Volume 10, No. 4
January, 1962

THE SOVIET JOURNAL OF

ATOMIC ENERGY

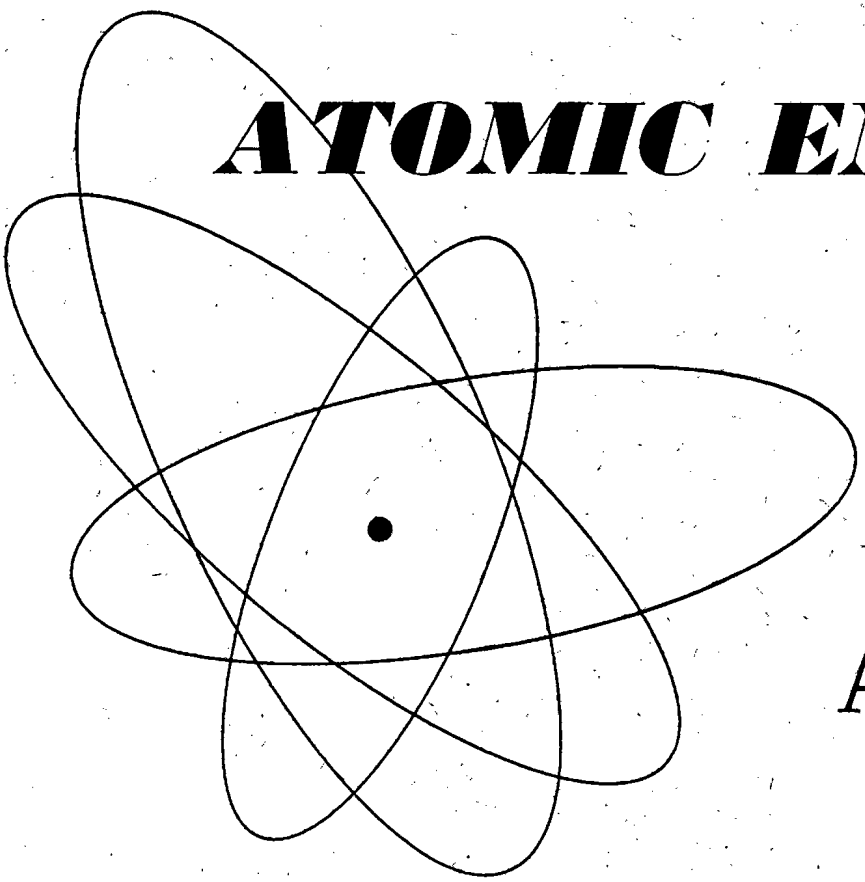

Атомная энергия

TRANSLATED FROM RUSSIAN

CONSULTANTS BUREAU

THE SOVIET JOURNAL OF

ATOMIC ENERGY

A translation of ATOMNAYA ÉNERGIYA, a publication of the Academy of Sciences of the USSR

(Russian original dated April, 1961)

Vol. 10, No. 4 January, 1962

CONTENTS

Annual subscription $ 75.00
Single issue 20.00
Single article 12.50

CONTENTS (continued)

NOTE

The Table of Contents lists all materials that appear in Atomnaya Énergiya. Those items that originated in the English language are not included in the translation and are shown enclosed in brackets. Whenever possible, the English-language source containing the omitted reports will be given.

Consultants Bureau Enterprises, Inc.

FIVE YEARS OF ACTIVITY OF THE JOINT INSTITUTE FOR NUCLEAR STUDIES

D. I. Blokhintsev

Translated from Atomnaya Énergiya, Vol. 10, No. 4, pp. 317-342, April, 1960
Original article submitted February 2, 1961

In March of this year, the Joint Institute for Nuclear Studies, the international scientific organization of the socialist countries, completed five years of existence. On this occasion, the Editorial Board publishes an abridged text of the main report delivered by the Institute's Director Prof. D. I. Blokhintsev to the Committee of Authorized Representatives of the Member Nations in November, 1960.

Most esteemed comrades!

The annual report to the Board of Directors of the Committee of Authorized Representatives, a report in which the immediate plans of the Institute are usually made public, has become our annual tradition.

Our international Institute will soon complete five years of existence; and it is therefore quite natural to report today not only of the results of the Institute's activities during the past year, but also to draw up a balance sheet covering our first five-year period of activity.

I. The Scientific Activities of the Institute

The scientific activities of our Institute have, during its existence, centered in the main on the development of high-energy physics.

In the beginning, we had to rely exclusively on the 680 Mev synchrocyclotron built at the Nuclear Problems Laboratory, the accelerator which we know as the veteran work-horse of Soviet high-energy physics. The year 1957 was marked by an event of first-ranking importance: the commissioning of the 10 Bev accelerator in the High-Energy Laboratory. Experimental work was carried out on this accelerator during 1958 in the practical realm, and significant scientific results were already available and reported by the High-Energy Laboratory at the 1959 Kiev Conference.

In the domain of low and intermediate energies, our scientific activities were comparatively limited, since the laboratories and facilities intended for this area of physics research were still in the planning and construction stages during those years.

I am happy to report to the Committee of Authorized Representatives that a pulsed reactor was successfully started up during the summer of 1960 and brought up to full power rating. At the present time, the Neutron Physics Laboratory, which has this unique facility at its disposal, enjoys splendid advantages for pursuing research in the field of classical neutron physics.

A second outstanding event in 1960 was the commissioning of the multiply charged ion accelerator at the Nuclear Reactions Laboratory. In mid-November, 1960, ion current and ion energy levels were attained with this accelerator adequate for producing reactions with complex nuclei.

The commissioning of these two machines means that the tasks posed during this five-year period in the development of low-energy and intermediate-energy nuclear physics at our Institute have been fulfilled. Nevertheless, the center of gravity of our scientific activities still falls primarily in the field of high-energy physics and elementary-particle physics. This area of research constitutes the front line of contemporary scientific investigation. Science enters here into the realm of new phenomena and new regularities.

Some idea of the extent to which the scales involved in this domain differ from the atomic and nuclear scales to which we are accustomed may be gathered by inspection of the schematic diagram in Fig. 1. The work at the Nuclear Problems Laboratory concerns dimensions hundreds of thousands of times smaller than the size of the atom

and ten times smaller than the size of the nucleus. At the High-Energy Laboratory, these scales are contracted again by a factor of ten, to the level of one hundredth of the size of the atomic nucleus.

This reduction in the scales studied is necessarily accompanied by an increase in the energy of particles whose beams serve as the tool of research, and also an increase in the energy associated with the nuclear processes being studied. In particular, the energy released when particles interact with antiparticles exceeds by hundreds of times the energy associated with nuclear reactions, and apparently constitutes the most complete liberation of the latent energy of matter that we are capable of imagining.

However, no one in the world yet has any idea how these numerous and varied elementary particles, the majority of which exist for only a negligible fraction of time (10^{-8} to 10^{-10} sec) might be put to practical use. Will means be found to render these transitory entities stable? Will ways and techniques be found to cause stable particles to yield up their energy? Will the enormous energy involved in this reaction of annihilation of matter be used for no other purpose than the devising of storage-ring and stacked-beam accelerators of colossal concentrations of energy? — or will other means be found for utilization of the energy contained in antimatter, e.g., circumventing the law of paired production of matter and antimatter? Answers to these questions still belong to the realm of fantasy, and no one today has any notion of how great the efforts called for will have to be or in what direction those efforts will be most fruitfully applied in searching for clues in the domain of high-energy physics.

At the present time, a formidable detachment of outstanding scientists the world over is working on problems of elementary particles in superbly equipped laboratories. These problems have become the central focus of contemporary physics.

We are pleased to acknowledge the fact that the Joint Institute for Nuclear Studies occupies a prominent place today in this work, and that the significance of the Institute's activities is constantly gaining new stature.

Let me report to you now on the most important achievements of the Institute during recent years.

2. The Most Important Results of Research in the Nuclear Problems Laboratory during 1956 to 1961

The point of central interest at the Nuclear Problems Laboratory has been occupied by research on interactions between nucleons and pions in the region of energies ranging from several hundred millions of electron-volts upward, the region which was quite happily dubbed the "classical" range of high-energy physics at the recently held Rochester Conference.

As a result of painstaking quantitative studies of proton, neutron, and meson (pion) scattering, including polarization effects (nucleon spin-dependent), highly important regularities in nuclear interactions were established for that energy range. The contribution of the Nuclear Problems Laboratory to this accomplishment was, if not decisive, at the very least eminently convincing.

Below we present a description, far from complete and in fact quite laconic, of the work completed at the Laboratory during the years in question.

1. An extensive round of research was completed at the Laboratory on establishing what is known as isotopic spin invariance; i.e., the law which unites under a single heading strong interaction between similar but oppositely charged particles (as forexample strong interaction between protons and neutrons).

2. The second grouping of research efforts is concerned with measurement of the meson-nucleon coupling constant f. This fundamental constant, which determines the mesic charge on a nucleon, has the same significance in nuclear forces as the charge of the electron has in electrical forces.

This constant has been determined to excellent precision at the Nuclear Problems Laboratory.

3. The third basic question toward which the Laboratory has made a significant contribution is an experimental proof for the so-called dispersion relations for meson scattering on nucleons. This means that the laws of causality and consequence generally accepted in physics retain their vigor in this new domain of physics, at least for scales of the order of 10^{-13} cm.

4. In addition, a wealth of other data has been accumulated at the Laboratory on nucleon and meson interactions (the "noncentral" character of nuclear forces, the significant role of "spin-orbit" coupling, quantitative data on nucleon polarization accompanying scattering, etc.).

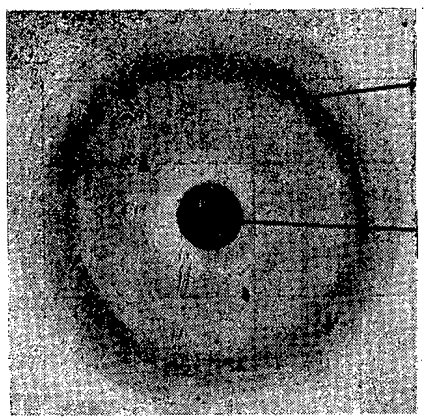

10^{-8} cm

ATOM

Electron shell; coupling energy of $\sim 1 \cdot 10$ ev

Nucleus (size $\sim 10^{-12}$ cm)

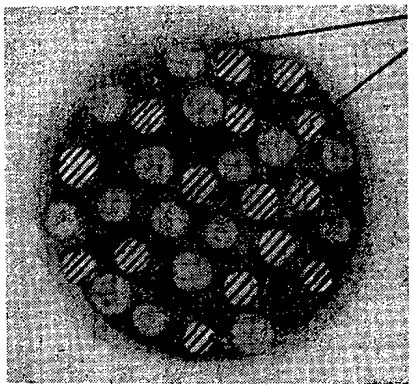

10^{-12} cm

NUCLEUS

Nucleons (proton-neutron); nucleon coupling energy in nucleus $\sim 1 \cdot 10^{7}$ ev

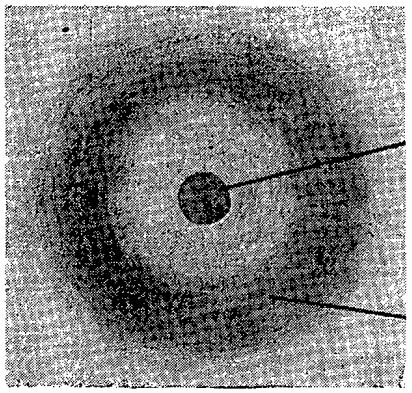

10^{-13} cm

NUCLEON

Core of nucleon (size $\sim 10^{-14}$ cm); rest energy $1 \cdot 10^{9}$ ev

Pion shell

Fig. 1. Comparative characteristics of scales and energies in atomic and nuclear physics and in the physics of elementary particles.

Figure 2 shows the angular distribution of particles upon scattering of neutrons by protons. The two lower curves were plotted from data obtained at the Nuclear Problems Laboratory, while the upper curve was obtained outside the USSR and refers to a lower energy range. From the position of vertical markings, it is apparent that an enormous

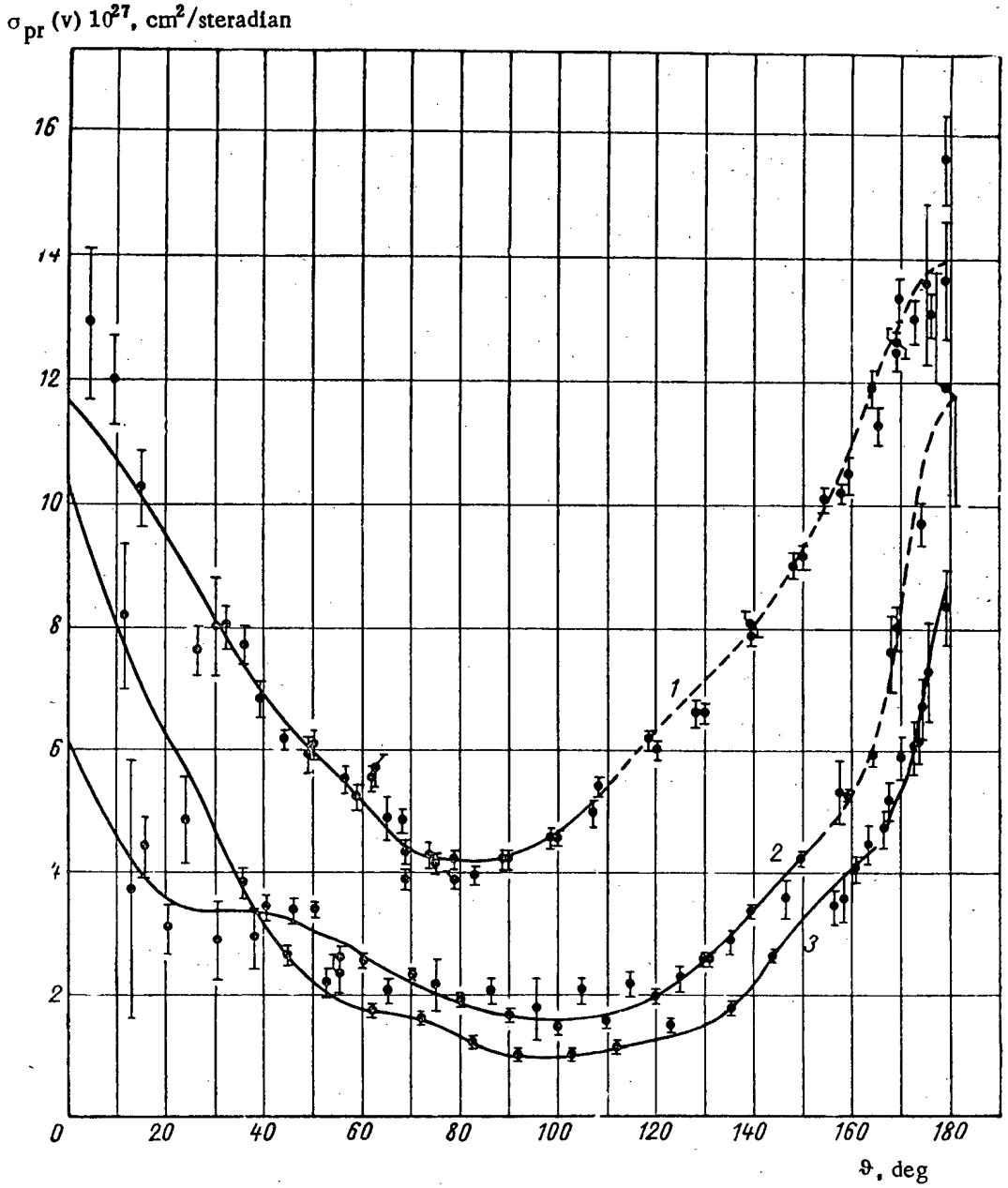

Fig. 2. Angular distributions of neutrons elastically scattered on protons. Curve 2 (at neutron energy 380-400 Mev) and curve 3 (at energy 630 Mev) obtained at the Nuclear Problems Laboratory. Curve 1 (for energy 90 Mev) was obtained abroad.

number of measurements have been performed. The relative part played by our Laboratory in these efforts also comes clearly to the fore. These data were used to prove isotopic invariance, and to obtain the value of the nucleon mesic charge.

Figure 3 shows resonance production of π^+-mesons in the $p + p \rightarrow \pi^+ + d$ reaction.

5. The Laboratory workers have recently obtained the first data on the now "fashionable" and quite important problem of interaction between unstable particles, in this case on mutual interaction between pions.

6. For the first time, the spin of the μ-meson was measured; this most important characteristic of the elementary particle, which many have considered the most enigmatic of all known particles.

7. Electron radioactive decay of the π^--meson has been established. This work, along with similar data from CERN on the π^--meson, furnish proof of the universal validity of the laws governing weak interactions.

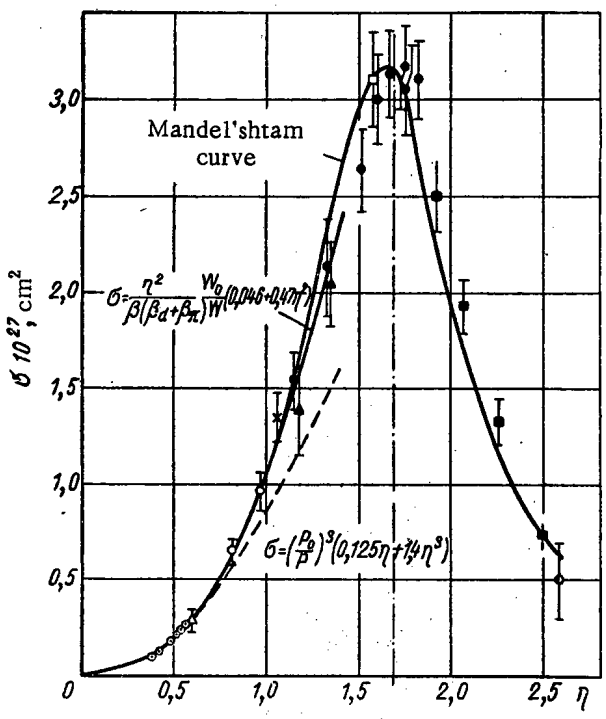

Fig. 3. Resonance relationship between total cross section of reaction $p + p \rightarrow \pi^+ + d$ and the momentum of the π^+-meson (here, η is the momentum of the meson in the center of mass system, in mc units): ●, ■ – data from the Nuclear Problems Laboratory; ○, ×, ▲, ◐, □, △, ⊙ – data obtained in other laboratories. Notation in the formulas: $\beta = v/c$ for incident proton $\beta_\pi = v_\pi/c$ for a meson in the center of mass system $\beta_d = v_d/c$ for a deuteron in the center of mass system P is the momentum of a proton in the center of mass system; P_0 is the momentum of a proton at threshold energy; w_0 is the reaction threshold energy; w is the kinetic energy of protons in the laboratory system.

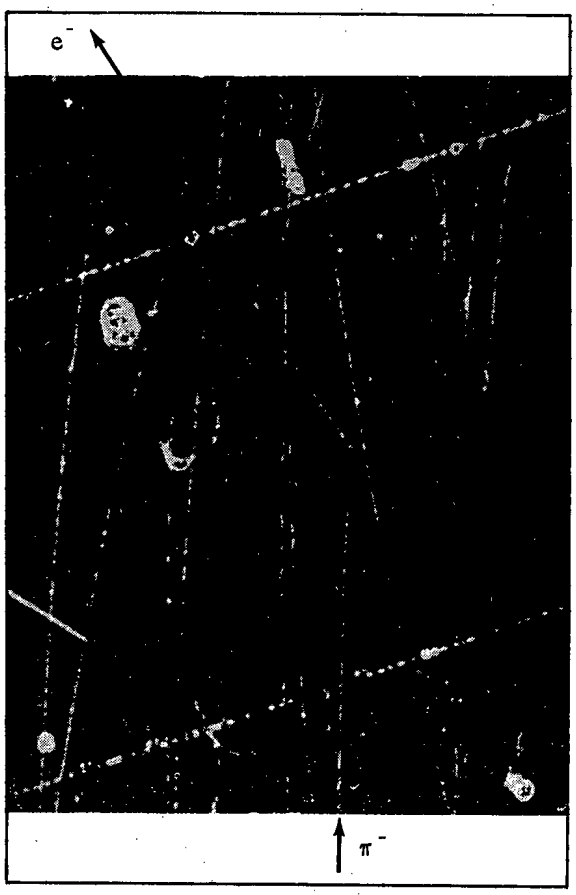

Fig. 4. Event of beta decay of a π^--meson: $\pi^- \rightarrow \rightarrow e^- + \tilde{\nu}$.

Figure 4 shows an event of radioactive decay of a π^--meson.

8. During the year, the curious phenomenon of excitation of atomic nucleus by μ-mesons, known as radiationless traditions in uranium, was proved as predicted by D. Zaretskii.

9. At the Laboratory, a considerable number of important projects have been carried out on methods and procedures: a device which automatically measures particle tracks has been designed, an ingenious hodoscopic system was devised, and an excellent liquid-hydrogen bubble chamber was built, in addition to many other accomplishments. Figure 6 shows the liquid-hydrogen chamber of 8 liters capacity. Figure 7 is a plate taken with that chamber (showing π^--meson scattering by protons).

Finally, highly vital investigations are proceeding at the Laboratory on the development of new accelerator concepts. Figure 8 shows a model of the accelerator built at the Laboratory in 1958-1959. This machine was used to prove the practical possibility of accelerating particles to relativistic energies in a cyclotron having a spatially varied magnetic field. We feel that this fundamental research will prove its value in the forthcoming development plans of the Institute.

3. Most Important Findings of the High-Energy Laboratory

All of the experimental research undertaken by the High-Energy Laboratory is based on the use of beams of particles accelerated by the 10 Bev synchrophasotron (proton synchrotron). This large machine was delivered to the Joint Institute for Nuclear Studies in the stage of assembly and run-in of individual components. Acceleration of a beam of protons to the design energy (10 Bev) was first achieved in April, 1957. It was then that the first experimental tasks were undertaken; but the beam intensity was still rather low.

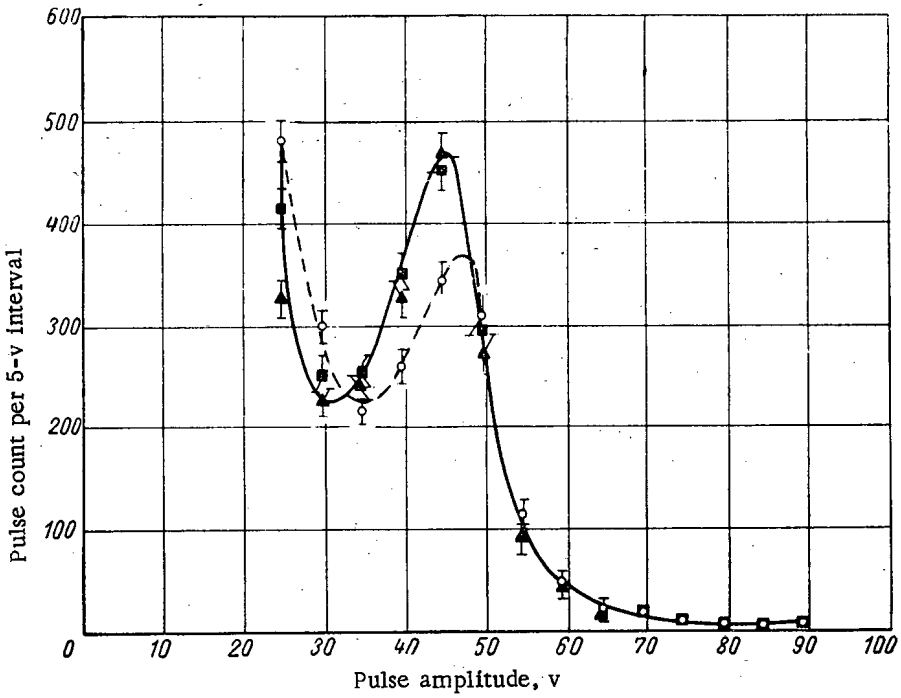

Fig. 5. Intensity of radiationless transitions 2p – 1S in mesic atoms of lead, bismuth, and uranium (radiationless transitions in uranium lower the number of pulses): ○ – U^{238}; ▲ – lead; ■ – bismuth.

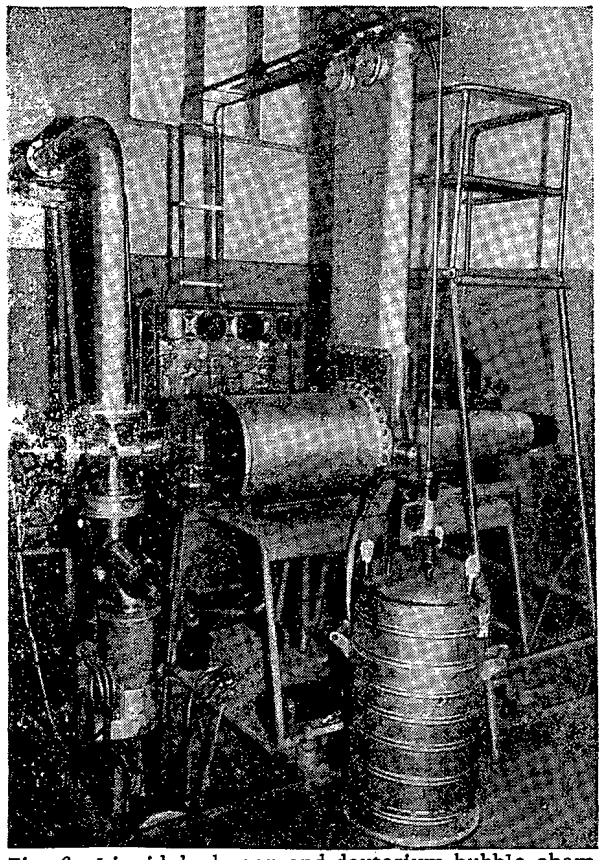

Fig. 6. Liquid-hydrogen and deuterium bubble chamber fabricated by the Nuclear Problems Laboratory staff.

The staff of the Laboratory has to its credit a large amount of work on perfecting the injection system, the vacuum system of the machine, and the supplies system for the electromagnet.

At the present time, the intensity of the protons is $1 \cdot 10^{10}$ particles per acceleration cycle, which makes it possible to successfully perform work using a multiplicity of beams and chambers installed to intercept them.

A new linear accelerator (see Fig. 9) designed at the High-Energy Laboratory and now in the testing and tryout stage was fabricated during the summer of 1960. This accelerator will make possible still higher beam intensities.

An enormous job was done in beam shaping and in installing bubble and diffusion chambers for obtaining plates of elementary processes, and setting up scintillation and Cerenkov counters.

At the present time, work is being done with the following beams:

1) a beam of π^--mesons with momentum of 9 Bev/c, with a propane bubble chamber (55 cm capacity), a xenon chamber (55 cm), and a liquid hydrogen chamber (25 cm);

2) a beam of negative particles with momentum to 6 Bev/c, with a liquid-hydrogen chamber (40 cm capacity), a Wilson chamber (50 cm), and work requiring the use of Cerenkov and scintillation counters;

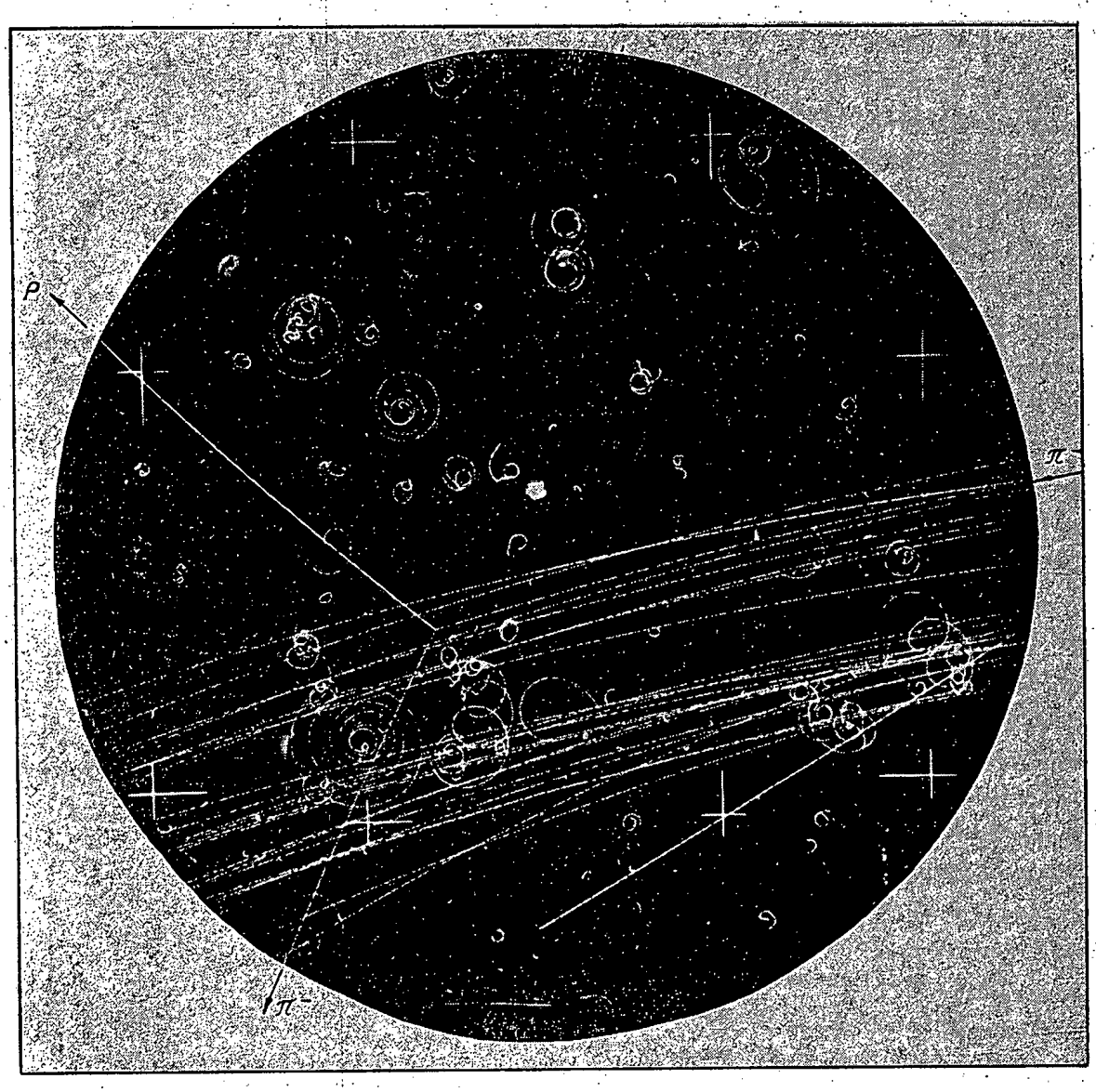

Fig. 7. Scattering of a π^--meson on protons: This photographic plate was made in the liquid-hydrogen and deuterium bubble chamber of the Nuclear Problems Laboratory.

3) a beam of positive particles with momenta attaining 5 Bev/c for work with K^+ mesons, with the aid of Cerenkov and scintillation counters and a similar beam with momentum to 2 Bev/c;

4) a beam of neutral K_2^0-mesons for work with a large diffusion chamber;

5) a beam of neutrons at high energies for work with a two-meter diffusion chamber;

6) on an energetic neutron beam for work with total-absorption Cerenkov counters.

Figure 10 shows the layout of now-existing beams, and those which will be shaped in the new experimental wing. Construction work on this wing is already completed.

A general view of the experimental wing of the High-Energy Laboratory is seen in Fig. 11. This photograph will remind many viewers of the totally empty appearance of this wing while it was quite new.

In Fig. 12 we see a xenon bubble chamber (55 cm capacity), and in Fig. 13 a liquid hydrogen chamber (40 cm capacity).

Work on building two new large-scale facilities for performing research on beams from the synchrophasotron is being continued.

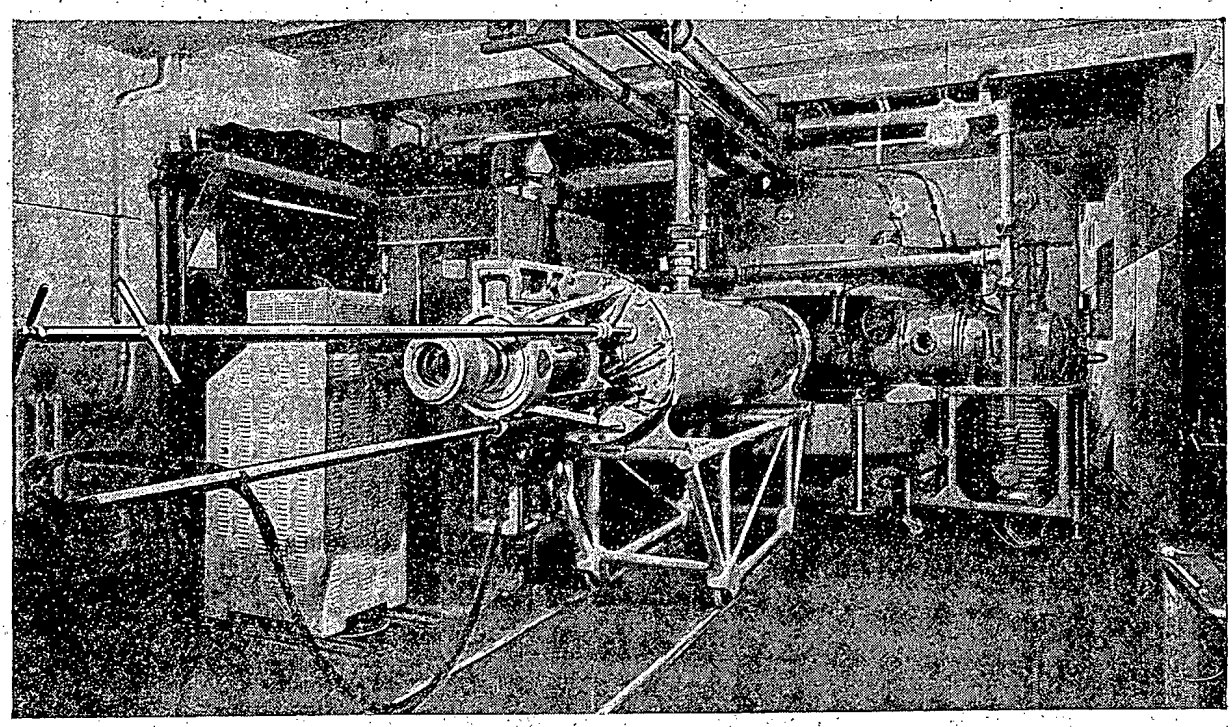

Fig. 8. Model of accelerator with spatially varying magnetic field.

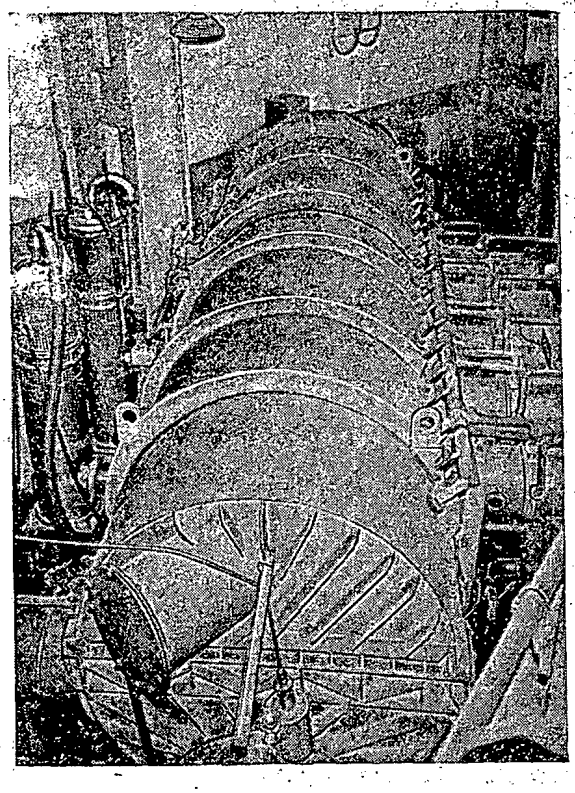

Fig. 9. New linear accelerator (injector) built by the High-Energy Laboratory.

In addition to the bubble chambers, the Laboratory staff has developed a large number of devices for processing and analyzing experimental data obtained by the use of various track chambers and thick-layered nuclear photographic emulsion stacks. Among these devices, we must single out for special mention the one developed in collaboration with the Drafting Bureau of the Institute, an automatic facility for processing emulsion plates obtained with the bubble chambers.

At the present time, the total number of plates obtained on the chambers at the High-Energy Laboratory has exceeded 200 thousand, and dozens of liters of emulsion have been irradiated. Processing of these experimental materials, in which scientists of the member nations of the Institute have played a great part, is far from complete, but the available data nevertheless provide sufficient ground for many new and important scientific inferences.

Below, we cite some of the most important scientific results of the Laboratory's work, which have enabled the Laboratory to take its deserved place at recent conferences on high-energy physics held at Kiev (1959) and Rochester (1960).

1. The first grouping of researches, to a considerable extent based on the use of nuclear emulsions (including the ingenious method of "perpendicular irradiation" developed at the Laboratory), covers the study of elastic and inelastic nucleon-nucleon and pion-nucleon interactions in the high energy region (6 to 10 Bev).

Figure 14 shows an example of similar phenomena, in this case an event of elastic scattering of a π^--meson of

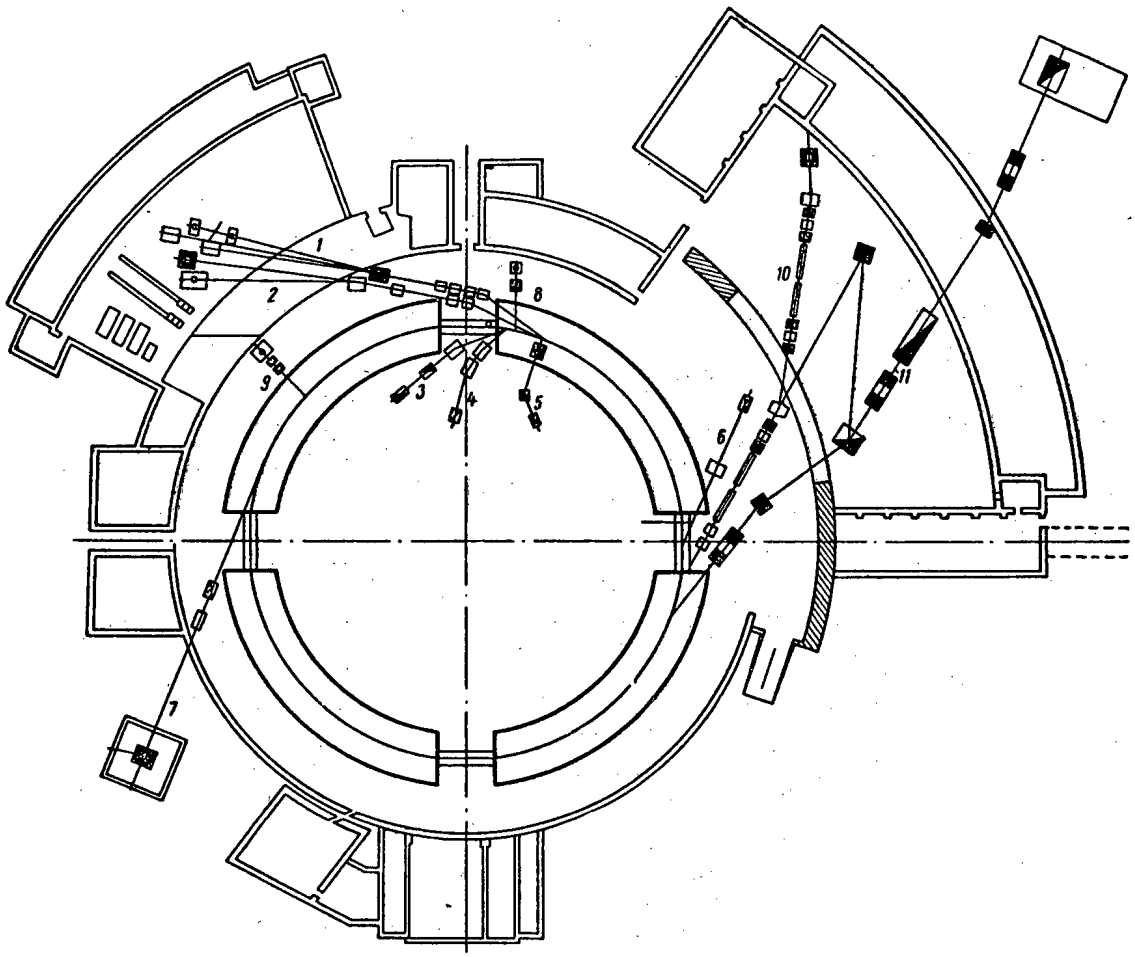

Fig. 10. Layout of synchrophasotron beams: 1) beam of π^--mesons with momentum to 9.2 Bev/c; 2) beam of π^--mesons with momentum to 5 Bev/c; 3,4,5) beams of positive particles; 6,7) beams of high-energy neutral particles; 8,9) beams of low-energy neutral particles; 10,11) planned beams of separated high-energy particles.

momentum 6.8 Bev/c on a nucleon. The plate was obtained from a propane bubble chamber. The typical small deflection of the π^--meson, attesting to the rarefied atmosphere of the nucleon, is characteristic. The study of such phenomena (multiplicity of pions generated, angular distribution, momentum transfer, etc.) has yielded many results supporting the concept of a complex structure for the nucleon: the concept of the nucleon (i.e., proton or neutron) as a system consisting of a dense core (of dimensions $\sim 10^{-14}$ cm) surrounded by a comparatively rarefied "mesonic atmosphere" (dimensions $\sim 10^{-13}$ cm) finds confirmation from several angles of approach in this work.

2. The second general grouping of problems concerns the study of the generation of strange particles. The most important result coming from these researches has been the discovery of the new positively charged particle, the antisigma-minus-hyperon ($\tilde{\Sigma}^-$). This discovery has made a new addition to the familiy of antiparticles, and has confirmed theoretical predictions on particle systematics. Figure 15 shows a photograph of this most remarkable event. Both the generation and decay of the $\tilde{\Sigma}^-$-hyperon are recorded in the photograph.

In Fig. 16, we have another interesting event: the generation of a Ξ -hyperon.

Cross sections and angular distributions in the generation of strange particles such as the Λ_0-particles, Σ-particles, K-mesons, and Ξ -hyperons have been measured at the Laboratory. These quantitative data are of course highly valuable. Nevertheless, even more interesting are the qualitative and new regularities uncovered in the generation of strange particles. In connection with these, we must draw attention to the following facts:

1) observation of D-events indicating interaction between K- and π-mesons (Fig.17). At first, this event was

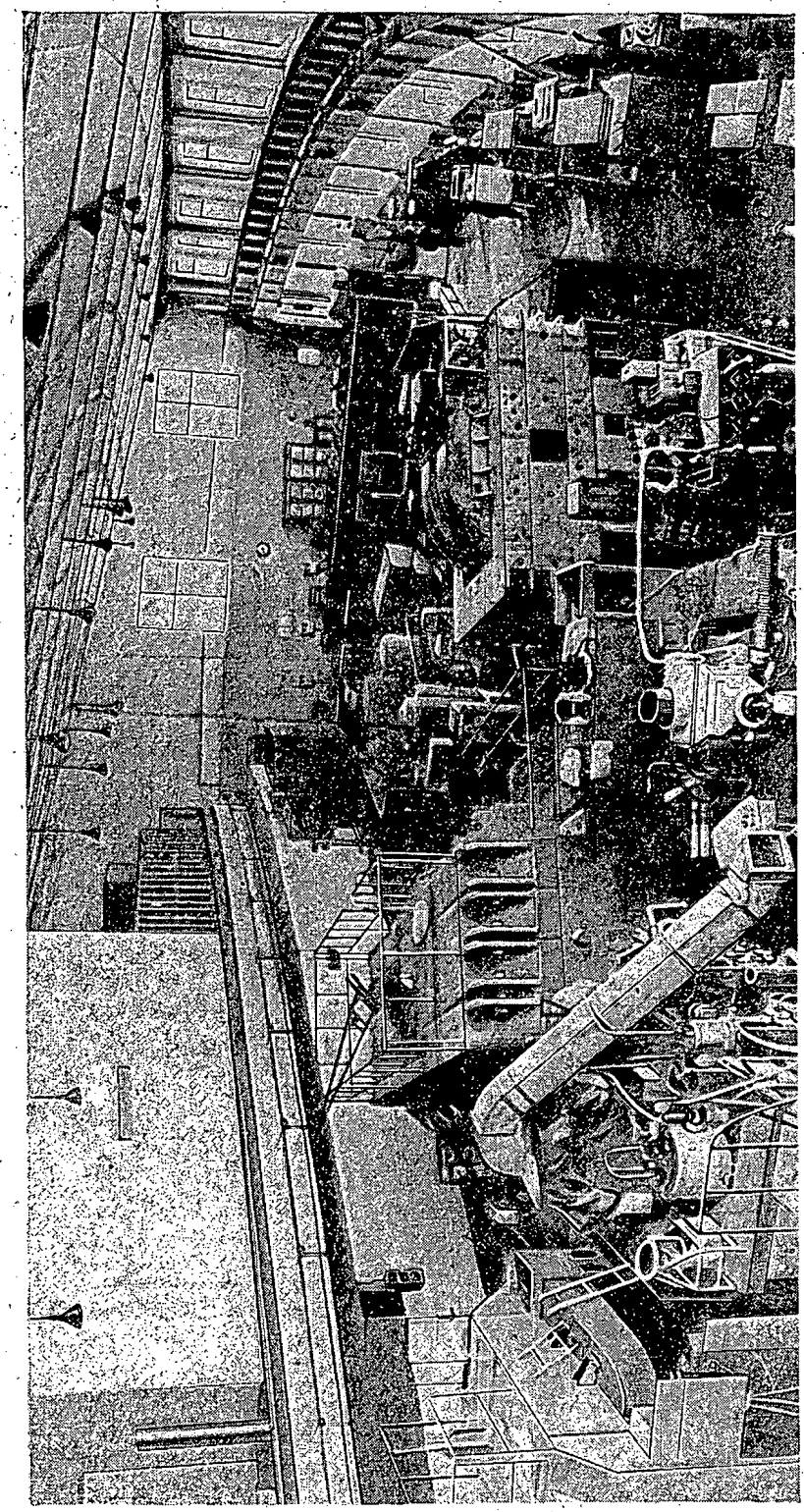

Fig. 11. Facilities for research with high-energy particles in the experimental wing of the synchrophasotron built at the High-Energy Laboratory.

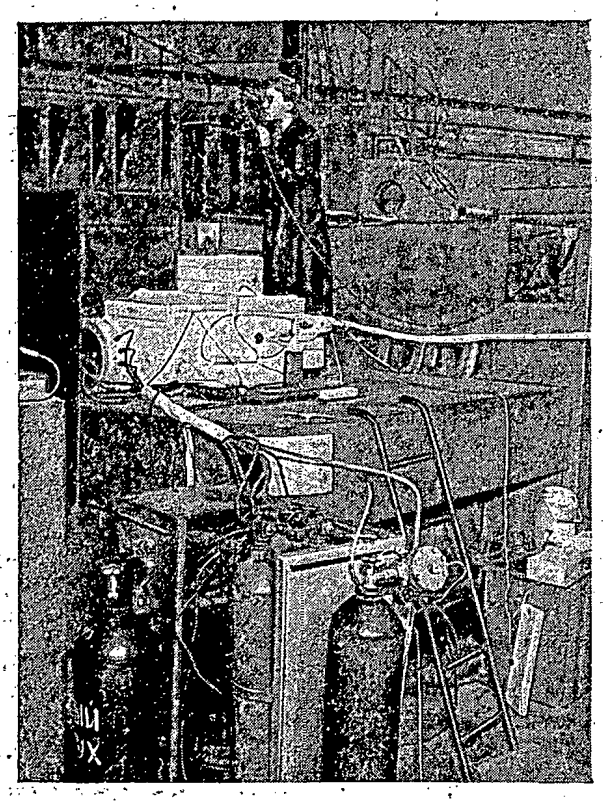

Fig. 12. Large xenon bubble chamber at the High-Energy Laboratory. The photograph was taken during assembly of the chamber. At the present time, over 100,000 photographs in beams of high-energy particles have been taken with the aid of this facility.

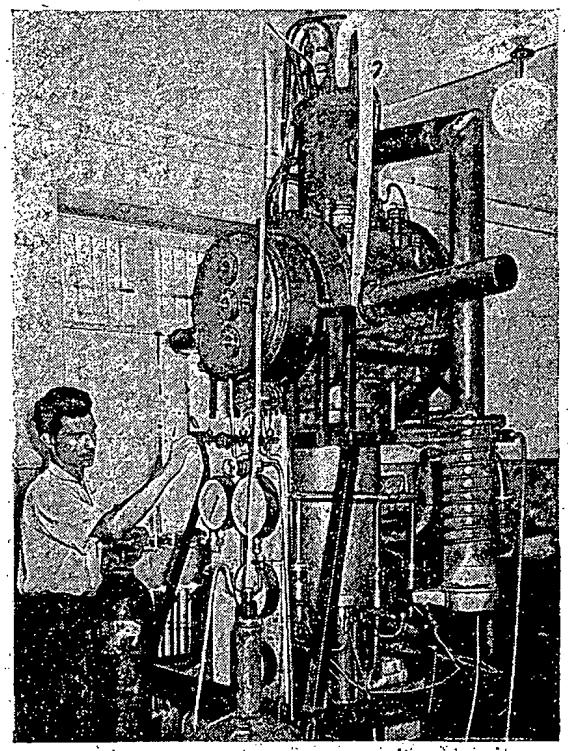

Fig. 13. General view of the 50-liter liquid hydrogen bubble chamber.

interpreted as either a decay in flight of a particle of approximate mass 1500, or else as evidence of a strong $K\pi$-interaction (or, again, possibly the formation of a $K\pi$-isobar). At the present time, we are inclined toward the second interpretation;

b) discovery of the longitudinal polarization of Λ_0-hyperons in their plane of generation. This fact is of basic significance, since it would imply the breakdown of spatial parity in strong interactions in strange particle production. A report on this phenomenon excited tremendous interest among the delegates to the 1960 Rochester Conference.

The study of momentum transfer and angular distributions demonstrates the following (see accompanying table):

a) the radius of the region in which events of interest generally occur in the course of interactions between energetic particles is practically the same for a broad class of phenomena (nucleon-nucleon and pion-nucleon interactions with production of all ordinary and all strange particles);

b) baryons evince a tendency to retain their individuality when they participate in various phenomena which are even remote and distinct in their properties at first glance. Nucleons and hyperons in particular proceed in the same direction, predominantly, following a reaction, in which the parent nucleon was moving prior to the reaction.

These facts point to the nucleonic "core plus atmosphere" structure referred to earlier. It is possible indeed that this fact will ultimately turn out to be no less significant than the discovery of the atomic nucleus per se.

In early 1960, a model of a new type accelerator, the ring phasotron, was put into operation. This accelerator, shown still in small scale for testing the principles of the mode of acceleration used, appears in Fig. 18.

These are the most important achievements to the credit of the High-Energy Laboratory.

4. Balance Sheet of the Work of the Neutron Physics Laboratory

Several years ago, work was initiated on the theory of a pulsed reactor at the Physics Institute of the State Committee on the Uses of Atomic Energy, and plans were laid for a fast-neutron pulsed reactor (the IBR).*

* Articles on the pulsed reactor will appear in coming issues of this Journal.

This unique facility is designed for physical research, functioning as a high-level neutron burst source at moderate average reactor power. In the summer of 1959 and winter of 1960, some work was carried out at the Neutron Physics Laboratory to test the underlying theory on critical assemblies. The reactor finally entered the assembly stage in 1960, and was brought up to rated power in June of that year.

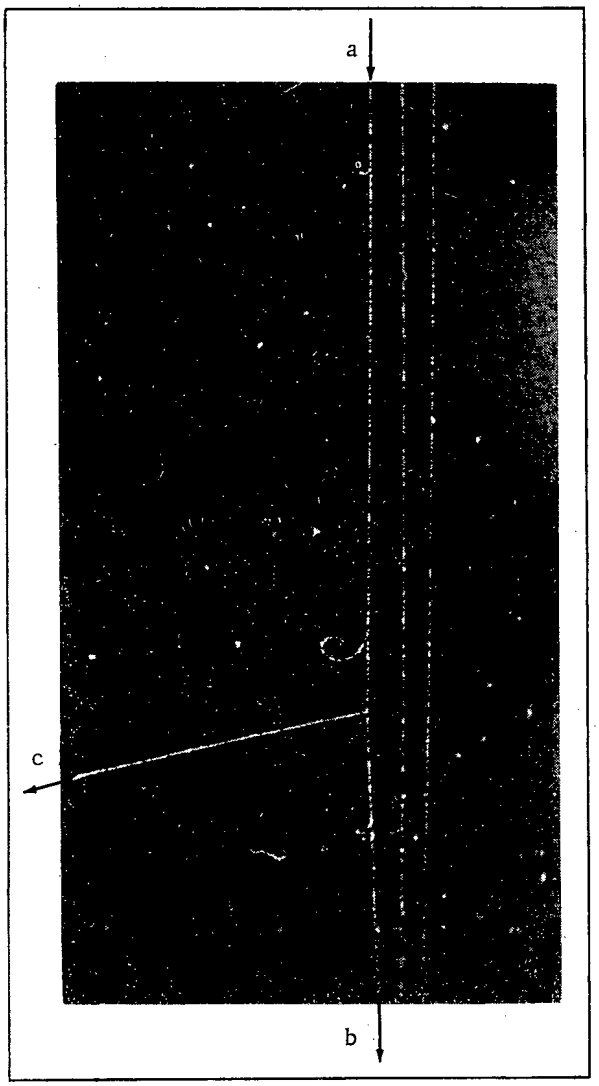

Fig. 14. Event of elastic scattering. This plate was made in the propane bubble chamber of the High Energy Laboratory. a) Track of primary π^--meson of momentum 6.8 Bev/c; b) track of same π^--meson primary after scattering on a hydrogen nucleus in the propane; c) track of recoil proton in this scattering event.

The following major trends stand out in the physics research at this Laboratory:

1) study of the reactor itself;

2) study of the cross sections of neutron reactions as a function of energy, particularly the study of neutron resonances;

3) study of solid and liquid molecules by the technique of inelastic scattering of slow neutrons.

Despite the difficulties associated with the incomplete state of the main building of the Laboratory, which is scheduled for completion only by the end of 1961, the needed equipment was nevertheless brought into readiness, especially the high-efficiency neutron detectors and pulse analyzers. Figure 22 gives a view of the neutron scintillation detector, 25 mm diameter, using methylborate; Fig. 23 gives a general view of the 1000-channel analyzer.

These and other improvements in technique have made it possible to get started on experimental research. Other interesting research projects are also underway at the Laboratory, including nuclear investigations using an electrostatic generator, studies of resonance absorption of gammas, etc.

The experimental work here is only the development stage, and the most important aspect is that the Laboratory is now not only a neutron laboratory, as its name indicates, but is also an excellent source of neutrons.

5. Balance Sheet of the Work of the Nuclear Reactions Laboratory

This Laboratory was built at Dubna during the past period, and an accelerator for multiply charged ions was installed in the Laboratory. The scientific activity is being carried out by a group in Moscow, at the I. V. Kurchatov Order of Lenin Institute of Atomic Energy.

The results achieved in the study of interactions heavy ions and nuclei were reported to the Second Geneva Conference (1958) on the Peaceful Uses of Atomic Energy.

The most essential and complicated research efforts were those conducted on synthesis of the element 102. The isotope 102^{253} was isolated in the autumn of 1957. A report on the synthesis of the isotope 102^{254} was made public somewhat later in the USA. Available data are still beset with contradictions, and work on further investigation into the properties of the element 102 stands high among the plans of the Nuclear Reactions Laboratory.

The complete state of the Laboratory building may be seen in Fig. 25, while Fig. 24 presents a photograph of the stage of progress reached in 1957 during construction of the building.

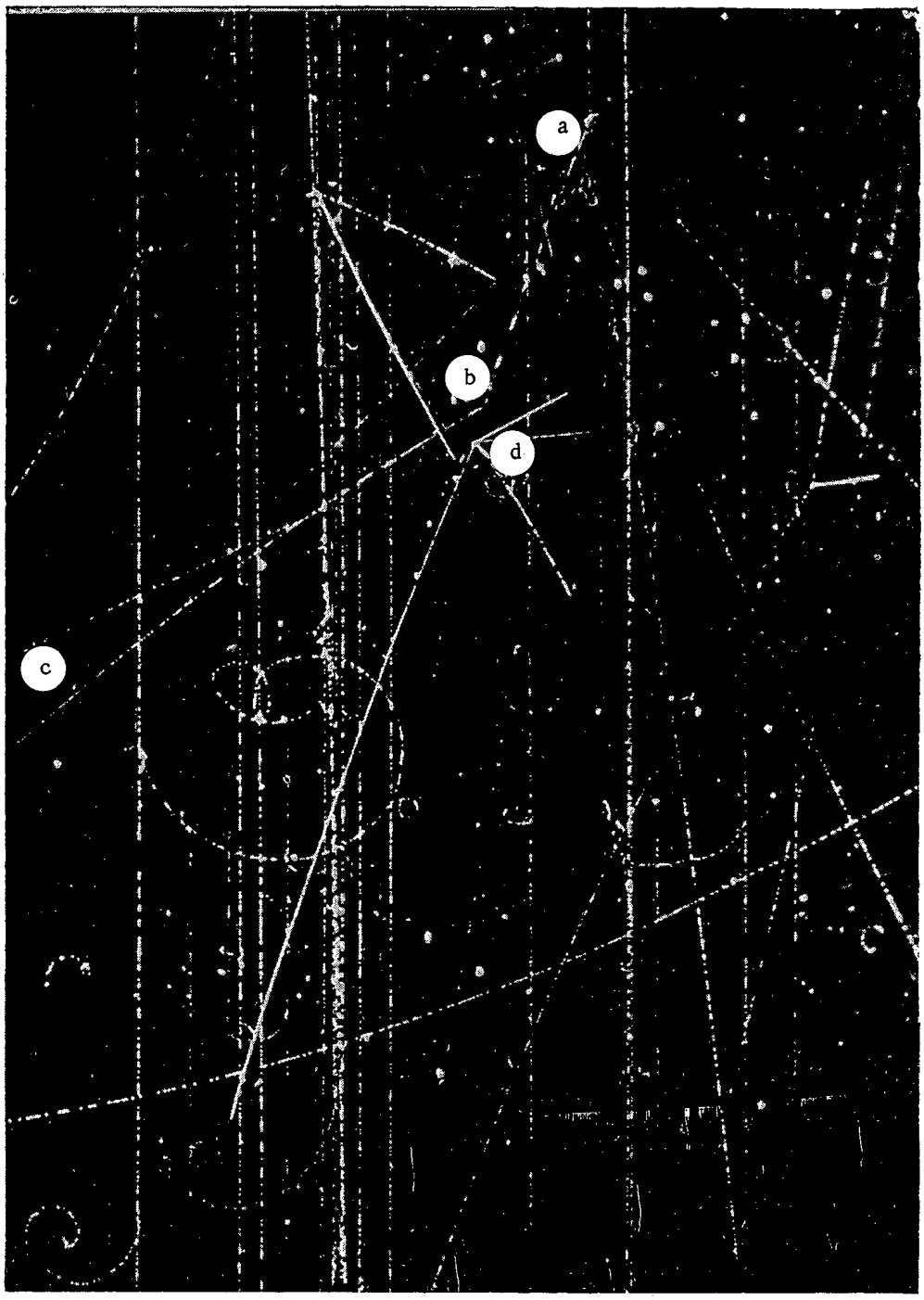

Fig. 15. Generation and decay of $\tilde{\Sigma}^-$-hyperon. Plate taken in propane bubble chamber. The antihyperon was generated by a π^--meson primary of 7 Bev/c momentum at point a. After proceeding in flight to point b, this unstable particle decayed to a π^+-meson (track c) and an antineutron, which annihilated at point d in an interaction with a carbon nucleus, yielding a large "star." In this plate, we see recorded for the first time an event of generation and decay of a charged antihyperon.

The most important achievement in the work of the Nuclear Reactions Laboratory staff was the commissioning of the accelerator for multiply charged ions. In Fig. 26, we see a general view of this accelerator. The first beam of accelerated particles was extracted from this accelerator in early September, 1960, and at the present time the accelerated ions have sufficient energy and intensity to support initiation of experimental studies of reactions in complex and heavy nuclei.

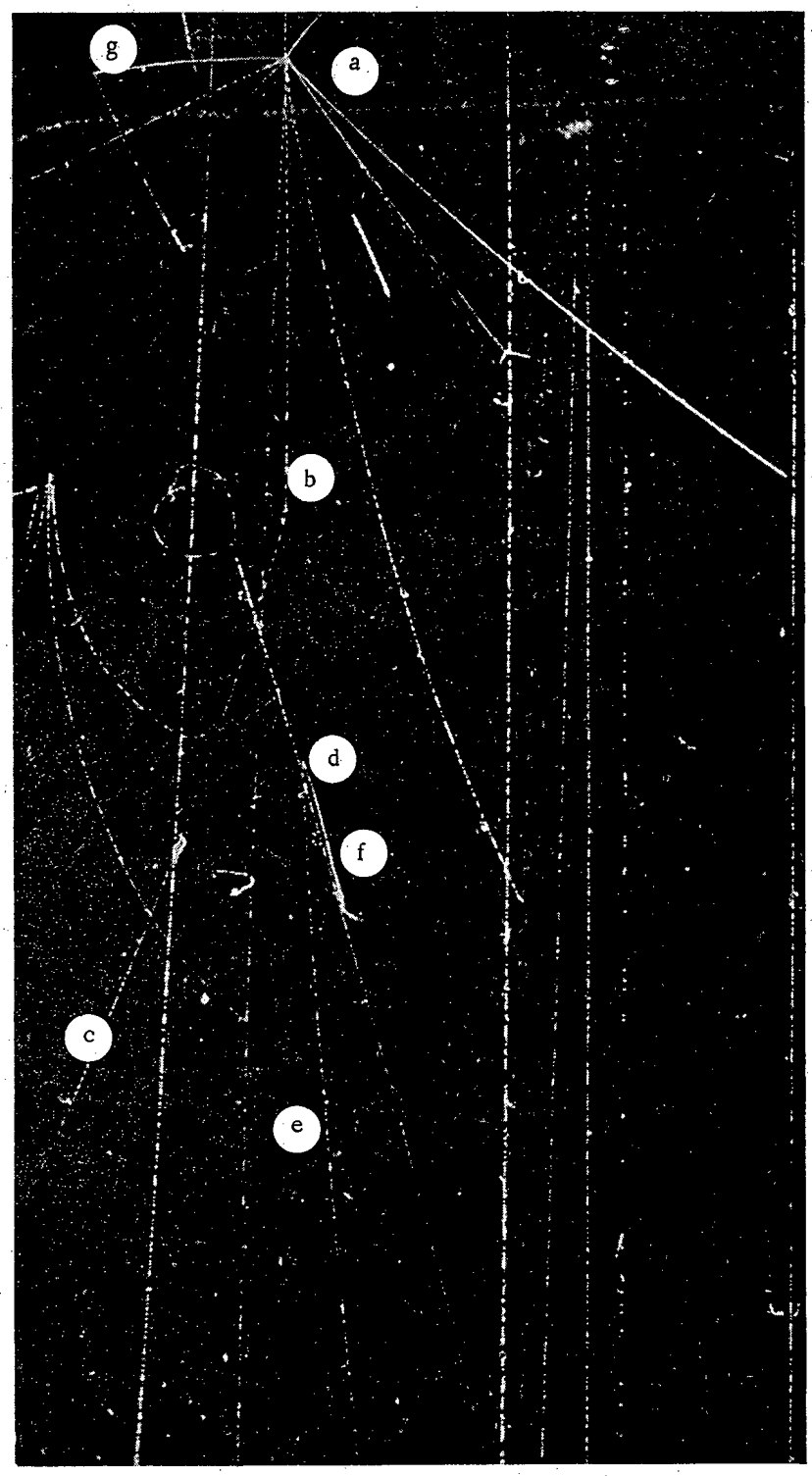

Fig. 16. Photograph showing a case of generation and decay of a Ξ^--hyperon: The Ξ^--hyperon was formed by a high-energy π^--meson at point a. After proceeding to point b, it decayed to a π^--meson (track c) and a neutral Λ-hyperon. The latter decayed at point d to a proton and π^--meson, producing the characteristic "fork" (tracks e and f). The birth of the Ξ^--hyperon was accompanied by the formation of several other particles, one of them, a K^+-meson, being brought to rest in the chamber at point g where it decayed to form a μ^+-meson.

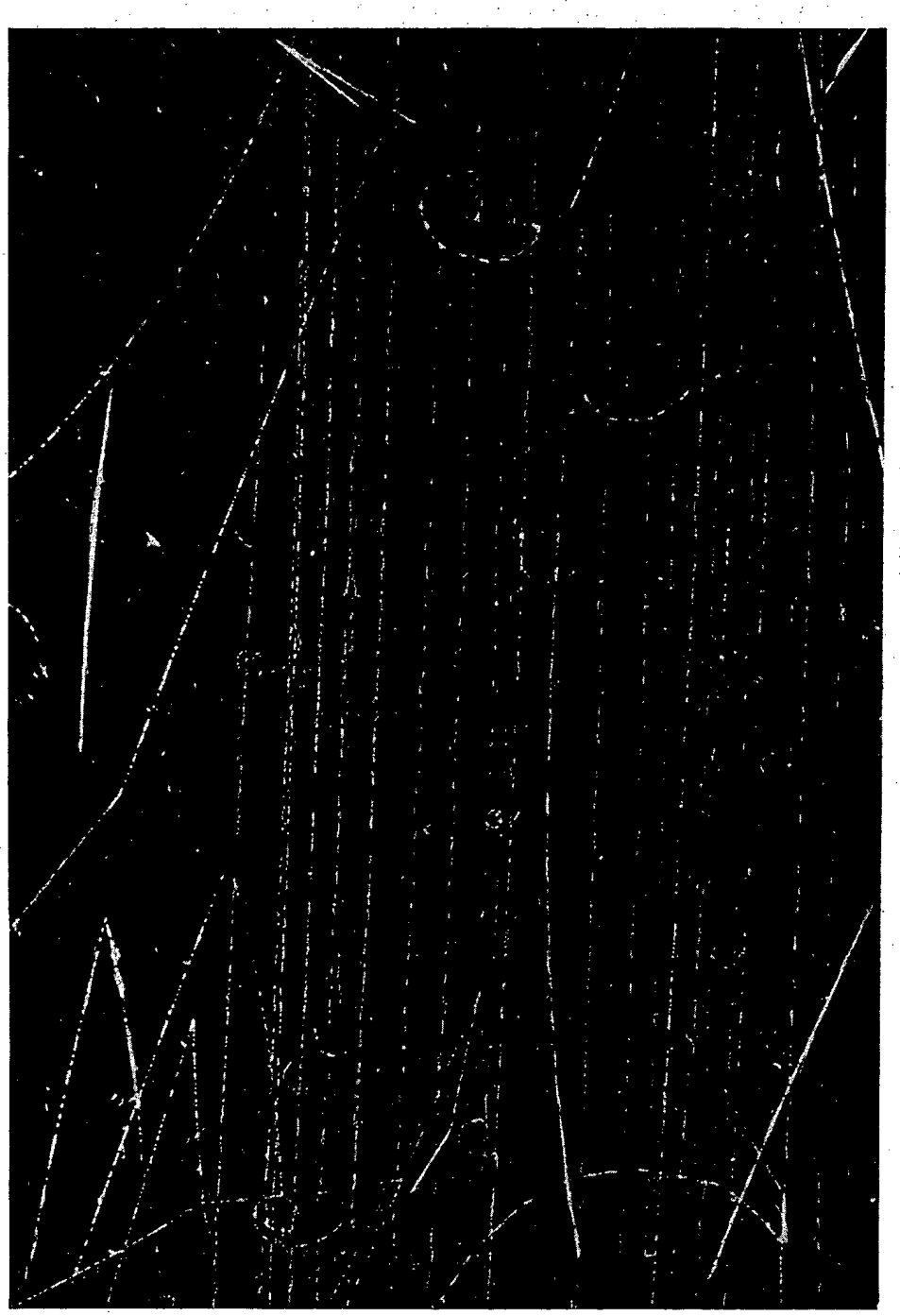

Fig. 17. A D-event. The plate was taken at Dubna during the summer of 1959, in the propane bubble chamber. This event is interpreted as a decay in flight of a particle of mass 1500 or as a case of a strong $K\pi$-interaction (possibly a formation of $K\pi$ isobars). At the present time, the second interpretation appears to enjoy more justification.

This Laboratory thus has been added to the number of functioning laboratories of the Institute.

6. Balance Sheet of the Activities of the Theoretical Physics Laboratory

In accordance with the five-year plan of development of the Institute, a building was erected in 1957 for the Theoretical Physics Laboratory (Fig. 27). This building will house the staff of theoretical physicists, a library, and

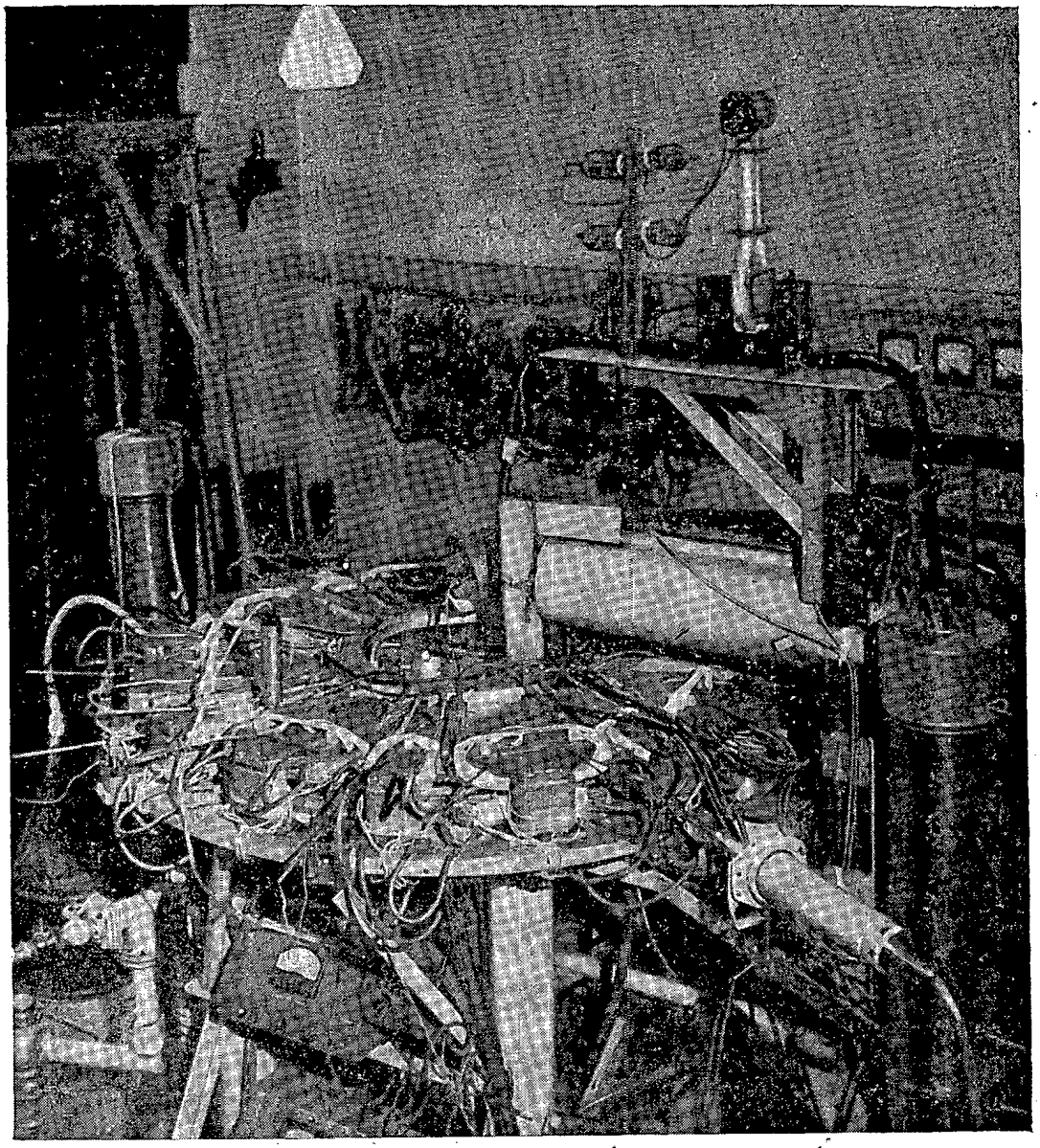

Fig. 18. General view of a model of the ring phasotron commissioned at the High-Energy Laboratory.

Average Values of Transverse Momenta of Various Particles Generated in Meson-Nucleon Encounters, Mev/c*

Number of prongs, n_f	Particle species					
	K^0	Λ^0	Σ^-	Σ^+	P	π^-
$n_f \leqslant 2$	394±42	395±47	523±48	428±70	380±70	384±26
$n_f \geqslant 4$	386±42	367±60	674±60	658±100	410±80	350±25
$\bar{n}_f$	393±35	388±35	587±53	559±85	390±40	361±20

* It is apparent that these values are mutually close for many collisional processes and for the production of new particles (only preliminary data are available with reference to Σ^--hyperons). This may be accounted for by the fact that the processes studied all take place in the same region of the nucleon.

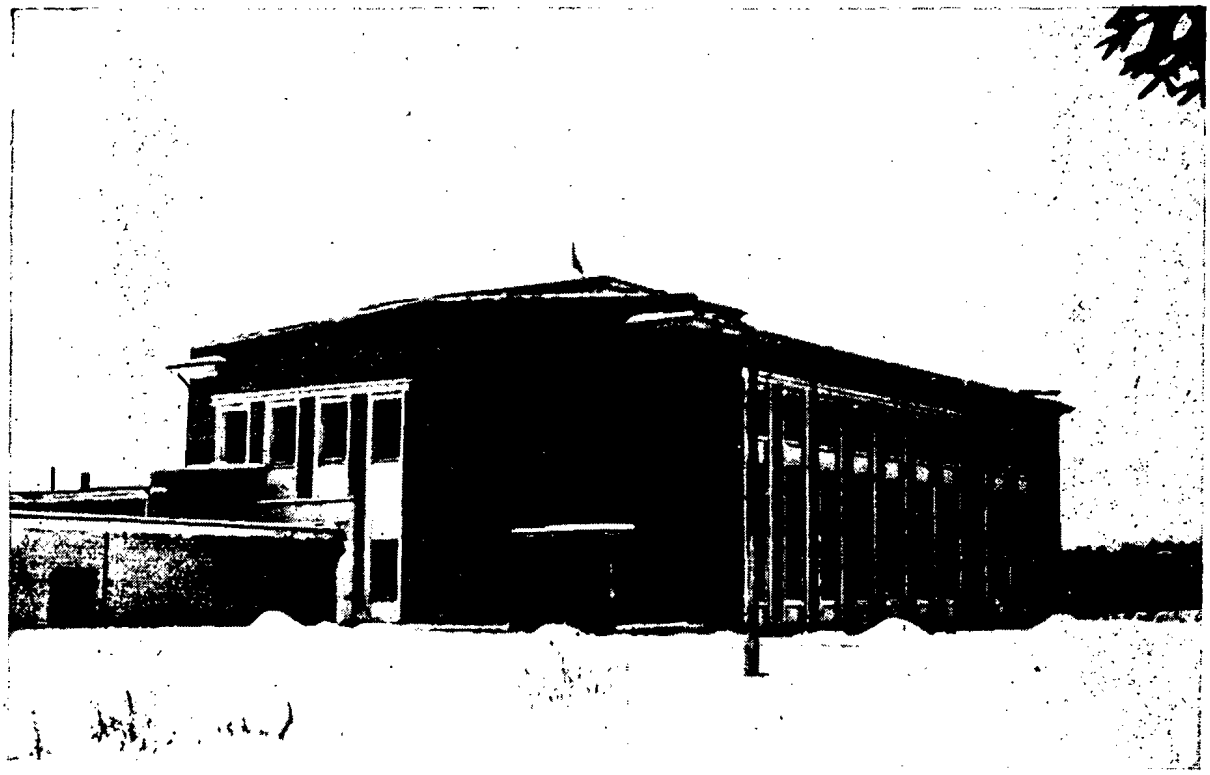

Fig. 19. General view of the pulsed reactor building of the Neutron Physics Laboratory.

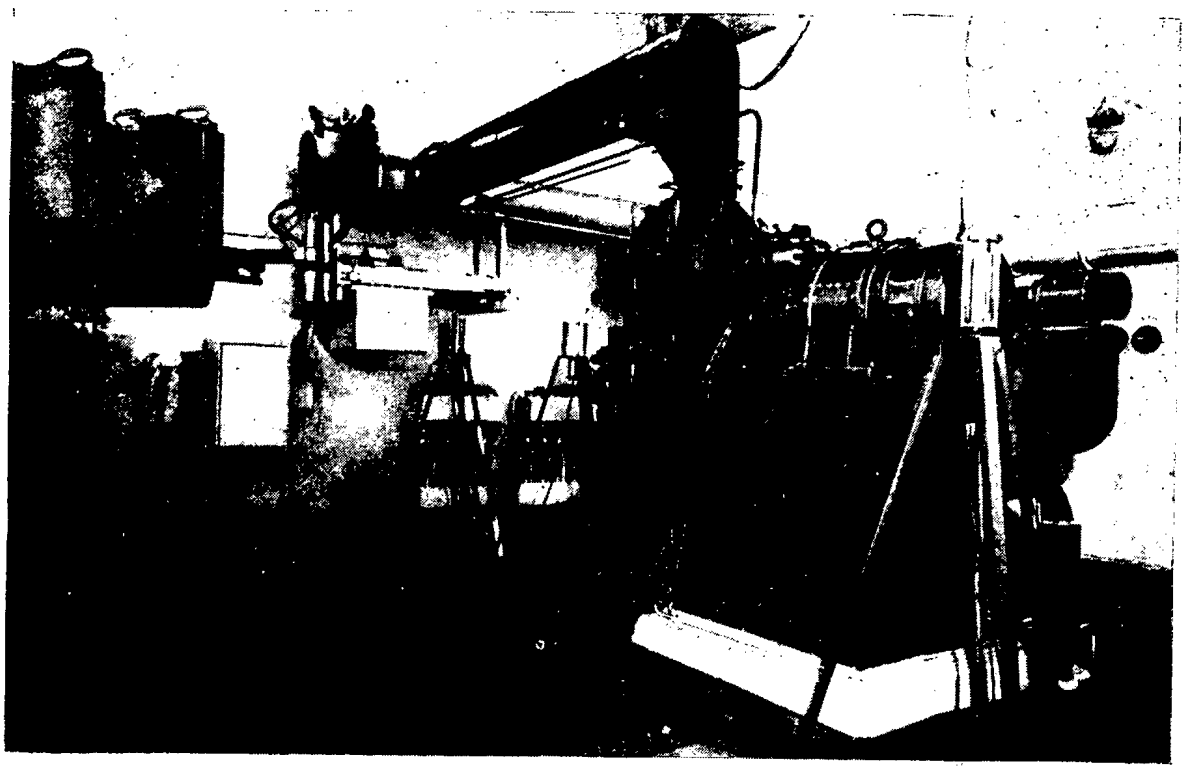

Fig. 20. General view of the reactor hall and general view of the facility.

a computing center. At the present time, the Laboratory is staffed by 88 theoretical physicists, among whom there number more than a few scientists of wide renown and exceptionally high ability.

The operations of this Laboratory will be directed toward the development of the fundamental principles of theory, to processing and interpretation of experimental findings obtained in the other laboratories of our Institute.

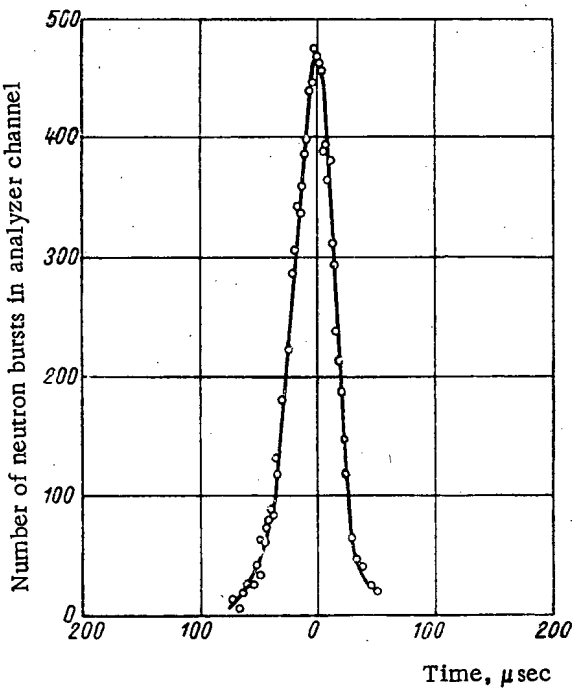

Fig. 21. Power excursion of the IBR pulsed reactor in the pulsed criticality mode. The curve was plotted from data taken from a time-of-flight analyzer of channel width 2 sec.

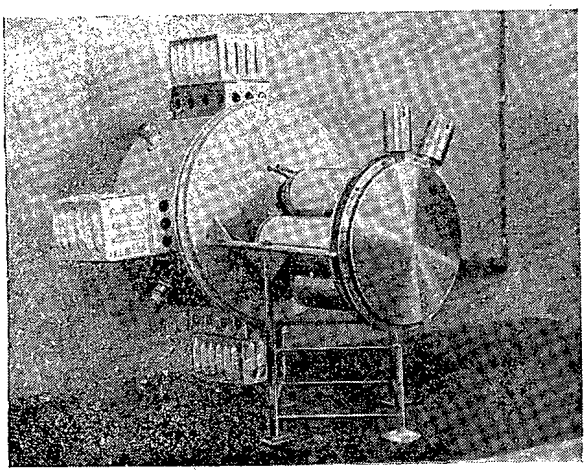

Fig. 22. General view of 250-mm diameter methylborate-filled neutron detector.

Imposing successes were achieved by the Laboratory staff in the development of the theory of dispersion relations, one of the most efficient tools for analyzing elementary processes in modern theoretical physics.

The theory of superconductivity (N. N. Bogolyubov) in its application to the atomic nucleus has undergone a profound development. Theoretical physics of the atomic nucleus has achieved a high standing in our work in the light of this theory.

The third major trend is work on the theory of elementary particles. The compound model of particles (M. A. Markov) was advanced and is being developed, and the structure of the nucleon is being studied on the basis of the concept of nucleon core and periphery, etc.

Interesting results have been obtained in the field of neutrino theory. B. M. Pontecorvo participated in this work (on assignment from the Nuclear Problems Laboratory).

The phenomonological theory of particle scattering and the theory of processing of experimental data have undergone successful development.

The activities of the Theoretical Physics Laboratory were reported on at international conferences, and many of the Laboratory's achievements have merited wide acclaim and recognition.

There is every reason for believing that the staff of the Theoretical Physics Laboratory will make no less significant contributions to the development of theoretical physics in the years to come.

7. The Computing Center and Automation

The computing center has become a part of the Theoretical Physics Laboratory. Until recently, we were working on keyboard calculators and the URAL-1 computer, which was entirely unsatisfactory for our needs. Many computational tasks had to be formed out to the already overlc 'ed Moscow computing centers.

At the present time, installation work has been completed on the new KIEV electronic computer (Fig. 28), and it is being put into operation.

One particularly important fact is that a new building was successfully completed in 1960 to house a still more sophisticated computer. It will be commissioned in early 1961.

Preparation of routine and standard computing programs is currently underway. Our Institute will thus have the services of a first-rate computing center in the very near future.

Another problem is closely linked to that of the development of the computing center; namely, the problem of automating measurements of photographic plate processing for plates obtained from chambers and emulsion stacks,

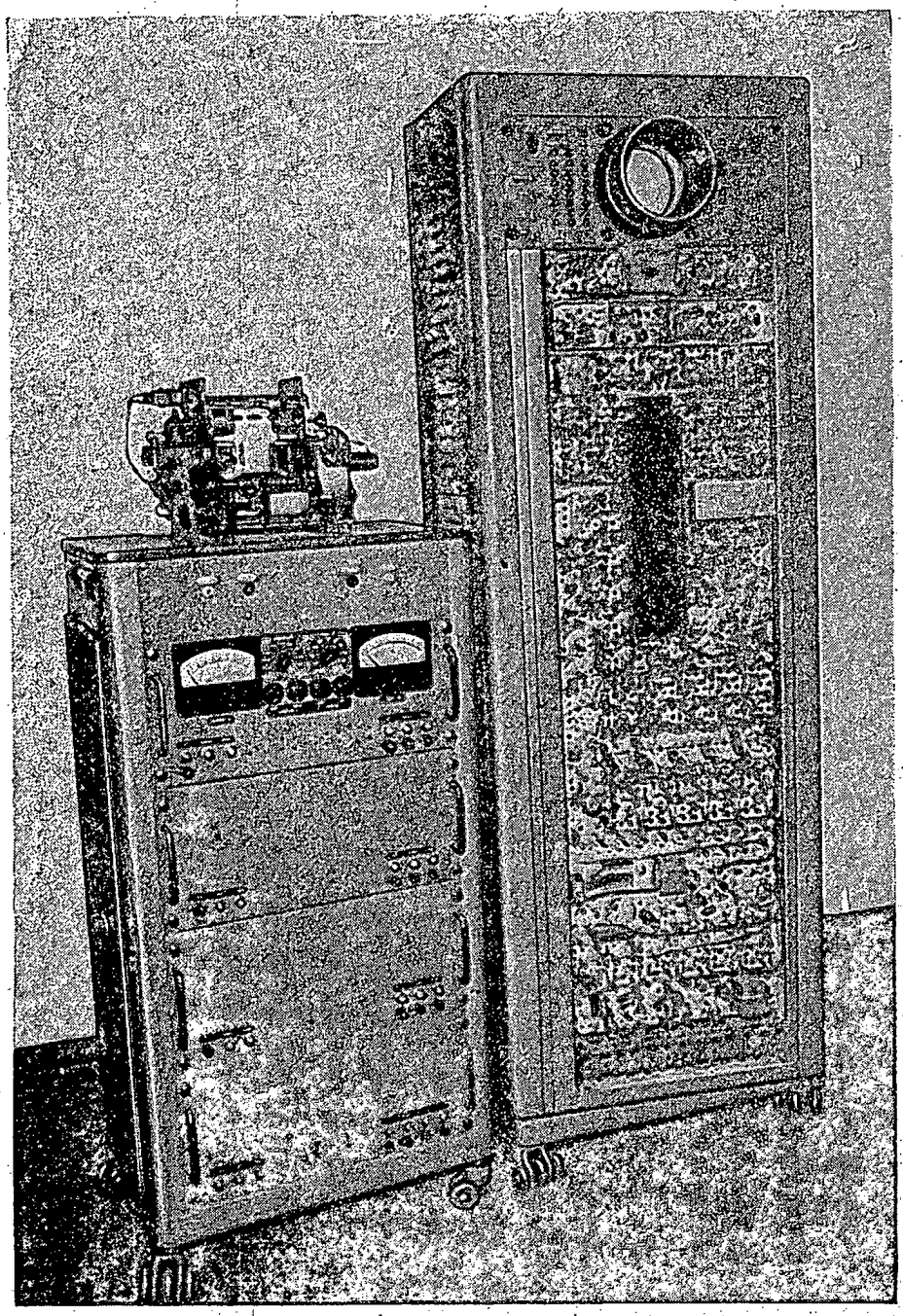

Fig. 23. 1000-channel time-of-flight analyzer with data processing accessories.

and running these measurements on computers. Three automatic facilities have been built to process photographic film: one of them was designed in the Drafting Bureau of the Institute and has met with high approval on the part of the Acquisitions Commission, while the second was built at the Nuclear problems Laboratory, and the third was built in Hungary and Poland.

Although we still have before us quite a lot of work ironing out problems associated with the introduction of computer and automation techniques into our regular work, the basis for a complete solution of those problems has already been laid.

8. The Cadres of the Institute

The number of the staff of the Institute increased significantly during the years 1956-1960, owing to the introduction of new laboratories and expansion of activities in already existing laboratories.

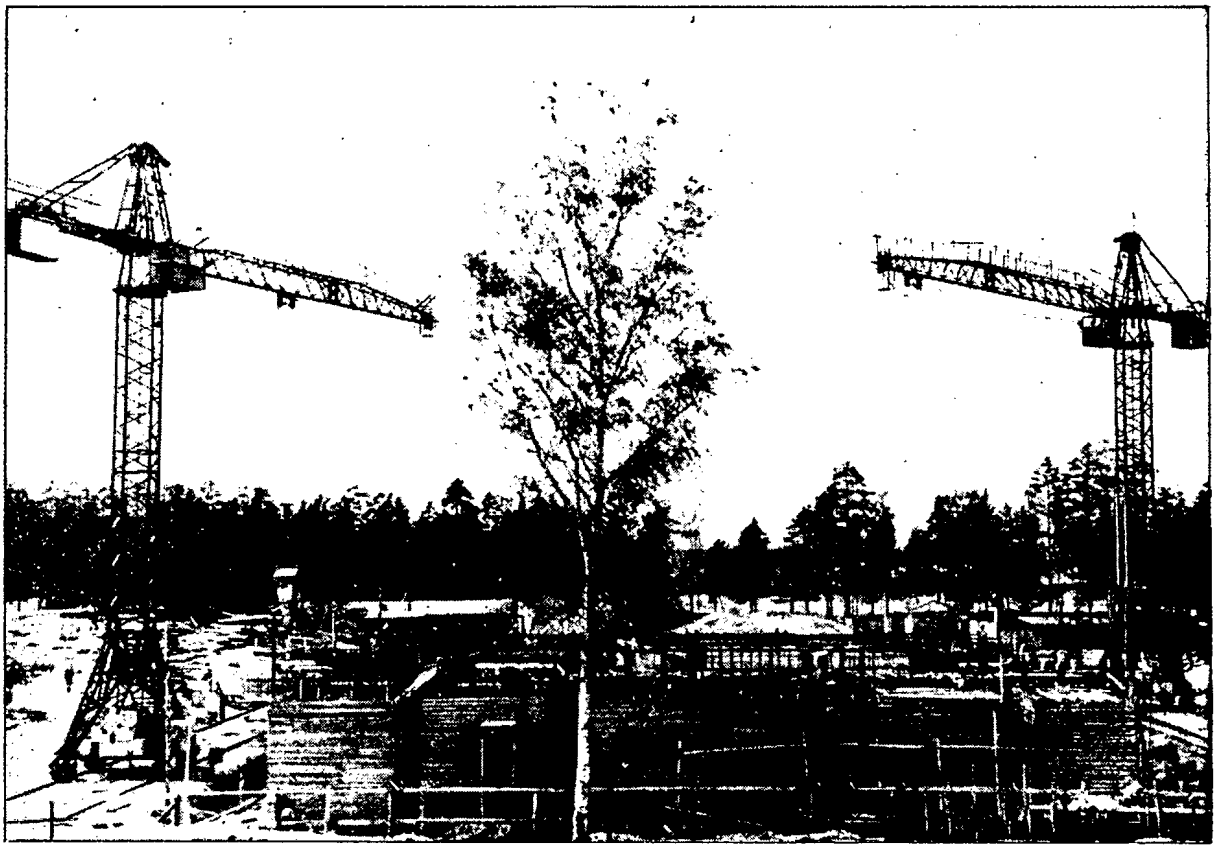

Fig. 24. General view of construction work at the site of the Nuclear Reactions Laboratory building. (photo taken May 13, 1957).

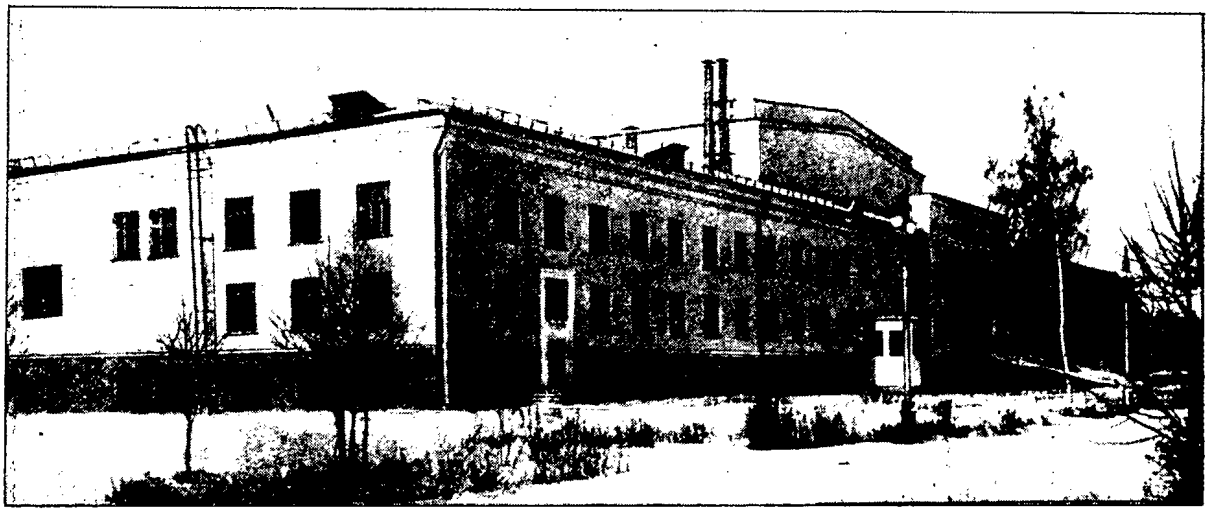

Fig. 25. General view of completed building of the Nuclear Reactions Laboratory. (photo taken November 20, 1960)

It is instructive to bear in mind the fact that, back in 1956, activities were developed in only one laboratory of the present complex, the Nuclear Problems Laboratory. At the present time, we have at our disposal five laboratories, the largest of them being the High-Energy Laboratory.

Moreover, scientific collaborators and engineers from member nations of the Institute other than the USSR have been drawn into the work of the Institute.

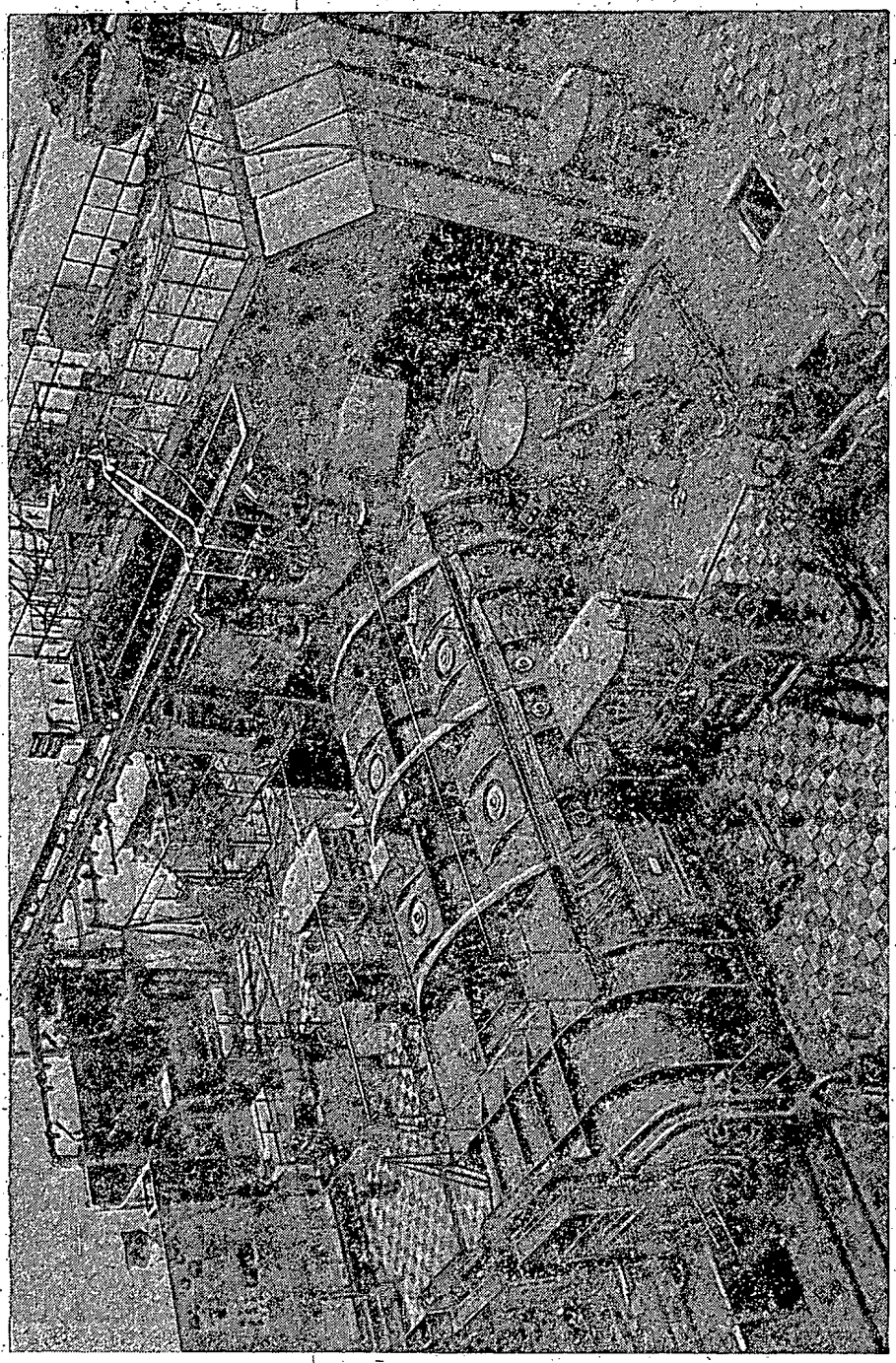

Fig. 26. General view of the cyclotron for multiply charged ions at the Nuclear Reactions Laboratory (November 20, 1960)

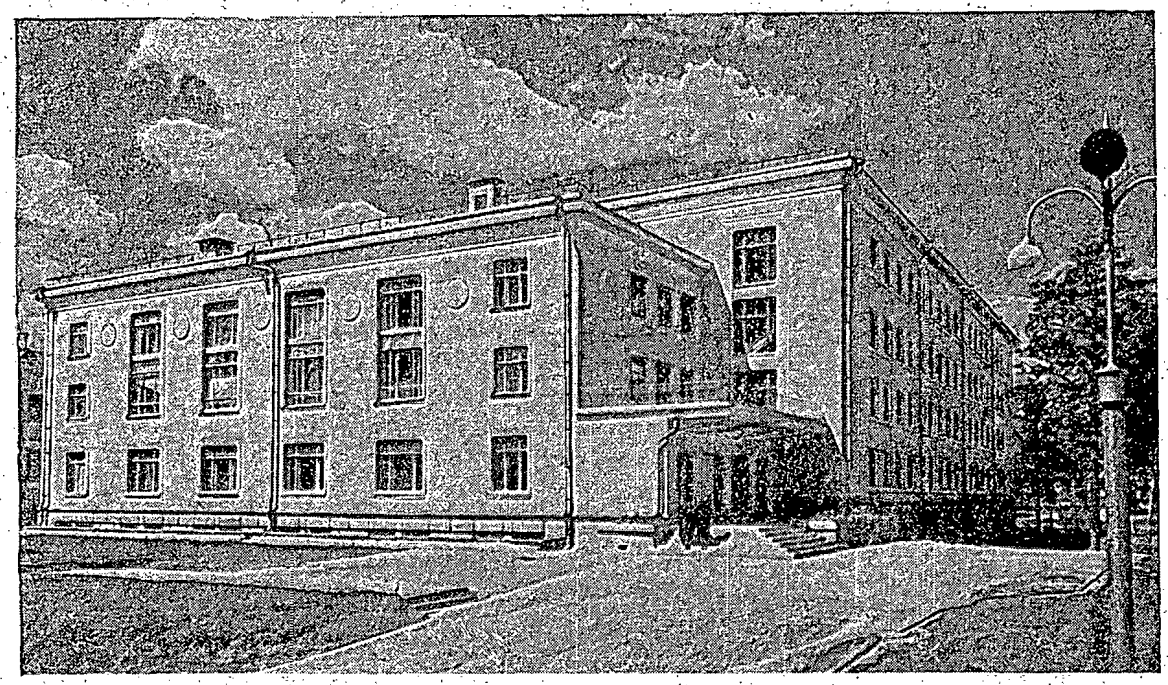

Fig. 27. General view of the building of the Theoretical Physics Laboratory (November 20, 1960).

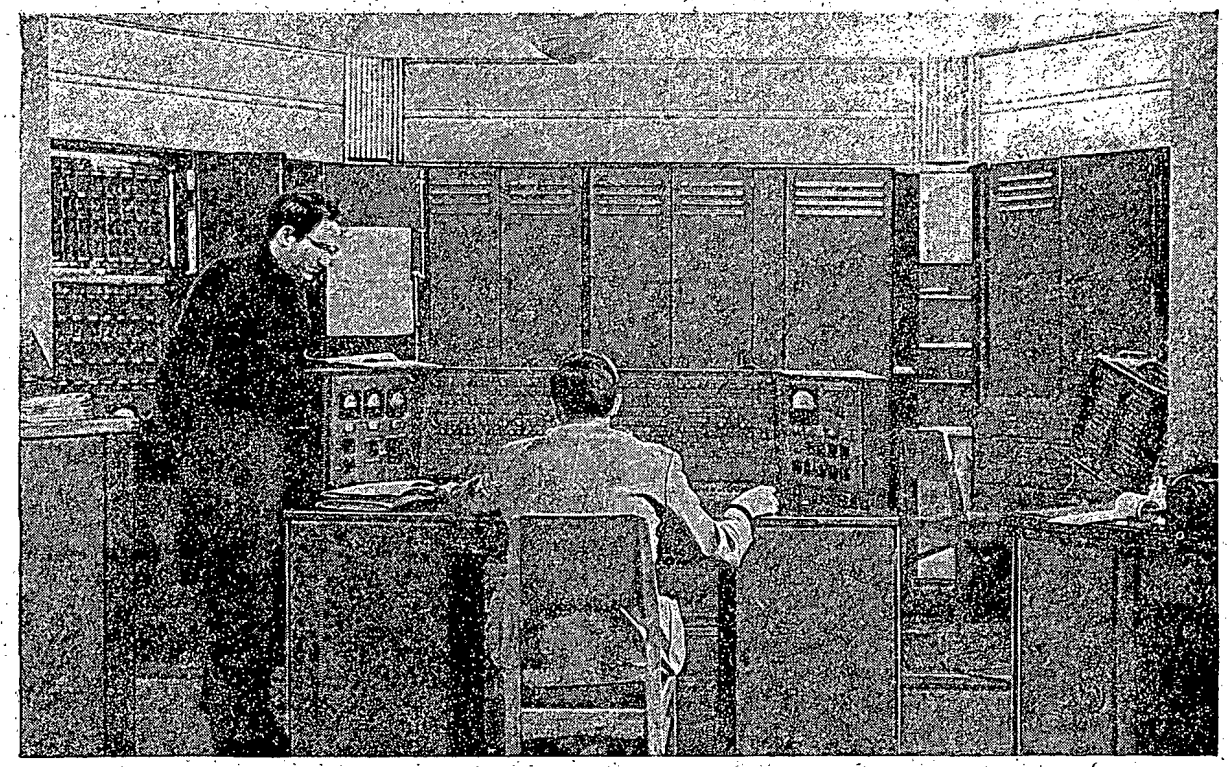

Fig. 28. The KIEV electronic computer.

At the present time, the number of colleagues who have been assigned to work at the Institute by other countries totals 200, and the total staff of scientific personnel at the Institute is 420. This fact convincingly demonstrates that out Institute has become transformed into a vital and capable international scientific organization.

However, the increase in the scientific staff of our Institute has led to some negative effects which are disturbing and which oblige us to take measures of correction. The increase in the Institute staff was accompanied by an decrease in the ratio of auxiliary personnel to scientific personnel. This unfavorable shift is acknowledged, and we realize the necessity of developing our Institute not only along the line of increasing the staff of research scientists, but also along the line of increasing the number of avilable laboratory technicians, mechanics, and other personnel in the subsidiary but vitally important work categories.

Youth still requiring aid and supervision on the part of the more experienced and more highly skilled scientists are conspicuous among the new additions to the research staff. The participation of a still larger number of qualified scientists from member nations in the activities of the Institute is therefore very important.

In 1961, a branch of the Physics Department of the M. V. Lomonosov Moscow State University will begin work at Dubna. This will further facilitate strengthening ties between the research level and the classroom level, and will contribute to the attraction of capable youth to the activities of our Institute.

9. The International Liaisons of the Institute

One of the problems facing the Joint Institute for Nuclear Studies, as stated in the 4th article of its constitution and by-laws, is that of "maintaining ties with interested national and international scientific research and other organizations in the cause of the development of nuclear physics and of the exploration of new opportunities for the peaceful uses of atomic energy."

Our liaisons with scientific research organizations in the member nations of the Institute are being developed thanks to the collaborative scientific research efforts and improvements in techniques achieved at the Joint Institute in the course of international scientific conferences, trips of Institute scientists to the member nations, and the exchange of scientific information.

Our contacts with other counties are realized in large measure through the participation of Institute scientists in international scientific conferences, visits of our scientists to scientific research centers in other countires, and, conversely, by visits of foreign scientists to our Institute, and also by the exchange of scientific information.

Our Institute collaborates with scientific organizations in the member nations, primarily in the field of investigations based on the use of nuclear emulsions irradiated in the Institute's accelerators, and bubble chamber plates.

Scientific investigations involving the use of nuclear emulsions irradiated at Dubna are being carried out by research institutes in Bulgaria, Hungary, the German Democratic Republic, the Peoples Republic of China, Poland, Rumania, and Czechoslovakia. A small photographic emulsion processing laboratory has been set up and equipped in Mongolia with the aid of our Institute, and will also take part in these investigations.

Organizational work on nuclear emulsion investigations is under the jurisdiction of a special committee on collaboration in that field headed by Prof. V. Petrilka.

The Board of Directors of the Institute will also tender support to this form of collaboration in the future, supplying nuclear emulsions to all laboratories participating in these investigations.

Collaboration in the field of investigations based on processing of bubble chamber plates will be organized in line with the introduction into service of propane and xenon bubble chambers and the preparation of large hydrogen and propane chambers.

Colleagues of the Nuclear Research Institute of Warsaw have been drawn into the new research projects, under the leadership of Prof. M. Danysz, and a team from the Nuclear Physics Institute at Miersdorf (German Democratic Republic) led by K. Lanius plus another group from the Central Physics Research Institute in Budapest have done likewise.

Collaboration based on investigations of plates taken with the aid of bubble chambers faces, we believe, great perspectives. Furthermore, collaboration is being realized in the field of radiochemistry, photoelectrets, fabrication of automatic devices, etc.

An important event in the life of the Institute took place in the organization of a low-energies panel of the Learned Council of our Institute, set up on the basis of the plan of collaboration in many fields as proposed by the State Committee of the Council of Ministers of the USSR in charge of uses of atomic energy.

The development of cooperative efforts along this line has already met with a reflection in the useful conferences held during the year. Courses for training specialists in radiochemistry and isotope engineering will be organized in the near future, in compliance with that plan of collaborative efforts.

The start-up of the pulsed reactor and the commissioning of the multiply charged ion accelerator at our Institute have laid a real material basis for the broadest development and cooperation in activities in the member nations, in this field of low energies. Henceforth, we intend to give increased priority to the development of activities in the low-energy field, since it is our understanding that this field of physics is especially interesting to the various countries in the practical sense. We have rendered material assistance to various countries in organizing laboratories, and those countries in turn have cooperated in many ways with our Institute.

The conferences held at the Joint Institute, with the participation of many scientists and engineers from the research centers of member nations, are of vital importance to the development of our collective efforts.

About thirty scientific conferences devoted to the outstanding trends in research have been held at Dubna since the founding of the Institute.

The Joint Institute also takes part in many conferences on nuclear physics organized in the member nations. The Institute's scientists participated in such conferences and gatherings in Poland, the German Democratic Republic, Rumania, Czechoslovakia, Hungary, and other cities in the Soviet Union, such as Moscow, Leningrad, Kiev, Kharkov, Uzhgorod, Erevan, and Sverdlovsk.

The number of countries benefiting from assignments of Dubna Joint Institute scientists has increased considerably. Many representatives of numerous countries around the world have visited the Institute. Exchange of scientific information has been facilitated and is today on a firm basis with many leading research centers throughout the world which are engaged in nuclear energy investigations.

The scientific achievements of the Joint Institute have enhanced the role and standing of the Institute in the eyes of the international scientific community. During the past two years, not a single significant international conference and not a single conference on high-energy physics or directly related branches of science took place without the participation of scientists from the Joint Institute for Nuclear Studies. Of particular importance was the participation of our scientists in the proceedings of the international conferences on high-energy physics held at Geneva in 1958, Kiev in 1959, Rochester in 1960, and the accelerator conference at CERN in 1959 and Berkeley in 1960. We venture to surmise that the scientific achievements made public by our Institute at those conferences were far from secondary. This, in brief outline, is the balance sheet of our international activities.

10. On the Development Plans of the Institute

In 1961, our Institute will enter upon the second five-year period of its existence, and we have before us, for our consideration, a plan covering our further development.

The principal concept of this plan is to continue on the basic course mapped out by our Institute, that of fundamental research in the field of the physics of elementary particles and of the atomic nucleus.

It is evident that to attempt to completely predict, in exact detail, the perspectives of development of an institution such as our Institute, whose activities are concentrated in the domain of the newest and most vigorously developing branch of physics, is naturally quite difficult, if not impossible. Life, as we are well aware, will introduce not a few correctives and addenda to our plans. However, it is certainly true to state that our further successes in the development of fundamental atomic physics will be governed by two factors: by increased precision and depth and scope in experimental work, and by boldness and profundity of theoretical thought.

We propose that our principal efforts in the field of the physics of elementary particles be directed to the study of a) the structure of those particles, concentrating on the structure of nucleons, b) on the laws governing particle production, and c) on the laws governing particle interactions.

In the microscopic universe, in the domain of quantum physics, all of the individual properties and peculiar features of the microscopic objects of research are studied through the prism of the statistical method. For that reason, whatever phenomenon we are studying, a rapid accumulation of a large number of events and the speedy processing of associated data are and will continue to be the most important prerequisites for success in our investigations. The first-ranking task of the coming years is, in this context, that of increasing the intensity of the beam of accelerated particles in our basic accelerator machines. It is perfectly clear to use that the total volume of statistical

material to be processed will, far from diminishing, increase to gigantic proportions. Therefore, the further development of automated processing of experimental data is our second-most task to be engineered.

In improving our accelerator machine and our methods for processing experimental data, we shall have created the material prerequisites for the discovery of new fundamental scientific facts, for the creation of an advanced physical theory of elementary particles and the atomic nucleus. We entertain no doubts about the fact that the further development of elementary particle physics will lead to a new and profound revolution in our knowledge of nature, and at the same time to a new increase in the power of man over the forces of the inanimate world.

In bringing this main report of the Board of Directors of the Institute to a close at this point, I hereby request the Committee of Authorized Representatives to undertake deliberations on the activities of the Institute and to approve our proposals for its further development.

THERMIONIC ENERGY TRANSFORMERS

B. A. Ushakov

Translated from Atomnaya Énergiya, Vol. 10, No. 4, pp. 343-346, April, 1960
Original article submitted December 19, 1960

The question of direct transformation of nuclear energy into electricity by thermionic methods is discussed. A comparison is made of the properties of various materials, containing fissionable matter, and at the same time having good thermoemissive properties. Results are given of transformation experiments in the active zone of a reactor. The experiments have shown that in the course of operation, a transformer filled with inert gas is converted into a cesium plasma diode. This eliminates the necessity of introducing cesium vapor into the transformer. In addition, it becomes possible to pump out the gases during operation, which prolongs the useful life and improves the thermionic properties of the transformer.

Introduction

One of the possible means for the direct transformation of thermal energy into electricity, the one based on the use of thermionic transformers, seems to be particularly promising if nuclear energy is used as the heat source. The thermionic transformer is essentially an ordinary diode, with a hot cathode and a cold anode [1]. The "hotter" electrons at the cathode-vacuum boundary overcome the potential barrier equal to the cathode work function, and move to the anode. After giving up to the anode a part of their energy equal to the anode work function, the electrons expend the rest of their energy as useful work in the external circuit.

In contrast with the diode, the transformer must have the electron space charge neutralized. One of the methods of neutralization is to introduce positive ions into the interelectrode space. It is important to work at high temperatures, since the efficiency of the transformer is markedly dependent on the temperature. With nuclear energy sources, it is possible to achieve high temperatures in the heat-producing elements, which are limited by the stability of the elements themselves.

At the present time, it seems possible to construct a transformer cathode and a reactor fuel element as a single unit, since a number of the materials containing fissionable nuclei have good thermionic emission properties.

Cathode Materials for Thermionic Transformers

The fuel element material, which is at the same time the cathode of the thermionic transformer, must be able to withstand high temperatures (about 2000°C), and it must have good thermoemissive properties, which are retained under intensive irradiation.

A number of materials have been studied, and reactor tests show that uranium and thorium carbides, as well as mixtures of uranium and zirconium carbides, are suitable for the purpose. In the combination thermionic-thermoelectric transformer [2], the heating element was made of uranium dioxide, with a titanium cladding. Uranium dioxide has a high melting point, but very low thermal conductivity, which produces a large internal temperature gradient. It is possible to get a heat flux of 100-150 watts/cm^2 through a 1 cm diameter uranium dioxide rod with a temperature drop above 700°C. Thus, with a temperature of 2400°C in the center of the rod, the surface temperature will only reach 1700°C. Therefore, it is preferable to use uranium and thorium carbides, and mixtures of uranium and zirconium carbides, which have high melting points, and better heat conductivity.

In experiments with a thermionic transformer having a ThC cathode and a nickel anode, in which cesium vapor was used to neutralize the electron space charge, good thermoemissive properties were exhibited by the ThC [3].

A useful electrical output of more than 15 watts/cm^2 was obtained at an efficiency of transformation greater than 15%.

Reference [4], which gives the results of the ThC studies, reports the following values for the thermoemission constants: φ = 3.2 v, A = 200 amp/cm^2 · deg^2.

Using these constants in Richardson's equation

$$I = AT^2 \exp\left(-\frac{\varphi}{KT}\right), \tag{1}$$

where φ is the work function in volts, T is the temperature in °K, and K = $8.61 \cdot 10^{-5}$ volts/deg (Boltzmann's constant), the saturation current may be found. The maximum output was found to be 16 watts/cm^2, at a transformation efficiency of 10-15%.

The thermoemissive properties of uranium carbide and the mixture of uranium and zirconium carbides have been described in [5]. However, the values of the thermoemission constants, obtained from this paper by substituting the experimental results in Eq. (1), were abnormally large.

In [6], an attempt was made to describe the data of [5] in terms of Eq. (1), using two sets of thermoemission constants corresponding with two temperature regions. The resulting values of the thermoemission constants are given in the table.

Values of Thermoemission Constants

Material	φ, v	A amp/cm^2 · deg^2	Temperature, °K	Reference
UC	4,57	$7{,}3 \cdot 10^5$	—	[5]
$(ZrC)_{0,8}$: $(UC)_{0,2}$	4,3	$6{,}6 \cdot 10^4$	—	[5]
UC	2,67	3,5	more than 1610	[6]
UC	3,62	90	more than 1590	[6]
$(ZrC)_{0,8}$: $(UC)_{0,2}$	2,53	0,3	more than 1650	[6]
$(ZrC)_{0,8}$: $(UC)_{0,2}$	3,53	55	more than 1610	[6]
UC	2,94	33	1200—2100	[7]
ThC	3,2	300	—	[4]

The authors of [7], who studied the thermoemissive properties of uranium carbide, found results differing from those of [5]. The experimental uranium carbide rods were made by covering a tungsten wire 5 mm in diameter with a nitrocellulose and ethyl ether solution containing 400 mesh UC powder. The constants φ and A from [7] are also given in the table.

The disagreement between the results obtained by different workers may be explained by a difference in vacua, or by a difference between the properties of solid and powdered UC.

Reactor Experiments

A serious problem in setting up the thermionic transformer is neutralizing the electron space charge. Reducing the effect of the space charge by using small interelectrode separation (~0.001 cm) involves great technical difficulties.

A promising method is to use the surface ionization of cesium vapor to form a low [8] or high [9, 10] pressure plasma in the interelectrode space. However, this method has some substantial drawbacks; namely: first, the necessity of getting the cesium into the transformer in the first place, second, the necessity of using a cathode material with an inherently high work function φ (about 4 v), so that the probability of surface ionization of the cesium atoms will be large enough. Further, the gaseous fission products of uranium (or thorium) raise the gas pressure in the interelectrode space, which interferes with the operation of the transformer. Pumping out causes a loss of expensive cesium. In [11], the proposal was made of using the uranium fission fragments in the cathode to produce an inert gas plasma in the interelectrode space. Every pair of fragments, which has a kinetic energy of about 150 Mev, forms ~10^6 ions. In this case, the gas may be pumped out at the rate at which it is produced by the transformer.

Some experiments have been made in the swimming pool reactor at the University of Michigan with a transformer filled with inert gas. The construction of the transformer, which was placed in the active zone of the reactor, is shown in the figure.

The UC discs were placed in a tantalum ring mounting. A tantalum screen was fixed in front of the surface of the disc facing the anode. The temperatures of the cathode and the aluminum anode, cooled by the water in the pool, were recorded with thermocouples. The temperature of the cathode, which depends on the reactor power level, went up to 2000°K (at reactor power level 1000 kw). The pressure of the inert gas could be changed during the course of the experiment.

The mechanical destruction of the cathode in one of the experiments, caused, probably, by the repeating heat loads, shows the necessity of producing high stability materials.

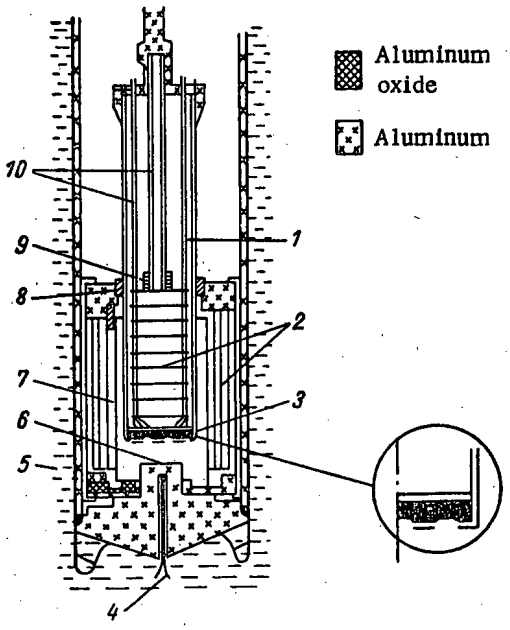

Inert gas plasma diode in reactor test chamber: 1) cathode thermocouple; 2) tantalum radiation shield; 3) uranium carbide cathode; 4) anode thermocouple; 5) water; 6) anode; 7) internal tantalum radiation shield; 8) insulator; 9) molybdenum; 10) aluminum oxide.

The 5 cm^2 UC disc, containing 7 gm U^{235} with a neutron flux density of $3 \cdot 10^{12}$ neutrons/$cm^2 \cdot$ sec at the surface of the sample, produced a heat output of about 400 watts. The short-circuit current was 0.02 amp at a minimum internal resistance of the diode equal to 30 ohms. The open circuit potential was 1.1 v. The indicated value of resistance leads to a very low level of ionization in the gas, of the order of 10^{-8}. However the mobility of the electrons in the inert gas is large enough to ensure a current of about 10^{-2} amp.

The values of the emission current from the cathode, found in [12], do not agree with the data given in [5]. This is a result of the fact that there was a certain amount of uranium oxide on the UC surface, formed during the fabrication of the transformer, and this reduces the emission considerably.

Conversion of an Inert Gas Diode into a Cesium Plasma Diode

About 5% of all the atoms that are formed in the fission of U^{235} are cesium atoms. At a cathode temperature of ~2000°C, it is reasonable to assume that all the cesium atoms evaporate from the surface of the cathode. The presence of cesium was also detected in the experiments described above. Thus, in working with a sealed diode, the cathode of which contains fissionable material, the pressure of cesium vapor in the interelectrode space is going to increase.

Calculations show that with a fission heat output of 80 watts per cm^2, a cathode area of 8 cm^2, and a system volume of 400 cm^3, the cesium vapor pressure reaches ~10^{-3} mm Hg after an hour's operation. A pressure like this has already been found associated with diodes working at low cesium-vapor pressure [8]. Therefore one can expect that a transformer filled with inert gas, as well as one working in vacuum, will in time start working as a cesium transformer. It is necessary though, for the density of cesium ions to be greater than the density of the inert gas ions. The cesium cannot condense on the cold parts of the transformer, and it must not react with other fission fragments to form substances, the atoms of which are not ionizable on the cathode surface.

SUMMARY

At the present time, experimental thermionic transformers have reached an efficiency of about 15% [3]. The efficiency of transformation may be raised to 20-25% by using optimum dimensions and operating temperatures for the transformer. The temperature of the anode can be high enough (about 1000°C) so that heat may be removed from it by a coolant, and then used in an ordinary steam turbine cycle, at an efficiency of about 30%.

Thus, in the combination reactor-transformer system, part of the thermal energy is directly converted into electricity, and the rest is transferred to a coolant and then converted to electricity in the usual steam turbine cycle. This makes it possible to increase the efficiency of such a system of 40-45% and, consequently, to reduce the specific capital costs of the electrical installation.

LITERATURE CITED

1. L. N. Dobretsov, Zh. tekhn. fiz. 30, No. 4, 365 (1960).
2. Nucleonics 18, No. 8, 84 (1960).
3. R. Fox and W. Gust, Bull. Amer. Phys. Soc. 4, 322 (1959).
4. N. D. Morgulis and Yu. P. Korchevoi, Atomnaya énergiya 9, No. 1, 49 (1960).°
5. R. Pidd et al., J. Appl. Phys. 30, No. 11,1575 (1959).

° Original Russian pagination. See C. B. translation.

6. G. Kuczynski, J. Appl. Phys. 31, No. 7, 1500 (1960).
7. G. Haas and J. Jensen, J. Appl. Phys. 31, No. 7, 1231 (1960).
8. G. Hatsopoulos, MIT Ph. D. Thesis, 1956.
9. K. Hernquvist, M. Kanefsky, and R. Norman, RCA Review 19, 244 (1958).
10. G. Grover et al., J. Appl. Phys. 29, 1611 (1958).
11. F. Jablonski, J. Appl. Phys. 30, 2017 (1959).
12. F. Jamerson, IRE International Convention Record, Part 9, 1960, p. 66.

All abbreviations of periodicals in the above bibliography are letter-by-letter transliterations of the abbreviations as given in the original Russian journal. *Some or all of this periodical literature may well be available in English translation.* A complete list of the cover-to-cover English translations appears at the back of this issue.

THE EFFECT OF NEUTRON IRRADIATION ON THE INTERNAL FRICTION OF ZINC MONOCRYSTALS AND POLYCRYSTALS

N. F. Pravdyuk, Yu. I. Pokrovskii, and V. I. Vikhrov

Translated from Atomnaya Énergiya, Vol. 10, No. 4, pp. 347-352, April, 1961
Original article submitted November 14, 1960

By an investigation of the effect of neutron irradiation on the internal friction of zinc polycrystals and monocrystals, we determined the value of the critical stress amplitude σ_{cr} before and after irradiation.

It was shown that the value of σ_{cr}, which may be related to the beginning of the motion of dislocations, increases as a result of irradiation. The increase of σ_{cr} in irradiated zinc is explained by the fact that the dislocations are held fixed as a result of interaction with point defects.

In addition, we studied the effects of the orientation of the basal plane (0001) with respect to the longitudinal axis of the zinc monocrystal specimen on internal friction and on σ_{cr}. The results of the investigations of the effect of orientation on internal friction and on σ_{cr} are compared with well-known representations of slippage obtained from static studies of monocrystals in tension along one axis.

Introduction

In report [1] information was published on the studies of internal friction and critical amplitude of the maximum stress σ_{cr}* before and after neutron irradiation of several metals, as well as on the effect of the orientation of the basal plane (0001) with respect to the longitudinal axis of the zinc monocrystal specimen on internal fraction and on σ_{cr}.

The present article reports the further results obtained after the irradiation of some of the zinc monocrystals studied in [1], as well as after the irradiation of polycrystalline zinc. In addition, the results of the investigations of the effect of orientation on internal friction σ_{cr} are compared with well-known representations of slippage obtained from static single-axis tests of monocrystals in tension.

The equipment and method of investigation are described in [1].

Results of the Investigations

The specimens used were zinc polycrystals and monocrystals with different orientations of the basal plane (0001), forming angles of 15, 40, 66, 76, 86, and 88° with the direction of the longitudinal axis. The monocrystal specimens with orientation angles of 15, 40, 76, and 86° were subjected to irradiation.

The measurements of internal friction were carried out with transverse vibrations with a frequency of ~300 cycles before and after irradiation in integrated neutron fluxes of $3 \cdot 10^{18}$ and $1.5 \cdot 10^{19}$ (thermal) neutrons/cm^2.** We studied the effect of irradiation on the change in internal friction of the polycrystalline and monocrystalline zinc as a function of the amplitude of the maximum stress (in the boundary fibers, where the specimen was gripped by the bracket); the amplitude of the maximum stress was calculated from the amplitude of the vibrations.

The results of the investigations carried out on zinc monocrystals with various orientations are shown in Figs. 1, 2, and 3.

Figures 4 and 5 contain the curves showing the change in $1/Q_M^{***}$ and σ_{cr} as functions of the orientation angle θ before and after irradiation; in the construction of these curves the values of $1/Q_M$ and σ_{cr} of Figs. 1, 2, and 3 were used; for greater clarity the values of σ_{cr} are shown again in the table.

*σ_{cr} is the value of the maximum stress amplitude, at which the internal friction begins to depend on stress amplitude.
** The ratio of the number of fast neutrons with energies > 1 Mev to the number of thermal neutrons is 1:10.
*** $1/Q_M$ is the minimum value of $1/Q$ measured for $\sigma < \sigma_{cr}$ and does not depend on the stress amplitude.

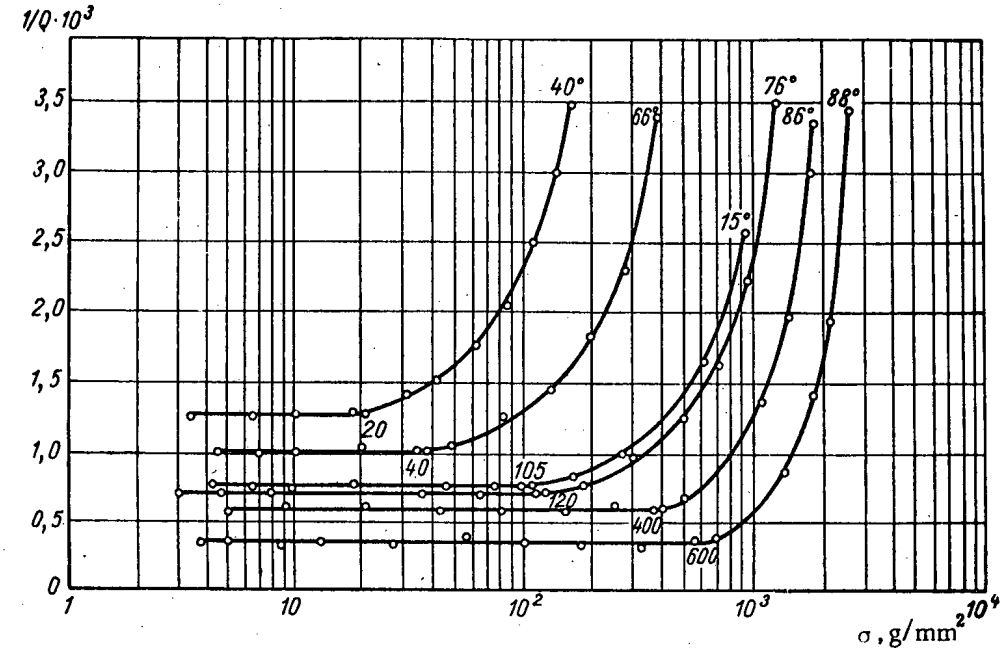

Fig. 1. Change in internal friction as a function of stress amplitude for unirradiated zinc monocrystals with angles θ = 15, 40, 66, 76, 86, and 88°, formed by the direction of the longitudinal axis of the specimen with the basal plane (0001). The values of σ_{cr} are shown on the curves.

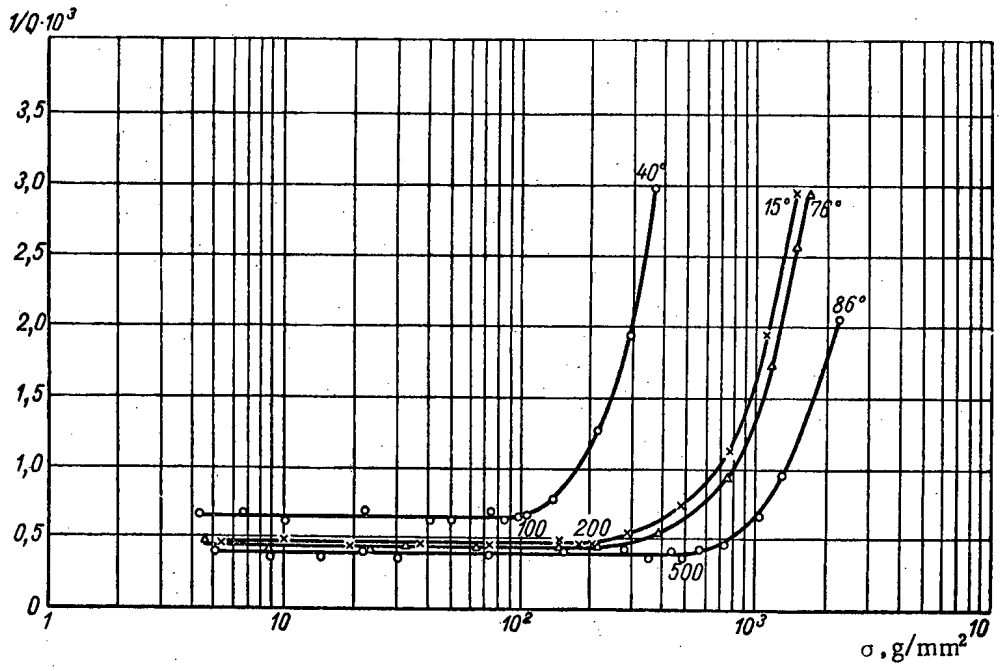

Fig. 2. Change in internal friction as a function of stress amplitude for zinc monocrystals irradiated in a flux of $3 \cdot 10^{18}$ neutrons/cm^2 and having angles of 15, 40, 76, and 86° formed by the direction of the longitudinal axis of the specimen with the basal plane (0001). The values of σ_{cr} are shown on the curves.

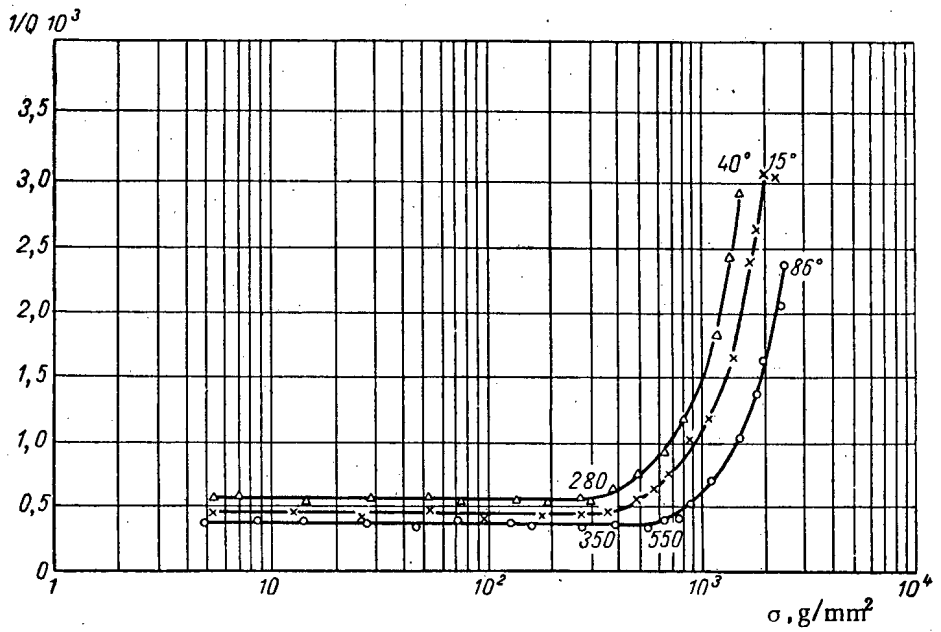

Fig. 3. Change in internal friction as a function of stress amplitude for zinc monocrystals repeatedly irradiated up to a flux of $1.5 \cdot 10^{19}$ neutrons/cm^2 and having angles of θ = 15, 40, and 86° formed by the direction of the longitudinal axis of the specimen with the basal plane (0001). The values of σ_{cr} are shown on the curves.

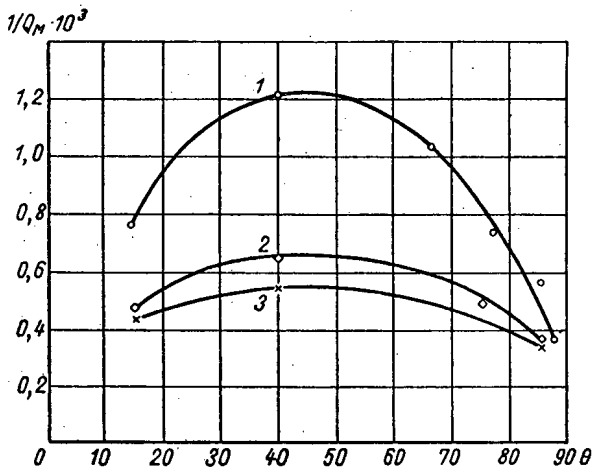

Fig. 4. Change in minimum internal fraction of zone monocrystals as a function of the angle θ formed by the direction of the longitudinal axis of the specimen with the basal plane (0001) before and after irradiation: 1) before irradiation; 2) after irradiation in a flux of $3 \cdot 10^{18}$ neutrons/cm^2; 3) after repeated irradiation up to a flux of $1.5 \cdot 10^{19}$ neutrons/cm^2.

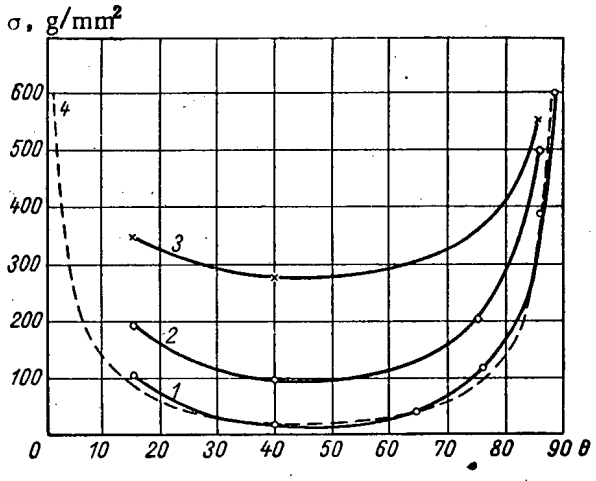

Fig. 5. Change in σ_{cr} of zinc monocrystals of the angle θ formed by the direction of the longitudinal axis of the specimen with the basal plane (0001) before and after irradiation: 1) before irradiation; 2) after irradiation in a flux of $3 \cdot 10^{18}$ neutrons/cm^2; 3) after repeated irradiation up to a flux of $1.5 \cdot 10^{19}$ neutrons/cm^2; 4) calculated curve of σ_{cr} as a function of θ before irradiation.

Examining the values of σ_{cr} shown in the table for all angles θ, we see that after irradiation they increased by comparison with the values of σ_{cr} obtained before irradiation; the values of σ_{cr} before and after irradiation were found to be minimum for an angle equal to 40°.

Such a minimum value of σ_{cr}, which is the normal stress acting in a plane perpendicular to the axis of the specimen and is associated with a crystal orientation angle of ~45°, may be represented as corresponding to the maximum shearing stress acting in the basal plane (0001). This is in good agreement with the known representations of the deformation of zinc monocrystals in tension. It is known that single-axis tension by a force P in a cylindrical crystal with a cross section of A results in a tangential stress in the slip element (Fig. 6); this stress is defined by the expression

$$\tau = \frac{P}{A} \cos\varphi \sin\theta.$$

If we designate $P/A = \sigma_{cr}$ as the yield point, then the expression for the critical shearing stress will have the form

$$\tau_{cr} = \sigma_{cr} \cos\varphi \sin\theta. \qquad (1)$$

In the explanation of the results of the investigations of the internal friction of zinc monocrystals the basal plane (0001) was taken as the slip element. The monocrystal specimen under study was placed so that $\varphi = \theta$. Then the expression for the value of σ_{cr} takes the form

$$\sigma_{cr} = \frac{2\tau_{cr}}{\sin 2\theta}. \qquad (2)$$

A quantitative estimate for τ_{cr} of the zinc monocrystals, made according to formula (2) using the experiment values of σ_{cr} (see Fig. 1), showed that on the average τ_{cr} is equal to 20 g/mm². If we substitute this average of τ_{cr} into formula (2), the variation of σ with θ may be represented in the form of curve 4 (see Fig. 5). Such a curve is found to be in good agreement with experimental curve 1, shown in the same figure.

Thus we see that the value of σ for the monocrystals which we studied can indeed be related to the beginning of the motion of dislocations along the basal plane (0001).

In order to find the relation between the σ_{cr} of the monocrystal and the σ_{cr} of the polycrystal, we took the variation of 1/Q with σ for polycrystalline zinc (Fig. 7, curve 1).

On examination of the value of σ_{cr} for the zinc polycrystal we see that this value, equal to 26 g/mm², is very close to the value of σ_{cr} for the zinc monocrystal with a basal plane (0001) orientation angle of 40°, which was equal to 20 g/mm².

Change in σ_{cr} for Zinc Monocrystal as a Function of the Angle θ Before and After Irradiation

	Degrees					
	15°	40°	66°	76°	86°	88°
σ_{cr} before irradiation	105	20	40	120	400	600
σ_{cr} after irradiation in a flux of $3 \cdot 10^{18}$ neutrons/cm²	200	100	—	200	500	—
σ_{cr} after irradiation in a flux of $1{,}5 \cdot 10^{19}$ neutrons/cm²	350	280	—	—	550	—

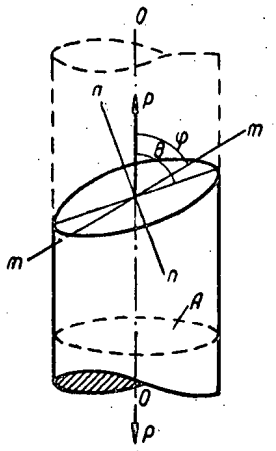

Fig. 6. Arrangement of the slip element and the direction of the tensile force: θ) angle formed by the line of action of the force and the slip plane; φ) angle formed by the direction mm of possible displacement in the slip plane with the axis of the specimen; nn – normal to the slip plane.

Hence we made the assumption that the individual grains of the zinc polycrystal behave approximately as do the monocrystals with an orientation angle most favorable for slipping. Consequently, the value of σ_{cr} of the polycrystal may also be related to the beginning of plastic flow in the crystallographically most favorably oriented grains; that is, with the motion of dislocation in the field of cyclic stress along the slip plane of these grains.

The results of the investigations of the effect of irradiation on the change in 1/Q of polycrystalline zinc as a function of σ are shown in the form of curves 1 and 2 in Fig. 7. Examining these curves, we see that the value of σ_{cr} before irradiation was equal to 26 g/mm² and increased after irradiation to 45 g/mm². As was shown by the results of [1] on other polycrystals (of copper, aluminum and magnesium), the value of σ_{cr} after irradiation can reach a considerably higher value when the integrated flux is increased. The observed increase in σ_{cr} of mono- and

polycrystalline zinc after irradiation may mean that the motion of dislocations is made more difficult as a result of the interaction of these with point defects caused by the irradiation.

To check the reversibility of the process which causes the internal friction, experiments were set up for the measurement of 1/Q of unirradiated specimens of mono- and polycrystals of zinc with an increase and decrease of the amplitude of the vibrations as σ increased beyond σ_{cr} to values equal to 500 g/mm^2 for polycrystals and 200 g/mm^2 for monocrystals with an orientation angle of 40°. The curves obtained from the experiments in the forward and reverse directions coincided. Such a reproducability of the 1/Q measurements indicates reversibility of the process causing internal friction for low stress amplitudes.

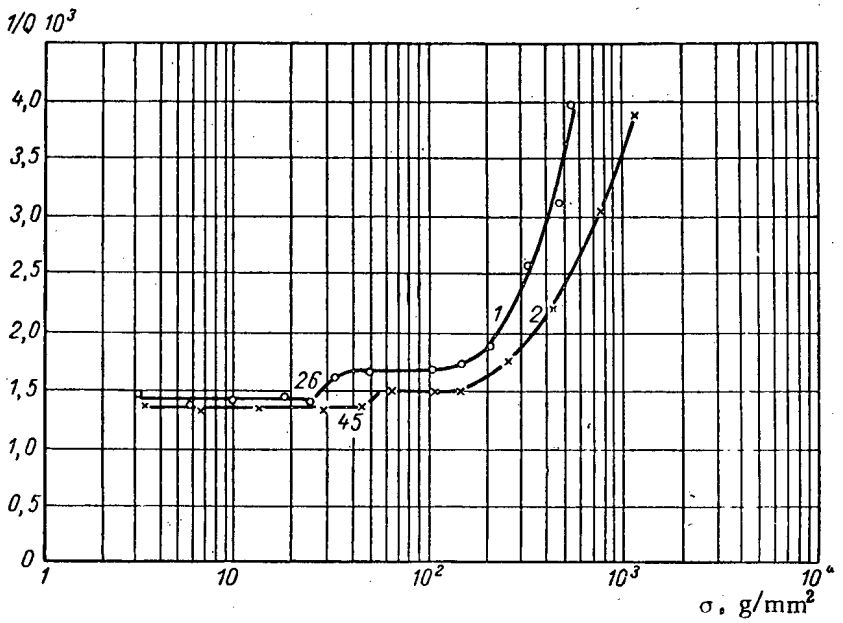

Fig. 7. Change in internal friction of polycrystalline zinc as a function of the stress amplitude before and after irradiation: 1) before irradiation; 2) after irradiation in a flux of $3 \cdot 10^{18}$ neutrons/cm^2. The values of σ_{cr} are shown on the curves.

At the same time we investigated the reproducibility of the measurements of 1/Q and the proper frequency of vibrations f of the specimen after tests with a large number of cycles of vibrations with amplitudes causing a stress greater than 500 g/mm^2 for polycrystals and greater than 200 g/mm^2 for monocrystals. The polycrystalline specimens were tested for stress amplitudes of 1000, 2000, and 3000 g/mm^2. The monocrystalline specimens with an orientation angle of 40° were tested for stress amplitudes of 200, 400 and 600 g/mm^2. The measurements of 1/Q before and after these tests were carried out for a wide range of stress values. The results of the tests of the polycrystalline specimens showed that if the stresses are equal to 1000 and 2000 g/mm^2, then the results are repeatable after $2 \cdot 10^6$ cycles of vibration. If the stress is equal to 3000 g/mm^2, then the results are no longer reproducible after 10^6 cycles of vibration. However, if the specimen vibrated at σ equal to 5000 g/mm^2, then changes were observed after 10^5 cycles, and the interval where the internal friction did not depend on amplitude was sharply reduced in the direction of low stress amplitudes (σ_{cr} decreased). The value of internal friction increased sharply (by a factor of three), and the value of the frequency dropped sharply. Shortly after this the specimen broke.

The results of the tests on monocrystalline specimens with basal plane orientation angle of 40° showed that if the stress are equal to 200 and 400 g/mm^2, then the results of the measurements are repeatable after $2 \cdot 10^6$ cycles of vibration. If the stress is equal to 600 g/mm^2, then the results are no longer reproducible, and the internal friction value increases sharply.

Thus, examining the results of these experiments, the curve of 1/Q as a function of σ (for mono- and polycrystalline zinc may be represented as consisting of 3 sections. The first section for the values $\sigma \leq \sigma_{cr}$ and the second section for the values $\sigma > \sigma_{cr}$ are sections with reproducible internal friction, and the third section for $\sigma \gg \sigma_{cr}$ has nonreproducible internal friction.

The higher internal friction of the second section, $\sigma > \sigma_{cr}$, was related to the motion of dislocations along the slip plane or to the beginning of plastic displacements. Since the internal friction value appeared reproducible, it is natural to assume that these displacements are reversible in nature.

The value of the σ_{cr} and the internal friction of the first section, as well as the internal friction of the second section of the curve, can be explained in more detail with the aid of a process suggested by Frank and Reed. This process consists essentially in the fact that the motion of a line of simple dislocation may give rise to an unlimited number of dislocations. This takes place on the application of the stress σ to the line of simple dislocation. For $\sigma < \sigma_{cr}$ in the first section, the line of dislocation only bends, and it is only when σ_{cr} is reached that the dislocations begin to spread, causing the formation of new dislocation loops and bringing about in the second section the increase in internal friction as the stress amplitude increases.

The third section $\sigma >> \sigma_{cr}$ with nonreproducible internal friction may be related to fatigue processes. This section requires more careful investigations. Such investigations are being carried on at the present time, and their results will be published.

The authors express their gratitude to S. T. Konobeevskii for his comments on the results of the work.

LITERATURE CITED

1. N. F. Pravdyuk et al., Proceedings of the Second International Conference on the Peaceful Uses of Atomic Energy (Geneva, 1958). Report of Soviet Scientists, Vol. 3, Moscow, Atomizdat, 1959, p. 610.

All abbreviations of periodicals in the above bibliography are letter-by-letter transliterations of the abbreviations as given in the original Russian journal. *Some or all of this periodical literature may well be available in English translation.* A complete list of the cover-to-cover English translations appears at the back of this issue.

THE USE OF ION-EXCHANGE MEMBRANES IN THE HYDROMETALLURGY OF URANIUM

B. N. Laskorin and N. M. Smirnova

Translated from Atomnaya Énergiya, Vol. 10, No. 4, pp. 353-361, April, 1961
Original article submitted October 29, 1960

Electrodialysis with ion-exchange membranes is important in chemistry, chemical technology and hydrometallurgy as a basic operation which eliminates the usual chemical neutralization and makes it possible to remove excess acidity and alkalinity, to separate mixtures of elements whose properties are similar and to extract radioactive products from waste waters.

This paper considers the possibilities of using the method of electrodialysis in the hydrometallurgy of uranium. It is shown that this method can remove excess acidity from sulfate, nitrate and chloride solutions. The method of electrodialysis is also used to remove ions from carbonate uranium solutions.

In connection with the further development of nuclear energy, the reduction in cost of uranium is increasingly important. One of the ways for reducing the cost of the finished production is to reduce the consumption of reagents during the hydrometallurgical treatment of uranium ores.

The systems used at the present time usually include neutralization. In the neutralization of solutions the acid and soda are lost and cannot be recovered; the salt composition of the solutions increases and hinders further treatment.

The recently developed sorption and extraction processes have considerably simplified the hydrometallurgical treatment of uranium ores. However, in these processes a large quantity of acids and alkalis is used.

We neutralized acid or soda uranium solutions by the method of electrodialysis using ion-exchange membranes. Furthermore, the method of electrodialysis with ion-exchange membranes was used for the electrochemical reduction of hexavalent uranium to tetravalent uranium from rich chloride solutions containing up to 300 g/liter uranium.

Ion-exchange membranes are new ion-exchange materials whose use in electrodialysis is based on their capacity to change the transfer number of ions. Thus, anion-exchange membranes are mainly permeable to anions and almost impermeable to cations; i.e., the transfer number of anions in the membrane approaches unity. Similarly, cation-exchange membranes are mainly permeable to cations [1-3].

In this work we used specimens of ion-exchange membranes prepared by the authors and also membranes prepared in the Scientific Research Institute for Plastics of the State Committee for Chemistry and in the D. I. Mendeleev Moscow Chemical and Technological Institute. In addition we studied foreign specimens of membranes: amberplex C-1 and A-1, permaplex C-10 and A-10 and nepton CR-51, CR-61 and AR-111.

The literature describes certain possibilities for using ion-exchange membranes in the hydrometallurgy of uranium. In 1955, papers were published [4, 5] on the electrochemical precipitation of uranium from acid desorption solutions in a two-chamber electrodialyzer with an anion- or cation-exchange membrane. A similar process was later patented [6]. A method was described for the electrochemical extraction of uranium and vanadium from carbonate solutions using ion-exchange membranes [7]. In this case, into the cathode part of the two-chamber electrodialyzer with an amberplex C-1 membrane was poured a carbonate solution containing 1.5 g/liter uranium and 9 g/liter vanadium. As a result of electrodialysis in the cathode part the uranium was precipitated, the completeness of which reached 92%. From 5 to 19% vanadium was coprecipitated with the uranium.

A method has been suggested [8] for the electrochemical precipitation of uranium from carbonate solutions in the cathode part of a two-chamber instrument, the chambers of which are separated by cation- or anion-exchange membranes; in the cathode part the uranium was reduced to the tetravalent state and precipitated in the form of the oxide.

At the Second International Conference on the Peaceful Uses of Atomic Energy at Geneva, three reports were presented dealing with the use of ion-exchange membranes in the Atomic Energy Industry. The use of cation-exchange membranes was described for the electrochemical reduction of hexavalent uranium to tetravalent uranium from chloride and chloride-fluoride solutions [9, 10].

The so-called flurex process has been suggested – the wet method for obtaining fluoride salts of uranium from aqueous solutions of uranyl nitrate. In the electrolyzer separated by anion- and cation-exchange membranes into three chambers, two processes occur simultaneously: the separation of uranyl and nitrate ions and the reduction of the uranyl ions at a mercury cathode to the tetravalent state [11].

All the above-mentioned work did not extend beyond laboratory tests. At the same time and independent of this work, over the course of a number of years, we have worked on the use of electrodialysis in widely differing regions of the uranium industry.

I. The Use of Ion-Exchange Membranes to Remove Excess Acidity from Uranium Solutions

We used electrodialysis with ion-exchange membranes to remove excess acidity from sulfate, nitrate and chloride uranium solutions. The investigations were carried out in sectional electrodialyzers made from plexiglas. We used two-, three- and twenty-chamber electrodialyzers with chamber volumes of 30-1500 ml. The electrode materials were platinum, tantalum, graphite, lead and stainless steel. The contents of the cells were mixed mechanically or by blowing air.

Removal of Excess Acidity in Two-Chamber Electrodialyzers

Sulfate solutions. The electrodialysis of sulfate solutions containing different amounts of uranium was carried out in two-chamber apparatuses using anion-exchange membranes. The electrodialysis of sulfate uranium solutions was more complex than the process carried out with nitrate or chloride solutions, since in a sulfate medium, in addition to the uranyl ion, there exist anion complexes of hexavalent uranium $[UO_2(SO_4)_2]^{2-}$ and $[UO_2(SO_4)_3]^{4-}$ and complexes of tetravalent uranium $[U(SO_4)_3]^{2-}$ and $[U(SO_4)_4]^{4-}$. Therefore in the electrodialysis of sulfate solutions using anion-exchange membranes, transfer of uranium to the anode part can be expected; i.e., to the returned acid.

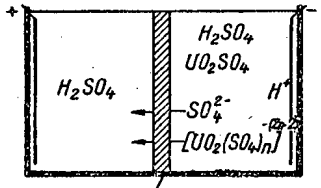

Anion-exchange membrane

Fig. 1. Electrodialysis of sulfate uranium solutions with an anion-exchange membrane.

As can be seen from Fig. 1, under the action of the current the sulfate ions transfer from the catholyte to the anolyte. At the anode water is decomposed according to the reaction $H_2O - 2\bar{e} \rightarrow \frac{1}{2}O_2 + 2H^+$; gaseous oxygen is liberated and the hydrogen ions remain in solution and form sulfuric acid with the sulfate ions. At the same time there is possible transfer of complex anions of hexa- and tetravalent uranium. During the removal of excess acidity from sulfate uranium solutions in the cathode part the hexavalent uranium is reduced to tetravalent uranium: $UO_2^{2+} + 4H^+ + 2\bar{e} \rightarrow U^{4+} + 2H_2O$.

The anion-exchange membrane protects the cathode part from oxidative conditions of the anode chamber, which also favors the reduction of uranium.

The kinetics of sulfate-ion transfer to the anolyte and the kinetics of reduction of uranium were studied in a two-chamber electrodialyzer with a chamber volume of 400 ml each. Into the cathode part of the instrument were poured solutions containing different amounts of uranium and the same amount of excess sulfuric acid – 1 g-eq/liter. A 0.1 N solution of sulfuric acid was poured into the anode part in all experiments; the current density was 40 ma/cm^2, the voltage was 5-6 v. After given intervals of time, samples were taken from the anolyte and catholyte to determine the concentrations of sulfate ions, the concentrations of tetravalent uranium and the total amount of uranium in the anolyte and catholyte. Figures 2 and 3 show the results for the determinations of sulfate-ion transfer to the anolyte and data on the kinetics of reduction of hexavalent uranium to tetravalent uranium. It can be seen from the figures that after 20 min in the catholyte the hexavalent uranium was completely reduced to tetravalent uranium. A change in acidity was observed in the anolyte and catholyte. When the excess acidity in the catholyte was reduced to 0.2-0.3 N the solution became turbid, and then on reduction of the pH to 4-5 the precipitate coagulated in the form of large dark green flakes. Some specimens of precipitates were subjected to x-ray analysis by the Debye powder method as a result of which it was found that a strongly hydrated uranium dioxide is precipitated in the cathode part.

To study the possibility of the partial separation of uranium from iron in the process of electrodialysis a series of experiments was conducted with pure solutions containing uranium, iron and sulfuric acid. The process was carried out until uranium was precipitated in the cathode part (pH = 3 – 3.6). The precipitate was collected and roasted until the mixed oxide was formed and the content of uranium and iron was determined in this material. During the electrodialysis the cathode was covered with metallic iron. This method could give a coefficient of purification of uranium from iron of about 1000.

Nitrate solutions. Electrodialysis of pure uranium solutions. The removal of excess nitric acid was studied with the example of solutions containing about 80 g/liter of uranium with varying excess acidity. The studies were carried out in a two-chamber electrodialyzer with an anion-exchange membrane. Acid uranium solutions were poured into the cathode part and a 0.05 N solution of nitric acid was poured into the anode part. The excess acidity was removed until a weakly acid solution was obtained in the catholyte with pH = 3 – 3.5. These solutions can be used for sorption purification on carboxyl resins without further treatment.

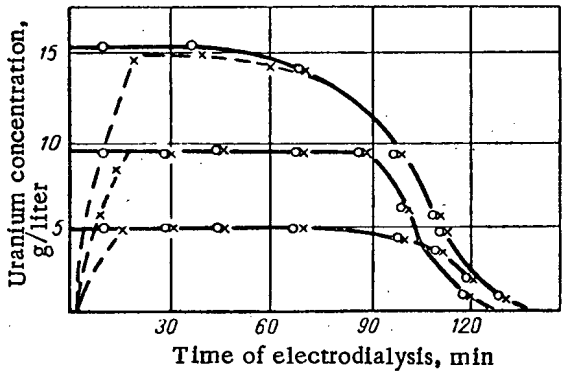

Fig. 2. Reduction of uranium in the catholyte during the electrodialysis of sulfate solutions: $-\circ--U^{6+}$ and U^{4+}; $-x--U^{4+}$.

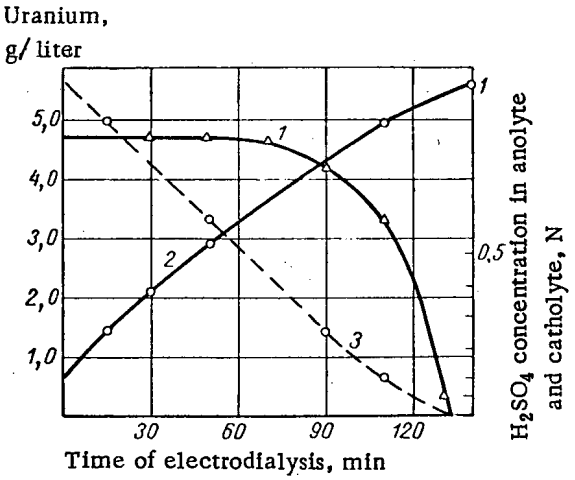

Fig. 3. Change in acidity in the anolyte and catholyte during electrodialysis: 1) uranium concentration in catholyte, g/liter; 2) H_2SO_4 concentration in anolyte, N; 3) H_2SO_4 concentration in catholyte, N.

In order to concentrate the nitric acid into as small a volume as possible during the process the anolyte was not renewed. Naturally in this process it was not possible to obtain high current efficiencies, since with increase in concentration of the acid in the anolyte there was a considerable reduction in the current efficiency due to the back diffusion of hydrogen ions through the anion-exchange membrane into the catholyte.

Almost all of the excess acidity could be removed from rich uranium solutions containing 80 g/liter of uranium and 25.6-63 g/liter of free nitric acid.

A very small amount of uranium was transferred into the returned acid. In some experiments when the conditions were not optimal there was maximum transfer of uranium into the anolyte. The concentration of uranium in the anolyte did not exceed 0.29 g/liter. The concentration of acid in the anode part was almost equal to the initial concentration, the obtained acid could be used repeatedly. The mean consumption of energy to obtain 1 kg of nitric acid in the anolyte was less than 10 kw-hr.

Therefore, the removal of excess nitric acid from concentrated uranium solutions can be successfully carried out without consuming reagents and increasing the salt composition of the solutions, which is particularly important in radiochemical production.

The Use of a Multichamber Electrodialyzer for Removing Excess Acidity

The consumption of electric energy on the recovery of acids can be considerably reduced if multichamber electrodialyzers are used having considerable design and operational advantages over the two- and three-chamber dialyzers. Two electrodes in this instrument serve a number of chambers, which sharply reduces the consumption of electrode materials and considerably simplifies and cheapens the whole system of current feed [1]. At the present time, for removing salt from various waters, multichamber electrodialyzers are used consisting of tens and even hundreds of chambers formed by alternating anion-exchange and cation-exchange membranes (Fig. 4).

As can be seen from Fig. 4, under the action of an applied voltage the cations and anions from chambers 1, 2, 3... migrate through the ion-exchange membranes into chambers 1', 2', 3'.... Consequently the solutions in some chambers will be purified and in the others they will be enriched with ions. A parallel flow of solutions to the chambers is most often used, but it can also be in series. The electrode chambers are usually washed separately, since acid or alkali and other electrode reaction products form in them.

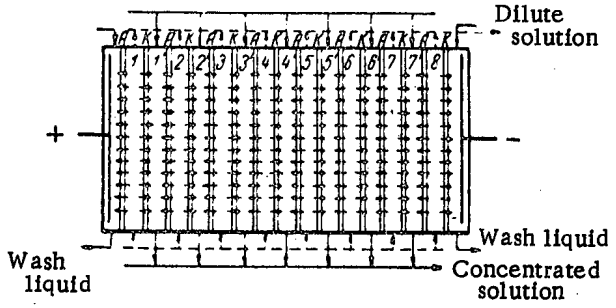

Fig. 4. Multichamber electrodialyzer used for salt removal (with parallel connection of the flow).

The consumption of energy during the electrodialysis depends on the concentration of the initial and obtained solutions. Without allowing for diffusion and electroosmosis the following simplified equation can be obtained for the energy consumption W [12]:

$$W = \frac{E(C^0 - C^1)}{37{,}4n\eta} \text{ kw-hr/liter of purified liquid.} \quad (1)$$

As can be seen from Eq. (1) with an arbitrarily selected value of $(C^0 - C^1)$ the energy consumption is directly proportional to the voltage E, inversely proportional to the number of chambers in the instrument and the current efficiency η. Equation (1) is convenient for a rough calculation of productivity of a multichamber electrodialyzer.

A multichamber electrodialyzer can be used to remove excess acidity from solutions containing acid and salt only if the cation-exchange membrane is permeable to hydrogen ions and impermeable to all other cations and the anion-exchange membrane is, thus, permeable only to anions of the recovered acid and impermeable to complex anions. The first condition can be satisfied if carboxyl membranes are used which are mainly permeable to hydrogen ions in acid media. This is due to the fact that in acid solutions there is only the hydrogen form of the carboxyl group. The transfer of all other ions can be accomplished only through a solution located in the pores between the active groups of the membrane.

We studied the regularities in transfer of certain ions through a carboxyl membrane in acid solutions with different molar ratios of acid and salt. Thus, the ratio of transfer of hydrogen and lithium ions $C^{H^+}_{fin}/C^{Li^+}_{fin} : C^{H^+}_{init}/C^{Li^+}_{init}$ for a carboxyl membrane with a ratio of $C^{H^+}_{init}/C^{Li^+}_{init}$ equal to 1-5 hardly changes and is 16.8 with a membrane thickness of 0.05 mm and 50 with a membrane thickness of 0.5 mm.

The excess acidity was removed from chloride and nitrate solutions in which, at acid concentrations that were not too high, there were no negatively charged complex anions. The studies were carried out on a twenty-chamber electrodialyzer with parallel distribution of the solutions in the separate chambers. Two insulated systems were used to deliver, distribute and take off the original acid and weakly acid solutions. The two-electrode chambers were washed separately.

The alternating membranes, anion-exchange (amberplex A-1) and cation-exchange, were prepared from polyvinyl alcohol and polymethacrylic acid, formed in the space between the anode and the cathode of the ten concentrated and ten purified chambers.

The electrodialyzer was tested on pure solutions containing 5-6 g/liter of uranium and 1 g-eq/liter of hydrochloric or nitric acid. The specific consumption of electric energy in the removal of excess acidity, as in the salt removal, for a given distance between the membranes and a given area of working cross section of the bath, is determined by the difference in concentrations of ions in the neighboring chambers. The higher the initial acidity, the greater the energy needed to remove excess acidity to a given level. The process is therefore best carried out in series; the number of stages should be greater the higher the initial acidity and the lower the final acidity. The removal of excess acidity from 1 to 0.1 g-eq/liter was carried out in three stages. The flow rate was selected on the basis of a decrease in concentration of the initial solution by 0.3 N at each stage. The arrangement of a three-cascade apparatus used to remove excess acidity is shown in Fig. 5.

According to our data, in a membrane of amberplex A-1 the transfer number of the chloride ion in 1.0 N solution of hydrochloric acid is 0.39. The transfer number of the chloride ion in a carboxyl membrane is ~0.02.

For 1 N chloride solutions the current efficiency is

$$\eta_1 = \eta_{\text{I}}^{\text{Cl}^-} - \eta_{\text{II}}^{\text{Cl}^-} = 0{,}39 - 0{,}02 = 0{,}37.$$

Similarly to the second cascade, where 0.7 N solution arrives, the current efficiency is η_2 = 0.42-0.02 = 0.40. For a 0.4 N solution in the third cascade η_3 = 0.46-0.02 = 0.44. The mean current efficiency for the three cascades is

$$\eta = \frac{0{,}44 + 0{,}40 + 0{,}37}{3} = 0{,}40.$$

The flow rate v can be calculated from the formula

$$v = \frac{\eta I n \cdot 0{,}0374}{\Delta C} \text{ liter/hr} \qquad (2)$$

where η is the current efficiency; I the current intensity; n the number of unit electrolytic cells (in this case 10); ΔC is the difference in concentrations of the incoming and outgoing initial solutions (g-eq/liter).

Using formula (2) we find the flow rate

$$v = \frac{0{,}37 \cdot 0{,}5 \cdot 10 \cdot 0{,}0374}{0{,}3} = 0{,}230 \text{liter/hr}$$

(in the calculation we take the minimum current efficiency as being 0.37). The transfer of water from the initial solution to the concentrating chamber during electrodialysis is rather high; therefore, the flow rate at the exit from the concentrating chambers is somewhat higher than at the inlet and the concentration is correspondingly lower. The energy consumption calculated from Eq. (1) per 1 liter of purified liquid in all three cascades was 0.0435 kw-hr. The experimentally found energy consumption was 0.0486 kw-hr per liter of 1 N hydrochloric acid. The transfer of iron and aluminum into the recovered acid does not exceed 0.2% of their initial amount. The concentration of uranium in the obtained acid varied from 5 to 10 mg/liter with its content in the initial solution of 5-6 g/liter.

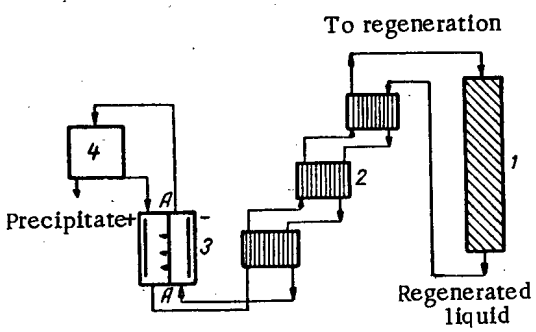

Fig. 5. Arrangement of a three-cascade apparatus for removing excess acidity: 1) sorption column; 2) multichamber electrodialyzers; 3) two-chamber electrodialyzer; 4) filter.

It follows that the use of a multichamber electrodialyzer for recovering hydrochloric acid and nitric acids is already economical, and further improvement in the process and reduction in the cost of electric energy will make this process even more economical. When an electrodialyzer was used to recover sulfuric acid the transfer of uranium through the anion-exchange membrane reached 10-15% of its initial content. The behavior of iron in sulfate solutions is similar to that of uranium.

II. The Use of Ion-Exchange Membranes for Separating Uranium

The electrodeposition of uranium from sulfate solutions containing ammonium sulfate. If sulfate solutions containing different amounts of ammonium sulfate are subjected to electrodialysis, then uranium can be precipitated in the cathode part and the excess acid can be transferred to the anolyte for further use.

In this process it is possible to use a two-chamber electrodialyzer both with an anion-exchange and a cation-exchange membrane. When using an anion-exchange membrane the sulfate ions transfer to the anolyte from the catholyte under the action of an electric current and the acidity in the catholyte decreases. A cation-exchange membrane leads to the migration of ammonium ions from the anode part through the membrane to the cathode. The transfer of ammonium ions increases the pH of the catholyte, since the hydrogen ions are discharged at the cathode. The acidity in the anolyte in this case increases due to transfer of ammonium ions to the catholyte and the accumulation of hydrogen ions obtained when water decomposes at the anode. In both cases the process can be carried out to complete precipitation of uranium in the cathode part.

The anolyte can be a solution of the corresponding salt. As a result of migration of anions or cations at the end of the process the anolyte will have the same acid-salt composition as the initial regeneration solution, and the anolyte can be used in the following cycle to regenerate the resin (Fig. 6). A certain transfer of uranium into the anolyte is possible in both cases.

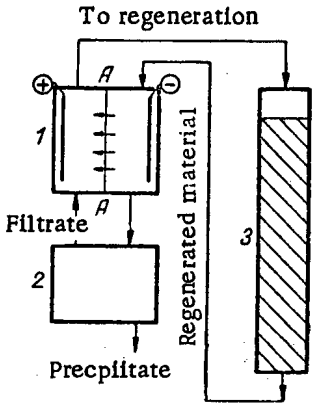

Fig. 6. Scheme for treating sulfate desorption solutions: 1) electrodialyzer with anion-exchange membrane; 2) filter; 3) column.

The catholytes used were solutions with differing contents of uranium, sulfuric acid and ammonium sulfate. Ammonium sulfate solutions were used as the anolyte. The current was passed until the pH of the catholyte approached 7. After this the current was stopped, the solutions were poured from the cells and the catholyte was filtered. In the catholyte the uranium content was determined, and in the anolyte the uranium content was determined and the acidity of the solution was measured. In all experiments in the cathode part a rapidly settling and easily filtered precipitate with a black-green color appeared. From the data of x-ray structural analysis this deposit was a strongly hydrated oxide of tetravalent uranium.

Uranium and acid from the regenerated sulfate solutions containing 5 and 10 g/liter of uranium can be obtained in a two-chamber electrodialyzer with an anion- or cation-exchange membrane. Figure 7 shows the dependence of the energy consumption for the precipitation of uranium on the amount of uranium in solution and the current density. From these data it follows that the energy consumption for the precipitation of uranium increases with the current density and, other conditions being equal, it decreases with increase in the uranium content from 5 to 10 g/liter. Thus, the precipitation of 1 kg of uranium from a solution containing 5 g/liter of uranium at a current density of 32 ma/cm^2 is 10.4 kw-hr, and for the precipitation of 1 kg of uranium from a similar solution containing 10 g/liter uranium 3.4 kw-hr is required; i.e., about a third.

In all experiments there is transfer of uranium into the anolyte. From a catholyte containing 5 g/liter of uranium 0.1 N H_2SO_4 and 0.9 N $(NH_4)_2SO_4$, not more than 25 mg/liter of uranium transfers into the anolyte during the electrodialysis through the anion-exchange membrane. With increase in the acidity there is an increase in the amount of anion complexes of uranium; therefore, with a high acidity of the solution entering the anode part a large amount of uranium is transferred into the anolyte. From a solution containing 5 g/liter of uranium 0.5 N H_2SO_4 and 0.5 N $(NH_4)_2SO_4$ the transfer of uranium to the anolyte through the anion-exchange membrane reaches 34-36% of its initial content.

Electrochemical Precipitation of Uranium from Desorption Solutions

In the treatment of uranium ores by the sorption system the anion-exchange materials are regenerated by weakly acid solutions of chlorides. When a two-chamber electrodialyzer is used the acid can be transferred to the anode part and can be used again for regeneration, and the uranium is then precipitated in the cathode part. As shown above, when working with sulfate solutions in this process anion- or cation-exchange membranes can be used.

In nitrate solutions the uranium can only be transferred to the anolyte due to diffusion, since the anion nitrate complexes of uranium hardly form at low acidities. The catholytes were solutions containing 2.5-10.0 g/liter of uranium, 0.1-0.5 N HNO_3 and 0.5-0.9 N NH_4NO_3; the anolytes were solutions containing 0.6-1 N NH_4NO_3. The current was passed until the pH in the catholyte was 7. In all experiments in the cathode part a yellow precipitate appeared which settled well and could be easily filtered. X-ray structural analysis showed that the uranium precipitates in the form of ammonium diuranate.

The precipitation of uranium with the simultaneous regeneration of acid from nitrate desorption solutions can be performed in a two-chamber electrodialyzer using both anion- and cation-exchange membranes. The composition of the treated solutions can be different, but, as in the case with sulfate solutions, it is much more effective to process solutions which are more concentrated with regard to uranium, containing 5-10 g/liter uranium.

Figure 8 shows the dependence of the power used to precipitate uranium (for an A-1 amberplex membrane) on the uranium content in the catholyte and the current density. The energy needed to precipitate uranium increases with the current density for all investigated solutions, but at the same time there is a reduction in the time of electrodialysis needed for complete precipitation of the uranium. The energy consumption in the precipitation of 1 kg of uranium decreases with increase in the amount of uranium in the desorption solution from 2.5 to 10 g/liter. Uranium is almost completely precipitated from nitrate solutions. Its content in the anolyte and catholyte does not exceed 0.005 g/liter.

In the electrodialysis of real desorption solutions with an anion-exchange membrane, in order to remove the excess acidity the transfer of main impurities and uranium into the recovered acid is small. The amount of uranium transferred to the anolyte increases somewhat with increase in the current density from 10 to 60 ma/cm^2; with a catholyte acidity of 0.825 N it reaches 3% of the initial amount. For all investigated current densities the iron and aluminum do not transfer into the anolyte; the anions SO_4^{2-} and PO_4^{3-} transfer. With increase in the current density there is an increase in the amount of acid transferred to the anolyte, but at the same time the current efficiency decreases.

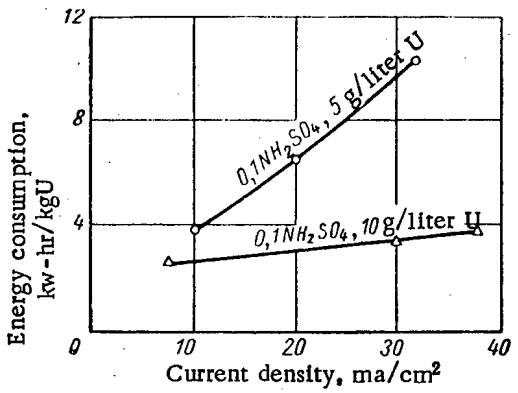

Fig. 7. Dependence of the energy consumption for precipitating uranium on the amount of uranium in the catholyte and the current density.

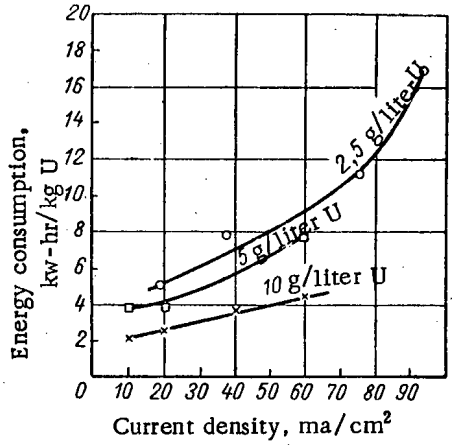

Fig. 8. Dependence of the energy consumption for precipitation of uranium on the uranium content in the desorption solution (for an amberplex A-1 membrane.

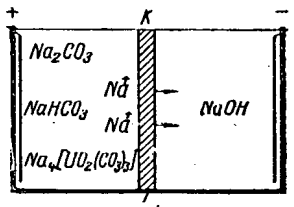

Fig. 9. Process for removing sodium ions from carbonate solutions by the method of electrodialysis with a cation-exchange membrane.

The energy consumption with increase in current density is proportional to the amount of recovered acid and the amount of uranium transferred to the anolyte. The uranium then partially transfers to the anolyte due to the presence of sulfate ions in the desorption solution.

III. The Use of Ion-Exchange Membranes for the Electrodialysis of Carbonate Uranium Solutions

It is known that the carbonate leaching of uranium ores is more selective than the acid leaching. In the subsequent treatment of carbonate uranium solutions it is necessary to breakdown the complex ions $[UO_2(CO_3)_3]^{4-}$, which leads to irreversible losses of soda and acid. We used electrodialysis with ion-exchange membranes to break up the carbonate complex and to return the alkali to the cathode chamber.

Figure 9 shows a scheme of processes occurring in a two-chamber electrodialyzer in the treatment of soda solutions using a cation-exchange membrane.

Into the anode part was poured an initial soda solution containing 0.3 g/liter of uranium, 24 g/liter of sodium carbonate and 15.3 g/liter of sodium bicarbonate, into the cathode part was poured a 0.1 N solution of alkali (2.56 g/ liter of the sodium ion). The cation-exchange membrane is permeable to sodium ions and practically impermeable to uranium; therefore, pure alkali accumulates in the catholyte, containing not more than 3 mg/liter of uranium.

If an anion-exchange membrane is used in the two-chamber electrodialyzer and the anolyte and catholyte change places, then soda can be obtained in the anode part and the diuranate can be precipitated in the cathode part. Naturally, in this case there can be partial transfer of uranium to the anolyte. The precipitation of sodium diuranate appears immediately after the start of the experiment due to the removal of carbonate ions, the current efficiency

for which decreases with increase in the amount of uranium precipitated. The transfer of uranium to the anolyte is rather high: 30 min after the start of the experiment the amounts of uranium in the anolyte and catholyte become the same.

The selectivity of the membranes is affected by the concentration of carbonate in the initial solution. With increase in the content of the carbonate ions in the initial catholyte their current yield increases and the consumption of electric energy for the precipitation of uranium decreases.

LITERATURE CITED

1. F. Nachod and D. Schubert, Ion-Exchange Technology [in Russian] Moscow, Metallurgy Press, 1959.
2. V. A. Klyachko, Collection: "Ion Exchange and Its Applications." Moscow, Acad. Sci. USSR Press, 1959, p. 285.
3. K. M. Saldadze, A. B. Pashkov, and V. S. Titov, Ion-Exchange High-Molecular Compounds [in Russian] Moscow, State Chemistry Press, 1960, p. 143.
4. P. Kirk, USAEC RMO-2506 (1955).
5. N. Frisch, USAEC RMO-2516 (1955).
6. R. Kunin, US Patent No. 2,832,727, 1958.
7. I. Saunders, USAEC RMO-2519 (1955).
8. R. Kunin, US Patent No. 2,832,728, 1958.
9. Mason and Parsi, Transactions of the Second International Conference on the Peaceful Uses of Atomic Energy (Geneva, 1958). Selected Reports of Non-Soviet Scientists, Vol. 7, Moscow, Atomic Energy Press, 1959, p. 451.
10. Higgins, Neill, and McNeese, Transactions of the Second International Conference on the Peaceful Uses of Atomic Energy (Geneva, 1958). Selected Reports of Non-Soviet Scientists, Vol. 7, Moscow, Atomic Energy Press, 1959, p. 468.
11. W. Schulz et al., Report No. 534 presented by the USA to the Second International Conference on the Peaceful Use of Atomic Energy (Geneva, 1958).
12. C. Horner et al., Industr. and Engng. Chem. 47, No. 6, 1121 (1955).

RADIOACTIVE PROPERTIES OF FRAGMENTAL PRODUCTS

A. G. Bykov, P. V. Zimakov, and V. V. Kulichenko

Translated from Atomnaya Énergiya, Vol. 10, No. 4, pp. 362-367, April, 1961
Original article submitted September 1, 1960

As a result of the difficulties of preparation and the high cost of sources of ionizing radiations from individual fragmental isotopes, it is expedient to examine the possibility of using sources of an unseparated mixture of uranium fission products. Theoretical and experimental data on the variation of energy and intensity of the total and also β- and γ-radiations with time are given for different fragmental isotopes and their mixtures. It is shown that the mean energy of β-active isotopes reaches a maximum for two-year fragments, while for γ-active isotopes the maximum is found in the case of two to six month fragments.

As a result of the increasing development of the atomic industry a continually increasing amount of radioactive waste, containing fragmental isotopes, is accumulated. Part of these isotopes may be used as sources of ionizing radiation (in chemistry, biology, agriculture, and in control and measuring apparatuses, etc.). Sources based on Sr^{90}, Cs^{137} and other individual isotopes, the separation of which from a mixture of fragments requires relatively complex reprocessing of radioactive waste, are already in use. For this reason, radiation sources from individual isotopes are comparatively expensive, which strictly limits their use as mass sources of ionizing radiations. The problem of the possibility and expediency of the use of unseparated-fragment sources, the cost of which must be considerably less, is therefore presented.

For this reason it is of considerable interest to investigate the radioactive properties of various preparations containing mixtures of fragmental isotopes.

Characteristics of Preparations of Unseparated Fragments

By the term "unseparated fragments" we understand all fragmental isotopes of practical importance (except those which are gaseous or volatile at ordinary temperatures), formed during the fission of uranium nuclei. Solid radioactive preparations intended for disposal by burial [1-3] may serve as an example of radiation sources containing a mixture of fission fragments.

As a result of the different rates of decay of individual isotopes, the composition of the fragments in such preparations will vary. Figures 1 and 2 give the calculated [4] and experimental data found by the radioelectrochromatographic method of analysis [5] for a preparation obtained from uranium slugs irradiated for 90 days.

Figure 3 shows the mean and mean-maximum energies of the β-radiation obtained by theoretical and experimental methods. Literature data on the values of the mean and maximum energies of the individual isotopes [6] and data on their percentage content in the total fragments were used for the calculation. The basis of the experimental method was that the absorption curves of radiation in aluminum were determined for a mixture of fragments of different ages. The β-spectra were constructed for these curves and the mean energy $\overline{E}_\beta$ was found from the latter [7-9]. As may be seen from this figure, the mean and mean-maximum energies reach a maximum value for fragments about two years old.

Figure 3 also gives the values of the mean energy of the γ-radiation of fragments of different ages,* determined by the calculation method. The mean energy of each individual isotope was found from literature data [5] and was multiplied by the percentage content of the isotope in the preparation. The values obtained were summated, and the total, divided by one hundred, was taken as the mean energy of the γ-radiation of the fragments.

* The mean energy of the γ-radiation of fragments is understood to be the sum of the energies of all the γ-quanta of the fragments, divided by the number of γ-quanta.

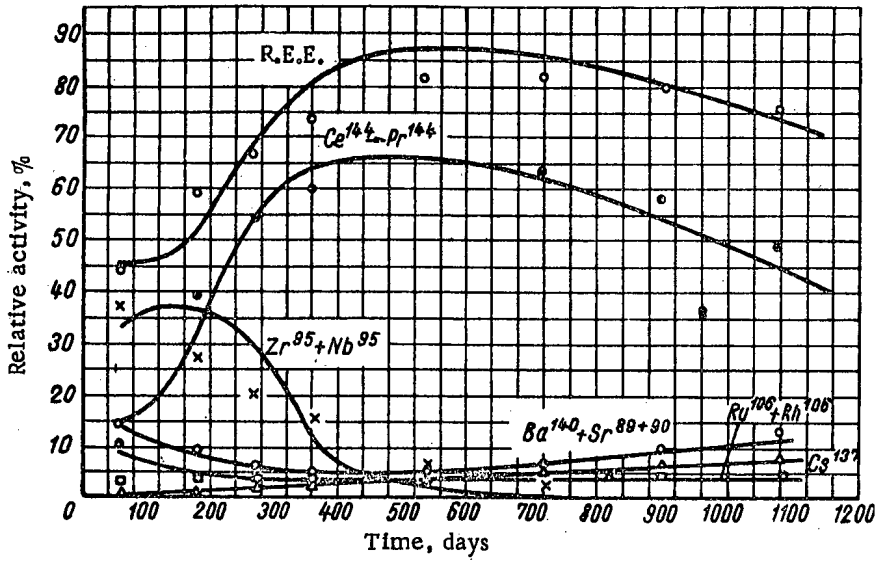

Fig. 1. Variation with time of the relative activity of the β-radiation of various fragmental isotopes (calculated data represented by lines: R.E.E. – rare-earth elements).

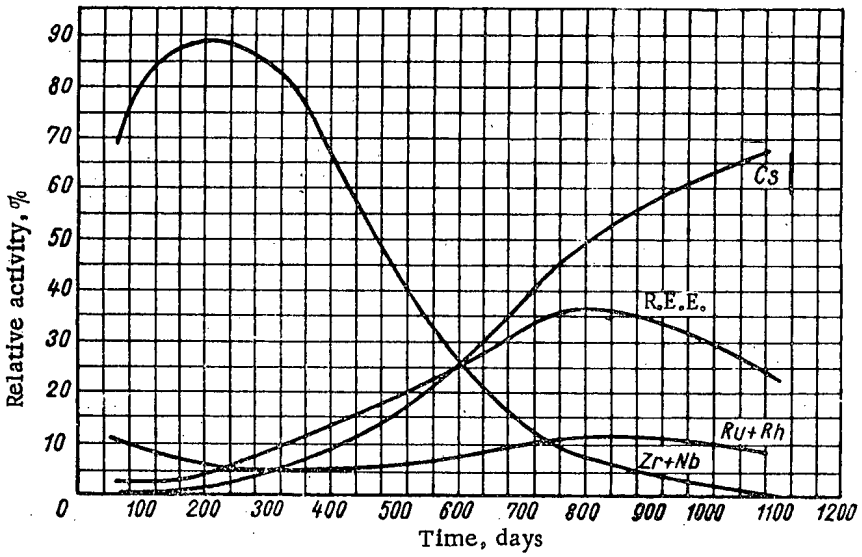

Fig. 2. Variation with time of the relative activity of the γ-radiation of various fragmental isotopes (R.E.E. – rare-earth elements).

The fall in the activity of fragmental preparations and the variation of the half lives of an unseparated mixture of fragments (with respect to β- and γ-radiations) with age are important characteristics of fragmental preparations. The decay of the activity was determined by measuring the activity of the target under the same conditions. The data obtained were compared with the calculated data [5]. As may be seen from Fig. 4, the experimental and theoretical data are close to each other.

The half lives of an unseparated mixture of fragments were found by the curves of the fall in the β- and γ-activities. With an increase in the age of the fragments the half lives of both β- and γ-radiations increase (Table 1).

For "young" fragments the β-radiation half lives are greater than the γ-radiation half lives. The difference in the half lives evens out with an increase in the age of the fragments.

The radiated power is one of the principal characteristics of an ionizing radiation source, particularly in radiochemistry. In the present case the radiated power of a preparation is understood to be the product of the specific activity (curie/liter) and the mean energy of the fragments (Mev). Figure 5 shows the variation of the radiated power with time. The fall in the radiated power of the fragments with respect to γ-radiation is far more rapid than for β-radiation. If we take the radiated power of a preparation from fragments with an age of 60 days as 100%, its power with respect to β-radiation will be 17% after 10 months, while with respect to γ-radiation it will be only 5%.

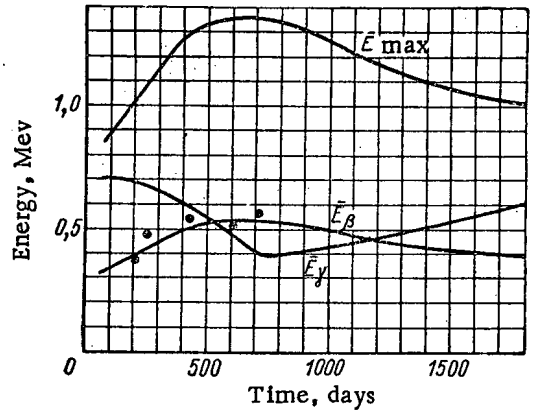

Fig. 3. Variation with time of the mean-maximum energy of the radiation of a mixture of fragments ($\bar{E}_{max}$) and the mean energy of β- and γ-radiations ($\bar{E}_\beta$, $\bar{E}_\gamma$) (calculated data represented by lines).

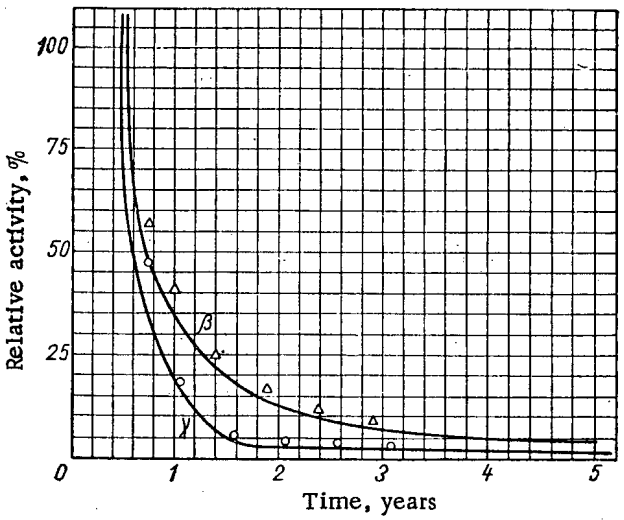

Fig. 4. Reduction of the activity of the β- and γ-radiations of a mixture of fragmental isotopes with time (calculated data represented by lines).

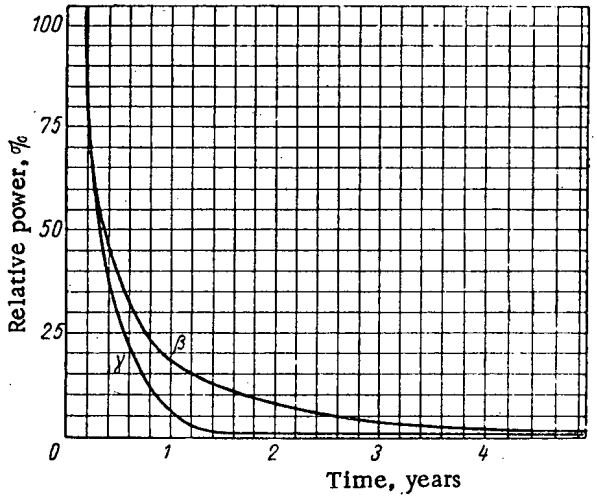

Fig. 5. Variation of the total radiated power of fragmental isotopes with time.

TABLE 1. Half Lives for a Mixture of Fragments of Different Ages (in days)

Type of radiation	Age of fragments, days				
	180	270	360	540	720
β-radiation	140	200	330	400	480
γ-radiation	75	80	95	240	–

Fragmental Preparations as Sources of γ-Radiation

Preparations from Ca^{137}, $Zr^{95} - Nb^{95}$, and unseparated fragments may be used as sources of γ-radiation (Table 2).

As may be seen from this table, a Cs^{137} preparation with an energy of 0.661 Mev for the γ-radiation emitted by its daughter isotope Ba^{137} is of a maximum interest as a γ-radiation source. In contrast to other fragmental sources of γ-radiation, the characteristics of which are given in Table 2, a Cs^{137} source has a maximum half life (fall in activity, only about 2% per annum), and its power hardly varies with time. Such preparations are more convenient to use than those whose power falls relatively rapidly with time. All the above-given facts relate to special Cs^{137} preparations obtained in the form of the chloride or sulfate. At the same time the proportion of Cs^{137} in the sum of the unseparated fragments is small. By the time the proportion of Cs^{137} in the mixture of fragments has reached a considerable value (43% in two years), the total activity of the fragmental source falls 30-40-fold.

Preparations from unseparated fragments may also be used as powerful sources of γ-radiation. Naturally, powerful sources from unseparated fragments will only be employed if they do not require special production and are considerably cheaper than a Cs^{137} source. Highly radioactive vitreous preparations intended for safe burial may be used for this purpose [1-3].

For this reason, the advantageousness of special production of γ-ray sources from $Zr^{95} - Nb^{95}$ is doubtful in view of the brief half life of the isotopes.

TABLE 2. Half Life and Radiated Power of Various Sources of γ-Radiation

Radiation sources	Half life			Radiated power, %		
	age of the fragments, years					
	1	1.5	2	1	2	5
$Cs^{137} - Ba^{137}$	33 years	33 years	33 years	100	98.0	92.0
$Zr^{95} - Nb^{95}$	75 days	75 days	75 days	100	2.1	0.0
Unseparated fragments	95 days	240 days	–	100	15.0	6.7
Unseparated fragments without Cs^{137}	95 days	150 days	250 days	100	9.1	0.6

TABLE 3. Mean Path of β-Particles of Fragments of Different Ages (in millimeters)

Medium	Age of fragments, days					
	60	180	360	720	1080	1800
Aluminum	1.23	1.52	2.02	2.20	2.00	1.53
Water	3.88	4.80	6.32	6.90	6.30	4.82
Air	2460.0	3060.0	4060.0	4400.0	4000.0	3100.0

TABLE 4. Self-Absorption of β-Particles of Fragments in a Layer of a Preparation with a Density of 2.7 g/cm³ (in percent)

Thickness of the layer of the preparations, mg/cm²	Age of fragments, days			
	60	180	270	360
2.7	5	2	1.5	1.5
27.0	35	16	13.0	13.0
135.0	79	55	46.0	45.0
270.0	89	74	66.0	65.0

Fragmental Preparations as β-Radiation Sources

To determine the zone of effect of a fragmental preparation as a β-ray source, it is necessary to determine the mean free path of the β-particles. This may be calculated on the basis of the values of the mean maximum energy, for example, from the formula

$$R_m = 0.543\bar{E}_{max} - 0.133,$$

where R is expressed in g/cm², and $\bar{E}_{max}$ is expressed in Mev. The approximate values of the mean paths of β-particles of fragments of different ages are given in Table 3.

From the data of Table 3 it may be concluded that in media with a density greater than 1 g/cm³, fragmental preparations should evidently not be used as β-sources, because the mean zone of effect of the β-particles is ~5 mm.

Moreover, when fragmental preparations are used as β-ray sources it is also necessary to determine the self-absorption of β-particles in the layer of the preparation. For this purpose it is necessary to know the thickness of the layer of half-absorption ($\Delta \frac{1}{2}$) of the β-particles of fragments of different ages. This thickness is found from the curves of the absorption in aluminum, determined in a T-25-BFL-type end-window counter with a window thickness of 1.2 mg/cm²:

Age of fragments, days	Thickness of half-absorption layer, mg/cm²
60	20
180	48
270	69
360	70

Knowing $\Delta_{\frac{1}{2}}$, the self-absorption P in a layer d (mg/cm^2) of different thickness can be determined from the formula [6]

$$P = \frac{\left(1 - e^{\frac{-0{,}693d}{\Delta_{1/2}}}\right)\Delta_{1/2}}{0{,}693d}.$$

With an increase in the thickness of the layer of the preparation, self-absorption increases, but decreases with an increase in the age of the fragments (to one year). Therefore, for use as β-ray sources, fragmental preparations should be as thin as possible and should be produced from fragments not less than six months in age. β-Ray sources are best prepared from fragments of age two years, at which the mean and mean-maximum energies are greatest Fig. 3). Table 5 gives the properties of fragmental β-ray sources from Sr^{90} and unseparated fragments; the age of the unseparated fragments is two years.

TABLE 5. Radioactive Properties of Fragmental β-Ray Sources

Source	Half life	Mean maximum energy, Mev	Mean maximum energy with respect to β-radiation, Mev	Free path of the β-particles, mm			Self-absorption in a preparation with different layers of density 2.7 g/cm^3 (%)		
				in air	in water	in aluminum	with a layer 27 mg/cm^2	with a layer 135 mg/cm^2	with a layer 270 mg/cm^2
Sr^{90} Y^{90}	28 years 61 hours	1.40	0.54	4800	7.35	2.31	10	38	58
Mixture of fragments	480 days	1.35	0.53	4400	6.90	2.20	13	45	65

From the data of Table 5 it is evident that preparations from Sr^{90} and from a mixture of two-year-old fragments hardly differ from each other as regards radioactive properties except for the half life, which is considerably greater for Sr^{90}. The activity of an Sr^{90} preparation decreases by only 3% in a year. However, preparations from unseparated fragments are cheaper and may be obtained with a greater specific activity. They may therefore find greater application.

SUMMARY

Preparations made from unseparated fragments may be used as β- and γ-ray sources. To reduce self-absorption, β-sources must be made in the form of thin layers. It is best to use β-active isotopes of age two years, at which their mean and mean-maximum energy is greatest. γ-Ray sources from unseparated fragments are best prepared from fragments of age two – six months, when the mean energy of their radiation is ~0.70 Mev. From the point of view of the fullest utilization of the whole energy of the fragments, the radiated power falls far more rapidly than for "old" fragments. From the aspect of convenience and simplicity of use, Sr^{90} and Cs^{137} preparations are of the greatest interest.

LITERATURE CITED

1. C. Amphlett, Progr. Nucl. Energy, III, Progress Chemistry 2, Pergamon Press, 1958.
2. P. V. Zimakov et al., Proc. 2nd International Conference on the Peaceful Uses of Atomic Energy (Geneva, 1958). Reports of Soviet Scientists [in Russian] 4, Moscow, Atomizdat, 1959, p. 247.
3. P. V. Zimakov and V. V. Kulichenko, Report given to the International Conference on the Reprocessing and Burial of Radioactive Waste (Monaco, 1959) [in Russian].
4. N. G. Gusev, V. P. Mashkovich, and G. V. Obvintsev, Gamma Radiation of Radioactive Isotopes and Fission Products [in Russian]. Moscow, Fizmatgiz, 1958.
5. Collection: Isotopes and Radiations in Chemistry [in Russian] Moscow, Academy of Sciences USSR Press, 1958, p. 303.
6. N. G. Gusev, Handbook on Radioactive Radiations and Protection [in Russian] Moscow, Medgiz, 1956.
7. A. Schopper, Z. Phys. 129, 416 (1951).
8. Das Gupta, Chaudhury and Phys. 22, 27 (1948).
9. H. Evans, Proc. Phys. London, A63, 575 (1950).

LETTERS TO THE EDITOR

A ROTATING PLASMA ARC IN A DISCHARGE IN A MAGNETIC FIELD

A. V. Zharinov

Translated from Atomnaya Énergiya, Vol. 10, No. 4, pp. 368-369, April, 1961
Original article submitted October 29, 1960

The discovery was reported earlier [1] of the stepwise increase in the ratio of electron current flowing to a probe to the ion current for a certain critical magnetic field. Subsequent experiments have been conducted with the same apparatus used in [1], supplemented with a thermocouple ionization gauge. The construction was also altered essentially with the disposition of an eighth probe connected with the plane anode, as shown in Fig. 1 (looking in the direction of the magnetic field, from the cathode side). As working gases, hydrogen, nitrogen, and argon were used. The critical magnetic field H_{crit} was studied for dependence on the pressure and the kind of gas. In Fig. 2 are curves depicting H_{crit} varying as a function of pressure for hydrogen, nitrogen, and argon.

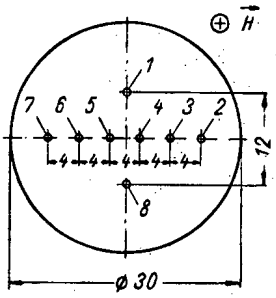

Fig. 1. Schematic arrangement of probes.

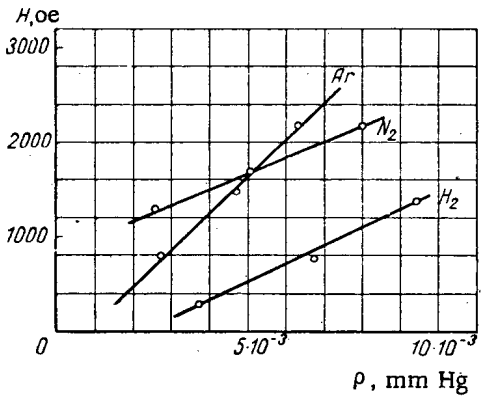

Fig. 2. Dependence of the critical magnetic field H_{crit} on pressure (I_p = 0.5 amp; V_p = 270 v).

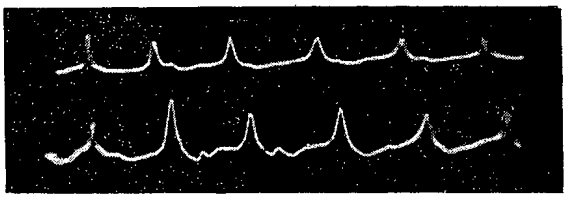

Fig. 3. Oscillogram of ion current to probes 1 and 6 (see Fig. 1) (I_p = 0.6 amp; V_p = 150 v; H = 3700 oe; p = $1.4 \cdot 10^{-2}$ mm Hg.

From the figure it is apparent that H_{crit} increases with increasing pressure according to a law which is nearly linear. In addition, one can observe an essential dependence of H_{crit} on the kind of gas. To explain the details leading to this relationship would be as yet premature. Pairwise oscillography of probe currents by means of the double beam oscilloscope DÉSO-1 has permitted us to establish the fact that near H_{crit} a transverse plasma arc is initiated in the discharge, which rotates in the direction of the ions around the primary electron beam. In Fig. 3 are shown oscillograms of the current to probe 1 (upper trace) and probe 6 (lower trace). Both probes were connected to the anode through a resistance of 5 kohm, and carried predominantly ion current. The repetition period of the recurrent peaks on the oscillogram had a value of 65 μsec. The peaks correspond to an increase in ion current to 30-40 μa, compared to the average background. The current to probe 6 lags the current to probe 1 in phase by 90°; this indicates a counterclockwise rotation of the arc in the same sense as the positive ions.

It is relevant to note the diverse modes of rotating arcs, which depend on the discharge parameters. Under certain conditions one can observe not one, but two synchronously rotating arcs escaping from the primary beam in diametrically opposite directions. The observations conducted do not as yet permit us to establish the relationship

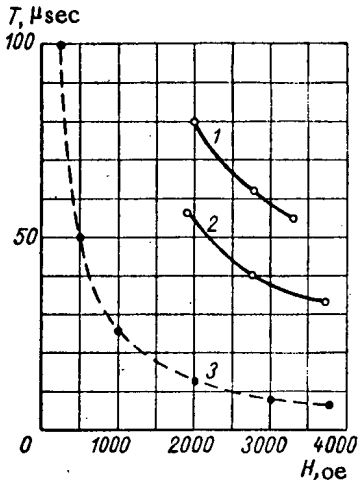

Fig. 4. Dependence of the period of rotation of the arc T on the intensity of the magnetic field: 1) I_p = 0.4 amp; V_p = 150 v; p ≈ 10^{-2} mm; 2) I_p = 0.6 amp; V_p = 120 v; p ≈ 10^{-2} mm; 3) $T = 2\pi/\omega_A$.

connecting the discharge parameters with the rotation period. However, there is no doubt of the tendency toward decrease in the rotational period with increasing magnetic field. In Fig. 4 are curves showing the dependence of the rotational period on the magnetic field. For comparison the addition curve 3 gives the variation of the Larmor period of rotation for argon ions. The rotational velocity of the arc was $1\text{-}3 \cdot 10^5$ cm/sec; this is correlated with the increasing drift velocity $c[EH]/H^2$ under corresponding conditions. One may speculate that the "anomalously high transverse diffusion," studied by Bohm et al. [2] under similar conditions, is due to the rotation of one of more arcs.

In conclusion we note that a similar rotation of a plasma arc was observed by Neidigh [3]. However, as he emphasized, under the conditions of his experiment the phenomenon occurred even in the presence of longitudinal gradients of pressure in the gas.

LITERATURE CITED

1. A. Zharinov, Atomnaya Energiya 7, 3, 215 (1959).*
2. A. Guthrie and R. Wakerling, The Characteristics of Electrical Discharges in Magnetic Field, New York, McGraw-Hill Book Co., 1949.
3. Neidigh and Weaver, Proc. Second United Nations International Conference on the Peaceful Uses of Atomic Energy [English Language Edition] (Geneva, 1958) 31, 315 (1959).

USE OF THE PRINCIPLES OF SIMILITUDE IN SOLVING PARTICLE TRANSFER PROBLEMS

Sh. A. Guberman

Translated from Atomnaya Energiya, Vol. 10, No. 4, pp. 369-371, April, 1961
Original article submitted November 10, 1960

The phenomena of particle and radiation transfer are described by the familiar kinetic equation, the solution of which presents considerable difficulties in many practically interesting situations. Therefore, setting up models has achieved great importance. The laws on which the models are set up are based on the theory of similitude, which allows the results of one experiment to be extended to a whole class of similar phenomena, thus considerably reducing the volume of experimentation required.

For phenomena of this sort, $x'_i/x''_i = C_{xi}$, where x'_i and x''_i are the values of the same physical quantity at similar points. To set up relations between the similitude constants, C_{xi}, according to the theory, the kinetic equation is reduced to dimensionless form, and divided into the independent dimensionless ratios:

$$\frac{vt}{\lambda};\ \frac{Stv}{\Phi};\ \frac{r}{\lambda};\ \frac{\lambda_a}{\lambda_s};\ \frac{v}{v_0};$$

with the further assumption that:

$$\frac{C_v C_t}{C_\lambda}=1;\ \frac{C_s C_t C_v}{C_\Phi}=1;\ \frac{C_r}{C_\lambda}=1;\ \frac{C_{\lambda_a}}{C_{\lambda_s}}=1;\ \frac{C_v}{C_{v_0}}=1.$$

* Original Russian pagination. See C. B. translation.

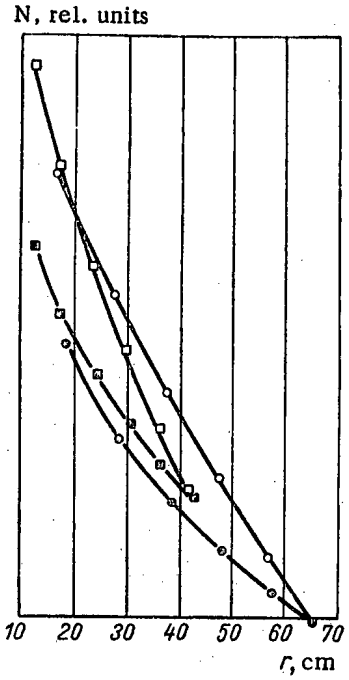

Fig. 1. Neutron density distribution along the axis of a crevice in a model, and in a real crevice 18 cm in diameter (similitude transformation); C = 1.6: ○) thermal neutrons in the model, □) thermal neutrons in the crevice, ◉) epithermal neutrons in the model, ▣) epithermal neutrons in the crevice.

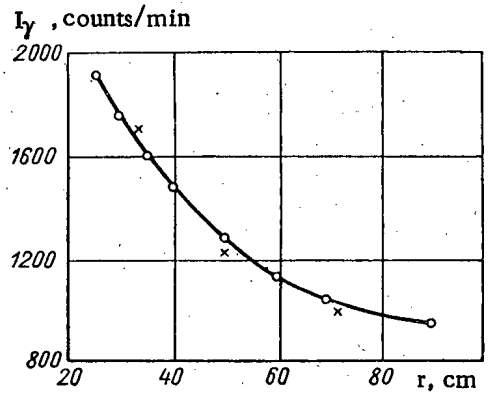

Fig. 3. Distribution of γ-quanta in soil (ρ = = 1.8 gm/cm^3). Source: Zn^{65} (E_γ = 1.12 Mev). ○) experimental points; ×) calculated by Eq. (3) from distribution in water.

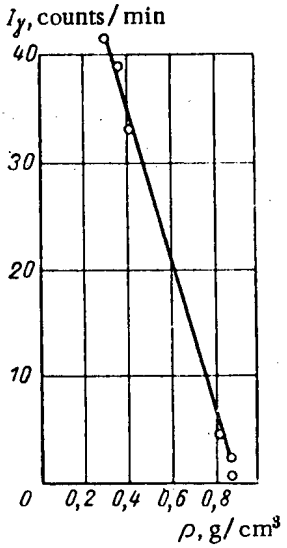

Fig. 2. Intensity of γ-radiation as a function of water density (r = 90 cm) obtained by the principle of similitude: ○) experimental data of [1].

Since all these equations must be satisfied simultaneously:

$$C_r = C_{\lambda_a} = C_{\lambda_s} = C_v C_t = \frac{C_\Phi}{C_s} = C. \qquad (1)$$

Similar geometries and similar initial and boundary conditions (Kirpichev – Gukhman theorem) can serve as the similitude condition of the phenomena. For phenomena described by the kinetic equation, these conditions are:

1. The media are geometrically similar $r'/r'' = C_r$.

2. At similar points

$$\frac{\lambda_s'(u)}{\lambda_s''(u)} = C_{\lambda_s}; \quad \frac{\lambda_a'(u)}{\lambda_a''(u)} = C_{\lambda_a}.$$

In view of the fact that the energy dependence of λ_s and λ_a is different for different nuclei, the equations can be satisfied strictly only if the similar points have constant chemical composition. Thus, $C_{\lambda a} = C_{\lambda s} = \rho''/\rho' = 1/C_\rho$, where ρ' and ρ'' are the densities of the medium at similar points. Since $\lambda_s(u)$ and $\lambda_a(u)$ are, generally speaking, not homogeneous functions of u, $\lambda(u')/\lambda(u'') = \text{const}$ at $u'/u'' = C_u$ for all the values of u'. This means that $C_u = 1$, and $C_v = 1$; i.e., the problem does not admit of similitude with respect to energies.

3. The sources are geometrically similar, have the same energy spectrum (this requirement arises out of the impossibility of similitude transformations in energy), and satisfy the equation:

$$\frac{S'(\bar{r}', t')}{S''(\bar{r}'',} = C_s,$$

where t' and t" are similar moments of time; i.e., $t'/t'' = C_t$.

Therefore, if the phenomena satisfy the three conditions given, they are similar, and Eq. (1) holds. Taking $C_v = 1$; $\Phi = Nv$; $C_N = C_\Phi / C_v = C_\Phi$, we obtain finally:

$$C_t = C_r = C_{\lambda_s} = C_{\lambda_a} = \frac{C_N}{C_s} = C, \tag{2}$$

which establishes the connection between the physical and geometric parameters of the similar phenomena described by the kinetic equations.

In particular, for the propagation of particles or radiation in similar media from a given point source Q:

$$C_s = C^{-3};\ C_N = C^{-2},$$

since:

$$Q' = \int S'dV' = C^3 C_s \int S''dV'' = C^3 C_s Q'',$$

i.e., for a particle density in the similar media given by:

$$N'(r', t') = \frac{1}{C^2} N''\left(\frac{r'}{C};\ \frac{t'}{C}\right). \tag{3}$$

Using these relationships, we can obtain a number of results of practical interest for phenomena, dealing, for example, with the propagation of neutrons and γ-quanta.

1. In nuclear geophysics, to solve the problem of the distribution of neutrons and γ-quanta in rocks, a model is made by piling up materials which differ in density from the real rocks by about 1.5 times. Using the theory of similitude, the conditions may be found, which the model must satisfy, so that the distribution of neutrons and γ-quanta in a real rock crevice, and in the model, will be similar. The relation between the density of neutrons or γ-quanta in the model, and that in the rock, is expressed by Eq. (3).

Let us, for example, make up a model of a stratum, traversed by a crevice of diameter d, filled with water. The density of the stratum in the model is C times less than the density of the real stratum. According to the principles of similitude, the model should be built in the following way: a crevice of diameter Cd is made in the built-up stratum, and is filled with water of density 1/C g/cm^3 (which is achieved by replacing part of the water with air). Results of measurements on such a model are given in Fig. 1.

2. In meteorology, a method has been used for measuring the density of snow and ice, using the attenuation of γ-radiation [1]. The relation between the intensity of the γ-rays and the density of the snow or ice may be obtained from experimental data on the distribution of γ-rays in water, with the aid of Eq. (3) (Fig. 2).

3. In view of the fact that the similitude conditions for the propagation of neutrons and γ-quanta are the same, it is possible to use the principle of similitude for the following problem: fast neutrons, emitted by a point source, are moderated in the surrounding medium and on absorption produce capture gammas, which may be detected some distance from the source (this phenomenon is widely used in nuclear geophysics to study crevices, and is known as the neutron-gamma method).

For the density of capture gammas in similar media:

$$N'(r', t') = \frac{1}{C^2} N''\left(\frac{r'}{C};\ \frac{t'}{C}\right).$$

The possibilities of the method of similitude are considerably broadened by the use of approximate models. For example, it is in some cases possible to assume that for a number of elements, λ_s and λ_a are independent of energy. Such elements may replace one another in the models, as long as they have equivalent values of Σ_s and Σ_a.

Another example is the propagation of thermal neutrons in strong 1/v absorbers (in minerals containing boron, manganese, lithium, chlorine etc.). The necessary conditions are established for the model with one of these elements, and are then extended to the remaining cases, keeping Σ_a the same.

The propagation of medium-energy γ -quanta in media containing light nuclei depends only slightly on the nature of the nuclei, and is determined principally by the electron density in the medium. Therefore, knowing the distribution of γ -quanta in water, and making use of Eq. (3), the distribution of γ -quanta may be found in sandstone, clay, and limestone (Fig. 3).

Models with dimensions exceeding the dimensions of the sample, make it possible to study nonstationary processes on a large time scale.

The results obtained have a general character and are applicable to the study of many phenomena described by the kinetic equations (transfer of radient energy in the atmosphere of stars, passage of electrons through matter, etc.).

In conclusion, the author wishes to thank S. A. Kantor and D. A. Kozhevnikov, who in many ways contributed to the completion of this work.

LITERATURE CITED

1. O. K. Vladimirov and V. A. Chernigov, Atomnaya Energiya 4, No. 5, 474 (1958).*

MEAN NUMBER OF NEUTRONS FROM FAST FISSION OF Np^{237}

V. I. Lebedev and V. I. Kalashnikova

Translated from Atomnaya Energiya, Vol. 10, No. 4, pp. 371-372, April, 1961
Original article submitted September 29, 1960

The measurement of the mean number of neutrons, ν, for the fast fission of Np^{237} was carried out relative to the well-known value of ν for thermal fission of U^{235}. The fission fragments were detected in an ionization chamber and the fast neutrons in a detector, consisting of a group of $B^{10}F_3$ counters, located in moderator. The value of ν was determined from the coincidences between the fragments and the fast neutrons from the fission. Apparatus and measurement technique have been described in earlier papers [1, 2].

A converter with a U^{235} sample, located in the neutron field near the reflector of the RFT reactor, was used as the source of fast neutrons to produce the Np^{237} fission. The formation of the beam of fast neutrons, and the spectral distribution, are discussed in [2], where it is also shown that the energy distribution of fast neutrons at the place where the target isotope is set up corresponds with the fission spectrum.

The neptunium sample used in the measurements was carefully purified of other fissionable contaminants by the chromatographic method. The degree of purity of the sample was so high, that it was not necessary to introduce any corrections for isotopic content into the final result.

The target consisted of about 1 mg/cm^2 thick layer of Np^{237}, on both sides of a thin (7 micron) platinum foil. Each of the layers contained about 20 mg of material. The standard U^{235} target was also made up in the form of a double layer about 0.3 mg/cm^2 thick on aluminum foil.

When the Np^{237} target was placed in the beam of fast neutrons, the fission fragment rate in the ionization chamber was about 4-5 per second, and the number of actual coincidences between fragments and fission neutrons

* Original Russian pagination. See C. B. translation.

was 0.6-0.7 per second. The ratio of the number of actual coincidences to the number of chance coincidences between fragments and the fast neutron background was of the order of unity.

Results of Several Series of Measurements of the Ratio $\nu(Np^{237})/\nu_T(U^{235})$

Measurement series	Isotope	No. of fragments	No. of actual coincidences	$\nu\omega\eta$*	$\gamma(Np^{237})/\nu_T(U^{235})$
I	Np^{237}	342 984	48 824	0,1424	1,1903
	U^{235}	612 480	73 244	0,1196	
II	Np^{237}	296 132	42 368	0,1431	1,2002
	U^{235}	58 232	69 764	0,1192	
III	Np^{237}	177 724	24 908	0,1402	1,2047
	U^{235}	352 896	41 056	0,1163	

*The quantity $\nu\omega\eta$ is equal to the ratio of the number of actual coincidences to the number of fragments counted in the same length of time: $\omega\eta$ is the efficiency of counting fission neutrons (taking account of the geometry of the experiment).

Because of the fact that the measurement of $\nu(Np^{237})$ is made with fast neutrons, while the measurement of $\nu_T(U^{235})$ is made with thermal neutrons, the conditions under which the fission neutrons are counted may not be the same in both cases, on account of the angular anisotropy in the ejection of the Np^{237} fission fragments. This fact could, with the geometry used, lead to some reduction in the efficiency of neutron counting, when making measurements on Np^{237}. However, as was shown in [3], the angular anisotropy for Np^{237} in the energy range 0.35-1.5 Mev is small (of the order of 10-15%), and calculations and simple control experiments have shown that the possible change in the efficiency of counting the fission neutrons lies far beyond the limits of accuracy of the experiment.

The basic data from the experiments is given in the table.

Thus, the desired ratio is:

$$\frac{\nu(Np^{237})}{\nu_T(U^{235})} = 1{,}197 \pm 0{,}012 .$$

Taking $\nu_T(U^{235}) = 2.47 \pm 0.03$ [4], we obtain for $\nu(Np^{237})$ the value 2.96 ± 0.05.

References [5 and 6] give results of measurements of $\nu(Np^{237})$ for fast fission. Thus, the work in [5], carried out by essentially the same method that we used, with the neutron spectrum issuing from a fast neutron reactor, gave the value $\nu(Np^{237}) = 2.72 \pm 0.15$. The measurements of [6], made by an indirect method on the "Topsy" and "Jezebel" critical assemblies with mean neutron energy spectra of 1.40 and 1.67 Mev, gave for $\nu(Np^{237})$ the values 2.81 ± 0.09, and 2.90 ± 0.04, respectively.

Experimental and calculational data on the uranium isotopes and Pu^{239} [7] show that the variation of the values of ν, with the energy of the neutrons producing fission, is linear, and the slope of all the straight lines is almost identical. If, with this in mind, we make a comparison of the results obtained in the critical experiments and in the present paper (making a very coarse estimate of the effective neutron energy spectra in all cases) we seem to be able to conclude that the data for Np^{237} do not contradict the linear dependance of $\nu(E_n)$, although it is possible that they indicate a more rapid increase in $\nu(Np^{237})$ with energy, than occurs with the other isotopes investigated. In this connection, the measurement of ν for Np^{237} in other neutron energy ranges is a very interesting matter.

The authors recognize their pleasant duty of expressing thanks to a group of radio-chemists: V. K. Markov, E. I. Rzhekhina, V. F. Gorbunov, and G. I. Khlebnikov, for the preparation of the high purity neptunium samples, and the fabrication of the high quality targets.

LITERATURE CITED

1. V. I. Kalashnikov et al., Session of the Academy of Sciences, USSR, on the peaceful uses of atomic energy (Meeting of the Division of Physical and Mathematical Sciences) [in Russian] Moscow, Academy of Sciences, USSR, Press, 1955, p. 161.
2. V. I. Kalashnikova, V. I. Lebedev, and P. E. Spivak, Atomnaya Energiya 2, No. 1, 18 (1957).*
3. B. M. Gokhberg, G. A. Otroshchenko, and V. A. Shigin, Dokl. AN SSSR 128, No. 6, 1157 (1959).
4. D. Hughes and R. Schwartz, Neutron Cross Section, BNL-325, Suppl., No. 1, January 1, 1957, p. 5.
5. B. D. Kuz'minov, L. S. Kutsaeva, and I. I. Bondarenko, Atomnaya Energiya 4, No. 2, 187 (1958).*
6. Leachman, First international conference on the peaceful uses of atomic energy (Geneva, 1955). Selected reports of foreign scientists, Vol. 2 [in Russian] Moscow, Atomizdat, 1959, p. 282.
7. I. I. Bondarenko et al., Transactions of the second international conference on the peaceful uses of atomic energy (Geneva, 1958). Reports of Soviet scientists, Vol. 1 [in Russian] Moscow, Atomizdat, 1959, p. 439.

*Original Russian pagination. See C. B. translation.

TERTIARY FISSION OF THE NUCLEI U^{233}, U^{235}, Pu^{239} and Pu^{241}

T. A. Mostovaya

Translated from Atomnaya Energiya, Vol. 10, No. 4, pp. 372-373, April, 1961
Original article submitted December 7, 1960

Recently many papers have been published dealing with tertiary fission of heavy nuclei [1-4]. In connection with the increased interest in this problem, it is not without interest to give some results which we obtained in 1954 and 1955 from measurements on the probability of tertiary fission of uranium and plutonium isotopes.

Relative Probability of Tertiary Fission

	Data of the present paper	Data of reference [6]	Data of reference [1]
$\frac{P_{af}(U^{233})}{P_{af}(U^{235})}$	1,16±0,05	1,25±0,22	1,22±0,06
$\frac{P_{af}(Pu^{239})}{P_{af}(U^{235})}$	1,04±0,06	1,14±0,23	1,18±0,06
$\frac{P_{af}(Pu^{241})}{P_{af}(U^{235})}$	1,34±0,07	—	—

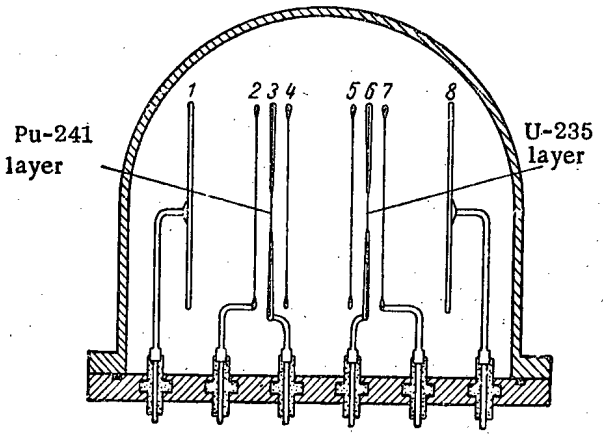

Diagram of ionization chamber.

In order to detect tertiary fission we used an ionization chamber, the construction of which is shown in the figure. Electrodes 1, 2, 3, 4 and 5, and 4, 5, 6, 7 and 8 formed two ionization chambers similar to the chamber which we used to measure the probability of spontaneous and induced tertiary fission in Pu^{240} [5]. In the present case it was possible to make measurements simultaneously with two different fissioning isotopes. The tertiary fission was detected by the coincidence between the impulse from fragments in chambers 2, 3 and 3, 4 with the pulse from the long-range α-particle in chambers 1, 2 and 4, 5. The probability of tertiary fission P_{af} is given by the equation

$$P_{af} = \frac{N_{af} - N_{afc}}{N_f},$$

where N_{af} is the number of coincidences recorded, N_{afc} is the number of chance coincidences and N_f is the number of fissions.

All the measurements were made in a beam of thermal neutrons from the RFT test reactor. The probability of tertiary fission of the isotopes U^{233}, Pu^{239} and Pu^{241} was measured relative to the probability of tertiary fission of U^{235} which was taken to be unity.

The layers of fissionable material used were 0.1 to 0.2 mg/cm^2 thick and were painted on nylon films which are transparent to fragments (~ 20 μg/cm^2).

We will be more detailed as to the measurements of the tertiary fission of Pu^{241}, since up to the present no data has been published on this problem. For the measurements we used a Pu^{241} layer having the total weight of 2 mg. The isotopic content of the sample was determined by measuring the total α-activity, the number of spontaneous fissions, the differential spectrum of the α-particles and the weight. The sample contained 88.5% by weight Pu^{241}, 8% by weight Pu^{239}, 2.9% by weight Pu^{240} and 0.6% by weight Am^{241}. The measurements with the sample of Pu^{241} were carried out at several threshold values for the discriminator to which the signals from chambers 1, 2 and 4, 5 were fed. In doing this the ratio of the number of coincidences for Pu^{241} and U^{235} did not change. Apparently the energy spectrum of the α-particles emitted in Pu^{241} fission does not differ materially from the spectrum of the long-range α-particles emitted in fission by other nuclei. The results of the measurements are given in the table.

After making corrections for the counting coefficient of the fragments and the long-range α-particles in the chambers, it was found that for Pu^{241} one tertiary fission occurs in 390 ± 25 ordinary fissions into two fragments. Thus the excitation of the Pu^{242} nucleus to tertiary fission behaves in the same way as the other isotopes studied.

LITERATURE CITED

1. V. N. Dmitriev et al., ZhÉTF 38, 3, 998 (1960).
2. N. A. Perfilov, Yu. F. Romanov, and Z. I. Solov'eva, Usp. fiz. nauk, 21, No. 3, 471 (1960).
3. V. N. Dmitriev et al., Doklady AN SSSR 127, No. 3, 531 (1950).
4. V. N. Dmitriev et al., ZhÉTF 39, 3, 556 (1960).
5. V. I. Mostovoi, Materials from the International Conference on the Peaceful Uses of Atomic Energy (Geneva, 1955) Vol. 2 [in Russian] Moscow, Fizmatgiz, 1958, p. 256.
6. K. Allen and J. Dewan, Phys. Rev. 80, 181 (1951).

NOTE ON THE THEORY OF AN ANNULAR CYCLOTRON

A. P. Fateev

Translated from Atomnaya Énergiya, Vol. 10, No. 4, pp. 373-375, April, 1961
Original article submitted July 26, 1960

The annular cyclotron, or ring cyclotron, is an interesting variant of the class of fixed-field accelerators [1]. The magnetic system of this cyclotron differs from the magnetic systems used in conventional sector-field accelerators in that the fields established in the sectors increase not radially, but along the vertical ($H \sim z_n$). The increase in field in the vertical direction has the result that the orbit traversed by the particles is shifted upwards as energy is increased, and that the orbit remains confined within a narrow cylindrical annulus. Alternation of the signs of the field assures stability of particle motion under certain conditions [1].

The stability may also be achieved with the aid of spiral field modulation. In that case, the annular cyclotron will have a "helical" magnetic field [2].

Since the orbital perimeter in an annular cyclotron is practically energy-independent, this machine is best used for accelerating electrons in the relativistic energy regions. In that case, the high-frequency system will be similar to that used in a conventional cyclotron, and particle currents equal to those attainable only in cyclotrons at the present time may be anticipated.

A previous contribution [1] considered the simplest variant of a radial-sector annular cyclotron in which the orbits traced out by the particles were plane curves formed of arcs of circles. This concept is obviously acceptable if and only if the effect of dissipated fields may be safely neglected and the field in each sector may be assumed axisymmetric. The motivation of the present note is to point out the existence of stable closed orbits in the general case, with boundary effects taken into due account. Particular attention is given here to the "symmetrical" variant where acceleration, stacking, and head-on collisions between particles belonging to two beams traveling in opposite directions are possible. The results obtained so far have aided the study of other modifications of the ring cyclotron.

The magnetic field of the ring cyclotron $\vec{H} = (H_r, H_\theta, H_z)$ in a cylindrical coordinate system r, θ, z, has the form [3]

$$\left.\begin{aligned}
H_r &= -\sum_k R_k \left(\frac{z}{\bar{z}}\right)^{n_k+1} \left\{\left[k^2 - n_k(n_k+1)\left(\frac{\bar{r}}{z}\right)^2\right]\frac{\Delta r}{\bar{r}} + \right.\\
&\left. + \frac{1}{2}\left[3k^2 + n_k(n_k+1)\left(\frac{\bar{r}}{z}\right)^2\right]\left(\frac{\Delta r}{\bar{r}}\right)^2 + \dots\right\} e^{ik\theta};\\
H_\theta &= -\sum_k \Theta_k \left(\frac{z}{\bar{z}}\right)^{n_k+1} \left\{1 - \frac{\Delta r}{\bar{r}} + \frac{1}{2}\left[2 + k^2 - n_k(n_k+1)\left(\frac{\bar{r}}{z}\right)^2\right]\left(\frac{\Delta r}{\bar{r}}\right)^2 + \dots\right\} e^{ik\theta};\\
H_z &= -\sum_k Z_k \left(\frac{z}{\bar{z}}\right)^{n_k} \left\{1 + \frac{1}{2}\left[k^2 - n_k(n_k-1)\left(\frac{\bar{r}}{z}\right)^2\right]\left(\frac{\Delta r}{\bar{r}}\right)^2 + \dots\right\} e^{ik\theta},
\end{aligned}\right\}$$

where $\Delta r = r - \bar{r}$; $n_k = n - iks$ (s is a parameter character characterizing the "field helicity"); $R_k = [\bar{z}/\bar{r}(n_k + 1)]Z_k$;

$$\Theta_k = \frac{ik\bar{z}}{\bar{r}(n_k+1)} Z_k; \quad Z_k = \bar{H}_{z,k}; \quad \bar{H}_{z,k} = H_{z,k}(\bar{r}, \bar{z});$$

$k = 0, \pm N, \pm 2N, \ldots$; N is the number of periodic elements. Putting $\bar{z}/\bar{r} = \Delta$, we find with ease

$$\left.\begin{aligned} &\bar{H}_{r,k} = 0, \ \bar{H}_{\theta,k} = \frac{ik\Delta}{n_k+1} \bar{H}_{z,k}, \ \frac{\partial \bar{H}_{z,k}}{\partial r} = 0, \\ &\frac{\partial \bar{H}_{z,k}}{\partial z} = \frac{n_k}{\bar{z}} \bar{H}_{z,k}, \\ &\frac{\partial \bar{H}_{r,k}}{\partial r} = \frac{k^2\Delta^2 - n_k(n_k+1)}{\bar{z}(n_k+1)} \bar{H}_{z,k} \ \text{etc.} \end{aligned}\right\} \tag{2}$$

According to previous findings [3, 4], orbits in fixed-field strong-focusing accelerators have in the general case a complex undulatory configuration. Let us assume that the "waviness" of the orbits

$$X = \frac{r - \bar{r}}{\bar{r}} \text{ and } Y = \frac{z - \bar{z}}{\bar{r}} \tag{3}$$

relative to some "mean" circle $\bar{r}$, $\bar{z}$ is small. Then we shall find, in an approximation [3, 4]:

$$\left.\begin{aligned} X_k &\simeq -\frac{\alpha}{k^2}\left[\bar{H}_{z,k} - \alpha \sum_{m \neq 0} \frac{\bar{H}_{z,m}\left(\bar{H}_{z,k-m} + \bar{r}\frac{\partial \bar{H}_{z,k-m}}{\partial r}\right)}{m^2}\right]; \\ Y_k &\simeq \frac{\alpha^2}{k^2} \sum_{m \neq 0} \left[\frac{\bar{H}_{z,m}}{m^2}\left(im\bar{H}_{\theta,k-m} - \bar{r}\frac{\partial \bar{H}_{r,k-m}}{\partial r}\right)\right], \end{aligned}\right\} \tag{4}$$

where X_k, Y_k are coefficients of a Fourier expansion; $X = \sum_k X_k e^{ik\theta}$, $Y = \sum_k Y_k e^{ik\theta}$. By definition of the mean circle

$$\bar{r} = \frac{1}{\theta_0}\int_0^{\theta_0} r(\theta)\, d\theta, \quad \bar{z} = \frac{1}{\theta_0}\int_0^{\theta_0} z(\theta)\, d\theta, \ \theta_0 = \frac{2\pi}{N} \tag{5}$$

we see that $X_0 = Y_0 = 0$. The dimensional parameter $\alpha = e\bar{r}/pc$ characterizes the position of the mean circle in space for a given momentum value, and is found from Eq. (5). The sign of α depends on direction of motion and type of particles (protons, electrons). It may be shown [3, 4] that in the general case

$$\alpha \simeq -\frac{\bar{H}_{z,0}}{2B} \pm \sqrt{\left(\frac{\bar{H}_{z,0}}{2B}\right)^2 - \frac{1}{B}}, \tag{6}$$

where

$$B = -\sum_{m \neq 0} \frac{\bar{H}_{z,-m}}{m^2}\left(\frac{3}{2}\bar{H}_{z,m} + \bar{r}\frac{\partial \bar{H}_{z,m}}{\partial r}\right). \tag{7}$$

At $\bar{H}_{z,0} = 0$, we arrive at $\alpha_1 = -\alpha_2$. In such a symmetrical field, particles of momentum $\pm p$ move in opposite directions around the same mean circle.

Substituting Eqs. (2) into (4), we find, for the annular cyclotron:

$$X_k \simeq -\frac{\alpha}{k^2}\left[\left(1 - \frac{\alpha\bar{H}_{z,0}}{k^2}\right)\bar{H}_{z,k} - \alpha \sum_{m \neq k,\,0} \frac{k+3m}{2m(k-m)^2} \bar{H}_{z,m}\bar{H}_{z,k-m}\right]; \tag{8a}$$

$$Y_k \simeq \frac{\alpha^2}{k^2\Delta}\left[\frac{n}{k^2}\bar{H}_{z,0}\bar{H}_{z,k} - \sum_{m\neq k,\,0}\frac{k(k-m)\Delta^2 - n_{k-m}(n_{k-m}+1)}{m^2(n_{k-m}+1)}\bar{H}_{z,m}\bar{H}_{z,k-m}\right]. \quad (8b)$$

The parameter α is expressed, as before, by Eq. (6), while

$$B = -\frac{3}{2}\sum_{m\neq 0}\frac{|\bar{H}_{z,m}|^2}{m^2}.$$

Where $\bar{H}_{z,0} = 0$ (case of a symmetrical annular cyclotron) and, in addition s = 0; then, for pure sinusoidal modulation of the field:

$$\left.\begin{aligned} X &\simeq \pm\frac{2\sqrt{3}}{3N}\cos N\theta + \frac{5}{12N^2}\cos 2N\theta; \\ Y &\simeq -\frac{\Delta}{3(n+1)}\left[1 - \frac{n(n+1)}{2N^2\Delta^2}\right]\cos 2N\theta. \end{aligned}\right\} \quad (9)$$

As we might well expect, the parameter α is independent, in the first approximation, of the pattern of field variation along the vertical.

It is clear from Eqs. (8) that an annular cyclotron has spatial orbits, while the frequency of vertical "waviness" in the symmetrical cyclotron is twice the frequency of radial waviness. Unfortunately, a field of configuration (1) fails to yield a precisely constant orbit perimeter, since the waviness component Y is dependent on particle momentum [the factor Δ in Eq. (8)]. This dependence may be minimized by choosing the "height" of the operating region $\Delta\bar{z} \ll \bar{r}$, i.e., $n \gg 1$. In that case $\bar{z} \simeq \bar{r} \simeq$ const and the orbital perimeter will be independent of momentum in the first approximation. A precisely constant perimeter is apparently possible in the case where the cylindrical "reference" surface is replaced by a suitable conic surface. This question requires further looking into. Calculations show that "geometrical similitude" of the orbits requires a field which grows exponentially with height: $H \sim e^{\gamma z}$, γ = const.

Studies of stability of particle motion have shown [3] that the condition of "dynamical similitude" is not fulfilled in a ring cyclotron [5]. In fact, in accord with Eqs. (8), the orbit configuration and, as a corollary, the betatron oscillation frequencies depend on particle momentum. However, the variation in oscillation frequencies and orbital perimeter during the acceleration process remain small during the acceleration process, as a general rule, and may be kept within tolerable limits arrived at, one the one hand, in terms of the phase stability of the accelerating voltage and on the other hand by the requirement that the operating point be located at least inside the stability region. Consequently, the condition of dynamical similitude is certainly desirable for a ring cyclotron, but not obligatory.

The stability condition in a ring cyclotron has a cumbersome form in the general case and requires numerical analysis [3]. It becomes simplified only in a symmetrical ring cyclotron; in this case, stability of particle motion requires that N > n.

The author expresses his sincere gratitude to A. A. Kolomenskii and B. N. Yablokov for their valuable comments relating to the work.

LITERATURE CITED

1. A. P. Fateev and B. N. Yablokov, Atomnaya Energiya 8, No. 6, 552 (1960).*
2. J. Teichman, Czech. J. Phys. 9, 262 (1959).
3. A. P. Fateev, Otchet FIAN (Bulletin of the Institute of Physics of the USSR Academy of Sciences) No. A8, 1960.
4. A. P. Fateev, Zhur. tekhn. fiz. 31, No. 2, 238 (1961).
5. A. A. Kolomenskii, Atomnaya Energiya 3, No. 12, 492 (1957).*

* Original Russian pagination. See C. B. translation.

A TRAVELING WAVE CASCADE GENERATOR – A NEW HIGH-VOLTAGE SUPPLY FOR ACCELERATOR TUBES

E. M. Balabanov and G. A. Vasil'ev

Translated from Atomnaya Energiya, Vol. 10, No. 4, pp. 375-377, April, 1961
Original article submitted September 22, 1960

The most suitable voltage supply unit for direct-acting ion and electron accelerators with energies in the multi-megaelectron-volt range and beam current of the order of 1 ma or higher is the cascade generator [1]. The principal defect inherent in the conventional cascade-generator circuit, aside from the high cost of capacitors, is the considerable energy storage in the capacitors ($\sim 10^4$ joules), which may result in irreparable damage to the accelerating tube in the event of a dielectric breakdown. Diminishing the amount of energy stored by reducing capacitance is out of the question, since the result would be increased voltage swings and a drop in the rectified voltage.

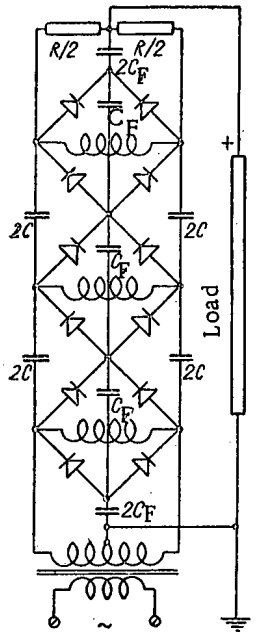

Fig. 1. Circuit of traveling-wave cascade generator (three filter sections shown): R) matching impedance; 2C) charge capacitors; C_F) filter capacitors (upper and lower capacitors of the filter column ($2C_F$) are charged to half voltage.

Investigations were conducted in 1957, at the Physics Institute of the USSR Academy of Sciences, on a traveling-wave cascade-generator circuit proposed by G. A. Vasil'ev [2]. The circuit (Fig. 1) operates as a high-pass LC-filter. Bridge rectifiers in each stage present additional resistance, resulting in lowered equivalent coil Q. If the filter network is matched, i.e., works into a resistive load R (see Fig. 1) equal to the surge impedance, the input impedance will also be purely resistive and equal to the surge impedance for frequencies exceeding the filter cutoff frequency $f_0 = 1/(4\pi\sqrt{LC})$. A cascade circuit thus behaves similarly to a section of a long transmission line in the traveling-wave mode.

In order to have the voltage across all stages equal at an assigned rectifier load current, and to minimize power dissipation in the matched impedance R, the LC-filter must be inhomogeneous. The surge impedance of the network must increase: an effect brought about by increasing the inductance or by simultaneously increasing the inductance and decreasing the capacitance of the charging capacitors.

Completed calculations have shown [2] that the number of stages present in a traveling-wave circuit may attain the sum of 1000, but that despite the increase in the number of stages used (far exceeding that of conventional circuitry) the capacitances in each stage not only show no increase, but rather an appreciable decrease. The energy stored up in the circuit capacitors is correspondingly reduced, the energy being determined in this case by the value of the capacitance of the high-voltage electrode relative to ground.

The circuit inductance coils (see Fig. 1) must be of large size to provide electrical strength and low heat losses. This results in increased equipment dimensions when the insulating properties of the space occupied are not used to full advantage. This difficulty may be overcome by making the inductors in the form of planar pancake coils stacked compactly as shown in Fig. 2. Here, each coil is inductively coupled to a large number (10 to 20) of stages on either side of it. An inductive coupling of this type may be used effectively to reduce heat losses in the coils and to lower the cutoff frequency. To achieve these goals, adjacent coils must be wound in opposing directions.

As the frequency of the supply voltage is reduced, the phase shift between currents in adjacent coils increases and tends to 180° (at the cutoff frequency). When the coils are wound in alternating directions, therefore, the magnetic fields established by adjacent coils operating near cutoff frequency will aid, increasing the effective coil inductance. The result will be a lowering of the cutoff frequency and a decrease in the current flowing through the inductance, i.e., a minimization of heat losses. At a given frequency, the arrangement of coils shown in Fig. 2 will favor a reduction in the capacitance of the charging condensors. The theory behind a similar high-pass inductively coupled LC-filter (known as a distributed transformer) will be published.

In the traveling-wave cascade circuit, the total ripple does not exceed the voltage ripple over a single cascade in order to magnitude, since the appreciable phase shift (100-150°) between variable voltages across adjacent stages tends to average out voltage oscillations. The capacitance of the high-voltage electrode relative to ground (several tens of picofarads under pressurized conditions) turns out to be much higher in this case than the output capacitance of the multiplication circuit per se (not higher than 10 $\mu\mu$f), a fact which also contributes to the suppression of voltage swings. As a result, the amount of ripple remains well within tolerance limits (~ 0.01%), despite the fact that the capacitance of the filtering capacitors is in this case an order of magnitude lower, while the number of stages is an order of magnitude higher, than in conventional circuits.

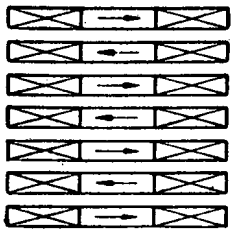

Fig. 2. Arrangement of coils for circuit in Fig. 1, based on the distributed transformer principle. The arrows indicate the direction of winding of the coils.

For the purpose of an experimental study of the properties of the traveling-wave cascade generator, we built the facility shown in the circuit diagram of Fig. 1, an arrangement consisting of fifty stages at 250 kv voltage and 1.5 ma current (operating frequency 7-10 kc). This arrangement is shown in cross section in Fig. 3. The height of each stage is 25 mm. To achieve uniform distribution of voltages over the stages, the inductance of the coils must increase (from 0.3 henry for the lower stages to 1.5 henry for the upper stages) and the capacitance of the charging condensors must fall correspondingly (from 600 to 120 $\mu\mu$f). KVKB-1 ceramic capacitors of 68 $\mu\mu$f rated capacitance were employed for the charging columns. By connecting these capacitors in parallel and using the technological spread in capacitances to good advantage, a smooth tapering off of capacitances can be achieved. The inductance coils (O. D. 210 mm) have a Q value Q = 100-200 at a frequency of 8 kc. AVS-7-3P type selenium rectifiers were used in the circuitry. Seven rectifiers were included in series in each arm of the bridge circuit (cf. Fig. 1). Four shunt-connected POV capacitors with a total capacitance of about 1500 $\mu\mu$f were used in each stage of the filtering column.

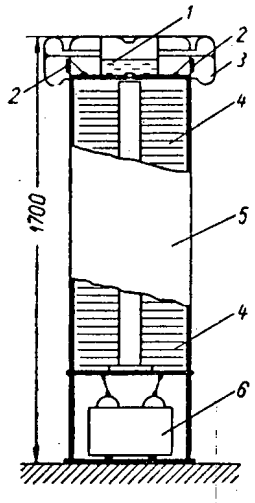

Fig. 3. Diagrammatic cross section through the cascade arrangement, based on a traveling-wave circuit, at 250 kv voltage and 1.5 ma current: 1) oil expansion chamber; 2) matched impedance; 3) guard electrode; 4) stages of multiplication circuit; 5) paper-bakelite tube (filled with pure transformer oil); 6) 4 kilovolt ferrite transformer.

About 200 w, comprising 20% of the total power consumed by the circuit, are produced in the 90-kiloohm matching impedance R (cf. Fig. 1) at full load current. When the load is cutoff, the voltage across the last stage increases 60%. The total rectified voltage thereby increases 30%.

The voltage across the transformer secondary (of the transformer supplying the multiplication circuit) is about 4 kv eff. at a rectified voltage of 250 kv (under load). The variable voltage source is a dynamo generator operated at a frequency f = 8 kc. The voltage oscillations in the arrangement described do not exceed several hundredths of a percent of the total rectified voltage, at full load.

The arrangement operated as a supply source for the accelerator tube. Since all of the capacitances are rather small, no malfunctioning of the multiplication circuit will result from dielectric breakdowns, and there is consequently no need for protective resistors. The circuit will sustain a short-circuit current (20 ma) without serious damage.

The traveling-wave cascade generator holds great promise for applications in high-current direct-acting accelerators with energies up to 5-6 Mev and beam current of about 1 ma.

Among the other advantages associated with this circuit, we may note the following:

1) the possibility of using a dielectric for the capacitors of the same compressed gas as is used to insulate the entire facility. Such capacitors can be engineered with ease into the over-all accelerator design, and are capable of post-breakdown recovery.

2) short rise time (~ 10 μsec).

3) the absence in the circuit of any excessively high variable voltage at high frequencies, and the associated coronal discharge.

4) improved operating conditions for semiconductor rectifiers.

5) the possibility of directly connecting the electrodes of the accelerator tube to the stages of the multiplication circuit without the intermediary of a voltage divider, which would consume addition current.

LITERATURE CITED

1. B. S. Novikovskii, Atomnaya Énergiya 4, No. 2, 175 (1958).*
2. G. A. Vasil'ev, Pribory i tekhnika éksperimenta, No. 5, 75 (1959).

MEASURING THE CHARACTERISTICS OF KINETICS OF A REACTOR BY THE STATISTICAL p-METHOD

A. I. Mogil'ner and V. G. Zolotukhin

Translated from Atomnaya Énergiya, Vol. 10, No. 4, pp. 377-379, April, 1961
Original article submitted August 25, 1960

In experiments carried out on one of the thermal subcritical assemblies containing enriched (~ 75% with respect to U^{235}) uranium with a hydrogen moderator, measurements were made of the mean lifetime of instantaneous neutrons and determinations were made of the constants connecting the count rate of the neutron detector with the units of K_{eff} and the absolute level of stationary power.

The measurements were based on the p_0-method described in [1] and relationships [2]

$$\psi(\alpha t) = Z\varphi(\alpha t);\quad Z = \frac{\varepsilon\nu(\nu-1)K_p^2}{(1-K_p)^2\bar{\nu}^2};\quad \varphi(\alpha t) = 1 - \frac{1-e^{-\alpha t}}{\alpha t}.$$

A proportional neutron counter SNM-5 was placed in the active zone of the studied reactor with a preamplifier at four silicon triodes P103. The impulses from the output emitter repeater of the preamplifier (R_H = 560 ohm) were taken by an RK-1 cable to a three-cascade amplifier at the silicon triodes. The total amplification of the signal was 10^4.

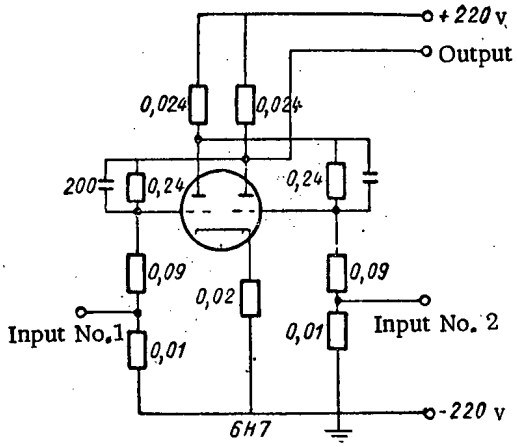

Fig. 1. Circuit of p-element (resistances in Meg, capacitors in $\mu\mu$f).

After passing through a standardizing discriminator the signal passed to the counting arrangement PS-64 (channel $\bar{n}$) and a probability p-element. The latter is controlled by two signals: the impulses of the detector, passing the discriminator, and the impulses of the timer giving the duration of the interval.

The timer was a very simple quartz generator at 60 kc on the 6Zh4 tube. The lower frequency was achieved using the counting systems.

The probability p-element (Fig. 1) is a trigger with two stable states and is controlled by impulses of negative polarity. After the signal of the timer the right triode remains in the closed state and the left triode remains in the open state. The impulses from the detector arriving at the input No. 1 only once during the interval change the state of the triodes and feed one impulse to the counting system of the p-channel. The impulse of the finish or start of the interval restores the initial state of the triodes of the p-element, preparing them to "receive" the impulses of the detector in the next interval. Therefore, the number of counts counted by the channel is equal to the number of intervals in which there is at least one impulse from

* Original Russian pagination. See C. B. translation.

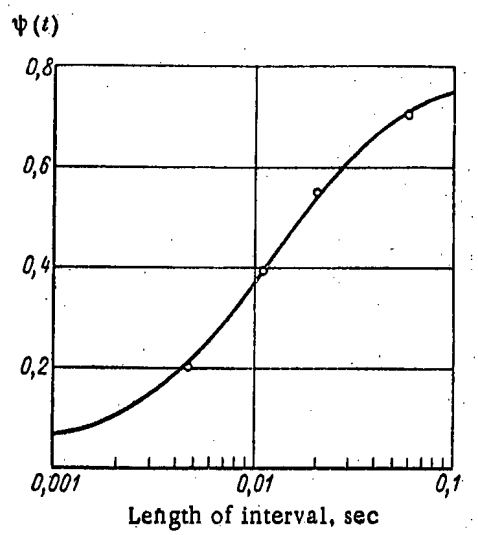

Fig. 2. The dependence of Ψ on the length of the interval of t for $\alpha = 139.8\ sec^{-1}$; Z = 0.806.

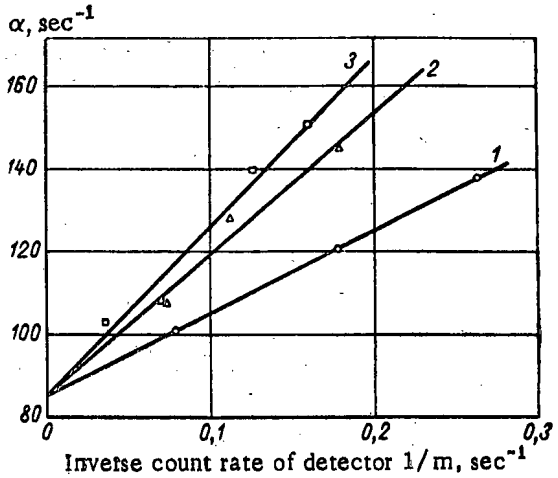

Fig. 3. The dependence of $\alpha = (1-K_p)/l$ on the inverse count rate 1/m of the detector for three series of measurements: 1) first series of measurements; 2) second series of measurements; 3) third series of measurements.

the detector. The total number of intervals is determined by the time of the measurement, the length of the interval is determined by the calibration, the mean load during the interval is determined by the recorded count rate (channel $\bar{n}$) and by the known length of the interval.

For each of the four lengths of the interval t (4.65; 11.0; 21.0 and 61.0 msec), the values of $\bar{n}$ and p_0 can be used to find the corresponding value of Ψ [1]. In order to determine the parameters α and z, the four values of Ψ were treated by the method of least squares. One of the curves of Ψ(t) together with the experimental values of Ψ is given in Fig. 2.

As a result of measurements of the values α and Z for several values of $(1-K_{eff})/\beta_{eff} = c/m$, we obtained values $\alpha_0 = \beta_{eff}/l$ and the constant c, which was determined from the linear equation

$$\alpha = \alpha_0\left(1+\frac{c}{m}\right),$$

and also the absolute effectiveness of the detector ε, connecting the count rate m with the fission counting rate $F = m/\epsilon$. The efficiency of the detector was determined from the mean value $r = Z(\alpha/\alpha_0)^2 = \epsilon\,\overline{\nu(\nu-1)}/\bar{\nu}^2\beta_{eff}^2$, where $\epsilon = 0.616 \cdot 10^{-4} r$.

Figure 3 shows the dependences of α_0 for three series of measurements, giving almost coinciding values of α_0 (85.2; 85.6; 85.2 sec^{-1}). The 50% reliable interval for α_0 calculated on the basis of experimental deviations from linearity is 3%. Assuming that $\beta_{eff} = 0.007$ for the mean life of instantaneous neutrons in the reactor we obtain $l = (0.82 \pm 0.025) \times 10^{-4}$ sec. This values agrees well with the result of a double group calculation ($0.8 \cdot 10^{-4}$ sec) and the value $l = 0.87 \cdot 10^{-4}$ sec obtained from a frequency analysis of reactor noise [3].

The values of K_{eff} calculated from the obtained values of c and m for different positions of the control rod agree with its calibrated curve.

It is very difficult to check the measured values of efficiency of the counter, which are satisfactory under the conditions of the experiments when the intensity of the neutron source in the reactor is only known approximately.

Good results were obtained using a magnetophone, on the film of which the detector impulses were recorded. Using the magnetophone the total time of measurements directly on the reactor was reduced (straight line 3 of Fig. 3) to 1 hr.

The authors would like to thank A. I. Leipunskii, V. V. Orlov, G. I. Marchuk, and V. A. Kuznetsov for their interest in the work and for discussing the results; they would like to thank V. V. Sapozhnikov and A. P. Tarasov for helping with the experiment.

LITERATURE CITED

1. V. G. Zolotukhin and A. I. Mogil'ner, Atomnaya Energiya 10, No. 4, 379 (1961).*
2. Scientific and Technical Fundamentals of Atomic Energy Vol. 2, Edited by K. Goodman. [Russian translation]. Moscow, Foreign Literature Press, 1950, p. 118.
3. C. E. Cohn, Nucl. Sci. and Engng. 5, 331 (1959).

DISTRIBUTION OF THE COUNTING OF A NEUTRON DETECTOR PLACED IN A REACTOR

V. G. Zolotukhin and A. I. Mogil'ner

Translated from Atomnaya Energiya, Vol. 10, No. 4, pp. 379-381, April, 1961
Original article submitted August 25, 1960

The distribution of the counting of a neutron detector placed in a stationary subcritical reactor differs from the Poisson law due to the existence of chains of genetically connected fissions. The mean counting during an interval is heterogeneous and depends on the number of recordings in the previous time interval. This fact forms the basis for the well-known Rossi alpha method [1] for measuring the parameters of kinetics of a reactor.

TABLE 1. Application of the Criterion χ^2 to the Negative Binomial Distribution

i	Experiment 1						Experiment 2					
	choice a			choice b			choice a			choice b		
	ν_i	Np_i	$\frac{(\nu_i-Np_i)^2}{Np_i}$	ν_i	Np_i	$\frac{(\nu_i-Np_i)^2}{Np_i}$	ν_i	Np_i	$\frac{(\nu_i-Np_i)^2}{Np_i}$	ν_i	Np_i	$\frac{(\nu_i-Np_i)^2}{Np_i}$
0	102	104,2	0,05	52	56,7	0,39	299	298,4	0,00	316	324,2	0,21
1	125	119,0	0,30	69	58,9	1,72	228	224,7	0,05	260	232,9	3,16
2	94	97,8	0,15	47	46,4	0,01	125	135,6	0,83	129	138,8	0,69
3	73	69,9	0,14	25	32,6	1,78	83	75,0	0,84	57	77,0	5,22
4	42	46,1	0,37	22	21,6	0,01	44	39,7	0,47	49	41,2	1,47
5	28	29,1	0,04	16	13,7	0,38	16	20,4	0,94	20	21,5	0,11
6	17	17,6	0,02	7	8,5	0,26	9	10,2	0,15	13	11,1	0,33
7	27	24,3	0,30	13	12,6	0,02	10	9,9	0,00	14	11,3	0,66
Total	508	508,0	1,37	251	251,0	4,57	814	814,0	3,28	858	858,0	11,85

Note: Here N is the total number of intervals; p_i is the probability of having i counts in the interval for i = 0,1.... 6; p_7 the probability of seven or more counts; ν_i is the actually observed number of intervals.

With heterogeneity of the mean counting it might be expected [2] that the actual distribution of the number of recordings is satisfactorily described by a negative-binomial distribution, the derivative function of which has the form

$$\Pi(z)=p_0+p_1z+p_2z^2+\ldots=[1-\psi(z-1)]^{-\frac{\bar{n}}{\psi}}, \quad (1)$$

where $p_k = 1/k!\,(d^k\Pi(z))/dz^k\,\big|_{z=0}$ is the probability of k counts in a given interval; $\bar{n}$ is the mean counting during the interval; the parameter Ψ is connected with the dispersion of the number of records by the relationship

$$\bar{n}^2-\bar{n}^2=\bar{n}(1+\psi).$$

* Original Russian pagination. See C. B. translation.

The Poisson law is obviously a limiting case of the negative-binomial distribution when $\Psi \to 0$.

For an experimental check for the distribution of (1), the impulses from a proportional counter SNM-5, placed in the reactor, were recorded together with the time readings on the film of a loop oscillograph and then counted visually. Tables 1 and 2 show the results for the use of the criterion χ^2 for two cases, each of which includes two selections. For three selections the agreement between the experimental data and the law of distribution (1) was good; in experiment 2b (see Tables 1, 2) "almost significant" deviation was detected, mainly due to the small number of intervals with three counts. However, the component selection including all 814 + 858 = 1672 intervals also shows good agreement with formula (1). The negative-binomial distribution therefore agrees well with the experimental data.

In [3] it was shown that in the case of a stationary subcritical reactor the dispersion of the number of counts of the detector is expressed by the formula

$$\overline{n^2}-\bar{n}^2=\bar{n}(1+\psi),\ \psi=\frac{\varepsilon\overline{\nu(\nu-1)}K_p^2}{(1-K_p)^2\bar{\nu}^2}\left(1-\frac{1-e^{-\alpha t}}{\alpha t}\right).$$

Here K_p is the multiplication factor at the instantaneous neutrons; $\alpha = (1-K_p)/l$; l is the mean lifetime of the instantaneous neutrons; t is the duration of the interval of measurement; ϵ is the efficiency of the detector (the counting for one division).

The measurement of Ψ makes it possible to determine the mean lifetime of the neutrons, the absolute power of the reactor and to calibrate the regulator in units of K_{eff}.

In the Feinman alpha method [4], similar to the correlation method of V. Gol'danskii and M. Podgoretskii [5], the values of $\bar{n}$ and $\overline{n^2}$ are measured directly. The measurement of the latter requires "memory" of the counting in a given interval, raising it to the square (during this time the circuit does not count) and feeding to the counting circuit for averaging over a large number of intervals. The limited volume of memory limits the count rate, which is particularly difficult to achieve in the case of a thermal reactor when comparatively long intervals are essential.

TABLE 2. Parameters Obtained by Treating Experiments in Table 1

	$\bar{n}$	Ψ	χ^2_{min}	P
Experiment 1:				
choice a	2.285	1.00	1.36	0.93
choice b	2.24	1.15	4.56	0.47
Experiment 2:				
choice a	1.378	0.81	3.28	0.66
choice b	1.365	0.90	11.8	0.04

Note: Here the parameters $\bar{n}$ and Ψ are found from the system of equations $\partial\chi^2/\partial\bar{n} = \partial\chi^2/\partial\Psi = 0$; $\chi^2 = \sum_0^7 (\nu_i - N_{pi})^2/N_{pi}$; $P = P(\chi^2 > \chi^2_{min})$ is the probability of obtaining $\chi^2 > \chi^2_{min}$.

A knowledge of the counting distribution makes it possible to avoid most of these difficulties, for which it is sufficient to measure $\bar{n}$ during time t and any probability p_k. From these experimental values it is possible to find the parameter Ψ. In particular, when $\bar{n} \lesssim 3$ it is sufficient to measure the probability p_0 of the absence of counts. As follows from the distribution (1), the parameter Ψ is connected with the experimental data by the following relationship:

$$Q \equiv \frac{1}{\bar{n}} \ln \frac{1}{p_0} = \frac{\ln(1+\psi)}{\psi},$$

where the value Q is determined by the simplest radiotechnical means, permitting the simultaneous measurement of Q for several lengths of intervals, which considerably reduces the duration of the experiment compared with the Feinman alpha method.

The calculations lead to the following expressions for statistical errors in the parameter Ψ:

$$N\overline{\left(\frac{\delta\psi}{\psi}\right)^2} = \frac{(1+\psi)[1+2(1+\psi)(\bar{n}+\psi)]}{\bar{n}\psi^2} \qquad \text{(Feinman alpha method);}$$

$$N\overline{\left(\frac{\delta\psi}{\psi}\right)^2} = \frac{1}{(1-1/\Theta)^2}\,\frac{\Theta+\dfrac{e^x-1}{x}-2}{x} \qquad (p_0\text{-method}),$$

where $x = \bar{n}Q$; $\Theta = Q(\Psi)(1 + \Psi)$; N is the total number of time intervals. In the region $\bar{n} \lesssim 3$ both methods lead to approximately the same errors.

For larger values of $\bar{n}$ the probabilities p_k or $q_k = p_k + p_{k+1} + \ldots$ should be measured for larger values of k. The analogy of the correlation bonds in the reactor and in problems which are usually solved by means of the technique of delaying coincidences or by the correlation method would seem to indicate that this method will also find application in this field due to the simplicity in the experimental technique and the possibility of operating with identity of particles emitted by the parent and daughter nuclei.

In [6] results are given for the application of the p_0-method to the measurement of characteristics of kinetics of one of the experimental reactors.

LITERATURE CITED

1. J. Orndoff, Nucl. Sci. and Engng. 2, 450 (1957).
2. G. Kramer, Mathematical Methods of Statistics [Russian translation]. Moscow Foreign Literature Press, 1950.
3. Scientific and Technical Fundamentals of Atomic Energy, Vol. 2, Edited by K. Goodman. [Russian translation]. Moscow, Foreign Literature Press, 1950, p. 118.
4. J. Bengston et al., Report No. 1783 presented by the USA to the Second International Conference on the Peaceful Uses of Atomic Energy (Geneva, 1958).
5. V. Gol'danskii and M. Podgoretskii, Dokl. AN SSSR, 100, 237 (1955).
6. A. I. Mogil'ner and V. G. Zolotukhin, Atomnaya Énergiya 10, No. 4, 377 (1961).*

THE DENSITY OF A VOLUME HEATED STEAM WATER MIXTURE

V. K. Zavoiskii

Translated from Atomnaya Energiya, Vol. 10, No. 4, p. 381, April, 1961
Original article submitted November 4, 1960

The density of the moderator in a homogeneous boiling reactor depends on the distribution of superheat in the liquid and on the distribution of centers of steam formation throughout the volume of the active zone. The problem of the relation between the density of the moderator and the reactor power output has so far not been solved.

In the present paper this relation is established for the special case that the superheat of the liquid is uniform throughout the whole volume and the centers of steam formation are located in the lower part of the active zone. There is reason to believe that these conditions are realized in reactors which have small steam content.**

The distribution of the density along the height with volume heating of the liquid between two electrodes arranged horizontally has been studied in another paper.*** Here the superheat of the liquid was uniform along the height and the steam bubbles were formed on the surface of the lower electrode.

It has been shown that in the space between the electrodes, the volume steam content φ increases proportionately to the square of the distance z from the lower electrode:

$$\varphi \sim z^2. \tag{1}$$

Above the top electrode the steam content remains constant and equal to the steam content on bubbling the steam to an extent which corresponds with the power developed between the electrodes. Thus for the region above the top electrode there exists the relation

$$N = k\varphi(H) \tag{2}$$

* Original Russian pagination. See C. B. translation.

** A more detailed consideration of this question will come out beyond the limits of this letter.

*** V. K. Zavoiskii, Atomnaya Energiya 10, No. 3, 272 (1961).

where N is the power developed between the electrodes, $\varphi(H)$ is the volume steam content over the top electrode, k is the proportionality coefficient and H is the distance between the top and bottom electrodes.

If we use the expression for φ from the paper mentioned [see Eq. (1)] the mean steam content in the liquid volume included between the electrodes will be

$$\bar{\varphi}=\frac{1}{H}\int_0^H \varphi dz=\frac{1}{3}\varphi(H). \tag{3}$$

Thus if other conditions are the same in the volume heated liquid, the mean steam content along the height is three times less than with bubbling steam.

Using the expression for $\varphi(H)$ from the Eqs. (2) and (3), we find

$$N = 3k\varphi. \tag{4}$$

Equation (4) relates the value of the mean steam content (the density of the steam water mixture) with the power developed in the volume heated liquid.

The results obtained are applicable in the case where steam entrainment by the liquid may be neglected.

STUDY OF THE SPECTRA OF THERMONEUTRONS IN TEST REACTORS WITH A MONOCHROMATOR

Yu. Yu. Glazkov, B. G. Dubovskii, F. M. Kuznetsov,

V. A. Semenov, and Pen Fan

Translated from Atomnaya Energiya, Vol. 10, No. 4, pp. 381-383, April, 1961
Original article submitted December 7, 1960

The experiments were carried out on a uranium graphite reactor in the center of which was placed an experimental subcritical assembly. Experiments were being made on different diameters of the subcritical assembly to determine the optimum (the number of fuel channels was being changed).

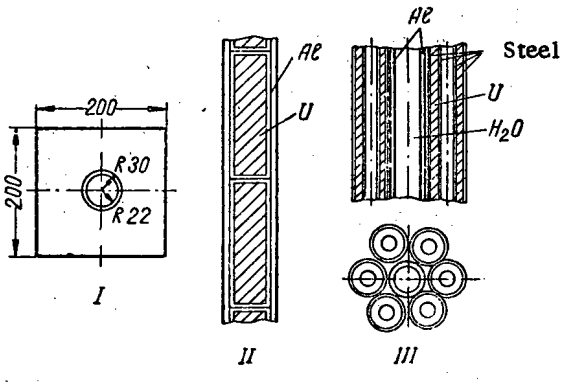

Fig. 1. Elementary cell and test channels. I) cell; II) channel with 2% enriched uranium; III) channel with 1.2% enriched uranium.

In this work a monochromator was being used which had been constructed for measuring the spectra of thermal neutrons from test reactors of small power output [1]. The number of neutrons going through the rotor and counted by the detector per second is given by the expression

$$N=\frac{n(v_0)v_0}{4}\frac{1}{2\pi}Sdh\frac{d}{H}\frac{S}{L}\frac{h}{L}\frac{v_0^2\eta\delta}{(\omega r_{cr})^2}\nu\frac{n}{60},$$

where N is the number of detector counts per second $n(v_0)v_0$ is the neutron flux in the center of the reactor corresponding with unit interval of velocity, n is the number of rotations of the rotor per minute, S, L, h are respectively the width, length and height of the collimator, d is the width of the rotor slit, H is the length of the rotor, r_{cr} is the distance from the axis to the middle of the rotor slit; ν is the

number of slits in the rotor; $v_0 = \omega r_{cr}/\alpha_0$ is the velocity of the neutrons being cutoff at a given angle of rotation of the rotor α_0 and a given angular velocity of the rotor ω; η is the efficiency of the detector for neutrons of velocity v_0; δ is a coefficient which takes account of the absorption of neutrons of velocity v_0 in air.

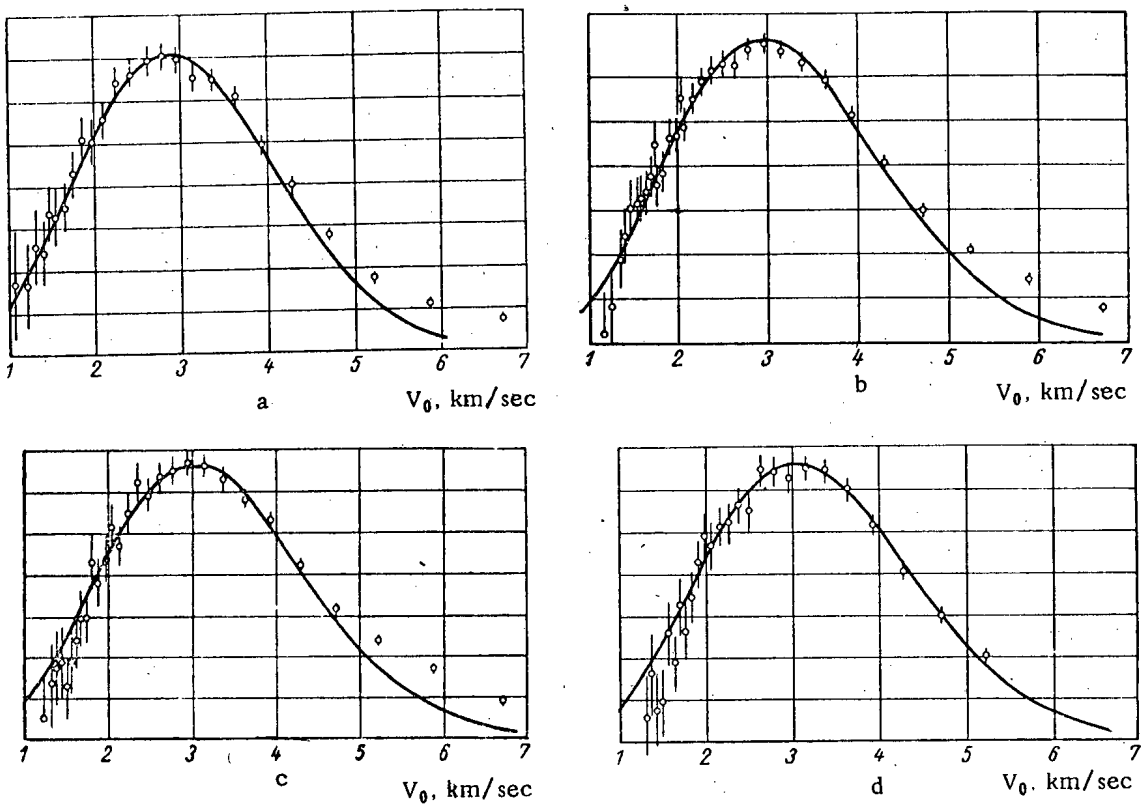

Fig. 2. Neutron spectra. a) Neutron spectrum in a lattice of test channels containing 2% enriched uranium ($\Phi = 0.0691\ v^3e^{-0.1862\ v^2}$, T = 325°K); b,c,d) neutron spectra in subcritical assemblies consisting of 13, 25 and 37 test channels respectively (b – $\Phi = 0.0612\ v^3e^{-0.1749\ v^2}$; T = 346°K; c – $\Phi = 0.0545\ v^3e^{-0.1652\ v^3}$, T = 366°K, d – $\Phi = 0.053\ v^3e^{-0.1634\ v^2}$, T = 370°K).

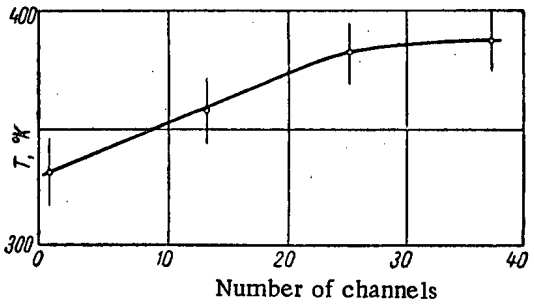

Fig. 3. Temperature of the neutron gas is a function of the number of test channels filled with 1.2% enriched uranium.

The resolution of the monochromator is given by the expression

$$\frac{\Delta v}{v_0} = \frac{v_0}{\omega r_{cr}}\left[\frac{S}{L} + \frac{1}{3}\frac{d}{H} + \frac{1}{4}\frac{h}{r_{cr}}\left(1 + \frac{H}{L}\right)\frac{\omega r_{cr}}{v_0}\right],$$

where Δv is the half width of the resolution curve, S/L + + (1/3)(d/H) is a half width of the static transmission curve (the number of neutrons passing through the rotor per unit of time as a function of α_0 the angle of rotation of the rotor when it is not moving relative to the beam of neutrons).

The values of the resolution of the monochromator at a rotor speed of 5000 revolutions per minute are as follows:

v_0, meters per second	Neutron energy, ev	$\Delta v/v_0$, %
1000	0.0052	8
1500	0.0116	11
2000	0.0207	14

v_0, meters per second	Neutron energy, ev	$\Delta v/v_0$, %
2500	0.0323	17
3000	0.0465	20
2500	0.0637	23
4000	0.0826	26
4500	0.1046	29
5000	0.1292	32

In the subcritical assembly, uranium with 1.2% enrichment was used. In the external zone of the reactor 2% enrichment was used. The dimensions of the elementary cell and the construction of the test channel are shown in Fig. 1.

The neutron beam was taken from the center of the subcritical assembly. A graphite plug was located in the cross section of the central test channel and the plain boundary of the plug served as a mirror for the beam. The diameter of the channel for taking out the neutron beam was 50 mm. The neutron spectrum was measured for three dimensions of the central subcritical assembly. The spectral distribution of neutrons approximating the experimental value was found by the method of least squares under the assumption that the neutron spectrum in the reactor is Maxwellian. Calculating the results of the measurements by the method of the least squares was done for a different number of experimental points; that is, with different upper limits of neutron velocity. This made it possible to exclude experimental points on which the spectrum in the intermediate range had an appreciable influence. The spectra were calculated up to $v_0 \sim 4000$ meters per second. The resolution correction was small and was not made in the calculations.

The experimental spectra and the neutron distributions approximating them for a lattice consisting completely of test channels with uranium enriched to 2% and for different dimensions of the experimental subcritical assembly are shown in Fig. 2.

Figure 3 shows the temperature of the neutron gas as a function of the number of test channels in the subcritical assembly. It follows from this curve that in the center of a subcritical assembly consisting of 37 cells of the type under study, a spectrum of thermal neutrons is established which is the same as the spectrum in a critical assembly consisting completely of test channels of the type under investigation.

The equivalent radius of a subcritical assembly consisting of 37 cells was equal to 68 cm. For the lattice under study the moderation length was $\sqrt{\tau} = 17$ cm, and the diffusion length was $L = 14$ cm.

With the monochromator described it is possible to make measurements on the thermal neutron spectrum in low-power reactors up to a velocity of about 5000 meters per second. The experimental accuracy is such that the effective temperatures of the neutron gas can be calculated (under the assumption that the neutron spectrum in the reactor is only slightly different from Maxwellian) with an accuracy up to about 4%.

In evaluating the errors no account was taken of the inaccuracy in measuring the power level of the reactor (in our case it amounted to about 0.5%) or the error caused by instability in the working of the apparatus, which can be substantial, in view of the one channel feature of the monochromator.

In measuring the neutron spectra for a velocity above about 5000 meters per second and a rotational speed of 5000 per minute for the rotor, difficulties arise from the need to make considerable resolution corrections. Improving the resolution of the monochromator by increasing the rotational speed presents mechanical difficulties.

LITERATURE CITED

1. A. P. Senchenkov and F. M. Kuznetsov, Atomnaya Energiya 5, No. 2, 124 (1958).*

* Original Russian pagination. See C. B. translation.

TURBULENT HEAT TRANSFER IN A STREAM OF MOLTEN METALS

V. I. Subbotin, M. Kh. Ibragimov, M. N. Ivanovskii,

M. N. Arnol'dov, and E. V. Nomofilov

Translated from Atomnaya Energiya, Vol. 10, No. 4, pp. 384-386, April, 1961
Original article submitted July 14, 1960

The present level of development in the theories of turbulence do not permit an analytical determination of the turbulent transfer of heat in a liquid stream. Widespread use has therefore been made of semiempirical theories of heat exchange based on the use of the analogy between heat transfer and the amount of movement. By making various assumptions the authors of these theories have calculated turbulent heat transfer, have found the temperature field in a liquid stream and the coefficients of heat transfer. The correctness of the assumptions in the semiempirical theories can be checked by measuring the temperature fields in molten metals. Due to the high thermal conductivity of molten metals the main temperature drop is concentrated not in the thin laminar sublayer, as in ordinary liquids, but is also extended into the turbulent nucleus. This permits a fairly accurate determination of the temperature gradient throughout the section of the tube and the assumptions in the semiempirical heat-exchange theories can be checked.

Martinelli was the first to apply the theory of the hydrodynamic analogy for molten metals with an allowance for molecular thermal conductivity in a turbulent nucleus. In the calculations it was assumed that the ratio of the coefficients of turbulent heat transfer and the amount of movement ϵ_a/ϵ_ν is independent of the radius and the rate of flow. Lyon obtained a general equation for the coefficient of heat transfer in a tube:

$$\frac{1}{Nu}=2\int_0^1 \frac{\left[\int_0^1 \frac{u}{w}\xi d\xi\right]^2}{\left(1+\varepsilon\frac{\varepsilon_\nu}{\nu}Pr\right)\xi}d\xi, \tag{1}$$

where $\xi = r/r_0$ and, using the main assumptions of Martinelli, he represented the results of the calculation for $\epsilon = \epsilon_a/\epsilon_\nu = 1$ by the formula

$$Nu = 7 + 0.025\,Pe^{0.8}. \tag{2}$$

Most of the experimental data on heat transfer to molten metals, obtained under conditions where the content of oxides and the purity of the heat-exchange surface are not controlled, is much lower than the values calculated from formula (2). Before the appearance of reliably measured temperature fields in a stream of molten metals the difference between the experimental data and the results of the Martinelli-Lyon theory were due to the incorrectness of the assumption that $\epsilon = 1$. Based on the high thermal conductivity of molten metals, Voskresenskii, Deissler, Jenkins and others tried to consider analytically the heat transfer by thermal conductivity from separate moles to the surrounding medium. The values of ϵ were much less than unity. Voskresenskii, Likoudis and Touluk'yan in the determination of the value of ϵ used certain experimental data on heat transfer to molten metals; however, they assumed incorrectly that the thermal contact resistance was absent in these data. The turbulent heat transfer and, consequently, the value of ϵ for the molten metals was therefore unnecessarily low.

The experimental data in the literature are not sufficient to reliably solve the problem on the value of ϵ for molten metals. On the basis of measured temperature fields in streams of water and molten metals, the authors of the present work tried to determine the coefficient of turbulent heat transfer and the ratio ϵ for molten metals and tried to find the effect of the thermal conductivity of the liquid on these values.

The coefficient of turbulent heat transfer was determined from the equation

$$\varepsilon_a=\frac{q/q_0}{\partial t/\partial\xi}\frac{r_0q_0}{c_p\gamma}-a. \tag{3}$$

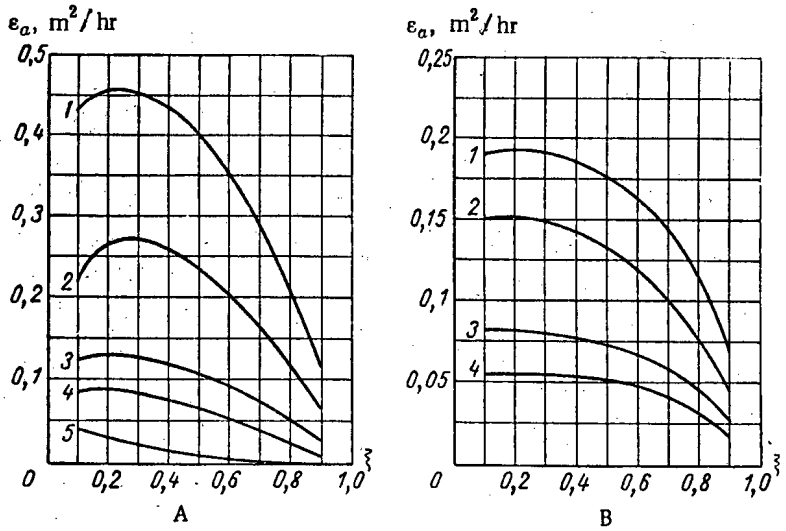

Fig. 1. Distribution of the coefficient of turbulent heat transfer throughout the section of a tube at different Re numbers: A) heavy metal. The values of the Re numbers are as follows: 1) 200,000; 2) 120,000; 3) 60,000; 4) 38,000; 5) 12,100; B) alkali metal. The values of the Re numbers are as follows: 1) 24,500; 2) 16,500; 3) 11,000; 4) 7900.

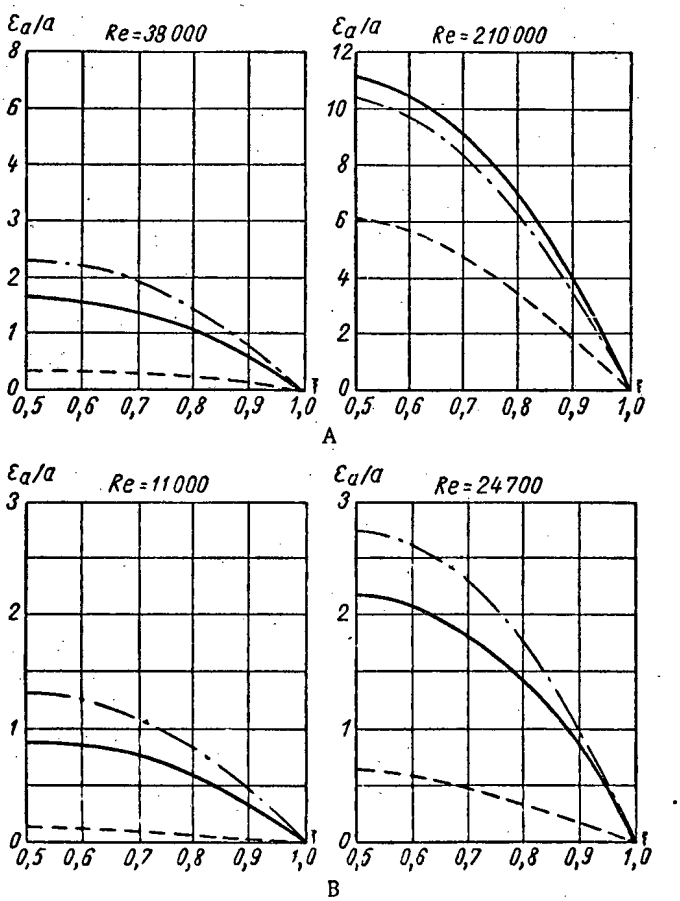

Fig. 2. Change in the ratio ε_a/a throughout the section of a tube for molten metals. (A is a heavy metal; B is an alkali metal): —— experimental curve; –·–·– curve calculated from the Lyon theory: – – – – curve calculated from the Voskresenskii theory.

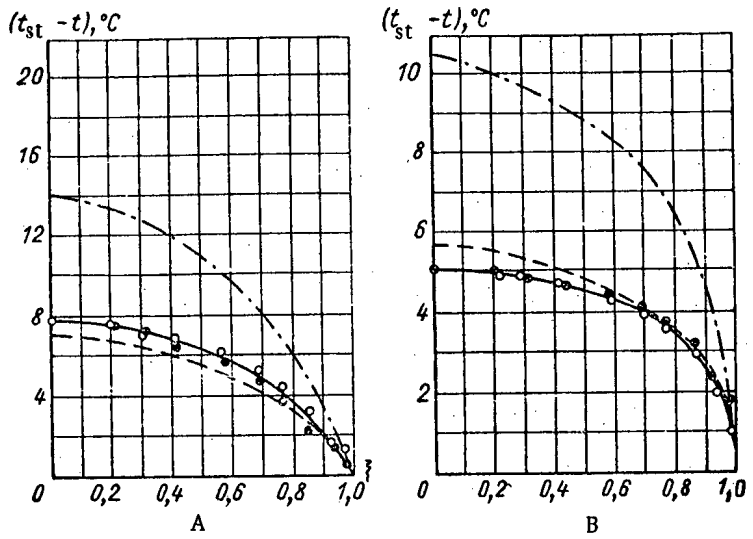

Fig. 3. Comparison of the experimental and calculated temperature field in a stream of heavy molten metal: A) Re = 26,900, Pr = 0.022, q = 18,700 kcal/m^2 · hr; B) Re = 228,000, Pr = 0.022, q = 47,600 kcal per m^2 · hr; —— curve averaging the experimental points (○ and ●) obtained by two thermocouples; – – – curve calculated by the Lyon equation (1); – · – · – curve calculated from the Voskresenskii formula.

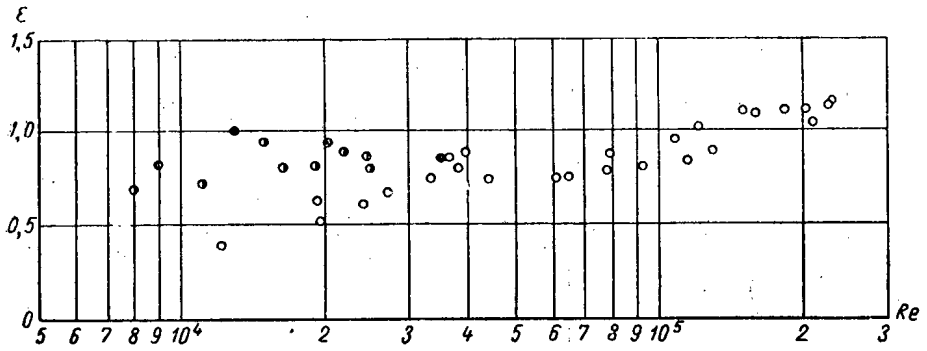

Fig. 4. Dependence of ϵ on Re at ξ = 0.8 for various liquids: ●) water (Pr ≃ 10); ◑) alkali metal; ○) heavy metal (Pr << 1).

The ratio of the local thermal stream to the stream at the wall was found from a relationship obtained from the equation of thermal balance of an elementary volume of liquid, using the law of universal distribution of rates,

$$q/q_0 = \frac{1}{\xi}\frac{u^*}{w}\left[(4{,}25 + 2{,}5\ln y^+)\xi^2 - 2{,}5\xi - 2{,}5(1-\xi^2)\ln\frac{r_0}{y}\right]. \qquad (4)$$

The graphically calculated temperature gradients were used to determine ϵ_a from formula (3). Figure 1 shows the distribution of ϵ_a throughout the section of the tube. The coefficient ϵ_a increases with distance from the wall and with increase in the criterion Re. It should be mentioned that the coefficient ϵ_a is not equal to zero at the axis of the tube. However, due to the high error in the determination of ϵ_a in the central zone of the stream (ξ < 0.4) it is difficult to talk of an accurate value of this coefficient in the center of the tube. Figure 2 compares the value of ϵ_a/a obtained experimentally with the results of calculations from the Lyon and Voskresenskii formulas. Heat transfer, even to molten metals having a high thermal conductivity, is largely determined by the turbulent heat transfer, especially at high Re numbers. In his calculations Voskresenskii overestimated the molecular heat transfer. This conclusion is

arrived at on comparing the temperature fields found experimentally and those calculated from the theoretical relationships of Lyon and Voskresenskii (Fig. 3). The temperature profile calculated from the Voskresenskii theory lies much higher than the experimental points. The experimental data agree more satisfactorily with the value of the temperature field calculated from the Lyon relationship (1). With an Re number ≃ 30,000 the experimental points lie higher, and with Re numbers ≃ 200,000 they are lower than the Lyon curve. The assumption that $\epsilon = 1$ apparently leads to an increased role of the turbulent heat transfer at moderate Re numbers and to a reduction at high Re numbers. This character of change in ϵ as a function of the Re number is very logical. It is probable that at small Re numbers the heat losses transferred by a mole, due to the high thermal conductivity of the liquid, can be higher than the losses of the amount of movement, i.e., $\epsilon < 1$. With strongly developed turbulent flow, moles can form for which the amount of movement is lost more rapidly than the heat ($\epsilon > 1$). Figure 4 gives the dependence of ϵ on the Re number for $\xi = 0.8$ for molten metals (Pr << 1) and water (Pr ≃ 10). The value ϵ_ν was calculated from the formula

$$\xi_\nu = \frac{u^*\left(1-\frac{y}{r_0}\right)y}{2{,}5}-\nu. \tag{5}$$

Within the limits of accuracy of the experiments it can be assumed that the Pr criteria have very little effect on the value of the coefficient ϵ. It is probable that for liquids with a different thermal conductivity the mechanism of turbulent heat transfer is the same and is mainly determined by the hydrodynamics of flow. Experiments showed that the value of ϵ changes with increase in the distance from the wall; however, in a region which determines the heat exchange ($\xi = 0.5$-0.9) this value was approximately constant.

The experimental values of the coefficient ϵ_a were used to determine the Nu criterion from formula (1). The Nu numbers found by this method are satisfactorily described by formula (2) at Re numbers equal to 500-5000; they coincide well with values of the Nu numbers which were calculated from the mean temperature head obtained from the measured temperature profile from the radius of the tube.

POWER LOSSES AND THE INITIAL TORQUE OF A SHAFT IN A FROZEN SODIUM SEAL

A. V. Drobyshev and N. M. Turchin

Translated from Atomnaya Energiya, Vol. 10, No. 4, pp. 386-387, April, 1961
Original article submitted December 10, 1960

Experience has shown that one of the most reliable seals for the shaft of a sodium pump is a seal of frozen sodium [1]. However, the operation of this seal involves unavoidable power losses due to friction.

In [2] it is stated that the power losses in the seal are several kilowatts. These investigations are not described in detail. The power losses due to friction in such a seal cannot be calculated accurately, because the detailed operating conditions of the seal are not known. The present work was therefore carried out in order to experimentally determine the power losses due to friction in a seal of frozen sodium. An apparatus was constructed which used a pump described previously [1]. The sodium in the seal was frozen by water cooling. The water passed through three independent sections.

At the section of the frozen sodium the temperature was measured by thermocouples at 18 points. The shaft was driven by a dc electric motor of 1.6 kw power. The speed of the motor was determined by a tachometer and stroboscope. The power used was measured by astatic instruments (ammeter and voltmeter) of class 0.5.

The experiments started with the measurement of power losses in the electric motor at different speeds in idle running. This made it possible to establish the total power losses due to friction in the antifriction bearings, in the cooling of the electric motor, etc.

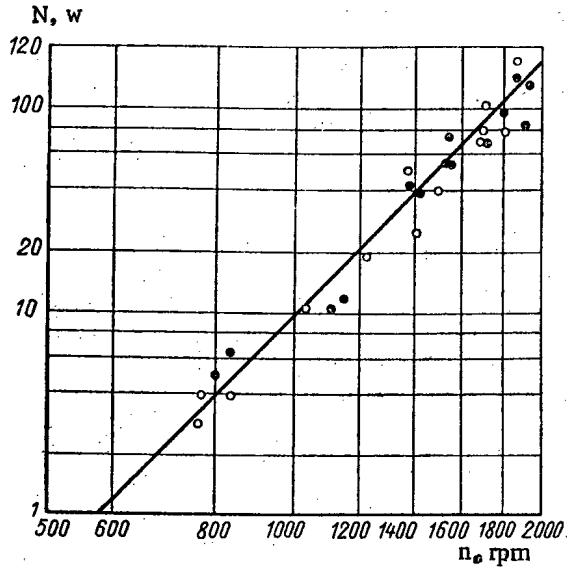

Fig. 1. Dependence of the power loss due to friction in a seal of frozen sodium on the shaft speed: ○) water; ●) sodium.

After the test in idle running, distilled water was poured into the apparatus. The power losses due to friction at the section which would be later occupied by frozen sodium were

$$N = 10^{-11} n^4,$$

where N is the power in watts; n is the number of revolutions per minute.

After the experiments with water the apparatus was dried and filled with sodium. The sodium temperature in the experiments was 400°C. The results of the measurements with sodium and with water coincided.

It can be seen from Fig. 1 that the power lost in the frozen sodium seals is 0.7-1% of the power needed to pump the sodium and, consequently, cannot be allowed for when designing such pumps.

The rate of leakage of the sodium through the seal is 2-3 cm^3/day. Assuming the flow to be laminar and knowing the pressure drop it is possible to evaluate the thickness of the molten sodium film. It is 15-20 μ.

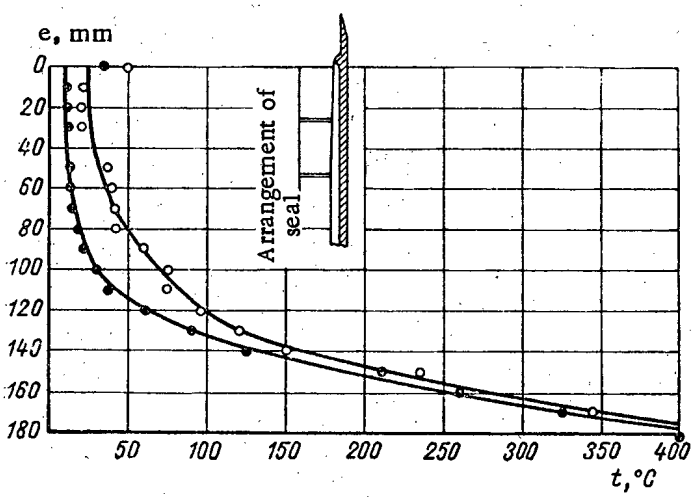

Fig. 2. Temperature distribution at the section of frozen sodium: ○) top section connected; ●) three sections connected.

Figure 2 gives the temperature distribution along the height l of a seal at different intensities of cooling. The length is measured from the top end of the upper section of cooling.

The second part of the work was to measure the initial torque needed to rotate the shaft. To the shaft of the apparatus described above, instead of the electric motor, a lever with a DS-0.2 dynamometer was fastened. As would be expected, when the sodium in the seal was in the liquid state the torque needed to rotate the shaft was very small. Reducing the temperature below the sodium solidification temperature led to a sharp increase in the torque. During the experiments the temperature distribution was measured along the height of the section of the seal, which made it possible to determine the size of the shaft surface in contact with the solidifying sodium.

The results of the measurements are shown in Fig. 3. The tangential stress τ is related to the torque by the following relationship:

$$\tau = \frac{2M}{\pi h d^2} \text{ kg/cm}^2,$$

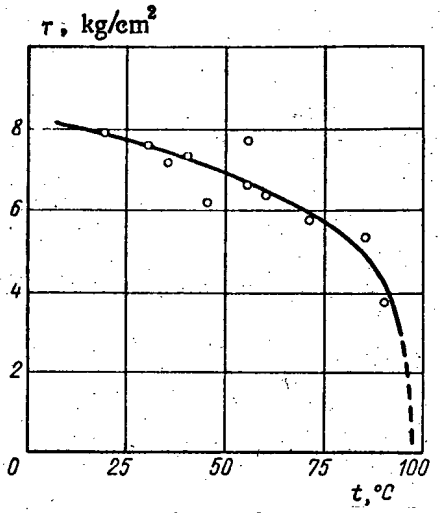

Fig. 3. Dependence of the tangential stress τ at the initial moment of rotation of the shaft on the temperature.

where M is the torque (kg·cm); h is the height of the solidifying sodium (cm), d is the diameter of the shaft (cm).

Finally it should be mentioned that with the pressure of the molten sodium increased from 0 to 3 atm the power losses due to friction and the torque of the shaft did not change.

LITERATURE CITED

1. P. L. Kirillov et al., Atomnaya Énergiya 7, No. 11 (1959).*
2. R. Saigan and A. M. Stell, Voprosy yadernoi energetiki No. 3, 40 (1957).

CALCULATING THE STREAMING OF FAST NEUTRONS ALONG THE CYLINDRICAL CHANNELS IN A BIOLOGICAL SHIELD

B. R. Bergel'son

Translated from Atomnaya Énergiya, Vol. 10, No. 4, pp. 388-389, April, 1961
Original article submitted November 21, 1960

When calculating the biological shield for reactors, especially reactors with gas coolants, serious difficulties arise when determining the streaming of neutrons along the hollow channels and the resulting weakening of the shield. In a number of published papers [1, 2] the main equation determining the streaming of neutrons along a channel is that of [3]:

$$I=\frac{I_0\pi\delta^2}{2\pi H^2}\left[1+A\frac{\alpha}{1-\alpha}+B\frac{4\delta\alpha}{H(1-\alpha)}\right]. \quad (1)$$

Here I is the neutron flux at the exit from the cylindrical channel of radius δ and length H; I_0 is the intensity of the isotropic plane source placed at the entry to the channel; α is the albedo of the walls of the channel. The first term of the right side of the equation determines the fraction of unscattered neutrons emitted directly from the source, the second and third terms determine the fraction of neutrons reflected by the walls of the channel. Equation (1) was obtained with the condition that the energy of the neutrons during scattering does not change and the angular distribution of the reflected neutrons has the form

$$\frac{dI_{\text{ref}}}{d\Omega}=\frac{A+2B\cos\vartheta}{2\pi}\alpha I'. \quad (2)$$

The coefficient A characterizes the isotropic distribution; the coefficient B characterizes the cosine distribution (A + B = 1).

The albedo of the walls of the channel was determined experimentally. In particular, for water and concrete it was found that $\alpha \simeq 0.1$ [4]. The scattering properties of various materials for fast neutrons of the fission spectrum are relatively close. It can therefore be assumed that α of the basic materials used in the shield has a value of the same order as α for water or concrete.

* Original Russian pagination. See C. B. translation.

When $\alpha \simeq 0.1$ and $\delta < H$, equation (1) becomes simpler:

$$I = \frac{I_0 \pi \delta^2}{2\pi H^2}. \tag{3}$$

Therefore the streaming of fast neutrons along a hollow straight channel in the shield according to Eq. (3) is determined by the geometrical collimation of the neutron beam by the walls of the channel. However, in [2] it is mentioned that for agreement between the results of calculation using formula (3) and the experimental data obtained for a plane isotropic source, the dimensions of which are much greater than the diameter of the channel, it is essential to introduce a correction factor β to formula (3), equal to 10.

The difference between the experimental data and the results obtained from formula (3) can be explained in the following way: with dimensions of the source which are large compared with the diameter (width) of the channel, the main part of the neutrons determining the streaming can arrive in the channel not directly from the source but by diffusing through the material of the shield from the source toward the walls of the channel.

If it is assumed that the attenuation of fast neutrons in the material of the shield is characterized by the relaxation length λ, then the flux distribution of these neutrons in a flat protective layer can be represented in the form

$$\Phi = \Phi_0 e^{-\frac{x}{\lambda}}. \tag{4}$$

Then the streaming of neutrons along the channel for the case of spherically isotropic distribution with respect to angles of neutrons emitted from the walls of the channel can be evaluated in the following way:

$$I = \frac{I_0}{2}\left(\frac{\delta}{H}\right)^2 \beta,$$

where

$$\beta = 1 + \frac{\Phi_0}{I_0}\frac{H^2}{2\delta}\int_0^H \frac{e^{-\frac{x}{\lambda}}}{(H-x)^2+\delta^2}\,dx. \tag{5}$$

the effective region of integration of Eq. (5) is $0 \leq x \lesssim 2\lambda$. Hence, it follows that to determine the streaming of neutrons along the channel it is necessary to know the distribution of neutron flux in the medium surrounding the channel at distances not greater than $\sim 2\lambda$ from the plane source.

We use an age approximation to find this distribution. We will consider a flat infinite layer of shield of thickness H, weakened by one straight cylindrical channel of radius δ and length H. Fast neutrons with an energy E_0 and intensity I_0 neutrons/cm^2·sec arrive at this layer (x = 0) from the "void." For most cases of practical interest the following conditions hold: $\delta \lesssim l_s$; $H \gg \lambda$ and $H \gg \delta$. Therefore when finding neutron flux distribution in the protective layer it is possible to neglect the effect of the boundary at x = H (the protective layer of finite thickness is replaced by a semiinfinite layer) and the perturbation of the stream introduced by the hollow channel can also be neglected.

The solution of the age equation $\partial q / \partial \tau = \Delta q$ with the boundary condition

$$I_0 \delta(\tau) = \frac{3}{4}\frac{1}{l_{tr}} q - \frac{1}{2}\frac{\partial q}{\partial x}\Big|_{x=0}$$

can be readily obtained by means of the Laplace transformation:

$$q(x, \tau) = 2I_0\left\{\frac{e^{-\frac{x^2}{4\tau}}}{\sqrt{\pi\tau}} - \frac{3}{2l_{tr}} e^{\left(x+\frac{3}{2l_{tr}}\tau\right)\frac{3}{2l_{tr}}}\left[1 - \operatorname{erf}\left(\frac{x}{2\sqrt{\tau}} + \frac{3\sqrt{\tau}}{2l_{tr}}\right)\right]\right\}. \tag{6}$$

With the condition that $\delta \lesssim l$ (l the length of the free path of a fast neutron in the material of the shield) and $\delta \ll H$, the presence of a hollow channel does not introduce noticeable perturbation into the distribution of neutrons in a protective layer. Expression (6) can therefore be assumed to hold near the hollow channel also.

For neutrons with an energy $E_0 \leq E' \leq E$, the coefficient β is expressed through the density of neutron attenuation $\beta(x, \tau)$ in the following way:

$$\beta = 1 + \frac{3H^2}{2l_0\delta} \int_0^H \frac{dx}{(H-x)^2+\delta^2} \left(\int_0^\tau \frac{q(x, \tau)}{l_{tr}} d\tau \right).$$

Since $H \gg 2\lambda \simeq 2\sqrt{\tau}$,

$$\beta = 1 + \frac{3}{2l_0\delta} \int_0^\infty dx \left(\int_0^\tau \frac{q(x, \tau)}{l_{tr}} d\tau \right). \tag{7}$$

Substituting expression (6) in (7) and integrating at first with respect to x and then with respect to τ, we obtain

$$\beta = 1 + \frac{4\bar{l}_{tr}}{3\delta} \left\{ e^{\left(\frac{3}{2\bar{l}_{tr}}\right)^2 \tau} \left[1 - \operatorname{erf}\left(\frac{3\sqrt{\tau}}{2\bar{l}_{tr}} \right) \right] + \frac{3}{\bar{l}_{tr}} \sqrt{\frac{\tau}{\pi}} - 1 \right\}. \tag{8}$$

Here $\bar{l}_{tr}$ is the transport length of neutrons averaged throughout the interval of energies E_0–E; τ – the age of neutrons with energy E.

At values of τ $(E_0, E) \gtrsim 2\bar{l}_{tr}^{-2}(E)$,

$$\beta \simeq 1 + \frac{4}{\delta} \left(\sqrt{\frac{\tau}{\pi}} - \frac{l_{tr}}{3} + \frac{2\bar{l}_{tr}^2}{9\sqrt{\tau\pi}} \right).$$

If the angular distribution of neutrons leaving the wall of the channel is assumed to be similar to (2), then

$$\beta \simeq 1 + \frac{4}{\delta} \left(\sqrt{\frac{\tau}{\pi}} - \frac{\bar{l}_{tr}}{3} + \frac{2}{9} \frac{\bar{l}_{tr}^2}{\sqrt{\tau\pi}} \right) \left(A + B\frac{\delta}{H} \right).$$

Cases are often encountered where the fast neutrons are incident on the layer of the shield with the channel not from a hollow, but from a medium having diffusion and attenuation properties close to the analogous characteristics of the shield material. In the case of a plane source in an infinite medium

$$q = \frac{I_0}{\sqrt{\pi\tau}} e^{-\frac{x^2}{4\tau}}$$

and instead of (8) we obtain $\beta \simeq 1 + (3\tau/2\delta l_{tr})$. If as the neutrons of the source we consider not the monoelectric neutrons but, for example, neutrons of the fission spectrum, then

$$\beta = \int_E^\infty \operatorname{sh}\sqrt{2E_0}\, e^{-E_0} \beta(E_0)\, dE_0.$$

Using these results the correction factor for (1) can be differentially calculated for each separate case.

LITERATURE CITED

1. B. Price et al., Protection from Nuclear Radiation [Russian translation] Moscow, Foreign Literature Press, 1959, p. 290.
2. T. Rockwell, Nuclear Reactor Shielding [Russian translation] Moscow, Foreign Literature Press, 1958, p. 212.
3. A. Simon and C. Clifford, ORNL-1217 (Rev.) March, 1954.
4. The Physics of Nuclear Reactors. Reports of the US Atomic Energy Commission [Russian translation] Moscow, Foreign Literature Press, 1956, p. 332.

THE SPECTRUM OF SCATTERED γ-RADIATION*

V. S. Anastasevich

Translated from Atomnaya Energiya, Vol. 10, No. 4, pp. 389-390, April, 1961
Original article submitted September 22, 1960

When studying the scattered γ-radiation it is possible to proceed from the kinetic equation used by Fano, Bethe and others to describe the passage of γ-radiation through a material. However, the solution of this equation involves considerable mathematical difficulties. The same problem can be solved using the condition of stationary states, first used to study the spectrum of attenuated neutrons.**

Let there be a point source radiating q γ-quanta in unit time. The initial energy of the γ-quanta is equal to ϵ_0. If the source is placed in a certain medium, then, due to the Compton effect, the energy of the quanta decreases during their movement. We will assume that the time passing since the moment of formation of a certain number of γ-quanta is included in the range t to t + dt. The energy of γ-quanta is then limited by the interval $[\epsilon, \epsilon + d\epsilon]$, $d\epsilon$ having a negative value, since with increase in time the energy decreases. We will designate the number of γ-quanta with an energy lying in this range by $-n(\epsilon)d\epsilon$, where $n(\epsilon)$ the density of the γ-quanta in the interval $[\epsilon, \epsilon + d\epsilon]$. If we do not consider the photoelectric absorption of γ-quanta, the condition of stationary states is written:

$$-n(\epsilon)d\epsilon = q\,dt. \tag{1}$$

We designate the mean energy which is lost during collision of a γ-quanta with an electron by $\overline{\Delta\epsilon}$. Then

$$d\epsilon = -\overline{\Delta\epsilon}\,d\nu, \tag{2}$$

where ν is the total number of collisions since the instant of generation of the γ-quanta:

$$d\nu = c\mu_s(\epsilon)\,dt. \tag{3}$$

Here c is the speed of light;

$$\mu_s(\epsilon) = n_e\Phi \tag{4}$$

is the linear coefficient of the Compton scattering of the γ-quanta (n_e is the number of electrons in unit volume of the scattering materials; Φ is the total effective cross section of scatter of the γ-quantum by an electron).

The value $\overline{\Delta\epsilon}$ is calculated by means of formula

$$\overline{\Delta\varepsilon} = \frac{1}{\Phi}\int_{\Omega}(\varepsilon - \varepsilon')\,d\Phi, \tag{5}$$

where $d\Phi$ is the effective differential cross section of the Compton scattering, determined by the Klein-Nishina formula; ϵ' is the energy of a γ-quantum after scatter at an angle θ.

Bearing in mind the known expression for $d\Phi$ and also the connection between ϵ' and θ, by elementary calculations we find

$$\Phi = \frac{\pi r_0^2}{\varepsilon}\left[4 + \frac{\varepsilon}{2} - \frac{\varepsilon}{2(1+2\varepsilon)^2} + \left(\varepsilon - 2 - \frac{2}{\varepsilon}\right)\ln(1+2\varepsilon)\right] \tag{6}$$

and

$$\int_{\Omega}\varepsilon'\,d\Phi = \frac{\pi r_0^2}{\varepsilon^2}\left[-\frac{1}{2} - \varepsilon + \frac{4}{3}\varepsilon^2 + \frac{1}{2}\frac{1}{1+2\varepsilon} - \frac{\varepsilon^2}{1+2\varepsilon} - \frac{\varepsilon^2}{3(1+2\varepsilon)^3} + \ln(1+2\varepsilon)\right], \tag{7}$$

where r_0 is the classical radius of the electron; Ω is a solid angle.

* The work was done in 1948.

** Flügge, Phys. Zs. H. 21-22, 445 (1943).

Substituting the obtained expressions in formula (5) we finally obtain

$$\overline{\Delta\varepsilon}=\varepsilon-\frac{-\frac{1}{2}-\varepsilon+\frac{4}{3}\varepsilon^2+\frac{1}{2}\frac{1}{1+2\varepsilon}-\frac{\varepsilon^2}{1+2\varepsilon}-\frac{\varepsilon^2}{3(1+2\varepsilon)^3}+\ln(1+2\varepsilon)}{4+\frac{\varepsilon}{2}-\frac{\varepsilon}{2(1+2\varepsilon)^2}+\left(\varepsilon-2-\frac{2}{\varepsilon}\right)\ln(1+2\varepsilon)} \tag{8}$$

From Eqs. (2) and (3) it follows that

$$\frac{d\varepsilon}{dt}=-c\mu_s(\varepsilon)\,\overline{\Delta\varepsilon}. \tag{9}$$

Considering the condition of stationary states (1) and (9), we find

$$n(\varepsilon)\,d\varepsilon=\frac{q\,d\varepsilon}{c\mu_s(\varepsilon)\,\overline{\Delta\varepsilon}}. \tag{10}$$

Equation (10) gives the dependence of the density of γ-radiation in the energy interval $[\epsilon, \epsilon + d\epsilon]$ without the readily-allowed-for photoelectric absorption of γ-quanta. For each $d\nu$ of the collisions accompanied by Compton scattering of the γ-quanta there are $[\mu_F(\epsilon)/\mu_s(\epsilon)]d\nu$ collisions, accompanied by a photoeffect, where $\mu_F(\epsilon)$ is the linear coefficient of photoelectric absorption. Therefore,

$$dq(\varepsilon)=-\frac{\mu_F(\varepsilon)}{\mu_s(\varepsilon)}\,q(\varepsilon)\,d\nu. \tag{11}$$

Here $q(\epsilon)$ is the number of γ-quanta generated in 1 sec and reaching the interval of energies $[\epsilon, \epsilon + d\epsilon]$.

From Eqs. (2), (3) and (11) we find

$$q(\varepsilon)=q\exp-\left(\int_{\varepsilon}^{\varepsilon_0}\frac{\mu_F(\varepsilon)}{\mu_s(\varepsilon)\,\overline{\Delta\varepsilon}}\right)d\varepsilon. \tag{12}$$

Substituting in (10) instead of q the value $q(\epsilon)$, we obtain the spectrum of scattered γ-radiation with an allowance for the photoelectric absorption:

$$n(\varepsilon)\,d\varepsilon=\frac{q\exp-\left(\int_{\varepsilon}^{\varepsilon_0}\frac{\mu_F(\varepsilon)}{\mu_s(\varepsilon)\,\overline{\Delta\varepsilon}}\,d\varepsilon\right)d\varepsilon}{c\mu_s(\varepsilon)\,\overline{\Delta\varepsilon}} \tag{13}$$

At high values of ϵ the photoeffect is practically absent and the integral in the exponent of formula (13) is equal to zero. Therefore for high energies the γ-radiation spectrum is determined by formula (10).

The character of the radiation spectrum is readily analyzed in two limiting cases: $\epsilon \gg 1$ and $\epsilon \ll 1$.

With an accuracy up to the value of higher orders of smallness from expressions (4), (6), (8) and (10) it follows that for $\epsilon \gg 1$,

$$n(\varepsilon)\,d\varepsilon=\frac{q\,d\varepsilon}{cn_e\pi r_0^2\ln 2e^{-\frac{5}{6}\varepsilon}} \tag{14}$$

If $\epsilon \ll 1$, then from these expressions we find

$$n(\varepsilon)\,d\varepsilon=\frac{q\,d\varepsilon}{\frac{8}{3}cn_e\pi r_0^2\varepsilon^2}. \tag{15}$$

Therefore, the spectrum of scattered γ-radiation depends weakly on the energy if $\epsilon \gg 1$ and changes $\sim 1/\epsilon^2$, if $\epsilon \ll 1$.

In the region of small energies (with certain values of $\epsilon = \epsilon_F$ of the order of several hundreds or tens, depending on the form of the scattering material), photoelectric absorption begins to have an effect and the integral in the exponent of formula (13) increases sharply and the γ-radiation spectrum tears.

If in a medium having an infinite length the γ-radiation sources are uniformly distributed, then γ-quanta reach every point of this medium, the time of formation of these quanta being different. The spectrum of the equilibrium γ-radiation can then be determined from formula (13). A more detailed consideration of this problem is beyond the scope of the present article.

THE MONTE CARLO CALCULATION OF THE PASSAGE OF γ-RADIATION FROM A PLANE DIRECTED SOURCE OF Cs^{137} THROUGH ALUMINUM UNDER CONDITIONS OF BARRIER GEOMETRY

A. F. Akkerman and D. K. Kaipov

Translated from Atomnaya Energiya, Vol. 10, No. 4, pp. 391-392, April, 1961
Original article submitted October 17, 1960

At the present time the Fano and Spencer method of polynomial expansions [1] is the generally accepted approximate method for solving the equation of γ-quanta transfer. Using this method, which is strictly speaking only applicable for an infinite medium by introducing the so-called factors of accumulation (energy, dose, absorption energy, etc.), the role of repeatedly scattered radiation could be correctly accounted for. In order to simplify the laborious calculations by this method [1], simple formulas were suggested for the accumulation factors [2]:

$$B = A_1 e^{-\alpha_1 \mu_0 z} + A_2 e^{-\alpha_2 \mu_0 z}, \quad (1)$$

where A_1, A_2, α_1, α_2 are parameters whose values were given in [3, 4] as a function of the energy and media for different substances; μ_0 is the linear attenuation factor of the γ-radiation in the material.

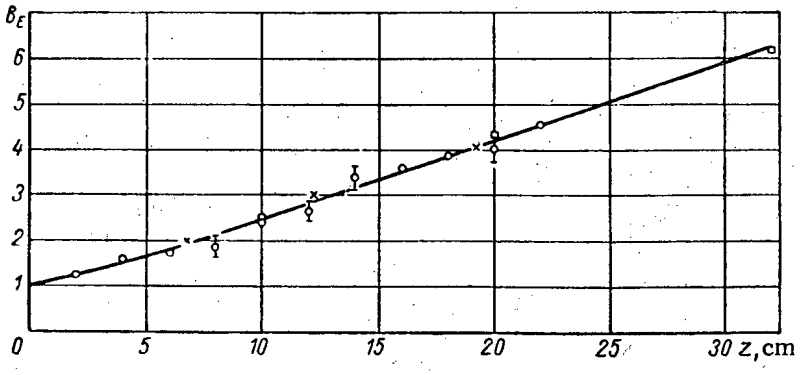

Fig. 1. Dependence of the energy factor of accumulation (source Cs^{137}) on the thickness of the layer: ○) our calculations; ×) results of [10]; □) results of [9].

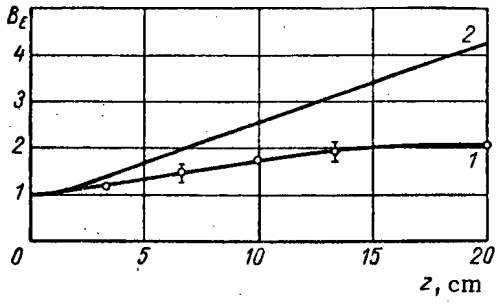

Fig. 2. Energy factor of accumulation of Co^{60} radiation.

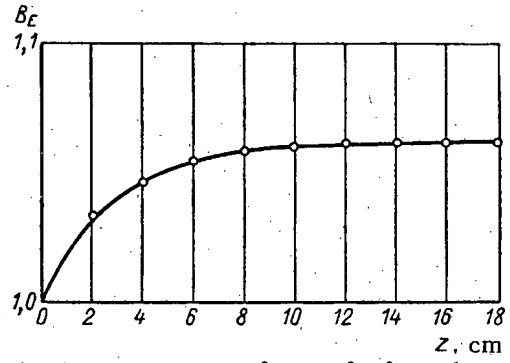

Fig. 4. Accumulation factor of reflected energy (source Cs^{137}).

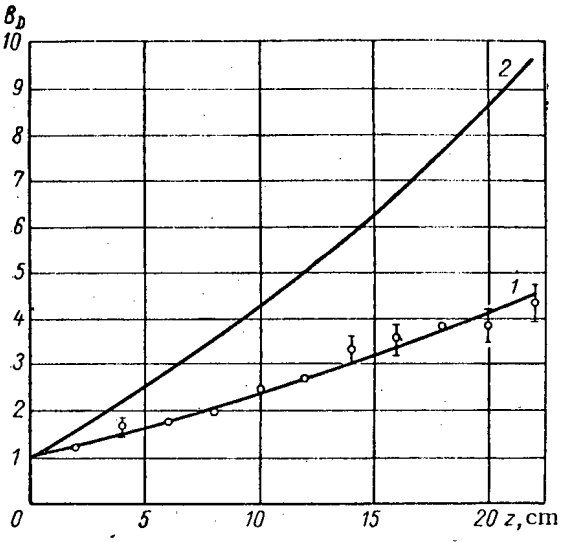

Fig. 3. Dose factor of accumulation of Cs^{137} radiation.

It has been shown in some papers [5, 6], however, that the accumulation factors calculated with formula (1) for media with a small atomic number are noticeably greater than the experimental values. The reason is that the theoretical accumulation factors are obtained under conditions of infinite geometry of the scattering medium, and, consequently, in them there is an allowance for the total flux of γ-quanta (energy) at a given point or through a given plane and under the conditions of barrier geometry we are dealing with flux in one direction; the reverse flux is practically absent. This difference increases with reduction in the energy of the source and is greatest when the depth of penetration of the radiation is not too high. To check these deviations and to obtain correct accumulation factors the Monte Carlo calculation method was used. The passage of γ-radiation was considered from a plane directed (angle of incidence 0°) source of Cs^{137} through aluminum under conditions of barrier geometry. The Monte Carlo method is most effective for these cases since the boundary conditions, even the complex conditions, are considered by it automatically. The method of the calculations was chosen on the basis of [7, 8].

An advantage of this method is the possibility of obtaining satisfactory accuracy in the calculations (in our case 9.5%) with a small number of studied "trajectories" of γ-quanta. This is achieved by an analytical allowance for absorption by means of the so-called "survival" factors and also the probability of exit or reflection of each of the studied γ-quanta in a given energy or angular interval.

Results of calculations. Figure 1 gives values for the energy factor B_E for Cs^{137} as a function of the depth of penetration z; it also gives the values of the factor obtained in [9, 10].* As can be seen from the figure, the agreement between the results is good.

For comparison in Fig. 2 the energy factor B_E is shown for Co^{60} (curve 1) which we calculated previously [8]; on this figure (curve 2) is shown the energy factor obtained from the data of [4].

Figure 3 gives the dose factor of accumulation B_D (curve 1) calculated from the formula

$$B_D = \frac{\sum_{i=1}^{20} \mu_e(E_i)\, I(E_i)}{\mu_e(E_0)\, I(E_0)} + 1, \qquad (2)$$

* In [10] the factor B_E was obtained for concrete with a mean atomic number and density close to the mean atomic number and density of aluminum.

where $\mu_e(E_i)$ is the absorption factor of the γ-quanta of energy E_i in air; $I(E_i)$* is the energy flux of the scattered radiation in the ith interval after passage through a layer of material of thickness z (in centimeters); $I(E_0)$ is the energy flux of nonscattered radiation at the same depth of penetration. This figure gives the dose factor calculated from formula (1) and the data of [3] (curve 2). A comparison of Figs. 2 and 3 confirms the above conclusion as to the increase in the difference between the theoretical and experimental results with decrease in the energy of the incident radiation. Figure 4 shows the energy factor of accumulation B_E^* for reflected γ-quanta. As can be seen from the figure, starting with a depth of 10 cm ($\sim 2\mu_0 z$) the energy of the radiation reflected from the diffuser hardly increases; therefore, a layer of aluminum of thickness more than $2\mu_0$ behaves as a semiinfinite medium. We notice that our value for the albedo of energy (0.062) agrees with the albedo calculated from the empirical formula of [11].

In conclusion the authors would like to thank N. S. Shtein, K. S. Yakovlev and Yu. G. Kosyak for taking part in the calculations.

LITERATURE CITED

1. L. Spender and U. Fano, J. Res. Nat. Bur. Standards 46, 446 (1951).
2. P. Roys, K. Shure, and I. Taylor, Phys. Rev. 95, 911 (1954).
3. B. Price, K. Harton, and K. Spinney, Protection from Nuclear Radiation [Russian translation] Moscow, Foreign Literature Press, 1959, p. 82.
4. T. Rockwell, Nuclear Reactor Shielding [Russian translation] Moscow, Foreign Literature Press, 1958, p. 300.
5. A. V. Bibergal', M. M. Korotkov, and I. G. Ratner, Atomnaya Énergiya 7, No. 3, 244 (1959).**
6. A. V. Bibergal' and N. I. Leschinskii, Atomnaya Énergiya 8, No. 4, 372 (1960).**
7. M. Berger, J. Res. Nat. Bur. Standards 55, 343 (1955).
8. A. F. Akkerman and D. K. Kaipov, Tr. Inst. yadernoi fiziki, Vol. 3, Alma-Ata, 1960, p. 106.
9. F. Perkins, J. Appl. Phys. 26, 1372 (1955).
10. F. Kirn, R. Kennedy, and H. Wyckoff, Radiology 63, 94 (1955).
11. B. P. Bulatov and E. A. Garusov, Atomnaya Energiya 5, No. 6, 631 (1958).**

A RADIOMETRIC METHOD FOR DETERMINING THE URANIUM CONCENTRATION IN SOLUTIONS CONTAINING IONIUM

N. N. Shashkina

Translated from Atomnaya Énergiya, Vol. 10, No. 4, pp. 392-393, April, 1961
Original article submitted December 9, 1960

In addition to rapid chemical methods for determining the uranium content in solutions in the hydrometallurgical treatment of uranium ores, it is also possible to use a radiometric method. The use of this method is especially advantageous when it is necessary to determine uranium in organic solutions whose chemical analysis involves difficulties.

The determination of uranium concentrations in solutions containing practically no other α-radiating elements by the radiometric method is straightforward. The α-radiation of solutions is measured in a thick layer by means of the B-apparatus with a P-349-2 attachment or the LAS apparatus. The uranium content in the solution is determined by comparing the α-radiation of the analyzed solution with the α-radiation of a standard [1] according to the formula

$$Q = q \frac{n_s}{n_{st}} \frac{\mu_{st} \rho_{st}}{\mu_s \rho_s}, \quad (1)$$

where q is the uranium content in the standard, g/kg; n_s, n_{st} are the number of impulses per minute from the sample and standard respectively; μ_s and μ_{st} are the stopping powers of the sample and standard for α-radiation; ρ_s, ρ_{st} are the densities of the analyzed solution and the standard.

* The values of $I(E_i)$ in our calculations were obtained from the energy spectra of scattered radiation. The energy interval 40-660 kev was split up into 20 energy intervals.

** Original Russian pagination. See C. B. translation.

Experience shows that even with considerable fluctuations of the salt composition of the solutions and the concentration of uranium in them, the product $\mu\rho$ remains practically constant, which makes it possible to assume that

$$\frac{\mu_{st}\,\varrho_s}{\mu_s\,\varrho_s}=1.$$

If necessary a standard is chosen which is close in composition to the measured solutions.

The sensitivity of the α-method for determining uranium in solution in measurements on the B apparatus with the P-349-2 attachment is about 0.3 g/liter. On an α-scintillation apparatus with the FÉU-3B (diameter of photocathode 200 mm) the sensitivity is increased to 0.05 g/liter.

In a number of cases the solutions obtained during the hydrometallurgical treatment of uranium ores, apart from uranium, contain ionium (Th^{230}). The relationship between the uranium and ionium in the solutions can differ, depending on the character of the ores and the methods of their treatment. There is usually an insufficiency of ionium compared with the amount equivalent to the amount of uranium existing in solution.

Results of Radiometric and Chemical Determination of Uranium

Concentration of α-radiating elements, g/liter of equivalent uranium	Concentration of β-radiating elements, g/liter of equivalent uranium	Correction for ionium, g/liter of equivalent uranium	Uranium concentration, g/liter		Difference between radiometric and chemical analyses %
			calculated from formula (2)	found by chemical analysis	
0,073	0,035	0,019	0,054	0,052	+3,5
0,086	0,037	0,020	0,066	0,066	0
0,155	0,054	0,030	0,125	0,132	—5,0
0,160	0,054	0,030	0,130	0,122	+6,5
0,343	0,139	0,076	0,267	0,256	+4,0
0,365	0,109	0,060	0,305	0,309	—1,0
0,413	0,191	0,105	0,308	0,320	—3,5
0,432	0,174	0,095	0,337	0,331	+1,6

The α-activity of these solutions is a function of the content not only of uranium, but also of ionium.

To determine the concentration of uranium in a solution containing ionium from the α-activity, a correction must be introduced for the α-activity of ionium, for which purpose it is necessary to know the content of ionium in the solution in units of equilibrium uranium. This determination is possible from the β-radiation $UX_1 + UX_2$ (E_{max} = 2.32 Mev).

When uranium minerals are dissolved, the isotopes of thorium Io and UX_1 transfer into solution in the same ratio in which they are present in the ore. Usually this ratio corresponds to radioactive equilibrium. Later in the solution, due to decay of UX_1, the initial ratio between the Io and UX_1 is disturbed. If the β-activity of the solution is determined not later than 2-3 days after obtaining the solution, it shows the content of ionium in the sample.

The β-radiation of the sample is measured in a thick layer, filling a flat cell with the solution or a cylindrical vessel surrounding the counter. With the presence in the solution of a β-radiator RaE, the measurements should be made by a β-counter with wall thickness of aluminum of about 0.25 g/cm^2, in order to almost completely absorb the β-radiation RaE (E_{max} = 1.19 Mev).

The standard is usually a solution of an old (prepared more than a year ago) salt of uranyl nitrate to which is added a small amount of a soluble salt of cerium or zirconium to prevent adsorption of UX_1 on the glass [2].

If the amount of ionium is calculated from results of β-measurement in units of uranium in equilibrium with the ionium, then the α-activity of ionium from measurements in a thick layer according to [1] will be equal to 0.55 of the α-activity of UI + UII.

Hence it follows that the true content of uranium in the solution can be calculated from the formula

$$Q_U = Q_\alpha - 0{,}55Q_\beta, \qquad (2)$$

where Q_α and Q_β are the α- and β-activities respectively of the analyzed solution in units of uranium.

A comparison of the results of radiometric and chemical analyses for uranium of solutions containing ionium is given in the table.

LITERATURE CITED

1. R. Evans, Phys. Rev. 45, No. 1, 38 (1934).
2. I. Starik, Usp. khim. 26, No. 4, 389 (1957).

THE PROBLEM OF THE SCALING FACTOR FOR THE QUANTITATIVE INTERPRETATION OF γ -LOGGING

A. M. Lebedev, S. G. Troitskii, and V. L. Shashkin

Translated from Atomnaya Energiya, Vol. 10, No. 4, pp. 394-396, April, 1961
Original article submitted November 21, 1960

The correct choice of the scaling factor, known conventionally as the infinite seam factor [1], is of great importance for the quantitative interpretation of γ -logging data of boreholes and blastholes. In radiometry this factor is usually expressed in microroentgen/hour* per 0.01% of equilibrium uranium or thorium.

The determination of infinite seam factors was the object of theoretical investigations [2]. Experimental data indicating the relation between the infinite seam factor and the material of the cathode counter and the thickness of its casing are given in [1, 3].

The relation between the infinite seam factor and the effective atomic number of an ore, the material of the cathode counter, and the thickness of the casing is linked to the different spectral sensitivity of the γ -ray collectors and to the difference in the spectral composition of the γ -radiation of large masses of ore and the radium (point) standard used for calibrating radiometers.

The aim of the present investigation was the experimental determination of the infinite seam factor for various types of ores by means of different γ -ray collectors. The experiments were carried out in models of an infinite seam, consisting of cubical iron boxes filled with crushed and thoroughly mixed ore. To ensure a degree of approximation of the models to the infinite seam of at least 97%, boxes with a side of 120 cm were selected for ores with $Z_{eff} > 12$,** and a side of 150 cm for ores with $Z_{eff} = 9$. An aluminum tube of diameter 7 cm, with a wall thickness of 1 mm, was installed in the middle of two opposite lateral walls of the box. The borehole model obtained in this way made it possible to carry out measurements in the center of the model of an infinite seam.

The boxes were hermetically sealed; the measurements were carried out after all the radon had been accumulated.

Average ore samples from each model were carefully analyzed for the radium content in three laboratories. The relative root-mean-square error in a radium determination was 3%.

The mean effective atomic numbers and the conversion factors to normal electron density were calculated from the data of the complete chemical analysis of the ores. The calculations were carried out by means of the formulas [2]:

$$Z_{\text{eff}} = \left[\sum_{(Z)} p_Z Z^{2,3}\right]^{\frac{1}{2,3}}; \quad \overline{N} = 2\sum_{(Z)} p_Z \frac{Z}{A_Z},$$

* The unit microroentgen/hour is employed here in the conventional sense used in prospecting radiometry: 1 mg of radium at a distance of 1 m, with recording of only primary γ -radiation, produces an intensity of 850 microroentgen per hour.

** The Z_{eff} of coal with an ash content of 20% is 9.1, the Z_{eff} of graphite is 13.

where A_Z is the atomic weight of an element with a number Z; P_Z is the relative gravimetric content of the element with a number Z in the ore.

The measurements were carried out in a PS-10,000 apparatus. The reproducibility of the measurement results is characterized by a relative root-mean-square error of 3%.

TABLE 1. Infinite Seam Factors from Measurements by Gas-Discharge Counters

Model No.	Z_{eff}	$\bar{N}$	Infinite seam factor, microroentgen/hour per 0.01% U							
			iron case of thickness 0.5 mm				iron case of thickness 4 mm			
			VS-4	MS-4	STS-2	GS-4	VS-4	MS-4	STS-2	GS-4
1	9,12	1,146	312	178	152	110	193	121	113	100
2	12,7	1,000	285	161	143	112	186	120	117	103
3	13,5	1,000	256	148	137	110	180	119	112	101
4	14,5	1,000	258	144	134	108	176	120	112	100
5	14,6	1,000	240	143	129	101	166	113	112	97
6	15,8	0,982	237	137	130	105	173	116	110	100
7	21,1	0,964	199	120	117	—	156	107	110	—
8	23,2	0,962	172	125	128	—	139	109	113	—
9	12,8	1,000	87	58	54	47	65	50	48	45
Uranium equivalent of thorium			0,31	0,36	0,38	0,42	0,35	0,42	0,41	0,44

TABLE 2. Infinite Seam Coefficients from Measurements by Scintillation Counters

Model No.	Z_{eff}	Infinite seam factor, microroentgen/hour per 0.01% U		
		without a filter	with an iron casing of thickness 4.6 mm	with a lead casing of thickness 4 mm
2	12.7	260	171	102
3	13.5	256	173	98
4	14.5	254	173	102
5	14.6	243	171	102
6	15.8	230	168	100
7	21.1	206	164	101
9	12.8	80	59	36
Uranium equivalent of thorium		0.31	0.35	0.36

The results of determinations with gas-discharge counters are given in Table 1. A comparison of the experimental and theoretical values of the factor of an infinite seam is given in Figs. 1 and 2.

All the models, except No. 9, contained uranium ore without thorium, while model No. 9 contained thorium ore. The small uranium content in this model was taken into account during calculations of the factor. The uranium equivalent of thorium was calculated as the ratio of the infinite seam factors for thorium and uranium ores of model No. 2, for which the effective atomic numbers were equal.

Determinations were also made of the infinite seam factors for two scintillation logging apparatuses – KRS and PRKS.

The gamma-radiation in the KRS apparatus was recorded by an NaI(Tl) crystal of height 40 mm and diameter 25 mm. The results obtained for KRS are given in Table 2. Measurements "with a filter" were carried out with screening of the container of the crystal and the photoelectron multiplier by only a compacted paper jacket for protection against light. The second series of measurements was carried out with the ordinary casing of the KRS apparatus; the third series was carried out with a lead casing.

In the PRKS logging radiometer the γ-radiation was recorded by an NaI(Tl) crystal of height 30 mm and diameter 18 mm. The factor was determined with only the ordinary casing of a radiometer (an outer iron jacket with a wall thickness of 3 mm and an inner lead insert with a wall thickness of about 1.2 mm). To check possible variations of the factor as a result of replacement of the photoelectron multiplier and the crystal, measurements were carried out with different combinations of FÉU-31 and the crystals. As a result of the measurements it was established that for a PRKS radiometer the infinite seam factor is independent of the effective atomic number of the ore and hardly varies with replacement of the photoelectron amplifier or recording crystal. The mean value of the factor was 117 ± 1.2 microroentgen/hour per 0.01% of uranium; confiding limits were calculated for the mean value within 0.95. The root-mean-square error characterizing the scatter of the individual determinations was 4.7 microroentgen/hour.

The results obtained allow the following conclusions to be drawn:

1. The character of the relation between the infinite seam factor and the effective atomic number of an ore, established theoretically, is confirmed satisfactorily by experimental data. The discrepancies in the numerical values are explained mainly by the difference in the spectral characteristics of the counters, used for the calculations and employed in the experiments.

2. The relation between the infinite seam factor and the effective atomic number of a rock is determined by the low-energy part of the γ-radiation spectrum. Therefore, this relation decreases with screening of the counter and with the use of a counter having a cathode of low-atomic-number material.

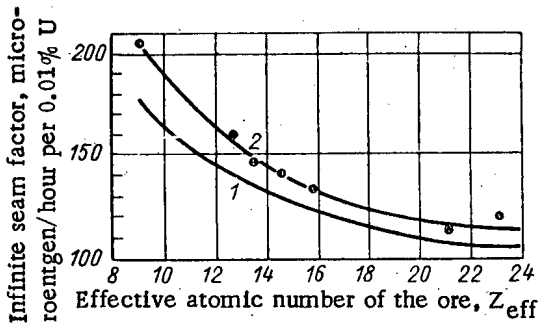

Fig. 1. Relation between the infinite seam factor and the effective atomic number of the ore for counters with a copper cathode: 1) theoretical curve from the data of [2]; 2) experimental curve for an MS-4 counter from data converted to normal electron density.

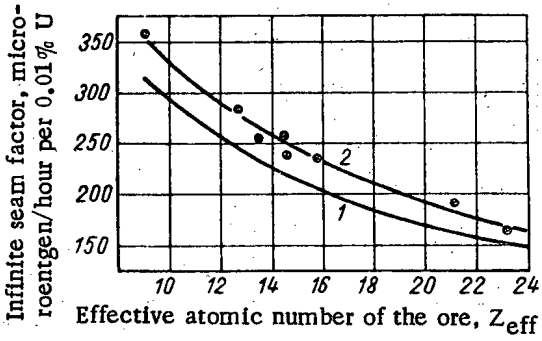

Fig. 2. Relation between the infinite seam factor and the effective atomic number of the ore for counters with cathodes of heavy elements: 1) theoretical curve for counters with a lead cathode; 2) experiment curve for a VS-4 counter (with a tungsten cathode) from data converted to normal electron density.

3. For counters of the MS type it is sufficient only to screen by an iron casing of thickness 4 mm to allow the infinite seam factor for rocks with an effective atomic number of 9-16 to be taken as constant and its mean value as equal to 117 microroentgen/hour per 0.01% of uranium.

4. For counters of the STS-2 type with screening by an iron casing of thickness 4 mm, the infinite seam factor is practically independent of the effective atomic number of a rock during variation of Z_{eff} from 9 to 23. The mean value of the factor is 113 microroentgen/hour per 0.01% of uranium.

5. With recording of γ-radiation by a KRS apparatus (with an iron casing of thickness 4.6 mm) the infinite seam factor is equal to 170 microroentgen/hour per 0.01% of uranium for ores with effective atomic numbers of 13 to 21.

6. From γ-measurements in infinite seams, the uranium equivalent increases from 0.31 to 0.44 with a reduction in the proportion of soft γ-rays in the recorded γ-radiation.

LITERATURE CITED

1. V. L. Shashkin, Atomnaya Energiya 2, No. 1, 48; No. 2, 157 (1957).*
2. G. M. Voskoboinikov, Intensity of γ-Radiation in a Homogeneous Radiating Medium. Proc. Mining-Geological Institute, Urals Branch, Academy of Sciences, USSR (Geophysical collection, No. 2) [in Russian], Sverdlovsk, 1958.
3. A. K. Ovchinnikov and T. F. Ivashchenko, Manual of γ-Logging [in Russian] Moscow, Gosgeoltekhizdat, 1957.

* Original Russian pagination. See C. B. translation.

PREPARATION OF URANIUM DODECABORIDE

Yu. B. Paderno

Translated from Atomnaya Energiya, Vol. 10, No. 4, p. 396, April, 1961
Original article submitted November 21, 1960

Uranium-boron alloys were prepared [1, 2] by the electrolysis of fused mixtures of boron oxide, boron fluoride, magnesium oxide and uranic oxide at a temperature of 1100°C. This gave uranium tetraboride and a mixture of the tetraboride and uranium dodecaboride. The individual compound uranium dodecaboride was not obtained by this method. As a result of thermal decomposition of uranium borohydride $U(BH_4)_4$ in the 150-200°C temperature range, uranium tetraboride is formed [3]. In [4, 5], uranium boride with the composition UB_4 was also obtained from the elements by synthesis. In [6], uranium borides with the composition UB_2 and UB_4 were obtained by synthesis from the elements. Uranium dodecaboride was not obtained in this work; the authors [6] explain this by the instability of this compound at the high temperatures at which borides are obtained.

In the present work we investigated the possibility of the preparation of individual uranium dodecaboride. The boride was obtained by the method developed for the preparation of rare-earth borides [7], i.e., by the reduction of uranium oxide by boron under vacuum at 1300-1900°C.

The product obtained had the appearance of a gray metallic powder. X-ray phase analysis by the Debye method, carried out in a chamber of diameter 143.25 mm in the K_α-radiation of copper, showed that a monophase product – uranium dodecaboride UB_{12} – is formed throughout the whole temperature range from 1300 to 1900°C. A determination of the period of the crystalline lattice of the boride gave the value α = 7.472 A, which agrees satisfactorily with literature data (α = 7.473 A [8]).

It is of interest to note that in spite of Brewer's statement regarding the instability of this phase at high temperatures [6], it was even obtained at 1900°C. This agrees with the results of investigations of the system uranium–boron [9, 10], according to which, uranium dodecaboride is stable up to the melting point (2235°C).

Therefore the method of reducing uranium oxide by boron makes it possible to obtain the individual compound uranium dodecaboride in a simple and practical manner.

LITERATURE CITED

1. L. Andrieux, Ann. chimie 12, 422 (1929).
2. L. Andrieux and P. Blum, Compt. rend. 229, 210 (1949).
3. H. Hoekstra and J. Katz, J. Amer. Chem. Soc. 71, 2488 (1949).
4. A. Zalkin and D. Templeton, Acta crystallogr. 6, 269 (1953).
5. A. Zalkin and D. Templeton, J. Chem. Phys. 18, 391 (1950).
6. L. Brewer et al., Amer. Ceram. Soc. Bull. 34, 173 (1951).
7. Yu. B. Paderno, T. I. Serebryakova, and G. V. Samsonov, Kristallografiya 4, 542 (1959).
8. F. Bertaut and P. Blum, Compt. rend. 229, 666 (1959).
9. B. Howlett, J. Inst. Metals 88, 91 (1959).
10. B. Howlett, J. Inst. Metals 88, 467 (1960).

A UNIVERSAL γ-APPARATUS FOR RADIATION-CHEMICAL STUDIES

N. G. Alekseev, K. N. Emel'yanov, G. K. Klimenko, B. V. Rybakov, and A. A. Rostovtsev

Translated from Atomnaya Energiya, Vol. 10, No. 4, pp. 396-400, April, 1961
Original article submitted July 2, 1960

In designing a γ-apparatus the problem was to develop a simple device for studying radiation-chemical processes. The requirements made of the apparatus were:

a) internal irradiated volume, with dose rate of 500 r/sec + 10%, about 50 cm^3 (depending on the distance of the source from the irradiated object, the dose rate of irradiation should be within the limits 150-15 r/sec);

b) the possibility of carrying out tests at controlled high temperatures and at low temperatures (liquid nitrogen);

c) remote control of the temperature and measurement of some controllable parameters of the radiation-chemical transformations;

d) operation and charging of the apparatus in situ without using water;

e) safety in operation and reliability, and also accessibility of the moving parts of the mechanisms for preventive maintenance and repairs.

The layout of a γ-apparatus satisying these requirements is shown in Figs. 1-4.

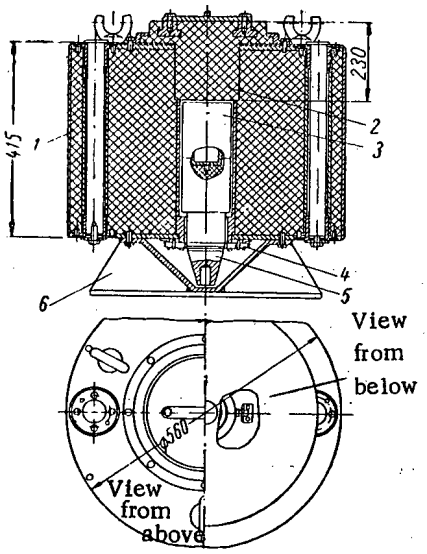

Fig. 1. Lead container: 1) steel vessel. 2) lead stopper; 3) aluminum vessel; 4) retainer; 5) end piece; 6) support.

The cylindrical radiator was assembled from 24 sources (Co^{60}) of height 160 mm and total activity 5000 g-eq Ra. The sources were placed in a circle of diameter 75 mm in two rows. Therefore, in the center of the radiator there is a volume equal to ~50 cm^3 (diameter 40 mm and height 55 mm) the dose rate in which varies within 10% of the mean value. The internal free volume of the aluminum vessel is 50 x 160 mm and contains the specimens to be irradiated, and permits the installation of temperature control blocks or Dewar flasks.

The radiator is placed in the lead container which can be used both in transporting and in operating. The container (see Fig. 1) of weight 1200 kg is made in the form of a cylinder of sheet steel and is covered with lead. Along the axis of the cylinder there is a hole for the radiator, and at the sides there are two holes with bushes, guiding the movement of the rods of the hoist mechanism during operation of the apparatus. When the radiator is transported the container is closed at the top with a lead stopper and at the bottom with an end piece. The lead shielding keeps the dose rate at the surface of the container during transporting at not more than 20 μr/sec with a total activity of 5000 g-eq Ra (measured with the PMR-1). In the working position the container is in a special recess in the floor of the shield cabin (see Figs. 2, 3). After the container has been put in place with a telpher (see Fig. 2), the stopper is removed and the top is covered with a protective plate moving in the recess of the cabin (see Figs. 2-4). The plate is moved by a motor with a screw pair (through a reducer) in two opposite directions. The reverse is electrical. In the extreme positions of the plate ("open" or "closed") the motor for the plate drive is switched off by the end switches (see Fig. 2), which are acted on by cams firmly fastened with the driving screw of the plate. The clearance between the top end of the container and the bottom plane of the plate is 5 mm. The plate weighs 600 kg and the time for withdrawal is 30 sec.

The device for raising the radiator into the working position and lowering it into the storage position consists of a lower tranverse with the radiator fastened to it by the end piece and an upper traverse to which is fastened a cable passing along the guide rollers from the telpher of lifting capacity 0,5 tons. On the cable of the telpher there

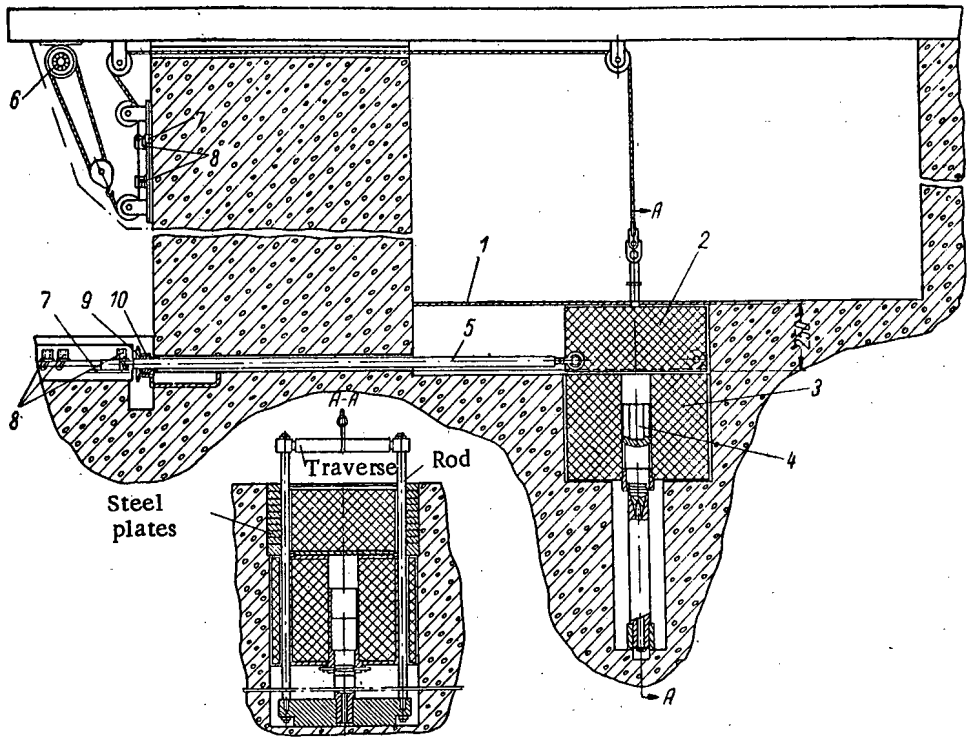

Fig. 2. View of apparatus in the "storage" position: 1) steel sheet; 2) plate; 3) container; 4) aluminum vessel with preparations; 5) lead screw; 6) telpher; 7) rests; 8) end switches type VK-211; 9) control wheel; 10) nut.

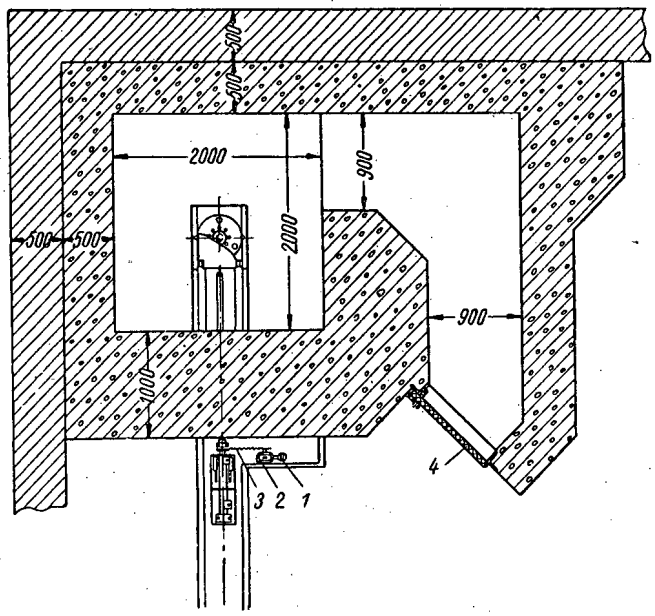

Fig. 3. Plan of apparatus and protective concrete cabin: 1) electric motor; 2) reducer; 3) chain drive; 4) lead door.

are cams which act on the final switches of the telpher motor at the instant of the extreme position ("up" and "down") of the radiator. The time for lifting or lowering (3 sec) makes it possible to carry out brief irradiations (up to 1 min).

The over-all view of the apparatus in the working position (without the working table) is shown in Fig. 4. In the cabin over the protective plate there is a special working table for fastening the irradiated objects in strictly fixed positions with respect to the radiator. On the inside wall of the cabin there is a board carrying leads and also water and gas pipes. An identical board is also placed on the outside wall. This provides remote control for the required measurements and the temperature system during irradiation.

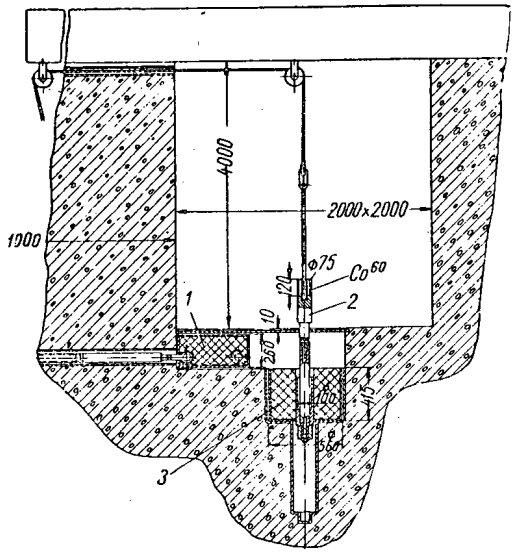

Fig. 4. Over-all view of apparatus in "working" position: 1) lead plate; 2) aluminum vessel with preparations; 3) lead container.

The dosimetry of the apparatus was provided by a chemical method, using a solution of iron sulfate in 0.8 N sulfuric acid and also with an ionization chamber of volume 2 cm^3 with a direct current amplifier. The nonuniformity in the dose rate in the internal irradiated volume was contained in the calculated figures.

Figure 5 shows the electric circuit for controlling the radiator and signaling the self-locking of the door and magnetic door fastening (DMZ). On the control panel there are four buttons, four magnetic starters giving reverse switching on of two electric motors, three signal lamps, the main switch off and the protectors. It can be seen from Fig. 5 that the operations of moving the plate and raising the radiator can only be carried out in strict sequence: withdrawing the plate (to the end), raising the radiator (the lamp 1 light up – the radiator is raised), the radiator is lowered (lamp 2 light up – the radiator is down), the plate is closed (lamp 3 light up – the plate is closed).

The coil DMZ is connected in parallel with the signal lamp 4; consequently, the cabin can only be entered when there is a feed voltage in the position of the radiator down and the plate fully closed. With the slightest movement of the plate the lamp lights up, a red light shows over the door of the cabin and the DMZ prevents the door from being opened. So that the mechanisms could not be switched on with the door open, automatic blocking was introduced into the circuit. The buttons (double) were mounted so that when several buttons are pressed together all mechanisms are switched off; the device can only be switched on if a strict order is observed when pressing the buttons. The arrangement not only provides safe operation, but also eliminates the possibility of the device breaking at points close to the source.

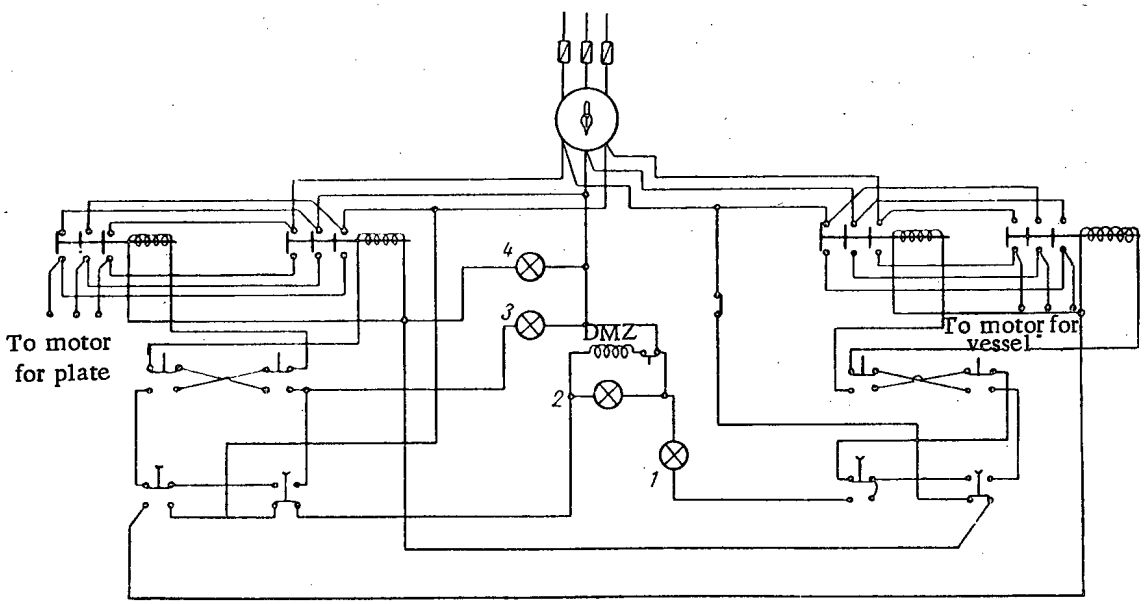

Fig. 5. Electric circuit for control of radiator, signaling, and automatic blocking.

If it becomes necessary to change the preparations, the UO-2 apparatus can be recharged in situ. For this purpose on the inside walls of the cabin there are rollers and there are extra devices (Figs. 6 and 7); lead tubing with a hole in the center 2 (the diameter of the hole is equal to the diameter of the hole in the container); there is a lead stopper 1 in the tubing with one hole at a distance from the axis of the stopper equal to the radius of the radiator; the special hopper and the magnetic manipulator are on flexible leads. The order of unloading can be seen from Fig. 6. Before operation, the tubing with the stopper is fastened on the cable of the telpher and the telpher raises it several centimeters from the plate; the plate is withdrawn and the tubing with the stopper are lowered onto the container and by rotating the stopper its hole is made to coincide with the socket of the radiator. This operation is carried out by means of an inclined mirror and a flashlight bulb. The hopper is then placed in the hole of the stopper (see Fig. 6). The dose rate of the scattered radiation at the operator does not exceed 5 μr/sec. The manipulator is lowered from the wall to the stop. The current is switched on. The Co^{60} preparation gripped by the manipulator is lowered to the stop in the upper floor of the hopper and it is brought into position over the bell of a sloping tube (up to the rest). The current is switched off and the preparation falls along the inclined tube into the previously placed container. If the preparation should accidentally break away, it falls onto an old spot. The intensity of the radiation is measured with a dosimeter. This operation is performed on all 12 sockets of the radiator in succession. The order of loading of the apparatus with preparations from the KIZ-4 container is the same as in the replacement of preparations (see Fig. 7). The storage valve for the preparations of the KIZ-4 container is opened by means of a mechanical screwdriver with an extended handle.

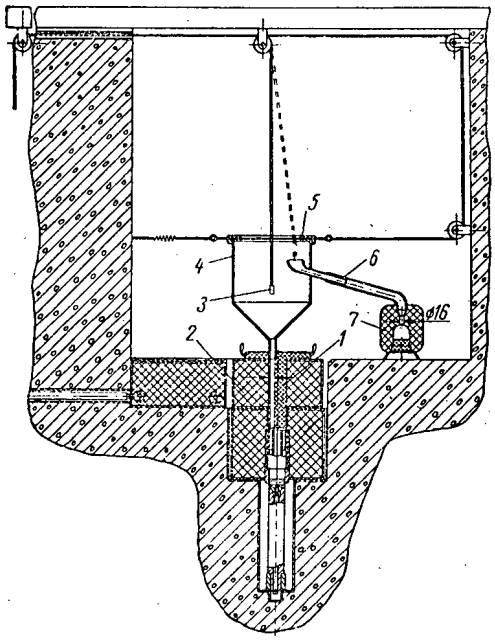

Fig. 6. Arrangement for unloading sources into the transport containers: 1) lead stopper; 2) lead tubing; 3) electromagnet; 4) hopper; 5) device for fixing electromagnet in the extreme positions; 6) pipe; 7) transport container.

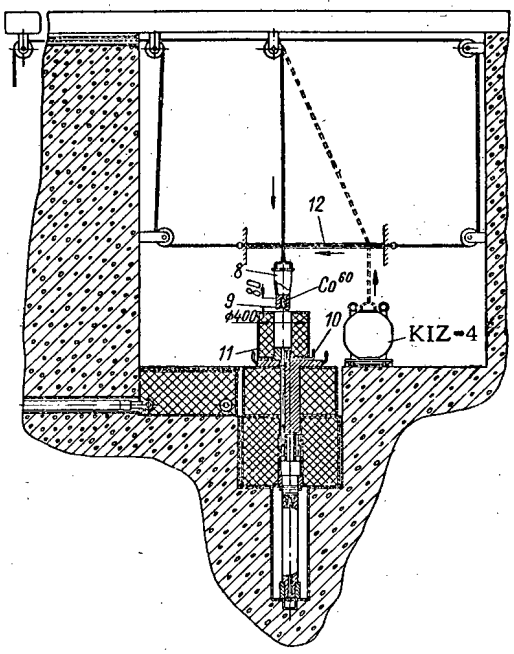

Fig. 7. Arrangement for charging apparatus with preparations from the KIZ-4 container: 8) KIZ-4 type stopper; 9) spring valve; 10) screw driver; 11) tubing; 12) device for fixing the KIZ-4 stopper in the extreme position.

According to the method described here, after prolonged operation the apparatus was recharged in two days (most of the time was spent on transporting the containers to and from the cabin). Three years of experience have shown that the apparatus is simple in operation and works without any accidents.

SELECTING A RADIOACTIVE ISOTOPE TO CHECK MATERIALS BASED ON THE USE OF BACK-SCATTERING OF γ-RADIATION

A. S. Rudnitskii

Translated from Atomnaya Energiya, Vol. 10, No. 4, pp. 400-402, April, 1961
Original article submitted June 21, 1960

To check the thickness or density of materials used in the production of large industrial components or articles, where access to them is only convenient from one side, with thickness from two to several tens of millimeters, it is advisable to use a radiometric method, based on the dependence of the intensity of back-scattered* γ-radiation on the thickness of the material (at constant density) or on the density (at constant thickness).

A measure of the thickness or density of a material is the relative intensity of back-scattered radiation of a radioactive source $I(x) = J(x)/J(0)$; $J(0)$ is the initial intensity of radiation in the absence of the checked material; $J(x)$ is the intensity of the scattered radiation with a thickness or density of the material x.

The curve for the dependence of $I(x)$ on the parameter x when checking the thickness is described by a function of the form

$$A(1-e^{-x\mu_{\Sigma}}), \tag{1}$$

where A is a constant, μ_{Σ} the total attentuation factor of the direct incident radiation, μ_0 the back-scattered radiation ($\mu_{\Sigma} = \mu_{0^\circ} + \mu_{180^\circ}$). The constant A includes the factors μ/μ_{Σ} and $I(\infty)$.

It can be seen from formula (1) that on reaching $x = x_{lim}$ ("saturation thickness"), $I(x)$ no longer depends on x; the measurement of the thickness x becomes impossible; therefore, the value x_{lim} is called the limiting measured thickness. For various values of the factor μ_{Σ}, the values of x_{lim} will also be different.

Starting from the character of the experimental curves $I(x) = J(x)/J(0)$, the authors of [1] found that the section of the curve of the form $A(1 - e^{x\mu\Sigma})$, which was the steepest and therefore gave the least error in checking the thickness, was limited by the value $x_{opt} \simeq 0.5\, x_{lim}$, where x_{opt} is the optimum thickness determined in the above way. On the other hand, for the same value of E_{γ} and different values of the atomic number Z of the material of the diffuser a family of curves (1) is obtained for which $\partial I/\partial x$ are different. The maximum values of $\partial I/\partial x$ occur at $20 \leq Z \leq 35$.

Other conditions being equal, $\partial I/\partial x$ causes a value of the graphically determined error in checking the thickness, depending on the statistical error δI_{stat}.

With regard to the dependence of the factor $\mu_{\Sigma} = \mu_{0^\circ} + \mu_{180^\circ}$ on the energy of the γ-radiation $E_{\gamma 0^\circ}$ and $E_{\gamma 180^\circ}$, the problem of the selection of the best value of $\partial I/\partial x$ for a certain value of Z amounts to a rational selection of $E_{\gamma 0^\circ}$ of the energy of directly incident γ-radiation. From expression (1) it follows that $\partial I/\partial x \sim \mu_{\Sigma}$, i.e., $\sim 1/E_{\gamma 0^\circ}$.

To check the thicknesses or densities of materials with this method, γ-active isotopes should be chosen which satisfy the following conditions:

1) the structure of the γ-radiation spectrum should be simple; if possible, the spectrum should be monochromatic (determined by the decay scheme of the isotope) [2]. The simplicity of the spectrum is essential for high reliability in separating in the γ-radiation spectrum that region of energy which corresponds to the back-scattered radiation ($E_{\gamma 180^\circ}$), when an electron diffuser is used for the directly incident and back-scattered radiation. For example, the Zn^{65} isotope should not be used due to the considerable intensity of the x-ray in the soft region of the spectrum ($E_{\gamma 180^\circ}$);

2) the energy of the γ-radiation should correspond to the desired value of x_{lim} and x_{opt};

3) the half life should be high in order to exclude the frequent recalibration of the scale of the pointer indicator of the thickness (density).

* By back-scattered radiation we mean, in the narrow sense of the word, scattering by 180 ± 10°.

Table 1 gives γ -active isotopes which satisfy these requirements [2].

TABLE 1. The Characteristics of Isotopes Suitable for Checking Materials by the Method of Back-Scattered Radiation

Isotope	$T_{1/2}$	$E_{\gamma 0°}$, Mev	$E_{\gamma 180°}$, Mev	Limiting measured thickness, mm					
				textolite	Al	Fe	Cu	Sn	Pb
Na^{22}	2,6 years	1,28	0,213	61	43	26	21,5	16	3,3
Co^{60}	5,24 years	1,33	0,215	—	—	—	—	—	—
		1,17	0,209	61	43	26	21,5	14	3,3
Mn^{54}	291 days	0,84	0,196	56	39	23,5	19,5	12	2,7
Cs^{137}	30 years	0,66	0,184	53	37	22	18,5	11	2,5
Ba^{133}	9,5 years	0,360	0,148	46	32	16,5	13	6,2	1,4
		0,290	0,135	44	30	15,5	11,5	5,0	1,1
Gd^{153}	230 days	0,103	0,073	34	20	5,5	3,5	0,9	0,20
Cd^{109}	470 days	0,087	0,065	30	18,5	4,5	2,6	0,6	0,13

The values of x_{lim}, for the materials shown in Table 1 were calculated by the author from the formula

$$x_{lim} = \frac{2-4}{\mu_{0°} + \mu_{180°}}, \qquad (2)$$

suggested in [1].

Of the γ -radiation listed in Table 1 the Cd^{109} isotope is not produced, nor are the isotopes that are not included in Table 1: Al^{26}, V^{50}, Rh^{101} [2]. The economically most suitable are Co^{60} and Cs^{137}. There are also suitable γ -radiators with $T_{\frac{1}{2}} < 0.5$: $Zr^{95} + Nb^{95}$, Sr^{85}, Ru^{103}, Sn^{113}, Cr^{51}, Hg^{203}, Re^{189}, Ce^{141} [2]. Of these Sn^{113} and Re^{189} are not produced in the necessary form.

To calculate x_{lim} in the range $0.3 < E_{\gamma 0°} < 2.0$ Mev, satisfactory results are given by the use of the empirical formulas $x_{lim} = mE^{k}_{\gamma 0°}$, where x_{lim} is expressed in millimeters and $E_{\gamma 0°}$ in megaelectron volts. The following values should then be used:

	Z=8	Z=13	Z=26	Z=29
m	58	41	24	20
κ	0,2	0,2	0,25	0,25

Isotopes with $T_{\frac{1}{2}} < 0.5$ year are less convenient in instruments; however, they are suitable for research work.

Table 2 compares values of x_{lim} calculated by formula (2) and found experimentally by the author in 1959 on a scintillation γ -spectrometer with FEU-19M, NaI(Tl), by the analyzer AADO-1 and PS-10,000 for the isotopes Cs^{137} and Cr^{51}.

A certain difference in the calculated values of x_{lim} and the experimental values is due to the fact that formula (2) does not completely accurately allow for the scattered radiation: the values of the factors $\mu_{0°}$ in the tables published for them are given for narrow beams of γ -radiation.

The values of x_{lim} given in Table 2, corresponding to the thickness of the diffuser material for $I(x) = 0.98\, J(x)_{max}$ can be calculated directly from formula (1).

Table 3 gives the maximum intensity of the back-scattered radiation $I(x)_{max}$ for various materials. The value of $I(x)_{max}$ is a limiting value of $I(x) = J(x)/J(0)$ when $x = x_{lim}$.

TABLE 2. Calculated and Experimental Values of x_{lim}

Material	Cs^{137}				Cr^{51}			
	0,661 Mev	0,184 Mev	x_{lim}, g/cm²		0,320 Mev	0,142 Mev	x_{lim}, g/cm²	
	$\mu_{0°}$, cm²/g	$\mu_{180°}$, cm²/g	calculated	experimental	$\mu_{0°}$, cm²/g	$\mu_{180°}$, cm²/g	calculated	experimental
Fire-refined copper	0,072	0,176	16 (1,8)	19 (2,0)	0,106	0,260	11 (1,2)	13,5 (1,5)
Brass	0,070	0,190	15,5 (1,85)	17,5 (2,0)	0,106	0,273	10,5 (1,3)	10 (1,2)*
Alloy D16/T	0,075	0,125	10 (3,7)	10,3 (3,8)	0,100	0,140	8,3 (3)	5,5 (2)*
								7,5 (2,7)
Magnesium MG	0,075	0,123	8,5 (4,8)	5,8 (3,2)	—	—	—	—
Textolite	0,076	0,125	7,5 (5,3)	6 (4,2)	0,103	0,136	6,3 (4,5)	5 (3,5)
Heat protective material	—	—	—	4,2 (3)	—	—	—	3,5 (2,5)
Tin	0,076	0,442	7,7 (1,1)	10 (1,5)	0,150	0,850	4 (0,55)	5 (0,7)*

Note: The asterisk shows the data of [3] and the brackets show values for thicknesses in centimeters.

TABLE 3. Maximum Intensity of Back-Scattered Radiation

Material	Cr^{51} ($E_{\gamma 0°} = 0,320$ Mev)	Cs^{137} ($E_{\gamma 0°} = 0,661$ Mev)	Co^{60} ($E_{\gamma 0°} = 1,25$ Mev)
Fire-refined copper	2,70±0,03	2,50±0,03	2,25±0,03
Alloy B16T	2,35±0,03	2,05±0,02	1,75±0,02
Magnesium MG	2,10±0,02	1,75±0,02	1,65±0,02
Textolite	1,95±0,02	1,66±0,02	1,46±0,02
Heat protective material PKM	1,70±0,02	1,55±0,02	—
Tin	1,58±0,02	1,73±0,02	1,78±0,02

The fact that the author obtained values of $I(x)_{max}$ for a number of materials somewhat greater than in [3] may be due to the better resolving capacity of the counting apparatus, in particular the quality of the NaI(Tl) crystals and the AADO-1 instrument. The counting-rate meters lower the value of $I(x)_{max}$ on the average by 5% compared with the scalers.

It is interesting to observe that, being represented graphically as functions of the atomic number Z of the diffuser, the curves of x_{lim} and $I(x)_{max}$ have the same character: for $20 \leq Z \leq 35$ on the curves of x_{lim} and $I(x)_{max}$ there is a maximum. It is due to the predominance of the Compton scattering of the γ-quanta over the other forms of reaction of quanta with the material; i.e., for $20 \leq Z \leq 35$, since $\mu_{0°}$ and $\mu_{180°}$ are additive values.

LITERATURE CITED

1. N. N. Shumilovskii and L. V. Mel'ttser, Theoretical Principles of an Automatic Control Device using Radioactive Isotopes [in Russian] Moscow, Acad. Sci. USSR Press, 1959, p. 74.
2. B. S. Dzhelepov and L. K. Peker, Decay Schemes of Radioactive Nuclei [in Russian] Moscow, Acad. Sci. USSR Press, 1958.
3. U. A. Ulmanis and N. A. Dubinskaya, Atomnaya Energiya 3, No. 6, 59 (1957).*

* Original Russian pagination. See C. B. translation.

CHANGE IN THE ACTIVITY OF U^{235} AND Pu^{239} FISSION PRODUCTS WITH TIME

F. K. Levochkin and Yu. Ya. Sokolov

Translated from Atomnaya Energiya, Vol. 10, No. 4, pp. 403-404, April, 1961
Original article submitted September 19, 1960

To solve some problems in radiometry and dosimetry it is essential to know the change in activity of U^{235} and Pu^{239} fission products with time. In the literature results are published of investigations [1-4] in which calculations

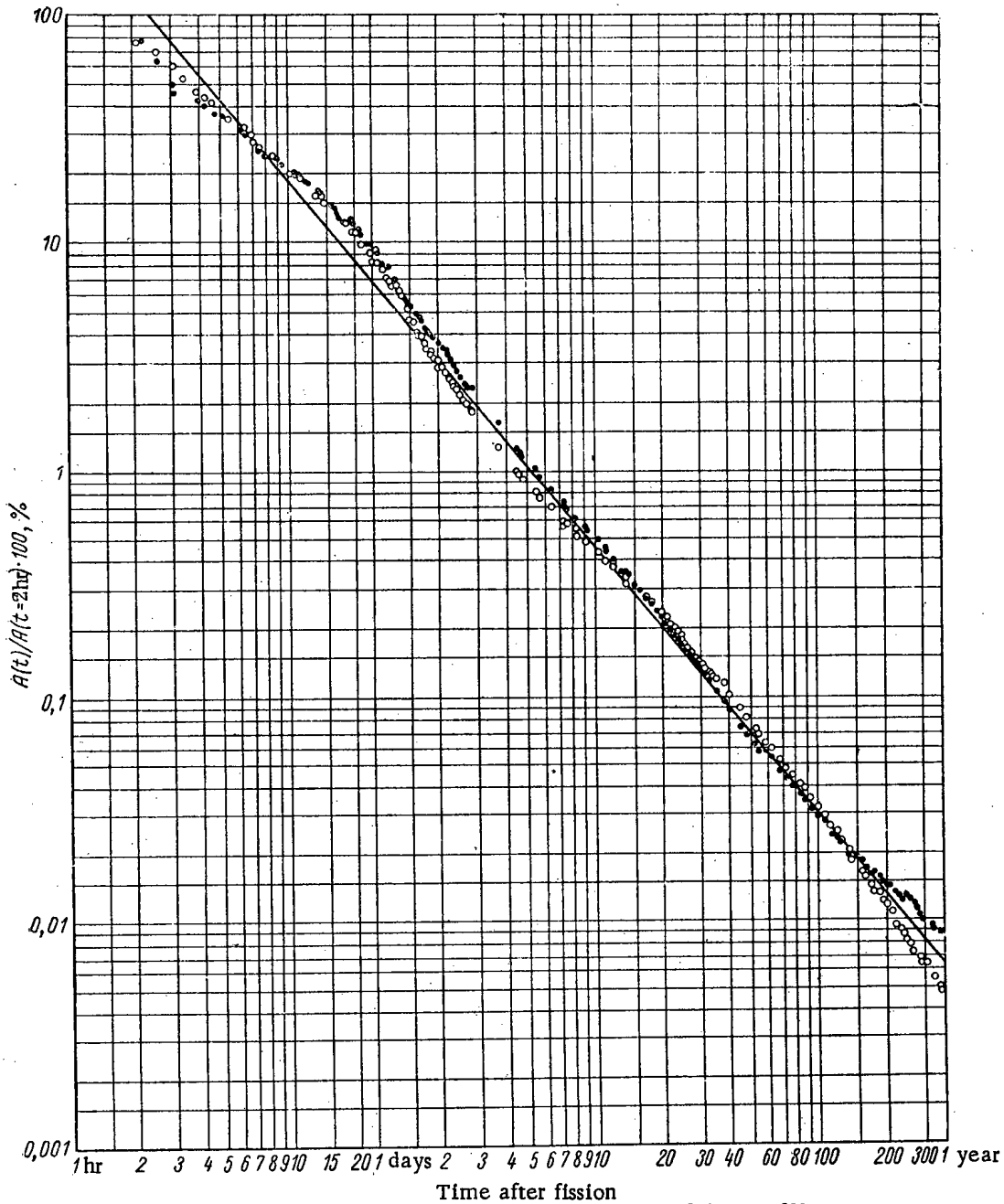

Change in time of activity of fission products: ○) U^{235}; ●) Pu^{239}.

were made of the isotope composition of a mixture of fission products and their activity at different instants of time after fission. Additional investigations are needed to improve the accuracy of the initial data (half lives of separate isotopes, yield of fission products, etc.).

In this work we studied the change in activity of U^{235} and Pu^{239} fission products over a period of time from 2 hr to 1 year. To carry out the work, hermetical sources were prepared in the form of two polythene films in the form of discs of diameter 30 mm and thickness 5 mg/cm^2 welded to one another around the perimeter. Uranyl nitrate enriched with U^{235} and plutonium nitrate were placed between the films. The sources contained 0.0001-0.1 mg of fissionable material. In all, 16 sources were prepared: eight to obtain U^{235} fission products and eight to obtain Pu^{239} fission products. In addition, to allow for the induced activity in the film, discs were prepared without fissionable material.

To obtain the fission products the prepared specimens were placed in an experimental block which was kept for 40 sec in the active zone of a reactor with a neutron flux of about 10^{12} neutrons/sec · cm^2. The activity of the fission products was measured by a comparative method with standard geometry using an end-window counter MST-17. The thickness of the absorbing layer (mica, air, and film) was 15.6 mg/cm^2; the statistical error of the measurement did not exceed 3%.

The results of the measurements are given in the figure where the time passing after fission is plotted along the abscissa axis and along the ordinate axis is plotted the activity of the fission products in percent, 100% being taken as the activity 2 hr after fission.

As can be seen from the figure, the change in activity of U^{235} and Pu^{239} fission products during a period of time from 2 hr to 200 days after fission is practically the same. Later a certain difference is observed in the rate of decrease in activity of U^{235} and Pu^{239} fission products, which gradually becomes more important and toward the end of the year reaches 60%. A comparison of the experimental curves for change in activity of U^{235} and Pu^{239} fission products with time (see figure) with analogous calculation curves, presented in [3, 4], showed that the difference between them is very small and in a period from two days to one year the curves coincide. The change in activity of the U^{235} and Pu^{239} fission products shown in the figure is satisfactorily described by the equation $A_t = A_{1t}^{-1.2}$ (continuous line) suggested in [1] for the products of fission of U^{235} by slow neutrons. The deviation of the experimental values of activity from those calculated with this equation does not exceed 40% in a period from 2 hr to one year.

The obtained experimental data and the calculated values given in the literature for the change in activity of U^{235} and Pu^{239} fission products with time are therefore in agreement.

LITERATURE CITED

1. K. Way and E. Wigner, Phys. Rev. 73, 1318 (1948).
2. H. Hunter and N. Ballow, Nucleonics 9, No. 5 (1951).
3. R. Björnerstedt, L. Löw, and S. Ulvönäs, Sweden, Preliminary Report to U. N. Scientific Committee of Effects Atomic Radiation (July, 1956).
4. K. Löw and R. Björnestedt, Arkiv fys. 13, No. 5, 85 (1957).

NEWS OF SCIENCE AND TECHNOLOGY

INTERCOLLEGIATE CONFERENCE ON TECHNIQUES FOR SEPARATION OF RARE METALS OF SIMILAR PROPERTIES

A. N. Zelikman

Translated from Atomnaya Énergiya, Vol. 10, No. 4, pp. 405-424, April, 1961

Among the engineering problems arising in the production technology of the rare metals, one of the most difficult ones is the separation of such close chemical analogs as zirconium and hafnium, niobium and tantalum, the rare earths, and several others generally found in association in their natural raw materials.

The main point which attracts attention, in questions involving the elaboration of techniques for separating elements of similar properties, concerns nuclear specifications for structural materials: in addition to the necessary physical-chemical and mechanical properties, certain nuclear properties are also required. This has given rise to the problem of extracting pure zirconium and pure niobium with minimal content of such analog impurities as hafnium and tantalum, which possess high thermal-neutron capture cross sections. The exceptional interest accruing to studies and isolation in pure form of distinct rare-earth elements is also intimately related to the increased applications of those materials in nuclear industry. Particular interest was aroused by the considerably high content of isotopes of the lanthanides in nuclear-fuel fission fragments. Detailed investigations have shown that individual rare earths possess some valuable and unique physical and nuclear characteristics, which have greatly broadened the range of applications for this group of elements, and has placed a premium on the development of industrially feasible separation techniques.

During the past ten years, new and efficient separation techniques have been worked out for elements of very similar properties, viz.,ion exchange chromatography, organic solvent extraction, fractional distillation of volatile compounds, techniques based on crystal physics, etc., and significant improvements have been achieved in earlier existing techniques, such as fractional crystallization and precipitation. Extensive research covering a variety of promising techniques has been conducted at various research institutes and technical colleges throughout the Soviet Union.

At the M. I. Kalinin Institute of Nonferrous Metals, an intercollegiate conference on separation techniques for rare materials of similar properties was held in November,1960, with the object of generalizing the experience accumulated in this field. The conference was the center of heightened interest. Over 250 delegates were in attendance, representing 10 technical college bodies, 13 institutes under the Academies of Science of the USSR and sister Soviet republics, and 20 industry-level research institutes plus delegates from some industrial plants.

Fifty-six reports were delivered in the four days the conference was in session. These papers discussed the physical-chemical foundations underlying various separation techniques and the results of research on the conditions governing separation of elements and applications to various forms of raw material as encountered in the Soviet Union.

The largest number of papers in one field took up separation of elements by solvent extraction techniques (19 papers), followed by ion exchange chromatography (13 papers), and fractional crystallization and precipitation (9 papers). The remaining papers shed light on methods of fractional distillation and rectification of volatile halides, fractional electrolysis, selective reduction or oxidation, and crystal physics techniques for ultimate purification of compounds.

In this brief treatment, it would be difficult to give a reasonably full account of all the reports made to the conference. We shall single out several of them, touching on various groups of separation techniques.

Ion-exchange techniques. Some interesting review papers relating to this grouping were made by M. M. Senyavin ("Chromatographic isolation of pure preparations of the rare earths") and B. N. Laskorin ("Ion exchange and chemisorption processes in nonferrous hydrometallurgy"). In the second of these, sorption and extraction processes were approached from a unified point of view. In particular, it was demonstrated that optimum conditions for absorption by liquid ion-exchangers could be predicted from available data on sorption on solid ion-exchange resins.

The mechanism operating in ion-exchange separation of bulk quantities of the rare earths was discussed in a report by L. I. Martynenko et al. The authors expounded the advantages of using several chelating agents in elution, rather than hydroxy acids.

Several papers were devoted to ion-exchange separations of tantalum, niobium, and titanium. The results of a pilot-plant verification of a method employing sorption from fluoride solutions were discussed in a report by N. P. Kalonina and N. P. Magda. Other reports (E. A. Subbotin, D. M. Chizhikov, etc.) demonstrated the feasibility of sorption from chloride solutions.

An appreciable number of contributions were delivered on ion-exchange separation of zirconium and hafnium. Among these, we may single out the interesting contribution by B. N. Laskorin, G. E. Kaplan, and A. M. Arzhatkin on continuous chromatographic separation of zirconium and hafnium. The possibility of effecting an ion-exchange separation of selenium and tellurium by employing sorption on cation and anion exchange resins was discussed in a paper by D. I. Ryabchikov et al.

Extraction techniques. A review of extraction techniques in rare-earth separations was made by G. V. Korpusov. Among the new trends stressed by the reporter and illuminated in other reports (by V. A. Mikhailov, V. G. Torgov), the use of complexing agents in rare-earth extractions, for example chelating agents to increase separation efficiency, and especially for the elements in the yttrium subgroup, show some promise. In addition to tributylphosphate, other organic extracting agents were studied, e. g., dibutylphosphate (Z. A. Shek and E. E. Kriss). Successful achievement of a continuous process for extraction separation of elements belonging to the cerium subgroup was discussed in a paper by N. I. Gel'perin, V. L. Pebalk and associates.

Judging by reports delivered by some research teams, the method of solvent extraction holds greatest promise for tantalum-niobium separations. A. I. Vaisenberg, T. F. Zhitkova, and L. A. Kolchina studied extraction conditions for tantalum and niobium, using cyclohexanone and tributylphosphate as extractants on fluoride solutions; G. E. Kaplan, B. N. Laskorin et al., showed the feasibility of tri-n-octylamine for that purpose; other investigators (V. K. Kulifeev, V. Z. Nepomnyashchii) studied extraction of tantalum, niobium, and titanium from chloride solutions using industrial alcohols.

One of the outstanding advantages in solvent extraction methods for tantalum and niobium separations is the possibility of simultaneously purifying those elements from titanium and silicon impurities.

Results of a study of extraction separation of zirconium and hafnium by using amines, organophosphorus compounds, and other extracting agents were compared in a report by G. E. Kaplan, G. A. Yagodin, and associates. Other reports dealt with extraction of zirconium and hafnium by cyclohexanone from sulfate solutions (F. L. Motov and T. G. Loshtaeva), and the isolation of pure hafnium dioxide by the method of rhodanide extraction (M. V. Vinarov et al.).

Fractional precipitation and crystallization. Although the brunt of the attention of researchers was directed to studies of new separation techniques, the methods of fractional precipitation and crystallization have not lost their significance. Results of a study of separation of titanium, niobium, and tantalum based on the solubility difference of their chloride complex salts (D. M. Chizhikov, B. Ya. Tratsevitskaya et al.), phosphate compounds (A. P. Shtin, A. K. Sharova), sulfate complexes (Ya. G. Goroshchenko) and other derivatives were announced in several papers. An ingenious technique for separating rubidium and potassium, based on the difference in the solubility of their bromochlorides, was made public in a report by B. D. Stepin and V. E. Plyushchev.

Distillation and rectification techniques. A review of separation and purification techniques for zirconium and hafnium, tantalum and niobium, based on the differences in the volatilities of their halides, was made in a paper by L. A. Nisel'son. The author discussed the problems of fractional separation of chlorides and metal chloride complexes using phosphorus oxychloride, and stressed the problems encountered in separating zirconium and hafnium by fractional distillation of their tetrachlorides under pressure. Other papers discussed results of studies and tungsten and molybdenum separations based on the differences in volatility of their chlorides and oxychlorides (A. N. Zelikman, O. E. Krein et al.), and thoroughgoing purification of tungsten and molybdenum salts via fractional distillation (V. N. Chernyaev and V. V. Krapukhin).

Miscellaneous techniques. Among the other separation techniques of interest, we might first mention research on separation of zirconium and hafnium via selective reduction of their chlorides (papers by V. A. Kozhelyakin and associates, and V. S. Emel'yanov, A. I. Evstyukhin et al.). The advantages of this method are the high separation coefficients and the obtaining, as a result of the separation, of products suitable for direct extraction of metal.

Mention should also be made of papers, discussed at the conference, on the behavior of zirconium and hafnium in fused salt electrolysis (V. M. Smirnov et al.), and purification of tungsten from molybdenum impurities by zone melting (P. I. Fedorov and N. V. Mokhosev).

In the discussion of the reports presented, and in the statements adopted by the conference, attention was drawn to the need for expanded research on the properties and basic physical-chemical constants of rare elements and their compounds, on the theoretical foundations of processes for separating elements, on the design and improvement of equipment and techniques for calculating pertinent data, engineering costs evaluations of various separation techniques, and perfection of analysis techniques. The conference itself served as a materialization of the coordination of the scientific efforts of various technical colleges and research institutes, thanks to the extensive information shared on the work carried out, and the personal contacts made.

The proceedings of the conference will be published in 1961 in a symposium to be prepared for press by the Metallurgical Press (Metallurgizdat).

FOURTH ALL-UNION CONFERENCE ON PHYSICOCHEMICAL ANALYSIS

Translated from Atomnaya Energiya, Vol. 10, No. 4, pp. 406-407, April, 1961

The N. S. Kurnakov Institute of General and Inorganic Chemistry and the A. A. Baikov Institute of Metallurgy, both under the Academy of Sciences of the USSR, sponsored the regular Fourth All-Union Conference on Physicochemical Analysis, which was held in Moscow, December 6-10, 1960. The Conference was scheduled on the occasion of the 100th anniversary of the birth of the renowned Soviet scientist N. S. Kurnakov. A certain portion of the reports included in the crowded agenda of the Conference (which heard a total of 142 reports) dealt with questions relating to nuclear industry.

A paper delivered by O. S. Ivanov discussed work on the physicochemical analysis of uranium, plutonium, thorium and their alloys, and on zirconium and beryllium; data were cited on phase transformations in uranium, plutonium, thorium, zirconium, and beryllium. Phase diagrams, the structure and the properties of alloys of these metals were systematized on the basis of the D. I. Mendeleev periodic table. The concluding section contained a description of the development of a method of physicochemical analysis pertaining to studies of metals of nuclear interest.

A paper presented by V. I. Spitsyn, "Radioactive phenomena and new problems in physicochemical analysis," noted some features in the properties of compounds with radioactive atoms. For example, the introduction of radioactive isotopes into sorbents has a drastic effect on sorptive power. The solution kinetics and the solubility of sparsely soluble substances varies sharply in response to radioactive bombardment. Similar phenomena related to effects of self-irradiation on the surface properties of solids must be taken into account in studying melting, evaporation, polymorphic transformations, polymerization, and other processes occurring in solid radioactive materials.

At a panel session on uranium alloys, reports discussed included a study of classical techniques of thermal, dilatometric, microscopic, and x-ray structure analyses of phase diagrams and of the structure of ternary systems in the region of solid state transformations, for such systems as: thorium–zirconium–uranium (G. K. Alekseenko and T. A. Badaeva), uranium–zirconium–molybdenum (G. N. Bagrov), uranium–zirconium–niobium (L. I. Gomozov), uranium–niobium–molybdenum (G. I. Terekhov).

At the panel on rare metals, a report was delivered by E. M. Savitskii on the physicochemical analysis of those metal systems containing rare metals. The author presented a review of the states of these research projects and indicated that Soviet scientists occupy advanced positions in some aspects of research on the structure of phase diagrams of plutonium, uranium, niobium, vanadium, rhenium, cerium, and lanthanum. However, the reporter noted that some investigations, especially projects on generalization of phase diagram data and constitution vs. property diagrams, as well as the development of modern theory of metal alloys, are undergoing retarded development, and must be given due priority in the present period.

A paper delivered by V. F. Terekhova presented a generalization of empirical and theoretical data on alloys of the rare earths. New phase diagrams were described for alloys of yttrium, neodymium and gadolinium with magnesium, yttrium and neodymium with aluminum, gadolinium with iron and nickel, and the magnetic properties of the latter were investigated. Recommendations were advanced on the industrial utilization of several alloys of the rare-earth metals. M. A. Tylkina, on the basis of a study of rhenium, tantalum, and tungsten alloys, presented some generalizations on the interaction between rhenium and the transition metals of the IV-VIII groups of the periodic table (titanium, zirconium, hafnium, vanadium, niobium, tantalum, chromium, molybdenum, tungsten, manganese, and cobalt), and also described the general features of the interaction between tungsten and tantalum with some transition metals of groups IV-VIII.

MATERIALS OF THE KINGSTON (ONTARIO) CONFERENCE ON NUCLEAR STRUCTURE

A. I. Baz' and V. M. Strutinskii

Translated from Atomnaya Énergiya, Vol. 10, No. 4, pp. 407-409, April, 1961

At the end of August and beginning of September, 1960, an international conference devoted to problems of the structure of atomic nuclei was held in Kingston, Canada. In a certain sense, this conference served the function of reviewing and summing up the results of nuclear physics developments over the past decade, during which the modern concepts of nuclear structure and of the mechanism of nuclear reactions took definitive shape. Simplified model representations reflecting one or another aspect of the over-all problem were introduced into the discussion to describe various aspects of nuclear physics. These models were, by their very nature, approximations, useful for describing a limited range of problems.

One of the outstanding successes attained in recent years has been the proliferation of simplified pictures used for description of nuclei, now acquiring a definitive shape in five principal models whose ranges of applicability may be reasonable accepted as understood. These models are:

1) the independent-particle model;

2) the optical model or cloudy crystal ball;

3) the collective model;

4) the "direct" mechanism in nuclear reactions;

5) the statistical model.

The first two models (the independent-particle model and the optical model) are intimately related. An enormous selection of papers devoted to these models were delivered at the conference, and may be summarized as follows.

The independent-particle model reflects the "single-particle" aspect of nuclear material; i.e., the fact that nucleonic motion within the nucleus occurs to a large measure independently of the motions executed by the remaining nucleons. The results obtained on the basis of these concepts show excellent agreement with a multiplicity of experimental data; the agreement proves to be even more noteworthy and complete than might have been anticipated. A striking affirmation of the independent-particle model has been ofered by P. Hillman, H. Tyrén, and T. Maris who studied the (p, 2p) reaction. The study of the energy and angular distributions of the two final protons provided direct evidence in support of the view that even inner nucleons contained within the nucleus exist at certain single-particle levels (the energy associated with those levels was established), and, consequently, move independently of each other in the first approximation.

Another affirmation, almost equally convincing, of the independent-particle model is the tremendous success enjoyed by the Nielson scheme: the scheme of single-particle levels for nucleons in the deformed nucleus, calculated on the basis of the independent-particle model. An overwhelming quantity of experimental facts accounted for in this scheme serves to confirm its correctness and,as a corollary, the correctness of the basic concept contained in the independent-particle model.

It is quite natural that the independent-particle model should be found applicable to the description not only of one particular problem, but of a whole broad range of problems in nuclear physics. The nucleons in the nucleus do not move entirely independently of each other, since some portion of the forces acting between nucleons (the residual interaction) may not be included in the self-consistent potential which defines the postion of single-particle levels in the independent-particle model. It is necessary to take this residual interaction into account in order to calculate the properties and the positions of the nuclear levels. The form and magnitude of the residual interaction remain as yet obscure, and this renders any detailed calculation of nuclear spectra impossible. Although those spectra which have been calculated agree quite well (sometimes even too well) with empirical data, the general problem of the residual interaction still awaits its definitive solution. In this sense, the hypothesis advanced by A. de Shalit (and based primarily on nuclear magnetic moment data) to the effect that the p-n interaction leads to a far smaller residual interaction than the p-p or n-n interactions seems quite intriguing.

The essential limitation upon the independent-particle model is the fact that, in its present form, it is inapplicable to the description of surfaces of nuclei: at the nuclear surface,correlation between nucleons is very strong and is not predicted by the independent-particle model. In general, the problem of the structure of the nuclear surface remains to this day one of the least clarified questions in the physics of the atomic nucleus.

The optical model is conceptually very closely related to the independent-particle model, since a particle incident upon a nucleus moves, according to the former, within the nucleus in some kind of self-consistent optical potential independently of the motion of the other nucleons contained in the nucleus. This a very simple model, requiring such parameters as the nuclear radius, radius of diffuseness of the nuclear surface, and the magnitudes of the real part V and imaginary part W of the self-consistent optical potential $V-iW$, and accounts satisfactorily for experimental data available on the size of total cross sections and elastic scattering cross sections.

One of the greatest successes of the optical model is generally agreed to be the agreement between the diffuseness parameters of the nuclear surface obtained from scattering experiments of various particles from nuclei (e, p, n, He). The mean radius of diffuseness obtained from those experiments was found to be $\sim 0.55 \cdot 10^{-13}$ cm. Even when W was assumed porportional to V, the calculated cross-section values could be brought into excellent agreement with experimental findings by a reasonable assignment of radial and energy relations for V. Agreement should have been poorer, according to theory.

In the course of the discussions at the conference, it was noted more than once that this should put us on guard and warn us against being over-complacent, and against any tendency to rest on the laurels won so far by the optical model. All the more so in that there are at hand facts which the optical model is as yet incapable of accounting for. As representative examples of such facts, we may cite the low value of the strength function in the region A = 100. Still another serious shortcoming is the fact that the optical model failed to yield the desired effect in the attempt to explain the experimental results reported by L. Rosen, where the energy and angular dependence of neutron and proton polarization at 3-7 Mev in scattering from various nuclides were measured.

There still remain troubling ambiguities in the optical model, which is far from fully clarified. The problem of the optical potential parameters has not been resolved definitively to the present writing, for instance, especially in the case where it is assumed that absorption takes place predominantly on the nuclear surface. Also obscure is the problem of the structure of the nuclear surface, and the problem of the behavior of the real and imaginary parts of the optical potential in that region.

Considerable time was devoted to the collective model of nuclei at the conference. The use of methods developed in superconductivity theory to resolve problems on the role of pairing forces has resulted in quantitative agreement between theoretical and experimental values of the fundamental constants characterizing collective motion in nuclei (moment of inertia, mass coefficient). It was found that one of the modes of collective motion, specifically vibration of the surface of nuclei, has in reality a much more complex nature that might be inferred from the earlier semi-intuitive model, and the very existence of collective motion in this form is attributed directly to nucleon pairing. Improved quantitative accord between theory and experiment also resulted in the case of some

nuclear reactions (stripping), radiative transition probabilities, and magnitudes of nuclear magnetic moments when pairing effects were taken into account. The problem of the relation between the vibrational model of nuclei and the model of the nonaxial nucleus was treated in detail. A presentation by A. S. Davydov, devoted to an explanation of new results in the model of nonaxial nuclei, drew considerable attention. The discussion took note of the great success scored by the theory in the interpretation of experimental findings. Some critical remarks were also voiced, in the main referring to the single-valuedness assumed by the nonaxial representation. Additional experimental research will be needed to arrive at any definitive confirmation of the nonaxial model of rotating nuclei, notably in the region of nuclei with maximum asymmetry ($\gamma \sim 10\text{-}20°$).

A presentation by L. V. Groshev (USSR) on the results of precision measurement of gamma-ray spectra accompanying thermal neutron capture, with the aid of a conversion spectrometer, was heard in connection with the formulation of the need for experimental proof of the existence of vibrational levels in spherical nuclei. This method is revealing the broad scope of its opportunities, particularly for discovering high-lying levels of zero spin.

The conference also heard reports presenting findings from some new research projects devoted to the microscopic description of dipole vibrational states of the nuclei (G. Brown, V. G. Shevchenko). This trend in research shows great promise, although the results obtained to date are far from perfect.

A better understanding of the theory of direct interaction processes led to a new success in the statistical theory of the compound nucleus. In the case of atomic nuclei of intermediate and heavy atomic weight, interference between direct interaction processes and processes taking place via the formation of a compound nucleus do not exist, for practical purposes. This makes it possible to separate the processes from each other without ambiguity and to introduce a substantial simplification in the interpretation of the nuclear reactions involved. This refers with particular emphasis to nuclear charge exchange processes. At the present time, we may consider it an established fact that the level density in the compound nucleus and the barrier penetration factor are the principal factors responsible for the decay of the compound nucleus. The dependence of level density on the magnitude of the compound nucleus leads to angular anisotropy of the emitted particles. The success of the theory utilizing these concepts was noted in a review paper on the statistical model of the nuclei (T. Erickson). Another verification of the compound nucleus model consists in the study of the properties and distribution of nuclear resonances. A review paper was devoted to this subject by J. Harvey. New data on fluctuations in the values of Γ_n, Γ_f, and Γ_γ for resonances in the thermal region are found to be in excellent agreement with the Porter-Thomas distribution for a reasonable assignment of the number ν characterizing the number of open channels ($\nu \sim 1$ for Γ_n and Γ_f, and $\nu \sim 30\text{-}100$ for Γ_γ). In this connection, one finds somewhat astonishing the result obtained by D. Hughes and colleagues, who discovered that the value of Γ_γ for a partial transition from 4.06 Mev in the nuclide U^{238} remains constant for the ten resonances investigated, i.e., ν_{eff} is large. On the other hand, it was shown in contributions by Argonne National Laboratory that $\nu_{eff} \sim 1$ for several partial transitions in the nuclear species Pt^{195} and Hg^{199}. New experimental data on the distribution of the distance between resonance peaks agree with the Wigner distribution, which serves as a confirmation of the hypothesis, underlying the statistical model, of the random phase of the wave function describing the complex state of the compound nucleus.

Problems related to fission of nuclei were discussed at the conference only to the degree that they were pertinent to nuclear structure. A proof of the existence of some analogy between the structure of states of the "intermediate" nucleus (i.e., the compound nucleus in a deformation corresponding to a saddle point) and levels of a deformed nucleus near ground state would be welcomed as of major importance. On the basis of the hypothesis first advanced by O. Bohr in 1955, some connection must prevail between the quantum-mechanical characteristics of the state of the compound nucleus and fission symmetry; two groups of neutron resonances characterizing strongly diverging values of $\overline{\Gamma}_\gamma$ must also be observed, the largest value of $\overline{\Gamma}_f$ being observed for resonances with spin 0, 2, 4 when the compound nucleus has positive parity, and 1, 3 for the case of negative parity. An analysis of available experimental data does not yet warrant any unambiguous conclusion on the validity of O. Bohr's hypothesis.

A good deal of space was devoted to an exposition of results obtained from an analysis of new data on angular distribution of fission fragments in the case of fission induced by intermediate-energy neutrons. The angular distribution of the fragments indicated the value of the parameter K_0^2 characterizing the anisotropy of the angular distribution. The value found empirically for this quantity was in excellent harmony with the theoretical prediction, once pairing effects were taken into account. The experimental angular distribution data also provide evidence for what we infer to be the presence of a phase transition in the intermediate nucleus at excitation energy ~ 7 Mev, when the moment of inertia of the nucleus becomes equal to the rigid-body value.

New data on "specific" fission problems were discussed in a review paper on fission. Here, we must take note of the new findings obtained by workers at the Chalk River laboratory (Canada). These findings support the view that the kinetic energy of the fragments decreases abruptly for symmetrical fission. A report by O. P. Komar stating that he and associates had detected the existence of three maxima in the mass distribution of photofission fragments of Th^{232} was received with great interest. In his review paper, J. Hahn also took note of the need for thorough investigation of effects possibly related to the size and orientation of the angular momentum of the frament. Available experimental data favor the inference that the angular moment of the fragments is large and is oriented along the direction of flight of the fragments. Clarification of this question may play an important role in future developments.

SYMPOSIUM ON ATOMIC-POWERED SHIPS

Translated from Atomnaya Énergiya, Vol. 10, No. 4, pp. 409-410, April, 1961

In mid-November, 1960, a symposium on marine nuclear propulsion plants and safety problems associated with their operation was held at Taormina, Italy (on the island of Sicily). The symposium was organized by the IAEA.

The following problems were discussed at the symposium: economics and national activities in the field of atomic shipbuilding, international problems and the over-all safety questions associated with atomic vessels, atomic vessel designs viewed from the standpoint of safety, marine reactor design problems, problems associated with the flow of seawater and design of hulls for atomic vessels, engineering maintenance of atomic vessels, and fuel reloading, safety in the operation of nuclear-propelled ships. Over 40 reports and other contributions were read on these questions.

The symposium showed that various countries have their own particular approach to the choice of reactor type for a ship with nuclear propulsion. Designs of nuclear ship propulsion plants incorporating an organic-cooled organic-moderated reactor (Britain, West Germany), a boiling-water reactor (West Germany), a pressurized-water reactor (USA), and a gas-cooled reactor (Britain) were discussed. In each case, specific attention was directed to shipboard functioning of the reactor types, with emphasis on safety problems.

Since civilian nuclear shipbuilding projects have not yet developed any broad scope (the only nonmilitary nuclear-propelled ship now afloat and in operation is the nuclear icebreaker LENIN), the subject matter of the overwhelming bulk of the reports was not based on experience, but rather dealt with suggestions and formulations of operating conditions and specifications applying to nuclear vessels, and conjectural descriptions of methods and techniques for realizing these conditions and requirements in practice. Most of the attention was therefore devoted to an analysis of aspects of the performance of conventional vessels which retain their validity for nuclear-propelled vessels (damage at sea, collisions, running aground), and to a discussion of associated problems. It must be affirmed, in general, that most of the attention in the reports was reserved for safety problems affecting nuclear-propelled vessels. This applies not only to the hazard that might be represented by a nuclear propulsion unit for the ship's crew, but also predominantly to the consequences which might possibly ensue from an accident at sea. L. Peffaut (France) made the forthright assertion that a nuclear ship would become a point of conflict between the opposing requirements of safety and costs feasibility. On the whole, the symposium showed that the risk associated with the use of nuclear ships may be reduced to a minimum, and does not present a danger for maritime traffic except under some exceptional combinations of circumstances.

Although the problems of nuclear shipbuilding economics were touched upon in several papers, this question was generally dealt with without going into specifics. One exception, we might add, was the paper submitted by G. Zamparo (Italy) on an economic analysis of maritime freighting via nuclear ships; reactors and fuel cycles were analyzed, and a comparison was made between several nuclear propulsion units for ships of the same type and displacement; diagrams were presented to illustrate choice of nuclear propulsion plant characteristics for a tanker with accessible operating costs. Results of costs investigations show that the most favorable economic prospects for some time to come are oil tankers.

The reports devoted considerable attention to the proper placement of the nuclear propulsion unit on board the ship, and to the effect of its positioning on ship safety conditions.

On the whole, the symposium demonstrated that nuclear shipbuilding is a topic of lively interest, and is being resolved in many countries around the world.

NEW RESEARCH IN THE STUDY OF THE GENESIS OF URANIUM DEPOSITS

A. N. Tugarinov

Translated from Atomnaya Énergiya, Vol. 10, No. 4, pp. 410-412, April, 1961

The 21st session of the International Geological Congress was held in Copenhagen during August 1960. The work of the session was divided among twenty panels; in one of the panels, the reports were entirely devoted to the problem of the genesis of uranium and thorium deposits. Fourteen reports, many of considerable interest, were heard at the sittings of the panel.

In his report, "Source of uranium in ore fields," R. Page (USA) reviewed the widely propagated concepts of genetic connection between hydrothermal uranium deposits and acid igneous rocks. Basing his work on the latest findings by American researchers, characterizing content of uranium in diabases and basalts, and also on the broad development of dikes of bedrock in spatial association with hydrothermal uranium deposits, association with uranium in ore veins of certain elements (Ni, Co, Cu, et al.) characteristic for deposits which are genetically related to mafic and ultramafic rocks, the author came to the conclusion that the uranium source could be provided by magma melts of basic and intermediate composition. The low uranium content in basic rock compared to acid magmas is due to the formation of larger amounts of uraniferous minerals in the latter. In discussing the source of uranium in deposits of different genesis, Page sums up the criteria determining which type the occurrence belongs to. Similar criteria are adduced for syngenetic occurrences in igneous and sedimentary species, and also for hypogene and supergene epigenetic occurrences.

A paper by M. Roubault and R. Koppens (France) shed light on results of a study of uranium distribution in the Mortagne granitic massif. The data cited provided a picture of the uranium content in the granites as a function of content of other elements.

A paper presented by A. Arrivas (Spain) cited new data on the mineralogy of hydrothermal deposits in Spain, and analyzed the position occupied by those occurrences in the European metallogenetic province.

Most of the attention at panel sessions was reserved for the topic of the genesis of "sedimentary deposits" of uranium, which was the subject of the most interesting papers. One of these, submitted by N. Katayama (Japan), had a programmatic character. It stressed the fact that most large payable uranium deposits are found in the continental facies of sedimentary rocks. The author proposed the following classification of occurrences under that heading: 1) syngenetic occurrences in lacustrine sediments; 2) occurrences formed by underground waters; 3) metamorphosed occurrences in ancient conglomerates. The second subtype, including occurrences of the highest value, was subdivided into:

a) occurrences in basal formations, principally in basal conglomerates. In these occurrences, one example of which is the Ningyo-Toge deposit (Japan), there is manifest a structural mineralization control effected by the beds of ancient streams;

b) lenticular deposits in sandstones with roe "rolls" (Colorado Plateau deposits);

c) deposits of the water table type, with an enriched zone found (presently or in the past) slightly below the ground water level.

The deposits formed in arid continental basins subject to the action of underground surface waters, precipitation of uranium from which took place as a result of reduction of hydrogen sulfide of biogenic origin. The absence

of any mineralization control by any fracturing structure, as well as other evidence, are interpreted by the author to completely refute any possibility of ore bodies forming in response to rising hydrothermal solutions. The differences observed in nonsynchronogenic deposits are accounted for in terms of metamorphism appearing after the uranium was deposited.

Occurrences in ancient conglomerates, overlain by thick sediment mass, have undergone hydrothermal infiltration leading to recrystallization of most of the ore minerals.

A discussion of the formation conditions of uranium deposits in continental sedimentary rocks received much attention, as a paper "Genesis of uranium occurrences" was presented by R. Nininger, D. Everhart, H. Aller, and J. Cratchman (USA). The authors lent their decisive support to the concept of formation of such deposits in response to underground waters. The principal geochemical factor affecting uranium distribution in sedimentary rocks is, in their view, the unequal solubility of compounds of hexavalent and tetravalent uranium in aqueous solutions. Reduction of the uranyl ion, leading to precipitation of tetravalent uranium, occurred predominantly through interaction with hydrogen sulfide, since the effect of bivalent iron was negligible. Hydrogen sulfide formation was due to reduction of the sulfate ion contained in bacteria in underground waters (bacteria are viable down to appreciable depths), during diagenesis of sediments. The bacterial attack on certain petroleum fractions is associated with the formation of uraniferous asphaltite in the largest of the Ambrosia Lake type deposits.

A report by E. Noble (USA) considered the conditions for localization of uranium deposits on the Colorado Plateau within the confines of extended mineral belts. This fact, as well as the absence of structural and lithological mineralization control, has brought the author to the view that the most important condition which could possible effect uranium transport and deposition is variation in pressure. The flow of uranium-enriched underground waters out of host rock is due to the pressure established by compaction of sediments and the action of tectonic forces. Lessening of pressure lowered the solubility of uranium compounds as the solutions entered into motion, and caused the precipitation of such compounds. The mineral belt is oriented at right angles to the presumed direction of flow of the streams. It is bounded on one side by a paleoisobaric surface corresponding to the pressure at which uranium began to settle from the solutions, and on the other side by a parallel surface beyond which no precipitation occurs because of depletion of the solutions.

In a very thoroughgoing paper submitted by J. Wier and W. Poffett (USA), "Affinity of uranium-vanadium and copper deposits of the Lisbon Valley district in Utah and Colorado, USA," a series of proofs was presented in support of a hydrothermal origin for the copper deposits, based on their morphology and the paragenesis of similar copper deposits found in granitic rock masses.

On the basis of a correlation of the features common to the geological structure and mineralogy of copper and uranium-vanadium deposits in the continental sandstones of the Colorado Plateau, the authors draw the inference that uranium-vanadium deposits as well as copper deposits formed through the action of low-temperature hypogene solutions, but at a great distance from the source and under other physicochemical conditions. In attributing the hydrothermal genesis of the deposits to the sandstones, the authors assume that the hydrothermal solutions underwent a change of composition as a result of mixing with stagnant and underground waters.

In a paper presented by L. Nell (Union of South Africa), "The problem of uraninite genesis in South African gold conglomerates," factual data supporting the hypothesis which assigns a sedimentary origin to the gold-uranium Witwatersrand deposits are summed up. It is noted that the geologists guided by this hypothesis succeeded in uncovering new ore fields. Prospecting criteria used were, in particular: 1) the distance from ore fields to the shore zone existing during the period of sedimentation; 2) interformational erosions leading to uranium enrichment of the conglomerates through erosion of more ancient ore beds.

In a highly interesting report, J. Armand and S. Landergren (Sweden) presented a detailed description of uraniferous peat bogs of the Narbotten district (Northern Sweden), the organic material (humus) of which contains an average of 0.09% uranium. Uranium enrichment of the peat bogs took place as a result of attack by underground carbonate waters. When the uranium content in the waters totaled $1 \cdot 10^{-5}$ %, 9000-fold uranium enrichment of the organic material took place via sorption. Experiments carried out on using an $NaHCO_3$ solution to leach uranium from the skarn and iron-ore-bearing rocks underlying the bogs confirmed the possibility of uranium becoming subtracted from the substrate in amounts sufficient to account for the presence of uranium in the bog material.

The problem of uranium distribution in an organic material during its fractionation was treated in a report by J. Muller (Chile). The results of a study of hydrothermally differentiated bitumens from Derbyshire (Britain) attested

to the fact that the O/C ratio varies directly as uranium content in the bitumens, while the H/C tends to vary inversely. A study of the behavior of organic matter in the zone of contact metamorphism, carried out by the author in one district in Chile, showed that uraniferous plant fossils graphitized as a result of being contact-metamorphosed by a batholith lost a considerable portion of the virtually uranium-depleted bitumens sublimating as a result of the contact. In contrast, the uranium content is found to increase appreciably in relict graphitized formations.

In addition to those heard at panel sessions, we may note the papers presented by J. Geffroy and J. Sarcia (France), "Experience in the classification of uraniferous vein deposits," V. Utenbogardt (Sweden), "Uranium mineralization in the Vestervik district," M. Alia (Spain), "The influence of surface morphology on uranium mineralization," and S. Miholic (Yugoslavia), "Secondary uranium enrichment of sedimentary rocks."

A TIMELY AND TOPICAL EXHIBIT ON "THE USES OF RADIOACTIVE ISOTOPES IN AUTOMATION AND PROCESS CONTROL"

V. M. Patskevich and S. A. Perepletchikov

Translated from Atomnaya Énergiya, Vol. 10, No. 4, pp. 412-415, April, 1961

An exhibit of timely interest devoted to the theme "Uses of radioactive isotopes in automation and process control" was open to the public of Moscow from November,1960 to February,1961, as part of a general exhibit displaying the achievements of the national economy of the USSR. The isotopes exhibit was held in the "Atomic Energy for Peaceful Purposes" pavilion. The goal of the exhibit was that of displaying the present state of the art and the assimilation into production techniques of automatic control and process control equipment and techniques based on the use of radioactive isotopes, and to generalize available experience and further promote the use of radiation devices in the national economy of the country.

The exhibit covered several distinct departments. The first of these was devoted to noncontact monitoring and control of levels of different media. Level gages and gamma-rays of various types capable of measuring and effecting automatic control over levels of liquids, free-flowing materials, and miscellaneous materials were on display in this section. Such instruments are being designed by NIITeplopribor (power instrumentation research institute), by the Institute of Automatic Control under the State Plan of the Ukrainian SSR, by TsNIIChermet (Central research institute for ferrous metallurgy), and other industrial organizations for use in the metallurgical, mining, ore processing, chemical processing, oil refining and petrochemicals, light industry, and other branches of industry. The instruments are being fabricated at the "Kaluga-pribor" plant, the Tallinn KIP experimental plant, and other enterprises.

An ARPU automatic level control produced in explosion,proof design by the Tallinn KIP plant is designed for contactless level sensing and control of the interface between two media of different specific weights, for on-stream performance in the chemical processing and petrochemical and oil refining industries. The instrument effects level control to within ± 40 mm.

Experimental devices still in the testing stage or being run through industrial pilot tests were also placed on display, in addition to mass-produced items. Design layouts and equipment for continuous sensing and control of blast-furnace charge levels were shown. These were designed by the TsNIIChermet in unison with the Ukrainian Ferrous Metallurgy Research Institute and the F. E. Dzerzhinskii Metallurgical Plant at Dneprodzerzhinsk. Also shown was a URU-6 type device for controlling the level of a stream of molten metal in crystallizers of continuous steel-casting machines. A URU-6 type device designed by TsNIIChermet is capable of recording levels to within ± 2 mm and may be employed in any branch of industry for automatic level control of liquids and free-flowing materials. An operating mock-up of a device designed to completely automate the process of hydraulic dust removal in a crushing mill was displayed. The device was designed by the Armenian SSR research institute for the mining and metallurgical industries.

A large portion of the section was occupied by a demonstration of devices incorporating radiation sources on the Yuzhny ore-dressing combine. These instruments allow workers at the combine to bring the entire process under

automatic control. One-hundred and eight GR-1 type gamma-ray relays put out by the Kharkov KIP plant were installed in the combine. The yearly savings occurring from the use of only 20 such devices in monitoring bottlenecks in load transfer in a crushing mill exceeded 900 thousand rubles.

The I. A. Likhachev Moscow automotive factory placed on display some instruments and circuits which have been at least partially engineered into the productive process for monitoring, alarm signaling, and control, with process control and some unit operation applications. An operating model of a facility for interlocking control of an automated cold-stamping press. The device, based on the use of a radioactive thickness gage, denies access to the press die to more than one workpiece at a time, eliminating any possibility of damage and shutdown of the automated line. This operating model proved a great attraction to the visitors.

The second section of the exhibit threw light on problems of noncontact sensing and control of densities, concentrations, pressures, and humidity. Among many other display items, we might single out the gamma-ray soil density gages used in an automatic control system for dredges. The gamma-ray soil gages are being used in many applications in dredgework in the construction of the Stalingrad hydroelectric power works. Several years' experience in using these instruments has shown that the productivity of labor may be increased 5%, and working conditions aboard dredges can be significantly improved with their aid. At the present time, river-duty suction degree barges are employing about 30 GK-1584 gamma-ray soil gages designed at the central drafting office of the river shipping ministry of the Russian Socialist Federated Soviet Republic. These devices are being used to measure, to ± 1% accuracy, and continuously record the content by volume of soil in pulp transported through the suction piping. The use of gamma-ray soil gages contributes to better organization of the dredging operations, and provides sizable economic advantages.

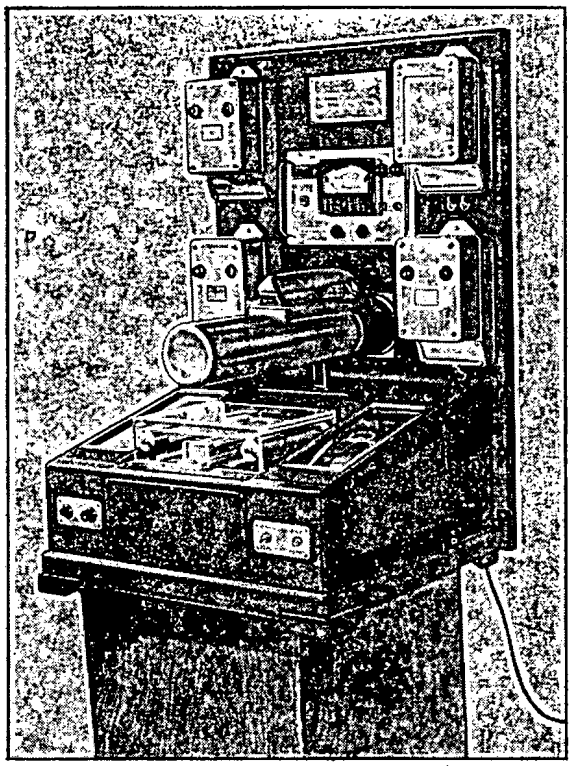

Fig. 1. General-purpose instrument for thickness measurement, URIT-1 type, designed by the Institute of Physics of the Latvian SSR in collaboration with the Tallinn KIP experimental factory.

This section also displayed devices for determining density in fluids and pulps, concentration of solutions, monitoring the cementation process, sensing the concentration of asbestos-cement slurry, and other applications. Instruments designed for automatic analysis of the composition of materials by means of radioactive isotopes were demonstrated, illustrating the great promise held forth for industrial monitoring and control of the composition of gases, fluids, and solids. These included instruments capable of efficient operation in chemically aggressive media. Also on display were instruments for monitoring sequential pumping of petrochemical products through pipelines, for pressure measurement in various gases, and radiometric bedrock density relays capable of automating the release of rock from jigging machines in ore processing plants, plus many others.

The theme "Noncontacting sensing and control of thickness and weight" was represented in the third section of the exhibit, by a line of assorted equipment now in mass production (Fig. 1). ITU-495 and ITSh-496 thickness gages on display are designed for continuous noncontacting measurement and control of the thickness of a moving metal strip in the cold-rolling process in applications to strip ranging from 0.03 to 1.0 mm thickness with a tolerance of ± 1.5% of the measured thickness. These devices are currently in widespread use in ferrous and nonferrous metallurgical plants. Their use has resulted in a sizable increase in the productivity of rolling mills through increase of rolling speed, reduction of scrap, and great savings in materials. Experimental specimens of cold-rolling-strip thickness gages with scintillation counters, differing from the ITU-495 model in their smaller size and weight as well as in wider range of thickness measurement (from 0.5 to 2.5 mm) were also on display. A device of this type, mounted for industrial trial tests on the line in the Leningrad steel-rolling plant, stepped up the productivity of an individual rolling mill by 40%.

Mass-produced instruments for measuring the thickness of coatings of different types, for spotting rough spots in fabric running through batting machines in the textile industry, noncontacting load cells, devices for sensing variations

in wall thickness of piping, thickness of sheet material admitted for working on only one side, and others were also displayed.

The section displayed an ROTOP-3 type instrument designed by the Makeev scientific research institute and manufactured by the Kharkov mine surveying instrumentation factory; this device is designed to measure the thickness of settled dust in place directly at the work site, in order to warn of the presence of surface concentrations presenting an explosion hazard. Data on a radioactive sensor developed by the Mining Institute of the USSR Academy of Sciences for coalface cutting machines were avilable. This device, used on coal cutters now in use, makes it possible to completely eliminate damage associated with deviation of the direction of bite of the cutting tool into the coal face, and improves the quality of the mined coal. This radioactive sensor served as the basis for the design of an automatic controller tested out on the KN-1 cutting and loading combine in pit No. 54 of the "Bokovantratsit" anthracite trust.

The fourth section of the exhibit was devoted to display of a varied line of radioactive relay-action equipment, built up on standardized circuits and components, beta and gamma emitters, transducers, and electronic relay units. This equipment, developed by the Tallinn KIP experimental plant, the Riga SKB "Avtoelektropribor" automatic electrical components factory, the Institute of Physics of the Latvian SSR Academy of Sciences, and other organizations, and now assimilated into production practice in enterprises under the jurisdiction of the Latvian and Estonian councils of the national economy, has facilitated the solution of the most varied types of engineering production problems. The savings accruing from the use of this instrumentation in Latvian plants and factories totalled one and a half million rubles yearly. A standardized assembly of equipment for measuring materials thickness and coating thickness with a self-adjusting relay unit was put on display. Also demonstrated were indicating instruments equipped with radioactive sensors functioning as current density controls in plating baths, alarm annunciators for voltage surge level in ac grids, etc.

The fifth section, on the theme "Radioactive isotopes for quality control of materials and products and investigation of physical and chemical processes," demonstrated a line of gamma-ray nondestructive testing equipment widely employed for quality control of weldments, castings, solders, etc. The resulting advantages are great economy in inspection time and cutting of inspection expenses combined with a simultaneous sharp reliability gain.

The GUP line of gamma-ray instruments displayed in this section, manufactured at the "Mosrentgen" x-ray equipment plant in Moscow, are used in many industrial applications. The Moscow branch of the Orgenergostroi power institute presented a RDB-2 model gamma radiography unit capable of measuring the density and detecting flaws of 1.5-2% of the thickness of the inspected specimen in prefabricated reinforced concrete members of up to 60 cm thickness with reinforcement filling to 100 kg/m^3. Measurement time at a single point is only 30 sec.

Several of the exhibit items reflected the development of the new ionization inspection technique, based on recording of variations in the intensity of emissions passing through the material under inspection by various detectors: an ionization chamber and gas-discharge or scintillation counters.

The advantages of employing this inspection technique at the "Uralkhimmash" chemical processing machinery works were that the source activity could be stepped down 100 times while speeding up the productivity of the inspection process by 50 times. Special stands were set up to display new work in the field of investigation and monitoring of wear on materials and parts with the aid of radioactive tracers. A special demonstration was made of the use of tracers in determining wear resistance of alloys, radiations in quality control of product, and process research in metallurgy and other fields at the V. A. Malyshev transportation machinery plant.

A special section gave an account of the use of radioactive isotopes in prospecting, exploration, and development of mining. On demonstration were a line of inspection instruments and techniques used in the development of oil fields to locate productive oil beds, in exploring oil fields to determine oil-water contacts by neutron-gamma logging and induced activity techniques. Devices for determining the injectivity profile in peripheral flooding and the hydraulic fracturing zone of a reservoir, and for quality control of drillhole completions were represented. Equipment and techniques for express assay of beryllium, boron, lithium, and other ore specimens were shown. Comprehensive analysis of the material composition of ores and minerals under field conditions has been made possible with the aid of the VIMS-58 facility (see Fig. 2) developed by the All-Union Mineral Raw Materials Institute. The relative precision achieved in analyses is 5-10% for a total of 20-30 min time spent per element in one run. The accomplishments of the "Azneftegeofizika" geophysical prospecting trust (Azerbaidjan) and Volga-Ural branch of the Geophysics Research Institute and other organizations in applications for radioactive techniques occupied a place of honor at the exhibit.

A special display reflected the activities of the All-Union "Izotop" central clearing office. Visitors to the exhibit had the opportunity of becoming acquainted with items available for delivery from "Izotop." A glass showcase was set up with models of nuclear radiation sources, next to which was placed an explanation of the routine to be followed in filling out order blanks. A representative of the "Izotop" office was available on a regular twice-weekly basis for consultations with visitors and routing of orders for instruments and equipment.

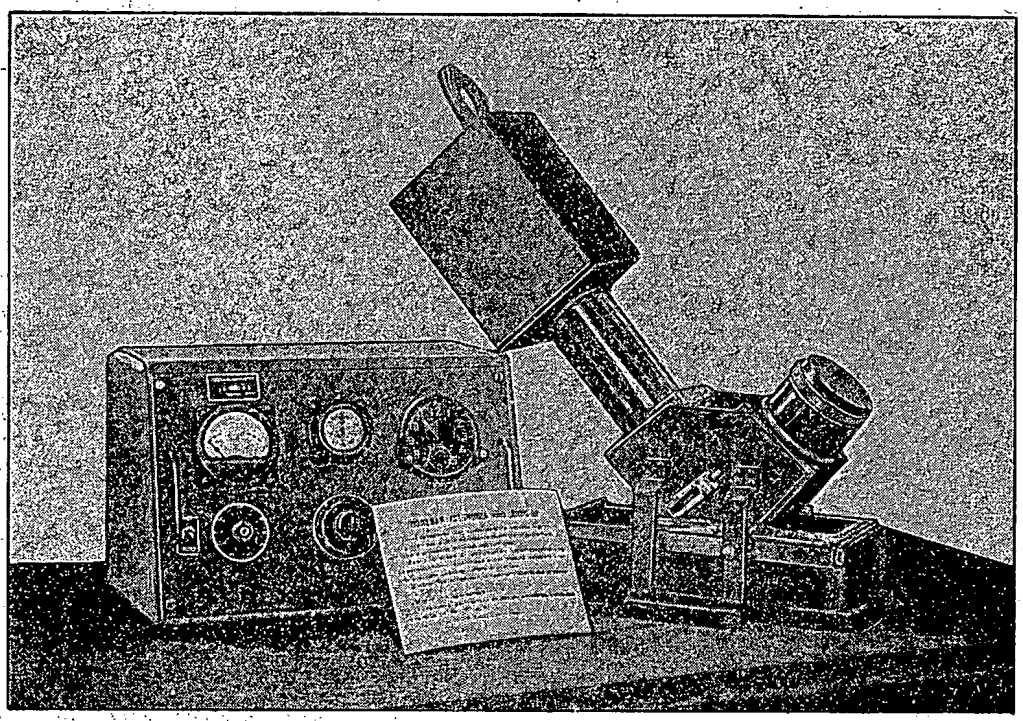

Fig. 2. VIMS-58 facility for comprehensive assay of material composition of ores and minerals under field conditions.

Another special section was devoted to safe working conditions and health physics in the handling of radiation sources. Some typical layouts of radiography laboratories worked out and approved by the State Committee of the Council of Ministers of the USSR on the Uses of Atomic Energy were exhibited, as well as specimens of protective equipment and lists of recommended personnel shielding items.

Regular consultations with qualified specialists in the field of applications of radioactive tracers and nuclear radiations from leading scientific research institute and R and D organizations and various industrial plants throughout the nation were arranged for visitors.

The total number of exhibits in this field were 150, presented by 138 different organizations engaged in the development or use of instruments based on nuclear radiation sources in process control and automation.

The over-all exhibit, which was well received by the visitors, hit home the fact that radioactive isotopes are capable of effecting monitoring and automation at an advanced technical level in the most varied branches of production, thereby contributing to the solution of the prime task facing the national economy—that of utilizing all available measures to increase labor productivity.

NUCLEAR POWER IN WEST GERMANY

Translated from Atomnaya Énergiya, Vol. 10, No. 4, p. 415, April, 1961

Materialization of most of the construction plans envisaged by West Germany for nuclear electric power stations and research projects are being delayed because of insufficiency of technical means. Some circles of industrialists who are interested in the development of nuclear power in West Germany have expressed their views on their dissatisfaction with the governmental financial policy currently pursued [1].

As an example, the Bonn government intends to cutback funds earmarked for nuclear industry by some 50 million marks, in favor of other budgetary items. This cutback affects the Stuttgart project primarily. The reason is conjectured to be a lagging rate of progress in construction and research. The government is moreover of the view that interested firms should step up their own appropriations to promote this work. It is further not excluded that this policy is the outcome of influence exerted by those industrial circles who see in a nuclear power station project a strong competitor to the building of conventional fossil fuel power installations.

Announced in 1957, this construction program for nuclear power stations aiming at a total power output of 500 Mw has been partially fulfilled only at the planning level, but not a single one of those projects has reached the construction stage [1-3].

Another important reason for the unsatisfactory state of progress on this program, as well as other programs, is the lack of a scientific research base to support national projects in general. For example, a pilot nuclear electric power station of 15 Mw(e) rating at Kahle-am-Main, built by private contractors, is a boiling-water reactor of American design, while the research associated with the high-temperature gas-cooled reactor was carried out at the Belgian nuclear studies center in Mol (construction work on this 15 Mw research reactor was begun in September,1960).

It is assumed that if the position of nuclear industry in the financial picture is not upgraded by the government and private firms, the level of development of nuclear power in West Germany will reach the level presently attained by Great Britain only by 1970.

The intense interest shown by the government in the development of nuclear propulsion units for seagoing vessels stands in contrast to the above picture, although there are those who feel that progress in this area is far from satisfactory. Projects for five such propulsion units were only half completed, and design work on a reactor for the tanker "Esso Bolivar" is still incomplete, although started in 1959 at Hamburg.

Another factor exerting a negative effect on the fulfillment of these projects is that firms engaged in building conventional type maritime engines frequently sit in on the discussions of the projects.

LITERATURE CITED

1. W. Kliefoth, Atomkernenergie 5, H. 10, 386 (1960).
2. W. Kliefoth, Atomkernenergie 5, H. 6, 232 (1960).
3. Atomnaya Énergiya 8, No. 3, 1960, p. 273.*

* Original Russian pagination. See C. B. translation.

NEW GENERAL-PURPOSE ENCLOSURE FOR HANDLING ALPHA, BETA, AND GAMMA EMITTERS

G. N. Lokhanin and V. I. Sinitsyn

Translated from Atomnaya Énergiya, Vol. 10, No. 4, pp. 420-421, April, 1961

A new general-purpose glove box system has been developed by Soviet industry to facilitate handling of alpha-, beta- and gamma-active materials.

The general-purpose box consists of a single-operator box type 1-KNZh, seen on the left in Fig. 1, and a biologically shielded type KSh junior cave (ball-joint manipulator box), with the two joined by a transfer chamber (see both Figs. 1 and 2).

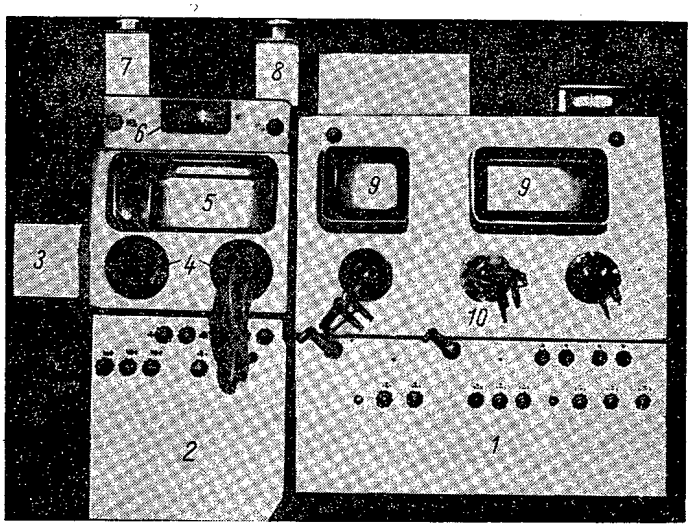

Fig. 1. General-purpose enclosure line (seen from the operator's side): 1) through-panel ball-swivel manipulator type KSh junior cave; 2) 1-KNZh type single-operator glove box; 3) transfer compartment; 4) rubber gloves; 5) viewing window (stalinite alloy); 6) water pressure gage; 7) exhaust filter; 8) inlet filter; 9) viewing windows (lead glass); 10) MShL-05 type through-panel ball-swivel junior manipulators.

Both enclosures are equipped with exhaust and inlet filters and with water pressure gages.

The 1-KNZh type glove box may be used for handling alpha and beta emitters, while the KSh type cave is useful for handling gamma-active materials with activities up to 50 milligram-equivalents of radium. The total volume of the enclosure line is one cubic meter (the volume of the 1-KNZh box is 0.4 m^3, and that of the KSh cave is 0.6 cm^3), and the air transfer volume is 25 volumes per hour.

The filter area in a 1-KNZh box is 0.11 m^2 (filter resistance of 13-21 mm H_2O), and that of the KSh cave is 0.25 m^2. Normal rarefaction in the boxes is 20 mm H_2O. The size of the general-purpose enclosure is 2970 x 2560x x 2320 mm. The total weight of the chamber is 5700 kg (the 1-KNZh box weighing 450 kg and the KSh box 5250 kg). The enclosure assembly may be used to carry out work at elevated temperatures and humidity levels in acid and alkali atmospheres.

The single-operator 1-KNZh glove box has been described in a previous article [1].

The KSh type junior cave has biological shielding. The cave is divided into a transfer compartment equipped with one MShL-05 through-panel manipulator and an operating compartment with two such manipulators. Transfer of radioactive material from one compartment to the other is carried out through the portal of the transfer chamber, which is sealed and remote-controlled by means of a dial system in the front panel, connected via a worm gear train.

The KSh type junior cave is equipped with the MShL-05 manipulators, a tray for holding instruments, daylight fluorescent lamps, a TNM-890 (0-125) water pressure gage, two-stage (0.25 m^2 area) inlet and exhaust filters, a vacuum suction for cleaning the inner surfaces of the box, a support for delivering containers with hot preparations inside the box, a solid waste carboy, carboy (type 10-KZhO) for liquid wastes, electric power leads, cold and hot water taps for operations and flushing down the cave interior, two spare nipples of special design for withdrawal of liquid wastes (into the drainage system, special-purpose drainage, and liquid waste carboy), and a device for discarding solid wastes into the proper carboy.

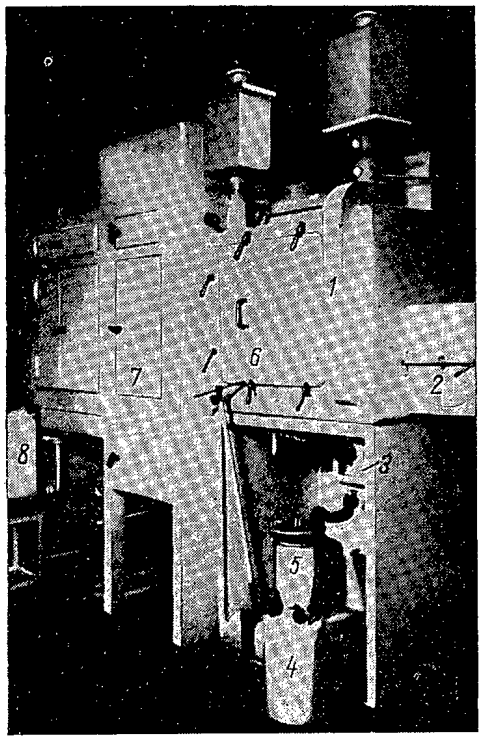

Fig. 2. General-purpose enclosure (seen from the maintenance approach side): 1) air lead; 2) transfer chamber portal; 3) drain for liquid wastes; 4) liquid wastes carboy; 5) solid wastes carbon and dolly; 6) back panel for placing equipment and instruments inside box, and for maintenance and other work inside box; 7) transfer compartment connecting KSh cave to 1-KNZh box; 8) exhaust filter in protective casing.

The size of the KSh junior cave is 1700 x 2540 x 2485 mm. The biological shielding used consists of cast-iron slabs 100 mm thick (front slab), 80 mm thick (bottom and side slabs), 50 mm thick (top, back, and in-between slabs), and a stack of lead glass windows 150 mm total thickness.

The supporting frame for the enclosures, 1700 x 980 x 940 mm in size, is made of carbon-alloy steel.

For the purpose of decontaminating the air emerging from the junior cave, a two-stage exhaust filter with a protective casing (of 40 mm wall thickness) is positioned across the outlet. The filter consists of glass fiber 200 mm thick and FPP-15-1.7 fabric sandwiched in four layers. The filter has a throughput of 25 cubic meters per hour.

The transfer compartment is made of 1Kh18N9T stainless steel (faced with cast-iron slabs) and is 450 x 706 x 732 mm. The working portion of the transfer chamber is made of stainless steel 3 mm thick, and is 900 x 706 x 725 mm.

A baffled funnel is mounted in the KSh table top to channelize liquid waste into a general drainage system, a special-purpose drainage system, or a 10-KZhO type carboy [2].

Removal of solid waste from the KSh junior cave follows the same pattern as observed for the 1-KNZh glove box.

The assembly of the 1-KNZh glove box includes two type 10-KZhO carboys for receiving and hauling liquid waste, a type 2T dolly with integral waste receptacle, two spare filter components, spare plastic pouches (25), a spare viewing window, spare rubber gloves, spare membranes (6), spare glove cuffs, and other items.

The KSh assembly includes filters (one inlet filter and one exhaust filter), plastic transfer pouches (25), 2Sh-2-57 and KSh-9-45 cuffs (2 each), DS-15 type membranes (6), 127-volt 75-watt fluorescent daylight fixtures (3), and miscellaneous items.

An engineering specifications plate, assembly and layout diagrams, filter inspection tags, pipe communications, liquid wastes casks, operating instructions, etc., are included in the general-purpose glove box accessories.

LITERATURE CITED

1. G. N. Lokhanin and V. I. Sinitsyn, Atomnaya Énergiya 9, No. 4, 344 (1960).*
2. G. N. Lokhanin and V. I. Sinitsyn, Atomnaya Énergiya 9, No. 4, 341 (1960).*

* Original Russian pagination. See C. B. translation.

THE M-2 MANIPULATOR

O. M. Ignat'ev

Translated from Atomnaya Énergiya, Vol. 10, No. 4, 421-422, April, 1960

The M-2 manipulator is designed to perform manipulative operations with encapsulated radioactive gamma emitters in loading, transfer, and maintenance of containers,both under laboratory and field conditions. The manipulator described below may be employed in radiography laboratories, radiation therapy clinics, radiation chemical laboratories, and other workplaces where encapsulated gamma emitters are being used.

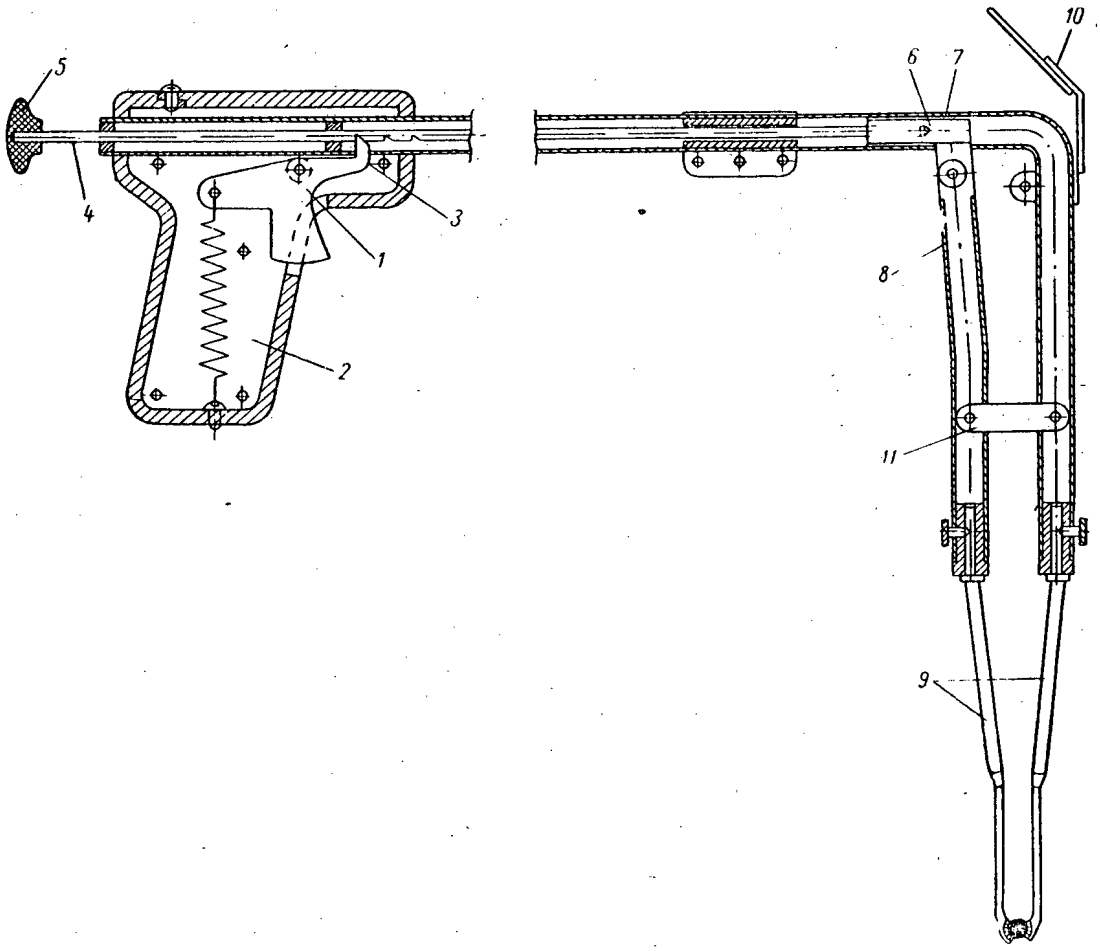

Fig. 1. Diagram of M-2 manipulator (general view).

The M-2 manipulator consists of two basic components (see Fig. 1 and Fig. 2); grip handles with actuating trigger and a jaw gripping device. When the actuating trigger 1 of the grip handle 2 (Fig. 1) is squeezed, the locking pin 3 of the trigger moves downward, releasing the rod 4, with head 5 fastened at one end, the far end being threaded into a slider 6. The slider may be displaced along the axis of the tube 7, within which it rides. A ball and swivel joint connects this tube with a lever 8, at the lower end of which is attached one of the gripping jaws 9 of the slave end. When the slider 6 is at the extreme righ of its travel, the distance between the slave jaws is at a maximum, i.e., the manipulator is ready for picking up the radioactive capsule.

To pick up a capsule with the aid of an M-2 manipulator, with the capsule located inside its container, one must: a) drop the jaws of the business end of the manipulator, in open position, into the interior of the container, as indicated in Fig. 2; b) while observing the mutual position of gripping jaws and capsule in the elbow mirror 10

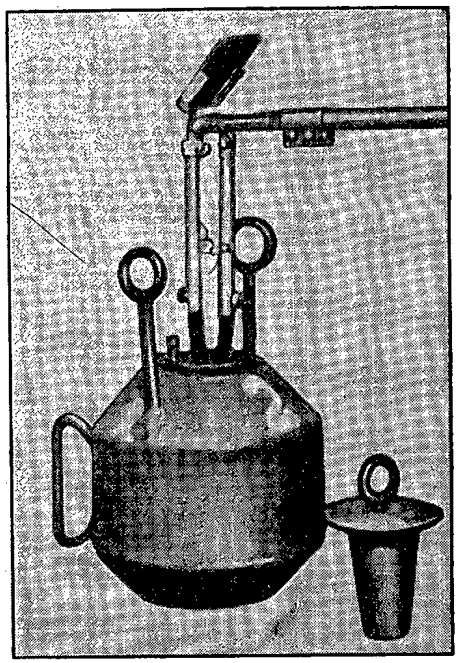

Fig. 2. Removal of a source from container cask with the aid of the M-2 manipulator.

(Fig. 1), position the jaws such that the capsule will be between the grip fingers; if there is insufficient illumination inside the container, and the capsule and fingers are difficult to observe in the mirror, a small light bulb positioned on the crossarm 11 of the slave end can be turned on; c) after the capsule is in the space between the fingers, squeeze the actuating trigger 1 and use the knob 5 to pull back the rod 4 with attached slider 6, after which release the trigger, thereby locking the position of the rod, and consequently of the capsule, which will be firmly grasped between the jaw fingers. The reliable operation of the capsule grip is brought about by the presence of leather pads securely attached to the inner surface of the fingers, which intimately contact the surface of the capsule, and also through the effect of the elastic forces of the steel jaws under compression.

The use of the M-2 manipulator for loading and unloading containers of radioactive emitters greatly eases the tasks of the operator carrying out this operation, shielding him from any exposure to direct beams. Moreover, there is the possibility of shielding all parts of the operator's body (including the hands) by means of a lead shield (while the capsule is still inside the cask). The lead screen of adequate thickness is placed between the cask and the operator's working position.

The M-2 manipulator may be made in different lengths (from 0.5 to 3 m, or longer), depending on the activity of the available sources, their radiation energy, the presence and thickness of an additional lead shield, etc.

BIBLIOGRAPHY

NEW LITERATURE

Translated from Atomnaya Énergiya, Vol. 10, No. 4, pp. 425-432, April, 1961

Books and Symposia

S. A. Prechistenskii. Radioaktivnye vybrosy v atomosferu [Radioactive venting to the atmosphere]. Moscow, Gosatomizdat, 1961, 176 pages, 66 kopeks.

This book reviews new techniques for decontamination of radioactive aerosols and toxic fumes in the air. Practical information of use in the planning and design of air decontamination apparatus is given. In the chapter devoted to filtration of aerosols, a procedure for designing filters of fiberglass, thin-fiber materials, and FP fabrics is outlined and recommendations on filter installation are given. The chapter on absorption of vapors and aerosols reviews the design and performance of foaming equipments of various types, cites the basic equations describing foaming performance, and hints on design techniques for such equipment. A chapter illuminating problems of aerosol centrifugation describes the design of the rotor for a centrifugal rotatory dust separator. This chapter also provides data on industrial tests for centrifugal dust separators which might prove useful in the design of industrial models.

A special chapter takes up combined decontamination methods. Here are described the decontamination of gases exiting from waste incinerator furnaces, decontamination of fumes from evaporators, sulfur oxide hood fumes, discharges from vacuum pumps, decontamination of process gases by cold trapping, venting of purified air to the atmosphere via high stacks, and new electrophysical techniques for removing fine aerosols from air.

The appendices to the book cite the critical tolerance concentrations for toxic fumes and dust in the air environment of work sites.

The book is written for engineering and technical workers responsible for the design and maintenance of air clean-up equipment.

W. Braunbek. Measurement techniques in nuclear physics. Translated from the German. Gosatomizdat, 1961, 88 pages, 36 kopeks.

This book provides a brief review of measurement techniques employed in nuclear physics, and their applications.

Techniques reviewed are: mass spectrography and mass spectrometry; measurement of nuclear moments; calorimetric measurements and charge measurements; measurements carried out with various types of ionization chambers; measurements of activity, dosimetric measurements and determination of decay constants; measurements of scattering, absorption, and range; spectrometry of radioactive radiations. The equipment required to perform these measurements is described.

The book will be found interesting by physicists and students majoring in physics.

A. M. Kuzin. Primenenie radioaktivnykh izotopov v biologii [Uses for radioactive isotopes in biology]. Vienna. International Atomic Energy Agency, 1960, 63 pages.

This brochure is the seventh publication in a series of reviews to be distributed by IAEA on the peaceful uses of atomic energy.

It presents a review of the literature since 1959 on applications for tracer methods in various fields of biological studies. Particular emphasis is given to the use of tracers in biochemistry in studies of protein biosynthesis, biosynthesis of nucleotides and nucleic acids, synthesis and turnover of lipids, carbohydrate turnover in animal organisms, etc. In the area of physiological research, attention is turned to work on the problem of premeability, diffusion, and sorption of matter, the physiology of the circulatory system, studies of malignant neoplasms. The review also includes a list of papers on tracer methods in plant physiology, microbiology, virology, and radiobiology, histomorphological research, hydrobiology, entomology, ichthyology, and genetics.

Five-hundred and seventy titles are included in the bibliography. The text of the brochure appears in both Russian and English.

Directory of nuclear reactors. Vol. III. Research, test and experimental reactors. Supplement to Vol. II. IAEA.

G. Dienes, G. Vineyard. Radiatsionnye effekty v tverdykh telakh (Translation of Radiation Effects in Solids, Interscience Publ.). Moscow, Foreign Literature Press, 1960. 244 pages, 1 ruble, 19 kopeks.

Articles from the Periodical Literature

I. Nuclear Power Physics

Neutron and reactor physics. Hot plasma physics and controlled fusion. Physics of charged-particle acceleration.

Doklady akad. nauk SSSR 135, No. 3 (1960).

L. V. Volod'ko et al., 560-563. Note on the interpretation of electron and vibrational absorption spectra of uranyl nitrates.

Zhur. tekhn. fiz. XXX, No. 12 (1960)

V. V. Afrosimov et al., 1381-93. Plasma research on the ALPHA machine.

V. A. Glukhikh et al., 1394-1403. Design data and basic performance parameters of the ALPHA facility.

V. A. Glukhikh et al., 1404-14. Studies of electrical and magnetic discharge characteristics on the ALPHA machine.

V. A. Burtsev et al., 1415-21. Measurement of flux of energy radiated by a plasma in the ALPHA.

A. N. Zaidel' et al., 1422-32. Spectral investigations on the ALPHA. I. Study of character of the spectrum and ion temperature.

A. N. Zaidel et al., 1433-36. Spectral investigations on the ALPHA. II. Oriented motion of ions.

A. N. Zaidel et al., 1437-46. Spectral investigations on the ALPHA. III. Time characteristics of plasma luminescence.

V. A. Anoshkin et al., 1447-55. Microwave plasma research on the ALPHA.

V. V. Afrosimov et al., 1456-68. A technique for investigation the flux of atoms emitted by a plasma.

V. V. Afrosimov et al., 1469-84. Investigation of flux of neutral atomic particles emitted by a plasma in the ALPHA machine.

O. V. Konstantinov, V. I. Perel', 1485-88. On the energy distribution of fast neutral atoms emitted by a plasma.

Zhur. éksptl. i teoret. fiz. 39, No. 6 (1960)

V. D. Rusanov et al., 1497-1502. Double electric probe studies of magnetoacoustic resonance in a plasma.

B. I. Patrushev et al., 1503-1507. Gyrotropic properties of a plasma in the propagation of an extraordinary wave.

M. S. Ioffe et al., 1602-11. Studies of plasma confinement in a magnetic mirror trap.

Izvestiya vyssh. ucheb. zaved. Radiofizika 3, No. 5 (1960)

M. S. Kovner, 746-57. Kinetic treatment of interaction between a stream of charged particles and a stationary plasma in a magnetic field. II.

Pribory i tekhnika éksperimenta, No. 6 (1960)

A. N. Pisarevskii, L. D. Shoshin, 3-13. Fast coincidence techniques with slow scintillators.

Yu. P. Betin et al., 23-27. Method for enhancing precision in measurements of flux of radioactive radiation.

D. V. Viktorov et al., 27-30. On a plastic-scintillator proportional counter.

E. K. Bonyushkin, V. V. Spektor, 30-34. Scintillation gamma-ray spectrometer features control channel.

V. S. Shevyrev, 35-40. Voltage-current characteristics of plane-parallel ionization chambers filled with air at atmospheric pressure.

A. I. Babaev, L. G. Lansberg, 40-42. New gas-filled Cerenkov counter.

A. T. Abrosimov, 48-51. Scintillation counter of large acceptance area records cosmic-ray particles.

G. A. Koval'skii, A. M. Rodin, 84-89. Separation of inert-gas isotopes in an electromagnetic isotope separator.

V. A. Gladyshev, L. N. Katsaurov, 113-14. Vapor-jet counter records charged particles.

Atomkernenergie 5, No. 12 (1960)

G. Brunner, 456-58. Superposition of pulses in high-pulse-density scintillation spectrometry.

Atomwirtschaft 5, No. 12 (1960)

K. Hagenow, R. Kippenhahn, 560. Thermonuclear fusion.

G. Lehr, 560-62. Fusion research in West Germany.

---, 567-72. Nuclear instrumentation at the INTERKAM exhibit.

Canad. J. Phys. 38, No. 12 (1960)

G. Milton, W. Grummitt, 1690-1701. Capture cross section of pile neutrons for Y^{91}.

Kerntechnik 2, No. 12 (1960)

A. Lösche, 389-91. Fundamentals of paramagnetic nuclear resonance. 3.

G. Lutz, 291-97. Experimental techniques in neutron diffraction.

Nucl. Energy 15, No. 152 (1961)

F. Paulsen, 29-32. Particle acceleration engineering.

Nucl. Instrum. and Methods 9, No. 1 (1960)

R. Bramlett et al., 1-12. Novel neutron spectrometer.

W. Smith, 49-54. Improved beam focusing in the region of a cyclotron ion source.

S. Waaben, 78-86. Synchrotron magnet power circuit with distributed banks of capacitors.

V. Dmitrievsky et al., 115-17. On particle losses at the critical radius of a synchrocyclotron.

II. Nuclear Power Engineering

Theory and calculations of nuclear reactors. Reactor design. Performance of nuclear reactors and nuclear power stations

Pribory i tekhnika éksperimenta No. 6 (1960)

V. I. Goman'kov et al., 45-48. Neutron diffraction facility at the IRT reactor.

Atomkernenergie 5, No. 12 (1960)

K. Bammert, 437-447. Optimum characteristics of a nuclear power station using nitrogen as working fluid.

H. Brüchner, 448-53. Boiling-water reactors for maritimeservice.

W. Kliefoth, 471-72. Review of proceedings of the Karlsruhe Atomforum conference.

Atomwirtschaft 5, No. 12 (1960)

H. Seidl, 538-43. Power reactors.

H. Daldrup, 544-46. Maritime nuclear power propulsion installations.

H. Fischerhoff, 551-52. Legislation in nuclear matters.

F. Sardemann, 563-64. The outlook for nuclear power development in Europe.

H. Liesegang, 575-82. Instrument holes and control rod and scram rod holes in the FR-2 reactor.

Energia Nucleare 7, No. 12 (1960)

S. Tassan, 821-32. Techniques for measuring physical parameters of heterogeneous reactor cores, using exponential experiments. 3.

L. Berardinelli et al., 833-43. Heat removal and various types of fuel elements of organic-moderated and organic-cooled reactors.

Jaderná Energie 6, No. 12 (1960)

L. Bohal, 398-403. The problem of thermal shock in gas mains of nuclear power stations.

Kerntechnik 2, No. 12 (1960)

W. Schilling, 398-400. Thermocouple measurements of neutron flux in the FRM reactor.

H. Uschwa, 400-404. Design of heat exchangers for high thermal loading.

---, 404. Techniques for leaktesting fuel element cladding.

P. Schranz, A. Stebler, 409-409. Reactor applications for magnetic amplifiers.

Nucl. Energy 15, No. 152 (1961)

N. Grassam, 19-28. Nuclear reactors in universities.

Nucl. Engng. 6, No. 56 (1961)

---, 1-2. Research reactors for universities.

---, 7. The Sizewell nuclear power station.

D. Hartley, 8-11. Thin tube sheets for high-pressure heat exchangers. 2.

---, 12-15. The Trawsfynydd nuclear power station.

G. Bracewell, 18-20. Studies of reactor scram conditions.

P. Warner, 21-23. Design of graphite cores for the Trawsfynydd reactors.

R. Bailey, J. Head, 25-27. Earthquake-proof core for the Tokai Mura (Japan) nuclear power station reactor.

W. Banks, 28-32. The EGCR experimental gas-cooled reactor.

---, 33-34. Nuclear maritime power installations. Review of the IAEA conference at Toarmina (Nov. 14-18, 1960)[see p. 406 this issue].

Nucl. Power 6, No. 57 (1961)

S. Cole, 71. Review of IAEA activities for 1960.

---, 74-81. Progress in technology. 1. Reactor design. 2. Instrumentation. 3. Chemistry. 4. Radiation processing.

O. Plail, 82-85. Techniques for irradiation of fissionable materials. 2.

R. Anscomb, 86-88. Nuclear maritime engines (IAEA conf., 1960).

J. Bolton, 89-91. Experience in operating the JASON reactor. 2.

---, 95-96. Design of the Sizewell power station.

Nucl. Sci. and Engng. 8, No. 5 (1960)

J. McDonald, 369-77. Investigation of natural convection heat transfer for liquid sodium.

W. Lyon, 378-80. Reactor neutron activation cross sections for several elements.

G. Hickman et al., 381-92. Water-moderated cores with boron-steel septa at elevated temperatures.

G. Calame, 400-404. Few-group theory of water gap peaking.

D. Klein, 405-409. Measurements of intensity of Pu and U^{235} fission in the neutron spectrum of a water-moderated reactor.

R. Babcock, S. Ruby, 410-415. A nondestructive assay device for determination of U^{235} and boron content in enriched fuel assemblies.

P. Michael, 426-31. Thermal neutron flux distribution in space and energy.

J. Mortenson, R. Ball, 448-49. Reactivity coefficients of rare-earth oxides.

G. Smith et al., 449-50. Comparative Monte Carlo measurements of the space distribution of resonance capture neutrons in a uranium rod.

Nukeonik 2, No. 6 (1960)

W. Häfele, 240-46. Neutron spectrum in a heterogeneous reactor using plate-type fuel elements. 2.

D. Emendörfer, M. Ritzi, 247-52. Effect of core-reflector gap on pile reactivity in the light of transport theory (P_L approximation).

W. Oldekop, 252-54. Exact multigroup diffusion theory of the finite heterogeneously charged reactor.

Nukleonika V, No. 10 (1960)

W. Dabek et al., 597-609. Ionization neutron detectors.

K. Jozefowicz, L. Adamski, 617-28. Gamma-ray spectroscopic studies of coolant water contamination in the WWR-S reactor.

Reactor Science 13, Nos. 1-2 (1960)

J. Lewins, 1-5. Derivation of the time-dependent adjoint equations for neutron importance in the transport, continuous slowing-down, and diffusion models.

W. Cooper, H. Rose, 6-13. Pile oscillator measurements of spent plutonium.

G. Rowlands, 14-24. Numerical method for investigating fast neutrons in a homogeneous medium.

W. Glendenin, 25-34. Model of a one-atom gas for themal neutron distributions in a physical moderator.

A. Baston et al., 35-36. Measurements of thermal neutron sections for Lu^{175} and Lu^{176}.

III. Nuclear Fuel and Materials

Nuclear geology and primary ore technology. Nuclear metallurgy and secondary ore technology. Chemistry of nuclear materials

Vestnik akad. nauk SSSR XXX, No. 12 (1960)

N. P. Lyzhnaya, 14-19. Development of physicochemical analysis.

Zhur. fiz. khim. 34, No. 10 (1960)

I. B. Rabinovich et al., 2202-04. Negative isotope effect in the viscosity of deuterated compounds.

E. M. Kuznetsova et al., 2370-71. Note on a new method for separating boron isotopes.

Pribory i tekhnika éksperimenta No. 6 (1960)

A. A. Ponomarev et al., 58-60. Inspection technique in the investigation of electrostatic precipitation of alpha-emitting isotopes.

V. A. Karnaukhov, V. L. Mikheev, 60-61. Facility for measuring the total thickness of alpha-active layers.

V. L. Tal'roze et al., 78-84. The RMS-2 mass spectrometer, designed for studies of chemical reactions and determination of free radicals.

V. I. Karpukhin, V. A. Nikolaenko, 96-98. Remote control facility for x-ray structural analysis of radioactive specimens.

Radiokhimiya II, No. 6 (1960)

S. Mints, S. Libus', 643-52. Investigation of the causes of selective extraction of uranyl nitrate by tri-n-butyl-phosphate.

N. M. Adamski, 653-58. Salting-out action of nitrates.

N. A. Balashova, N. S. Merkulova, 699-703. Adsorptive and electrochemical methods for separating radioactive zirconium and niobium.

V. P. Shvedov et al., 711-714. Application of continuous electrophoretic techniques to the separation of rare-earth group of photofission fragments of U^{238}.

I. E. Starik, K. F. Lazarev, 749-52. Effect of crushing minerals on the leachability of radioactive elements.

Uspekhi khimii XXIX, No. 12 (1960)

R. Tsaletka, A. V. Lapitskii, 1487-97. The presence of transuranium elements in nature.

Atomwirtschaft 5, No. 12 (1960)

G. Matz, 548-49. Reactor fuel elements.

H. Steinert, 550-51. Fluctuations in the uranium sales picture.

Chem. Engng. News 38, No. 39 (1960)

---, 114. Preparations for the production of Cm-242 for nuclear thermopiles.

---, 116-17. Continuous countercurrent process for foam separation of strontium from nuclear process effluents.

Energia Nucleare 7, No. 12 (1960)

B. Brogoli, 845-48. Numerical methods in distillation column calculations.

G. Camozzo, S. Pizzini, 849-61. Fluorination techniques and a facility for production of fluorine and fluorine halides.

Jaderná Energie 6, No. 12 (1960)

L. Simon, 409-412. Neutron activation analysis of rock.

J. Inorg. and Nucl. Chem. 15, Nos. 3-4 (1960)

F. Butement, P. Glentworth, 205-209. New rare-earth radioisotopes.

J. Forrest et al., 210-214. Ratio of UZ activity to UX_2 activity.

R. Doering et al., 215-21. Rapid method for detecting Sr^{90} in Y^{90}.

J. Alstad, A. Pappas, 222-36. Radiochemical investigations of fission products of lanthanum and lanthanides. I.

J. Inorg. and Nucl. Chem. 16, Nos. 1-2 (1960)

J. Gilat, 147-48. Method for determining Sr^{90} using tagged Sr^{85} as carrier.

J. Ellis, C. Forrest, 150-53. Investigation of the interaction between uranyl fluoride and chlorine trifluoride.

T. Sato, 156-58. TBP extraction of uranyl nitrate in the presence of nitrate salting-out agents.

J. Nucl. Materials 2, No. 4 (1960)

T. Blewitt et al., 277-98. Radiation hardening of copper single crystals.

A. Saulnier, 299-309. Investigation of the structure of thin beryllium specimens in an electron microscope and by microdiffraction techniques.

L. Russell et al., 310-20. Plutonium-base compounds with a perovskite type lattice.

A. Sawatzky, 321-238. Distribution and heat transport of hydrogen in zircaloy-2.

C. Tucker, F. Norton, 329-49. Arrangement and motion of noble-gas atoms in metals.

R. Chang, 335-40. Phase transformation, twinning, and inelastic phenomena in zirconium dihydride.

D. Smart, 341-49. A technique for measuring the thermal diffusivity coefficient of irradiated materials.

F. Norton, C. Tucker, 350-52. Isolation of krypton from uranium metal.

S. Bronisz, A. Gorum, 353-55. Plastic flow of monoclinic α-plutonium.

Kerntechnik 2, No. 12 (1960)

Anders, 388. Production of B^{10}.

H. Pischel, 405-408. Compacting and sintering techniques and their use in the fabrication of uranium oxide fuel elements.

Nucl. Energy 15, No. 152 (1961)

J. Amman, T. Sprague, 11, 13-16. Liquid metal research and prospects for applications.

Nucl. Engng. 6, No. 56 (1961)

---, 24. Industrial method of graphite impregnation.

Nucl. Power 6, No. 57 (1961)

G. Darwin, 93-94. Steels for reactor loops. Review of proceedings of the conference of the Iron and Steel Institute (November, 1960)

---, 98-99. Production of impregnable graphite.

Nucl. Sci. and Engng. 8, No. 5 (1960)

M. Bradley, L. Ferris, 432-36. Recovery of uranium and thorium from graphite fuel elements. I. The grind-leach process.

Nukleonik 2, No. 6 (1960)

B. Weiss-Hollerwöger, 222-27. Effect of neutron bombardment on phase transformations in chrome steels.

Nukleonika V, No. 10 (1960)

W. Trzebiatowski, A. Jablonski, 587-96. Some phase relations in the $BaO-UO_2-O_2$ system.

I. Krawczyk, 649-59. Ion exchange separation of uranium and rare earths in solutions of EDTA.

Z. Rozmej et al., 661-70. Study of uranium sorption in peats.

R. Gwozdz, S. Siekierski, 671-76. Isolation of plutonium in various valence states by reversed-phase partition chromatography.

IV. Nuclear Radiation Shielding

Radiobiology and radiation hygiene. Shielding theory and techniques. Instrumentation.

Doklady akad. nauk SSSR 135, No. 1 (1960)

A. A. Peredel'skii et al., 185-88. Dispersion of radioisotopes in soil by burrowing action of earthworms.

Izvestiya akad. nauk SSSR, seriya biol. No. 6 (1960)

I. V. Bulyakin, E. V. Yudintseva, 874-85. Plant uptake and crop accumulation of some radioactive fission products.

Pribory i tekhnika éksperimenta No. 6 (1960)

O. M. Kovrizhnykh et al., 69-72. Investigation of industrial phototube multipliers in driven mode of operation.

G. I. Zabiyakin, V. N. Zamrii, 126-27. Transistorized decade scalers.

Sel'sko-khoz. Uzbekistana No. 11 (1960)

F. K. Rasulov, 90-92. Effect of radioactive radiation on the dark brown fluor beetle.

Trudy inst. genetiki akad. nauk SSSR No. 27 (1960)

I. E. Glushchenko, G. M. Zakharova, 304-10. Effect of ionizing radiations on the development of wheat and oat plants.

V. K. Karapetyan, 311-14. Effect of gamma rays on wheat heredity.

V. K. Karapetyan, 315-18. Effect of gamma rays on soft wheat and rye.

Archives Environmental Health 1, No. 6 (1960)

M. Udel, 497-501. Legistlative problems and control of ionizing radiations.

Atomkernenergie 5, No. 12 (1960)

H. Peter, 453-55. Thermoluminescence of samarium-activated calcium sulfate, and possibilities for its use in dosimetric instruments.

K. Stierstadt, M. Papp, 459-61. Aerosols as carriers of natural radioactivity.

Atomwirtschaft 5, No. 12 (1960)

R. Palm, 557-58. Nuclear reactor safety.

H. Levi, 558-59. Disposal of radioactive wastes.

L. Lassen, 582-89. Purification of radioactive aerosols from air. II.

Energia Nucleare 7, No. 12 (1960)

R. Bonalumi, 862-64. Measurement of neutron age in diphenyl-impregnated graphite.

L. Colli et al., 865-66. Alpha-particle detector in the form of a discharge chamber.

Jaderná Energie 6, No. 12 (1960)

J. Klumpar et al., 404-408. Determination of trace concentrations of radium in water, based on scintillation measurements of fission products of electrostatically separated radon.

J. Scient. Instrum. 37, No. 12 (1960)

B. Cohen, 475-78. Geiger counter background.

Kerntechnik 2, No. 12 (1960)

---, 412-19. Readily deactivated corrosion protection for hot laboratories.

Nucl. Energy 15, No. 152 (1961)

L. Babin, 43-44. Air monitoring system at the Isotope Research Center.

Nukleonik 2, No. 6 (1960)

H. Engler, 215-222. Silicon alloy diodes as particle counters.

C. Heusch, 228-40. Inelastic moderation of fast monoenergetic neutrons.

Nukleonika V, No. 10 (1960)

T. Florkowski et al., 629-34. Gamma-ray spectrometry applied to analysis of radioactive fallout at Krakow.

Radiation Res. 13, No. 4 (1960)

H. Rossi et al., 503-20. Dependence of RBE on energy of fast neutrons. 1. Design of source and measurement of absorbed dose.

W. McLaughlin, 594-609. Dosimetry of megaroentgen dosimetry employing photographic plates without processing.

Radiation Res. 13, No. 5 (1960)

C. Henderson, N. Miller, 641-43. A study of extinction coefficients for ferric and ceric ions.

T. Osborn, J. Bacon, 686-90. Radiosensitivity of seeds. I. Reduction or stimulation of seedling growth as a function of gamma-ray dosage.

V. Radioactive and Stable Isotopes

Labeled-atom techniques. Use of radioactive radiations. Direct conversion.

Azerb. neft. khoz. No. 10 (1960)

A. G. Khanlarova et al., 40-41. Labeled atoms in studies of the anticorrosive action of AzNII-7 lubricant additive.

Izvestiya Kazan. filiala akad. nauk SSSR, seriya khim. nauk No. 5 (1960)

A. F. Bogoyavlenskii, 155-62. Tracer techniques in the study of anodic passivation of aluminum, and the theory of the mechanism of oxide film formation. Report delivered to the conference on the mechanism of electrolytic grinding of metals (June, 1957).

Zhur. Vsesoyuz. khim. ob-va im. Mendeleeva 5, No. 5 (1960)

A. F. Bogoyavlenskii, 600. On the fabrication of radioactive radiation sources using oxide films on aluminum and aluminum alloys.

Trudy nauchno-issled. inst. betona i zhelezobetona akad. stroitel'stva i arkhitektury SSSR No. 9 (1959)

V. M. Moskvin, I. I. Kurbatova, 83-87. Preparation of radioactive calcium hydrosulfoaluminate preparations.

V. M. Moskvin, I. I. Kurbatova, 88-95. S^{35} tracer studies of the effect of sulfate corrosion in sodium sulfate solutions.

Atomkernenergie 5, No. 12 (1960)

H. Moser, W. Rauert, 462-71, Tracer applications in hydrology.

Atomwirtschaft 5, No. 12 (1960)

H. Sauer, 546-47. Radioactive isotope applications.

Energia Nucleare 7, No. 12 (1960)

F. Strassman, 843-44. Problems regarding exposure of technical personnel engaged in handling of radioactive materials.

For the Information of Readers:

During the third quarter of 1961, Gosatomizdat press will publish the book Plasma Chetvertoe Sostoyanie Veshchestva (Plasma, the Fourth State of Matter) by Dr. Phys.-Math. Sci. Prof. D. A. Frank-Kamentskii. The book, in semi-popular presentation, will have a tentative price of 24 kopeks.

The book presents, in a form accessible to all and shorn of complex mathematics, but with deep scientific content and precision in language, a concise and complete review of the fundamental physical concepts of science on plasma and the possibilities of using it in practical applications.

The book is written for a broad readership interested in this new frontier of science. The basic text is supplemented by more detailed comments for those interested in probing deeper into the subject.

Orders will be accepted by Gosatomizdat, address: Moscow, B-180, Staromonetnyi pereulok, 26.

Soviet Journals Available in Cover-to-Cover Translation

ABBREVIATION	RUSSIAN TITLE	TITLE OF TRANSLATION	PUBLISHER	TRANSLATION BEGAN Vol.	Issue	Year
AÉ	Atomnaya énergiya	Soviet Journal of Atomic Energy	Consultants Bureau	1	1	1956
Akust. zh.	Akusticheskii zhurnal	Soviet Physics – Acoustics	American Institute of Physics	1	1	1955
	Antibiotiki	Antibiotics	Consultants Bureau	4	1	1959
Astr(on). zh(urn).	Astronomicheskii zhurnal	Soviet Astronomy–AJ	American Institute of Physics	34	1	1957
Avto(mat). svarka	Avtomaticheskaya svarka	Automatic Welding	British Welding Research Association (London)		1	1959
	Avtomatika i Telemekhanika	Automation and Remote Control	Instrument Society of America	27	1	1956
	Biofizika	Biophysics	National Institutes of Health*		1	1957
	Biokhimiya	Biochemistry	Consultants Bureau	21	1	1956
Byull. éksp(erim). biol. i med.	Byulleten' éksperimental'noi biologii i meditsiny	Bulletin of Experimental Biology and Medicine	Consultants Bureau	41	1	1959
DAN (SSSR) / Dokl(ady) AN SSSR	Doklady Akademii Nauk SSSR	The translation of this journal is published in sections, as follows:				
		Doklady Biochemistry Section	American Institute of Biological Sciences	106	1	1956
Life Sciences		Doklady Biological Sciences Sections (Includes: Anatomy, biophysics, cytology, ecology, embryology, endocrinology, evolutionary morphology, genetics, histology, hydrobiology microbiology, morphology, parasitology, physiology, zoology sections)	American Institute of Biological Sciences	112	1	1957
Life Sciences		Doklady Botanical Sciences Sections (Includes: Botany, phytopathology, plant anatomy, plant ecology, plant embryology, plant physiology, plant morphology sections)	American Institute of Biological Sciences	112	1	1957
Chemical Sciences		Proceedings of the Academy of Sciences of the USSR, Section: Chemical Technology	Consultants Bureau	106	1	1956
Chemical Sciences		Proceedings of the Academy of Sciences of the USSR, Section: Chemistry	Consultants Bureau	106	1	1956
Chemical Sciences		Proceedings of the Academy of Sciences of the USSR, Section: Physical Chemistry	Consultants Bureau	112	1	1957
Earth Sciences		Doklady Earth Sciences Sections (Includes: Geochemistry, geology, geophysics, hydrogeology, mineralogy, paleontology, petrography, permafrost sections)	American Geological Institute	124	1	1959
Earth Sciences		Proceedings of the Academy of Sciences of the USSR, Section: Geochemistry	Consultants Bureau	106-123	1-6	1957-1958
Earth Sciences		Proceedings of the Academy of Sciences of the USSR, Sections: Geology	Consultants Bureau	106-123	1-6	1957-1958
Mathematics		Doklady Soviet Mathematics	The American Mathematics Society	131	1	1961
Physics		Soviet Physics–Doklady (Includes: Aerodynamics, astronomy, crystallography, cybernetics and control theory, electrical engineering, energetics, fluid mechanics, heat engineering, hydraulics, mathematical physics, mechanics, physics, technical physics, theory of elasticity sections)	American Institute of Physics	106	1	1956
Physics		Proceedings of the Academy of Sciences of the USSR, Applied Physics Sections (does not include mathematical physics or physics sections)	Consultants Bureau	106-117	1	1956-1957
Derevoobrabat. prom-st'.	Derevoobrabatyvayushchaya promyshlennost'	Wood Processing Industry	Timber Development Association (London)		9	1959
	Élecktrosvyaz	Telecommunications	Massachusetts Institute of Technology*		1	1957
Éntom(ol). oboz(renie)	Éntomologicheskoe obozrenie	Entomological Review	American Institute of Biological Sciences	38	1	1959
Farmakol. (i) toksikol(ogiya)	Farmakologiya i toksikologiya	Pharmacology and Toxicology	Consultants Bureau	20	1	1957
FMM	Fizika metallov i metallovedenie	Physics of Metals and Metallography	Acta Metallurgica*	5	1	1957
Fiziol. zhurn. SSSR (im. Sechenova)	Fiziologicheskii zhurnal im. I. M. Sechenova	Sechenov Physiological Journal USSR	National Institutes of Health*		1	1957
Fiziol(ogiya) rast.	Fiziologiya rastenii	Plant Physiology	American Institute of Biological Sciences	4	1	1957
	Geokhimiya	Geochemistry	The Geochemical Society		1	1958
FTT	Fizika tverdogo tela	Soviet Physics–Solid State	American Institute of Physics	1	1	1959
Izmerit. tekh(nika)	Izmeritel'naya tekhnika	Measurement Techniques	Instrument Society of America		1	1959
Izv. AN SSSR, O(td). Kh(im). N(auk)	Izvestiya Akademii Nauk SSSR: Otdelenie khimicheskikh nauk	Bulletin of the Academy of Sciences of the USSR: Division of Chemical Sciences	Consultants Bureau		1	1952

Declassified and Approved For Release 2013/03/04 : CIA-RDP10-02196R000600060003-0

continued

Izv. AN SSSR, O(td). T(ekhn). N(auk): Met(all). i top.	(see Met. i top.)				
Izv. AN SSSR Ser. fiz(ich).	Izvestiya Akademii Nauk SSSR: Seriya fizicheskaya	Bulletin of the Academy of Sciences of the USSR: Physical Series	Columbia Technical Translations		1 1954
Izv. AN SSSR Ser. geofiz.	Izvestiya Akademii Nauk SSSR: Seriya geofizicheskaya	Bulletin (Izvestiya) of the Academy of Sciences USSR: Geophysics Series	American Geophysical Union		1 1954
Izv. AN SSSR Ser. geol.	Izvestiya Akademii Nauk SSSR: Seriya geologicheskaya	Izvestiya of the Academy of Sciences of the USSR: Geologic Series	American Geological Institute		1 1958
Kauch. i rez.	Kauchuk i rezina	Soviet Rubber Technology	Research Association of British Rubber Manufacturers	18	1 1959
	Kinetika i kataliz	Kinetics and Catalysis	Consultants Bureau	1	3 1960
	Koks i khimiya	Coke and Chemistry USSR	Coal Tar Research Association (Leeds, England)		1 1958
Kolloidn. zh(urn).	Kolloidnyi zhurnal	Colloid Journal	Consultants Bureau	14	1 1952
	Kristallografiya	Soviet Physics – Crystallography	American Institute of Physics	2	1 1957
Metalov. i term. obrabot. metal.	Metallovedenie i termicheskaya obrabotka metallov	Metal Science and Heat Treatment of Metals	Acta Metallurgica	6	1 1958
	Metallurg	Metallurgist	Acta Metallurgica		1 1957
Met. i top.	Metallurgiya i topliva	Russian Metallurgy and Fuels	Eagle Technical Publications		1 1960
Mikrobiol.	Mikrobiologiya	Microbiology	American Institute of Biological Sciences	26	1 1957
OS	Optika i spektroskopiya	Optics and Spectroscopy	American Institute of Physics		6 1959
	Pochvovedenie	Soviet Soil Science	American Institute of Biological Sciences		1 1958
	Priborostroenie	Instrument Construction	British Scientific Instrument Research Association		1 1959
Pribory i tekhn. éks(perimenta)	Pribory i tekhnika éksperimenta	Instruments and Experimental Techniques	Instrument Society of America		1 1957
Prikl. matem. i mekh.	Prikladnaya matematika i mekhanika	Applied Mathematics and Mechanics	American Society of Mechanical Engineers		1 1958
PTÉ	(see Pribory i tekhn. éks.)				
	Problemy Severa	Problems of the North	National Research Council of Canada		
Radiotekh.	Radiotekhnika	Radio Engineering	Massachusetts Institute of Technology*	12	1 1957
Radiotekh. i élektronika	Radiotekhnika i élektronika	Radio Engineering and Electronics	Massachusetts Institute of Technology*	2	1 1957
	Stanki i instrument	Machines and Tooling	Production Engineering Research Assoc.		1 1959
	Stal'	Stal (In English)	Iron and Steel Institute		1 1959
Stek. i keram.	Steklo i keramika	Glass and Ceramics	Consultants Bureau	13	1 1956
Svaroch. proiz-vo	Svarochnoe proizvodstvo	Welding Production	British Welding Research Association		4 1959
Teor. veroyat. i prim.	Teoriya veroyatnostei i ee primenenie	Theory of Probability and Its Applications	Society for Industrial and Applied Mathematics		1 1956
Tsvet. Metally	Tsvetnye metally	Nonferrous Metals	Primary Sources		1 1960
UFN	Uspekhi fizicheskikh Nauk	Soviet Physics – Uspekhi (partial translation)	American Institute of Physics	66	1 1958
UKh	Uspekhi khimii	Russian Chemical Reviews	The Chemical Society (London)		1 1960
UMN	Uspekhi matematicheskikh nauk	Russian Mathematical Surveys	London Mathematical Society	15	1 1960
Usp. fiz. nauk	(see UFN)				
Usp. khim(ii)	(see UKh)				
Usp. matem. nauk	(see UMN)				
Usp. sovr. biol.	Uspekhi sovremennoi biologii	Russian Review of Biology	Oliver and Boyd		48 1959
Vest. mashinostroeniya	Vestnik mashinostroeniya	Russian Engineering Journal	Production Engineering Research Assoc.		4 1959
Vop. gem. i per. krovi	Voprosy gematologii i perelivaniya krovi	Problems of Hematology and Blood Transfusion	National Institutes of Health*		1 1957
Vop. onk.	Voprosy onkologii	Problems of Oncology	National Institutes of Health*		1 1957
Vop. virusol.	Voprosy virusologii	Problems of Virology	National Institutes of Health*		1 1957
Zav(odsk). lab(oratoriya)	Zavodskaya laboratoriya	Industrial Laboratory	Instrument Society of America	25	1 1959
ZhAKh Zh. anal(it). khimii	Zhurnal analiticheskoi khimii	Journal of Analytical Chemistry USSR	Consultants Bureau	7	1 1952
ZhETF Zh. éksperim. i teor. fiz.	Zhurnal éksperimental'noi i teoreticheskoi fiziki	Soviet Physics–JETP	American Institute of Physics	28	1 1955
ZhFKh Zh. fiz. khimii	Zhurnal fizicheskoi khimii	Russian Journal of Physical Chemistry	The Chemical Society (London)		7 1959
ZhMÉI Zh(urn). mikrobiol. épidemiol. i immunobiol.	Zhurnal mikrobiologii, épidemiologii i immunobiologii	Journal of Microbiology, Epidemiology and Immunobiology	National Institutes of Health*		1 1957
ZhNKh Zh(urn). neorgan(ich). khim(ii)	Zhurnal neorganicheskoi khimii	The Russian Journal of Inorganic Chemistry	The Chemical Society (London)		1 1959
ZhOKh Zh(urn). obshch(ei) khimii	Zhurnal obshchei khimii	Journal of General Chemistry USSR	Consultants Bureau	19	1 1949
ZhPKh Zh(urn). prikl. khimii	Zhurnal prikladnoi khimii	Journal of Applied Chemistry USSR	Consultants Bureau	23	1 1950
ZhSKh Zh(urn). strukt. khimii	Zhurnal strukturnoi khimii	Journal of Structural Chemistry	Consultants Bureau	1	1 1960
ZhTF Zh(urn). tekhn. fiz.	Zhurnal teknicheskoi fiziki	Soviet Physics–Technical Physics	American Institute of Physics	26	1 1956
Zh(urn). vyssh. nervn. deyat. (im. Pavlova)	Zhurnal vysshei nervnoi deyatel'nosti (im. I. P. Pavlova)	Pavlov Journal of Higher Nervous Activity	National Institutes of Health*		1 1958

*Sponsoring organization. Translation through 1960 issues is a publication of Pergamon Press.

Declassified and Approved For Release 2013/03/04 : CIA-RDP10-02196R000600060003-0

the latest Soviet techniques!

CONTEMPORARY EQUIPMENT for WORK with RADIOACTIVE ISOTOPES

A comprehensive review of the Soviet methods and technological procedures used in the production of isotopes and the preparation of labelled compounds from them. The shielding and manipulative devices are described as well as illustrated in detail. It is an excellent guide for all scientists and technologists concerned with radioactive isotopes.

CONTENTS

durable paper covers 67 pages illus. $15.00

CONSULTANTS BUREAU
227 W. 17th ST., NEW YORK 11, N. Y.